Andrea Laghi

*Editor*

# MDCT Protocols
# Whole Body and Emergencies

*With contributions from*
A. Bozzao, R. Ferrari, F. Fraioli,
M. Rengo, L. Romano

Springer

# MDCT Protocols

Andrea Laghi
Editor

# MDCT Protocols
## Whole Body and Emergencies

*With contributions from*
A. Bozzao, R. Ferrari, F. Fraioli, M. Rengo, L. Romano

Springer

*Editor*
ANDREA LAGHI
Department of Radiological Sciences, Oncology and Pathology
"Sapienza" University of Rome, Polo Pontino, Latina, Italy

*Co-authors*
ALESSANDRO BOZZAO
Neuroradiology,
NESMOS Department
Faculty of Medicine and Psychology
"Sapienza" University of Rome
Rome, Italy

F. FRAIOLI
Chest Imaging Team
Department of Radiological Sciences
Oncology and Pathology
"Sapienza" University of Rome
Rome, Italy

RICCARDO FERRARI
Department of Radiology
San Giovanni Addolorata Hospital
Rome, Italy

MARCO RENGO
Department of Radiological Sciences
Oncology and Pathology
"Sapienza" University of Rome
Polo Pontino, Latina, Italy

LUIGIA ROMANO
Department of Diagnostic Imaging
A. Cardarelli Hospital, Naples, Italy

# Preface

Multidetector-row computed tomography (MDCT) is currently the imaging modality of choice for the study of many anatomical districts in different clinical settings, as it provides a fast, reliable, and accurate simultaneous evaluation of different organs, including parenchyma, hollow viscera, vessels, and bony structures.

The technological catalyst behind the revolution in CT began a little more than 10 years ago, with the introduction in 1998 of 4-slice systems. Rapid progress quickly led to the 320-slice and dual-source scanners of today. These developments have had obvious consequences on CT study techniques, which have become increasingly refined and focused on the clinical query of the examination. In fact, the most frequent causes of diagnostic error are no longer due to limitations of the scanners but rather to inappropriate patient preparation and an incorrect choice of acquisition protocol.

Moreover, recent-generation MDCT scanners offer new diagnostic opportunities to the radiologist, who nowadays is frequently called on to confer with clinicians in fields from which he or she was previously completely excluded (e.g., the heart, the peripheral circulation, and the colon). This is a new and stimulating challenge for radiologists, which at the same time requires further cultural progress to facilitate such multi-specialty collaborations. Indeed, while on the one hand multi-slice scanners have opened up new fields of study, on the other they have also given rise to particular problems, which require specific training, of both a technical and a clinical nature.

The aim of this volume is to provide the general concepts for optimizing an MDCT study by taking into consideration the differences between the various anatomical regions and the diagnostic potential of MDCT for each one. This is achieved also through the presentation of numerous cases, whose intention is neither a complete description of the disease nor a comprehensive explanation of the imaging characteristics of the different lesions, but to demonstrate the optimal imaging

protocol in different clinical settings. Each case is, in fact, accompanied by a detailed presentation of the factors determining the overall quality of the examination (patient preparation, contrast material injection modality and parameters, scan delay), which the radiologist must bear in mind. A meticulous description of the acquisition techniques (collimation, effective slice thickness, reconstruction interval) does not accompany the cases, as these features have become nearly standardized on the most recently marketed MDCT systems and the most important general concepts are nonetheless given in the Introduction. In the choice of study protocol, which at all times is correlated with the clinical indications of the examination, consideration is always given to radiation dose, particularly in young patients, with acquisitions being suggested only in the enhancement phases, after the injection of contrast material, as they are necessary for diagnostic purposes.

We truly hope that this booklet is of help in clinical practice, especially for general radiologists and specialists in training but also for all practitioners facing the challenges posed by the new MDCT technology.

Rome, October 2011                                          Andrea Laghi

# Contents

## Technical Basis

## Clinical Cases

# Contributors

DAVIDE BELLINI
Department of Radiological
Sciences, Oncology and Pathology
"Sapienza" – University of Rome
Polo Pontino, Latina, Italy

DAMIANO CARUSO
Department of Radiological
Sciences, Oncology and Pathology
"Sapienza" – University of Rome
Polo Pontino, Latina, Italy

VALENTINA CIPRIANI
Neuroradiology
NESMOS Department
Faculty of Medicine and Psychology
"Sapienza" University of Rome
Rome, Italy

STEFANIA DANIELE
Department of Diagnostic Imaging
A. Cardarelli Hospital
Naples, Italy

CARLO NICOLA DE CECCO
Department of Radiological
Sciences, Oncology and Pathology
"Sapienza" – University of Rome
Polo Pontino, Latina, Italy

LORENZO FIGÀ TALAMANCA
Neuroradiology
NESMOS Department
Faculty of Medicine and Psychology
"Sapienza" University of Rome
Rome, Italy

ANDREA FIORELLI
Chest Imaging Team
Department of Radiological Sciences
Oncology and Pathology
"Sapienza" University of Rome
Rome, Italy

NICOLA GAGLIARDI
Department of Diagnostic Imaging
A. Cardarelli Hospital
Naples, Italy

PAOLA LUCCHESI
Department of Radiological
Sciences, Oncology and Pathology
"Sapienza" – University of Rome
Polo Pontino, Latina, Italy

MARCO MARIA MACERONI
Department of Radiological
Sciences, Oncology and Pathology
"Sapienza" – University of Rome
Polo Pontino, Latina, Italy

STEFANELLA MEROLA
Department of Diagnostic Imaging
A. Cardarelli Hospital
Naples, Italy

SILVANA NICOTRA
Department of Diagnostic Imaging
A. Cardarelli Hospital
Naples, Italy

MARCELLO OSIMANI
Department of Radiological
Sciences, Oncology and Pathology
"Sapienza" – University of Rome
Polo Pontino, Latina, Italy

PASQUALE PAOLANTONIO
Department of Radiology
San Giovanni Addolorata Hospital
Rome, Italy

ANTONIO PINTO
Department of Diagnostic Imaging
A. Cardarelli Hospital
Naples, Italy

GIANLUCA PONTICIELLO
Department of Diagnostic Imaging
A. Cardarelli Hospital
Naples, Italy

SILVIA PUGLIESE
Neuroradiology
NESMOS Department
Faculty of Medicine and Psychology
"Sapienza" University of Rome
Rome, Italy

STEFANIA ROMANO
Department of Diagnostic Imaging
A. Cardarelli Hospital
Naples, Italy

GIUSEPPE RUGGIERO
Department of Diagnostic Imaging
A. Cardarelli Hospital
Naples, Italy

GIOVANNA RUSSO
Department of Diagnostic Imaging
A. Cardarelli Hospital
Naples, Italy

MARIANO SCAGLIONE
Department of Diagnostic Imaging
Pineta Grande Hospital
Castel Volturno, Caserta, Italy

GIACOMO SICA
Department of Diagnostic Imaging
Pineta Grande Hospital
Castel Volturno, Caserta, Italy

AMELIA SPARANO
Department of Diagnostic Imaging
A. Cardarelli Hospital
Naples, Italy

CIRO STAVOLO
Department of Diagnostic Imaging
A. Cardarelli Hospital
Naples, Italy

MICHELA TANGA
Department of Diagnostic Imaging
Pineta Grande Hospital
Castel Volturno, Caserta, Italy

FABRIZIO VECCHIETTI
Department of Radiological
Sciences, Oncology and Pathology
"Sapienza" – University of Rome
Polo Pontino, Latina, Italy

DANIELA VECCHIONE
Department of Diagnostic Imaging
A. Cardarelli Hospital
Naples, Italy

# Technical Basis

# 1 Introduction

Multidetector-row computed tomography (MDCT) has become the technique of choice for the study of many anatomical districts in different clinical settings, as it provides a fast, reliable, and accurate simultaneous evaluation of different organs, including parenchyma, hollow viscera, vessels, and bony structures.

Exploiting the enormous potential of this imaging modality requires thorough knowledge of the technical characteristics and performances of the different scanners currently in clinical use as well as the optimal study technique. Indeed, inappropriate patient preparation and an incorrect choice of the acquisition protocol, rather than scanner limitations, are among the most frequent causes of diagnostic error. This is particularly true with respect to protocols for contrast medium injection, which should be adapted to the contrast agent used, the acquisition protocol, and, more importantly, the patient's characteristics.

The potential risk derived from an overuse of MDCT scanners is related to dose exposure. Again, knowledge of the different systems enabling dose reduction, developed by the MDCT vendors and including software that carries out iterative reconstructions, is essential. Moreover, the radiologist must pay particular attention to the optimization of acquisition parameters as this will provide the best image quality with the lowest dose exposure.

The first part of this booklet consists of a brief overview of the different technological features of modern MDCT scanners, together with a detailed explanation of optimal contrast enhancement for both arterial and parenchymal studies. Considerable attention is then given to more sophisticated examinations requiring greater care by the radiologist in choosing the imaging protocol, whether CT-angiography, cardiac-CT, or CT-colonography.

In the second part, the application of the various imaging protocols is illustrated through a large number of clinical cases covering the different diagnostic possibilities of MDCT, including emergency radiology and neuro-imaging.

# 2 The Technology

## 2.1 Scanner Characteristics

### 2.1.1 Anatomical Coverage

Multidetector computed tomography (MDCT) expanded the volume coverage per gantry rotation and revolutionized the imaging of many body regions. The most dramatic advances in MDCT technology profited from the increase in the number of detector rows. In general, the wider the detector, the larger the anatomical coverage. The dimension of the detector can be calculated by multiplying the width of a single detector's element by the number of elements. Currently, the widest anatomical coverage is 16 cm and it is obtained using a 320-slice detector with 0.5-mm slice thicknesses ($320 \times 0.5$ mm = 16 cm).

The main advantage of wider volume coverage is faster MDCT acquisition, which is extremely important to decrease motion artifacts. A second advantage is the capability to evaluate whole-organ perfusion (e.g., cardiac stress imaging, whole liver and brain acquisition) without table movement, thus reducing related artifacts. The possibility to acquire large body segments also enables fluoroscopic examinations of the upper gastrointestinal tract and visualization of joint instability with dynamic imaging.

### 2.1.2 Temporal Resolution

Temporal resolution refers to the time needed to acquire a complete data set for image reconstruction. Superior temporal resolution improves the ability to freeze moving structures such as the heart. The temporal resolution of a single X-ray MDCT tube and detector system is one half of the gantry rotation time, because image reconstruction requires approximately 180°

plus the fan angle. The rapid evolution of multidetector technology has improved gantry rotation speeds, reducing temporal resolution. When the MDCT standard reached 64 slices per gantry rotation, the gantry rotation time was 360 ms but it is now as low as 270 ms.

Temporal resolution also can be improved by the introduction of a second X-ray MDCT source with an independent detector system. Dual-source MDCT features two X-ray MDCT sources and detector systems separated from one another by 90°. Consequently, when both MDCT tubes are used, the temporal resolution is halved, from 165 ms to 83 ms, because only a quarter gantry rotation is needed for reconstruction. This implies, for example, the possibility to perform cardiac studies in patients with a rapid heart rate, without the need to administer beta-blockers but still obtaining high-quality images.

### 2.1.3    Spatial Resolution

The spatial resolution of a MDCT system refers to its ability to separate two structures and is determined by measuring the ability of the system to separate line pairs. Voxel size has become the surrogate parameter for spatial resolution; it is determined by the field of view (FOV), image matrix, detector efficiency, number of projections (sampling frequency), and section thickness. Even before the advent of 64-row MD-MDCT, most MDCT image reconstruction algorithms included isotropic voxels, which means that the $x$, $y$, and $z$ dimensions are cubic with equal lengths along each side. Isotropic voxels enhance image post-processing, achieving excellent image quality in any plane and the generation of excellent volumetric reconstructions. High spatial resolution is critical for the analysis of small structures such as the coronary arteries or implanted stents. Currently, a 0.35-mm spatial resolution is achievable with the latest-generation MDCT scanners.

The signal to noise ratio (SNR) is another important parameter intimately related to spatial resolution. SNR is defined as the amount of signal, or information, that can be used for interpretation divided by the image noise. There is no information in noise; it is akin to an imperfect canvas on which the image data, or signal, is painted. As the MDCT slice thickness decreases, so does the amount of tissue per slice and hence the signal. However, a significantly higher SNR data set, i.e., less noisy images, can be obtained when images are reconstructed at double the slice thickness, for example 0.8 mm instead of 0.4 mm.

### 2.1.4 Contrast Resolution

Recent advancements in the composition of detector materials have improved MDCT contrast resolution, which is the ability to distinguish between differences in intensity within an image. Contrast resolution in MDCT can be changed with the application of different filters. Less filtering makes the beam softer and yields a higher-contrast image but it is also associated with higher radiation exposure because soft radiation is more readily absorbed by biologic tissue. Conversely, more filtering yields lower-contrast images while reducing radiation exposure. The effect may be negligible on unenhanced MDCT scans but is clearly apparent on scans obtained after the administration of an iodine-based contrast agent, mainly because of the differences in the radiation absorption of different energies by iodine.

## 2.2 Systems for Reducing Dose Exposure

### 2.2.1 Limiting z-Axis Length

In everyday practice, scan coverage is set up visually on the scout-topogram. Since the total radiation dose delivered is directly proportional to $z$-axis coverage, the accurate adjustment of scan length is important for optimization of the dose-length product (DLP).

### 2.2.2 Tube-Amperage and Tube-Voltage Adjustments

Adjustment of the tube current and/or the voltage applied to the X-ray tube reduces the number and/or average energy of the photons generated, respectively. Furthermore, both directly affect image SNR. The radiation dose is approximately proportional to the number of mAs and is adjustable, thereby allowing amperage values to be customized according to body mass. Failure to adjust this parameter downwards for thin patients will result in unnecessary radiation. It is important to reduce mAs as much as possible while ensuring a high enough SNR to obtain diagnostic-quality images.

Another approach to reduce the dose delivered to the patient is to reduce the tube voltage. Tube kVp affects both peak photon energy

and image contrast. Tube voltage has a more dramatic effect on radiation dose, which is exponentially proportional to kVp. However, the use of photons with a lower average energy leads to an increase in the attenuation values of elements of higher atomic number and greater absorption coefficients because of the increased interaction resulting from the photoelectric effect; the greater disadvantage of this approach is a reduction in diagnostic accuracy caused by increased beam-hardening artifacts in the calcified plaque as well as a reduction of the SNR, even if the latter is compensated by a slight increment in tube current.

### 2.2.3    Automatic Modulation of Tube Current

Another option is based on anatomy-adapted tube-current modulation. Thus, according to the individual characteristics of the patient, the X-ray tube current can be adjusted using attenuation values quantified by the patient's initial scout image. The pixel noise in a MDCT image is largely attributable to the projections in which the greatest attenuation occurs; the intensity of the radiation can be reduced in projections with less attenuation. Thus, the tube current will be reduced in thin patients, or rather in those with reduced anteroposterior thickness (*xy* plane), and greater in obese patients, in order to obtain optimal image quality.

### 2.2.4    Iterative Reconstruction

Iterative reconstruction techniques have demonstrated the potential to improve image quality and to reduce the radiation dose in MDCT relative to the currently used filtered back-projection techniques. The most noticeable benefit of iterative reconstruction is that it is able to incorporate into the reconstruction process a physical model of the MDCT system that can accurately characterize the data acquisition process, including noise, beam hardening, and scatter. This ability dramatically improves image quality, especially in the case of low-dose MDCT scans, in which the propagation of non-ideal data during image reconstruction becomes more significant than in routine MDCT scanning. Iterative reconstruction is also superior to filtered back-projection in handling insufficient data. Recent advances in iterative

reconstruction allow a significant reduction in the number of required projection views while still producing acceptable image quality. Iterative reconstruction techniques thus have the potential to substantially reduce the radiation dose in MDCT. With computational power growing quickly, the clinical implementation of iterative reconstruction algorithms is within delivery.

## 2.3 Multi-Energy

Multi-energy computed tomography (MECT), i.e., the acquisition of data sets at different photon spectra in a single MDCT acquisition, can provide information on the material composition of the tissues based on differences in photon absorption. This enables materials of similar density but different elemental composition to be distinguished from one another, especially materials with large atomic numbers such as iodine.

In particular, the use of dual-energy post-processing software, based on three-material decomposition principles (soft tissue, fat, and iodine), allows the contrast agent to be distinguished and isolated from other materials. The possibility to accurately recognize iodine distribution enables the generation of a virtual unenhanced or virtual angiographic data set. The generation of virtual unenhanced images may obviate the routine need for a pre-contrast scan, thus decreasing patient radiation exposure especially in multiphasic acquisitions or repetitive MDCT examinations. Indeed, as reported in the literature, this means a dose reduction of about 30% .

The ability to accurately discriminate parenchymal iodine distribution using a color-coded image implies improved quantification of both subtle tumor vascularization and the response to anti-angiogenic therapy.

Liver MECT may permit the rapid detection and quantification of hepatic iron overload in thalassemia patients.

Finally, the advantage of different energy acquisitions has been investigated, with the results showing that hypervascular lesions are better visualized and show increased conspicuity at 80 Kv than on a standard 120-Kv scan.

# 3 Contrast-Medium Administration

The optimization of any contrast medium injection protocol should be aimed at achieving the best arterial and/or parenchymal enhancement according to the clinical indication. Arterial and parenchymal enhancements influence the accuracy of the MDCT examination and are generally affected by different kinetics. Arterial enhancement is determined mainly by the iodine dose delivered per unit of time and parenchymal enhancement by the total iodine dose. However, both are significantly related to patient-specific factors, such as body size, cardiac performance, gender, and age. Moreover, the goal of any MDCT examination is to achieve the best image quality using the lowest volume of contrast medium (CM), because most adverse CM reactions are a consequence of the total iodine dose administered to the patient.

## 3.1 Arterial Enhancement

### 3.1.1 Body Imaging

Two important variables determine the time-course of arterial enhancement: the iodine delivery rate (IDR) and the injection duration (ID). Arterial enhancement is also influenced by patient-specific variables such as cardiovascular status (i.e., cardiac output) and individual body-size indexes (i.e., distribution volume). IDR is expressed in gI/mL, is operator-controlled, and determined by modifying the injection flow rate (FR) and the iodine concentration of a given CM. The required value can be obtained with virtually any concentration of CM according to the formula:

$$IDR = ([I]/1000) \times FR$$

where [I] is the CM concentration (expressed in mgI/mL). If the acquisition of an arterial phase for body imaging is required, the IDR should not be < 1.2 gI/s; optimally, the value should be around 1.6 gI/s, since this provides higher conspicuity of hypervascular lesions. As an

example, in order to achieve an IDR of 1.6 gI/s, CM must be injected at a concentration of 320 mgI/mL, at a FR of 5.0 mL/s, and a CM concentration of 400 mgI/mL with a flow rate of 4.0 mL/s.

Patient-specific factors contribute to the magnitude of vascular and parenchymal enhancement; the most important are patient body size and cardiac output. The latter is the most relevant factor affecting the timing of contrast enhancement and cardiovascular circulation. A reduction of cardiac output results in delayed CM arrival, higher peak arterial enhancement, and prolonged parenchymal enhancement. The slower the CM circulates, the slower its clearance and the higher its concentration. The magnitude of the aortic peak and of parenchymal enhancement increases substantially in patients with reduced cardiac output, while the magnitude of hepatic enhancement peak increases only slightly. A 60% reduction in cardiac output increases the magnitude of aortic peak enhancement by about 30% but that of hepatic enhancement by only 2%. The factors with the greatest effects on cardiac output are sex and age. It has been demonstrated that the CM bolus arrives slightly earlier in female than in male patients because of a smaller (around 5–10%) distribution volume in the former. The demonstration of a lower cardiac output proportional to age suggests that a 10% reduction in iodine dose and injection rate in elderly patients will yield an enhancement of the same magnitude.

IDR should also be modified according to the patient's body size. As previous studies demonstrated, IDR should be determined according to the patient's lean body weight (LBW) as, among other body size indexes (eg. total body weight: TBW; blood volume: BV), it provides the best hepatic arterial enhancement with reduced patient-to-patient variability.

Flow rates for CM with different iodine concentrations and TBWs are suggested in Table 3.1.

**Table 3.1** Suggestions for injection flow rates of contrast medium, with different iodine concentrations, according to total body weight (TBW)

| Iodine concentration (mgI/mL) | BW IDR (gI/s) | < 55 1.2 | 56-65 1.4 | 66-85 1.6 | 86-95 1.8 | > 95 2.0 |
|---|---|---|---|---|---|---|
| 300 | | 4 | 4.7 | 5.3 | 6 | 6.7 |
| 320 | | 3.7 | 4.4 | 5 | 5.6 | 6.2 |
| 350 | FR (mL/s) | 3.4 | 4 | 4.6 | 5.1 | 5.7 |
| 370 | | 3.2 | 3.8 | 4.3 | 4.8 | 5.4 |
| 400 | | 3 | 3.5 | 4 | 4.5 | 5 |

*IDR*, Iodine delivery rate; *FR*, flow rate

### 3.1.2    CT Angiography

The delay between the intravenous injection of CM and its appearance within the arterial compartment is defined as the CM transit time ($t_{CMT}$). This parameter, as discussed above, is markedly variable in different patients and is linked to the efficiency of the cardiovascular system. The bolus-tracking test and automatic monitoring techniques are used to establish the $t_{CMT}$, which can then be set to determine the scan delay; this is defined as the time required for the CM to arrive in the vascular bed and to produce an enhancement of around 100 HU.

For angiographic studies, once the injection FR is chosen, the contrast volume should be set on the injector screen. If the acquisition of an arterial phase is required, the CM volume depends on the injection duration (ID) according to the formula:

$$\text{Volume} = \text{FR} \times \text{ID}$$

For example, if the FR is 4.0 mL/s (for CM at 400 mgI/mL) and the ID is 13 s, the total volume needed is 52 mL.

Injection duration influences vascular enhancement only in longer acquisitions (> 10 s): the longer the ID, the greater the arterial enhancement. This is due to the cumulative effects of bolus recirculation, which contributes to a 10–20% increase in peak arterial enhancement and in the magnitude of intravascular enhancement. For abdominal acquisition times (> 5 s for liver imaging) this parameter is not as important. Injection duration should be longer than the scan time and scan acquisition should be delayed until the maximum intravascular attenuation is achieved. As a ballpark rule for abdominal angiographic acquisitions, the scan delay should be 8 s after a 100-HU threshold in the aorta is reached. Injection duration is thus calculated as follows: for a 5-s acquisition, the injection duration should be 5 s + 8 s = 13 s. The scan delay s modified according to the particular clinical needs and especially according to the organ to be studied. This is discussed elsewhere in this volume.

#### 3.1.2.1  Fast CT Angiography (< 10 s)
In the case of a short scan time, as achieved by the new-generation MDCT scanners, and high FR protocols, the transit time cannot be used in a mathematical fashion. Instead, adding 8 s to the $t_{CMT}$ is advisable. This practical rule is applied on the basis of the technical times required

for repositioning the patient tray (it is nonetheless advisable to avoid setting bolus tracking too far from the beginning of the scan). In addition, visualization of the images obtained with bolus-tracking techniques are not produced in real-time but rather as reconstruction times, which vary according to the MDCT manufacturer (around 3 s). There are also delay times associated with the change of collimation. This empirical rule enables the exact scan time to be determined, but it is also advisable to lengthen the injection duration by around 8 s, bearing in mind the delay, which needs to be adapted to the iodine concentration of the specific CM (refer to the flow-volume tables in the product information). This widens the window available for performing the scan and enables the desired iodine administration rate to be achieved. By way of example, if we wish to perform a scan of the abdominal aorta and the scan time is around 8 s, we need to position the region of interest (ROI) so as to monitor the bolus at the level of the abdominal aorta and then set a diagnostic delay of 8 s from the moment when 100 HU is reached. If the CM concentration is 350 mgI, then around 69 mL of CM should be injected at an injection FR of 4.3 mL/s for an injection duration of 16 s. With a high-concentration CM (400 mgI), the volume becomes 61 mL and the injection FR 3.8 mL/s.

### 3.1.2.2   Slow CT Angiography (> 10 s)

We have already analyzed the strategies to be implemented in order to correctly evaluate the arterial vessels when the scan times are very short. For long scan times, other factors need to be taken into consideration. The mean transit time (between the vein of the arm and the abdominal aorta) is calculated with automatic techniques, but there is evidence in the literature that even the mean transit time between the abdominal aorta and the popliteal arteries is highly variable (between 4 and 24 s). This value corresponds to a bolus FR of 29–177 mm/s. The table speed should be set at the lower limit of this range to avoid the phenomena of the bolus being overtaken by the scan. A table speed of around 30 mm/s translates into a scan time of around 40 s when we want to cover large volumes, such as in studies that include the abdominal aorta and the arterial vessels of the lower limbs.

Modern 64-slice systems allow for table speeds of around 80 mm/s in the basic configuration. The speed can be lowered by reducing the pitch; if this is not enough, the gantry rotation speed can be increased. A widely used strategy therefore consists of setting the table speed to

around 30 mm/s, or simply setting the scan parameters to obtain a scan that lasts for around 40 s.

For studies with these scan durations, the CM administration strategy should involve an injection duration of around 35 s, considering that the time required for the enhancement of the abdominal aorta is excluded from the automatic techniques of bolus tracking and that the minimum scan delay is around 3 s. Accordingly, the use of a constant injection FR (5.7 mL/s for iodinated CM with a concentration of around 350 mgI/mL) requires the administration of a much higher quantity of iodine (in our case $35 \times 5.7 = 199.5$ mL of CM at a concentration of 350 mgI/mL). Correct enhancement of the entire vascular tree of the aorta and the lower limbs can be obtained without the need to administer > 120 mL of CM at a concentration of 350 mgI/mL, by using lower volumes of high-concentration CM with a strategy of dual-phase injection at different FRs. This strategy requires the use of an initial bolus of CM at a high FR (around 40 mL at 5 mL/s) and a maintenance bolus (around 80 mL) at a variable FR: for normal-weight patients (60–90 kg) the FR should be set at 3 mL/s, whereas for heavier patients the quantity of CM should be increased and the FR adapted to obtain a fixed injection duration of around 35 s.

## 3.2    Parenchymal Enhancement

Parenchymal enhancement is governed by the relationship between the total iodine dose (mgI) and the total volume of distribution (intravascular and interstitial spaces).

Historical studies have demonstrated that it is necessary to deliver an adequate amount of iodine, in the range of 500–600 mgI per kg TBW, to achieve optimal parenchymal enhancement of the liver (around 50–60 HU). To calculate the required volume of CM, with a concentration of 300 mgI/mL, it is necessary to deliver 2 mL/kg TBW. This value (2 mL/kg) should be adapted to the iodine concentration, thus resulting in 1.7 mL/kg for 350 mgI/mL and 1.5 mL/kg for 400 mgI/mL.

However, it has been demonstrated that TBW is not the optimal body-size index for adjusting iodine dose because blood volume and liver weight are not directly proportional to TBW. For example, obese patients may have abundant body fat, which has a small vascular and interstitial space and thus contributes little to dispersing or diluting the CM in the blood. In these patients, adjusting the iodine dose so that it

is proportional to TBW may lead to an overestimation of the amount of CM needed. Some experiences reported that calculating the CM dose on the basis of LBW leads to increased patient-to-patient uniformity of hepatic parenchymal and vascular enhancement. LBW can be measured using an electronic body-fat monitor, which estimates the body-fat percentage (BFP). Thus, LBW can be calculated according to the formula:

$$LBW = TBW(1\text{-}BFP)$$

Once the patient's LBW is evaluated, the amount of iodine required to achieve adequate enhancement of the liver parenchyma is calculated as:

$$VI = LBW(\Delta HU/77.9)$$

where I is the amount of iodine (g) and $\Delta HU$ represents the desired maximum hepatic enhancement (MHE), which should be around 50–60 HU. The amount of iodine needed, divided by the CM concentration (in g), results in the exact CM volume in mL.

## 3.3    Timing

Determination of the optimal temporal window for body scanning is mandatory to correctly identify and characterize focal or diffuse parenchymal disease.

The CM transit time ($t_{CMT}$), as referred to above, is the time between the start of intravenous administration of a CM bolus and its arrival in the vascular region of interest. Thus, especially in patients with cardiovascular disease, scan delay should be based on the patient's $t_{CMT}$. The $t_{CMT}$ can be determined using a test bolus injection or by automated bolus-triggering techniques.

The use of a fixed delay time is no longer recommended, since it cannot guarantee optimal separation between dynamic phases due to inherent variability among individuals, such as patient size and cardiovascular status. Instead, a more rational use of MDCT can be accomplished using either a test bolus or bolus-tracking software.

The test-bolus technique is based on the injection, at the same FR as calculated for the diagnostic injection, of a small CM bolus (15–20 mL) while acquiring multiple low-dose sequential scans at the starting level of the diagnostic scan. The time-enhancement curve obtained is a reliable method to determine the $t_{CMT}$ from the intravenous injection site to the arterial territory of interest. The $t_{CMT}$ equals the time to peak

enhancement interval and is measured in a ROI placed within a reference vessel. Furthermore, time-attenuation curves obtained from one or more ROIs can be used for individual bolus-shaping techniques using set mathematical models. A test bolus is particularly useful in determining the $t_{CMT}$ if unusual CM injection sites must be used (e.g., lower extremities) or for very short (< 3 s) scan times when a bolus-triggering software is not suitable.

Many MDCT scanners have automatic bolus-triggering software built into their system. This allows the real-time detection of a circular ROI placed within the target vessel on a non-enhanced image. After 5–10 s from the start of the CM injection, a series of low-dose sequential scans are acquired every 1–3 s whereas the attenuation within the ROI is monitored or inspected visually. The $t_{CMT}$ equals the time at which a predefined enhancement threshold is reached (e.g., 100 HU), plus a diagnostic delay determined according to the specific organ to be studied. The diagnostic delay is the time between reaching a predefined enhancement threshold and the start of the MDCT acquisition; it depends on the scanner model and on the longitudinal distance between the monitoring series and the starting position of the actual MDCT series. Bolus triggering is a very robust and practical technique for routine use and has the advantage of not requiring an additional test-bolus injection.

## 3.4    Saline Flush

During fast-acquisition scans, a substantial volume of the injected CM remains in the dead space of the right heart, peripheral veins, and injection tubing. Flushing the venous system with saline immediately after CM administration pushes the CM column into the systemic circulation. Thus, a saline flush is helpful in optimizing CM volumes as it allows a reduction of the iodine dose without significant influence on the level of contrast enhancement. The reduction of CM volume is reportedly between 12 and 50 mL, with a positive effect on the risk of CM-induced nephropathy.

The most convenient technique for routine saline flush after CM injection uses the newly available programmable double-piston power injectors (one syringe for CM, one for saline).

In the field of body MDCT, there is little evidence that a saline flush influences vessel and parenchymal enhancement. A positive effect of saline flushing on aortic, portal, and hepatic enhancement has been

reported, along with a significant increase in the aortic peak but no evidence of improved hepatic enhancement. However, a saline flush does not improve the magnitude of liver parenchyma enhancement in clinical imaging, whereas in time-density analyses it significantly improves the time to peak of liver, portal vein, and aortic enhancement. Furthermore, the CM left in the dead space contributes to vascular enhancement by a slow and late flowing. The clearing of this CM volume is reflected in a more rapid decline of intravascular attenuation after the peak such that scanning during this period may result in insufficient contrast enhancement.

# 4 Special Examinations

## 4.1 Thorax

### 4.1.1 Image Analysis

**Multiplanar Reconstruction**

With MPR algorithms, images can be easily obtained and oriented in all planes of vision while modified by the operator in real time. The raw data are used for the reconstruction such that there is no loss of image quality. The MPR technique can be applied to increase the diagnostic sensitivity in the evaluation of diffuse lung diseases, allowing improved determination of their location and extent. The radiologist profits from the ability to select the orientation plane that best reveals a key aspect of the disease, thus raising the diagnostic power of the method.

**Maximum Intensity Projection**

In MIP, higher voxel attenuation values are projected on a two-dimensional image. This technique is undoubtedly of fundamental importance in assessing the distribution of pulmonary nodules. In the lung, vascular structures are brighter than the surrounding air-filled acini. On thick reconstructions, this difference allows visualization of the branching vessel and thus peri-vascular nodule assessment.

### 4.1.2 Detection and Characterization of Lung Nodules

**Computer-aided Detection**

Computer-aided image analysis methods can aid the radiologist in detecting lung nodules. These computer algorithms have been enabled by

high-resolution thin-section MDCT data. CAD techniques have been shown to increase the detection of small pulmonary nodules while maintaining time efficiency for diagnosis.

All CAD systems rely on a discrimination mechanism based on densitometry gray-level thresholding. First, a gray-level threshold is determined for segmentation of the thoracic structures from the background. A binary image is thus constructed in which pixels with a gray level greater than the selected threshold are turned "on" and those with a lower level are turned "off." The thoracic contour is then delineated along the outermost border of the "on" region. Second, regions of interest (ROI) with threshold values between 50 and 225 HU are selected. In the segmented lung volumes, pixels ranging in value from 50 to 225 HU are automatically "turned off" and excluded from the analysis such that all structures that are nodule candidates are visualized. Volumetric processing and the selection of nodule CAD devices for nodule identification have been primarily investigated in the context of a second reader, in which CAD identifications are viewed subsequent to an initial review by the radiologist. In this setting, a 50–76% increase in reader sensitivity for the detection of pulmonary nodules has been demonstrated. More recently, CAD has been applied as a valid tool in the follow-up of pulmonary nodules or in pulmonary metastases, with the advantage that it reduces interobserver measurement variability and provides a more precise evaluation in terms of volume, rather than two-dimensional axial images.

### 4.1.3    Nodule Enhancement Characteristics on MDCT

While an option when 18 Fluorodeoxyglucose Positron Emission Tomography (18 FDG PET) imaging is not available, MDCT nodule enhancement is a method that is otherwise not frequently used. This technique has several technical considerations. It is limited to the characterization of nodules > 7 mm and < 30 mm with no obvious calcifications, cavitations, or ground-glass attenuation.

Multicenter trial experience has shown that repeated scans should be performed before and 1, 2, 3, and 4 min after intravenous contrast administration. The nodule's pre-contrast attenuation is subtracted from the maximal attenuation after intravenous contrast injection, as measured with a ROI placed over a majority of the nodule on its largest cross-section as determined in thin-section MDCT images. An enhancement ≤ 15 HU suggests a benign etiology. To avoid false-negatives, a 10-HU threshold for

enhancement and follow-up imaging with MDCT are recommended. Based on a 15-HU threshold, a sensitivity of 98% and a specificity of 58% have been reported. Given the lower specificity of this technique, an increase > 15 HU may indicate either malignant or inflammatory disease.

Lung nodules can also be characterized with MDCT perfusion, when available. A sensitivity for malignancy of 99%, with a specificity of 54%, positive predictive value of 71%, and negative predictive value of 97%, has been achieved using 20-s MDCT perfusion with a threshold > 30 HU. The analysis of contrast-enhanced data for nodule perfusion can potentially benefit from image-processing techniques, including volumetric enhancement analysis and semi-quantitative enhancement maps. Only a few investigations have addressed compartmental modeling with MDCT. In this approach, enhancement data are analyzed for quantitative measures such as blood volume and volume-transfer constant ($K_{trans}$) parametric maps. These parameters have been investigated primarily in lung cancer. $K_{trans}$ describes the portion of blood flow that enters the extravascular space. Despite the potential of compartmental modeling, a trade-off exists between the number of imaging time points needed and the radiation exposure to the patient. Low-dose techniques with low kVp, reduced mAs, and limited coverage imaging have been used to minimize radiation exposure.

## 4.2   Heart

### 4.2.1   Patient Preparation

In order to obtain good image quality, the patient's heart rate (HR) should be < 65 bpm. This can be achieved by the use of chronotropic agents, such as beta-blockers. These drugs are administered according to their pharmacodynamics, either orally (e.g., metoprolol tartrate 50–200 mg 45–60 min prior to the examination) or intravenously (metoprolol tartrate in bolus 5 mg at 1 mg/min, 15 mg maximum, or esmolol 0.5 mg/kg in 1 min, followed by continuous infusion at 0.05 mg/kg/min). The use of these agents is limited by the following contraindications: congested heart failure and cardiogenic shock, grade II and grade III sinoatrial and atrioventricular block diseases, COPD, marked hypotension (systolic blood pressure < 100 mmHg), and bradycardia (HR < 50 bpm).

If the examination is performed to evaluate the myocardium, the pericardium, the anatomy of the large vessels, or myocardial function, patients

with higher HRs or atrial fibrillation (with low ventricular response) can be pre-treated with chronotropic agents and then more accurately studied.

The administration of nitroglycerin derivatives (e.g., isosorbide dinitrate, 5 mg sublingually) immediately prior to the examination produces a vasodilatation of the coronary arteries and improves the evaluation of stenoses, particularly in small-diameter segments. The administration of these agents is contraindicated in patients with severe aortic stenosis, severe hypotension, and those taking sildenafil citrate.

When the ideal HR has been reached, the patient can be positioned on the examination bed and the ECG electrodes connected. To obtain a correct ECG trace, three electrodes should be placed on the patient's chest: at the right shoulder, the left shoulder, and the left hypochondrium. To avoid irregularities in the ECG trace, direct contact of the electrodes with the deltoid, pectoral, and intercostal muscles should be avoided. At this stage, the regularity of the ECG trace needs to be checked and a test breath-hold performed, since the latter can markedly reduce the HR or cause the appearance of premature beats.

### 4.2.2   Calcium Score

Quantification of coronary artery calcium may provide a great deal of information in terms of risk stratification and interpretation of the angiographic examination. The examination is acquired under baseline conditions with ECG synchronization and spiral (retrospective gating) or axial technique (prospective triggering). The axial acquisition with prospective triggering is generally preferred due to the lower radiation dose delivered to the patient (around 1.5 mSv). This type of examination can be used to obtain three types of scores; the Agaston score, which was standardized and indexed with electron-beam CT (EBCT) and has been transferred to MDCT technology, the mass score, and the volume score. Numerous studies in the literature have demonstrated a correlation between the coronary calcium score, the presence of calcified stenoses, and the extension of atheromatous disease. The threshold score suggests that coronary artery disease corresponds to an Agatston score ≥ 400. This stratification should prompt not only a suspicion of hemodynamically significant stenoses, but also of the high probability that the patient will suffer an acute coronary syndrome.

Given the difficulty with which CT coronary angiography evaluates

plaques with large concentric calcifications, this technique allows the a priori selection of patients in whom a diagnostic examination cannot be obtained (calcifications of the left main coronary artery or a proximal segment), allowing them to be sent directly to conventional coronary angiography.

### 4.2.3    Prospective Triggering

Acquisition with prospective triggering involves the delivery of X-rays, and therefore image acquisition, during a brief pre-established period of the cardiac cycle based on the patient's HR. The procedure reduces the time the patient is being radiated and therefore allows a drastic reduction of the delivered dose. Some authors have used this type of acquisition with kV values weighted according to the BMI of the patient and have thus greatly reduced the dose absorbed by the patient (to as low as 1.5 mSv).

This approach is highly sensitive to variations in HR since it involves calculation of the preselected phase of the R-R interval during one heart beat and image acquisition in the subsequent beat. Clearly, the presence of an early beat will result in image acquisition during the wrong phase, with image quality suffering significantly. Another factor influencing image quality is the HR itself. Thus, to perform an examination with prospective triggering, the patient's HR needs to be lowered and stabilized as much as possible, and kept below 60 bpm.

It should be noted that the data necessary to functionally evaluate the cardiac chambers and valves cannot be obtained with prospective triggering.

### 4.2.4    Retrospective Gating

In the acquisition with retrospective gating, X-rays are delivered during the entire cardiac cycle. To obtain images without motion artifacts, the datasets need to be retrospectively reconstructed. The phase with the least residual motion is generally the end-diastolic phase (65–75% of the R-R interval) for HRs < 65 bpm. It is known that with increasing HR the duration of diastole progressively decreases, whereas the duration of systole is about the same. This means that with elevated HRs (> 70 bpm), high-quality images can even be obtained in the end-systolic phase (25–45% of the R-R interval). However, the examination should not be

performed in patients with HR > 70 bpm if a scanner with a temporal resolution > 165 ms is used. Instead, these patients should be treated with negative chronotropic agents to reduce the HR to < 65 bpm.

The acquisition with retrospective gating exposes the patient to a high dose of radiation, between 12 and 20 mSv, but it does yield data covering the entire cardiac cycle, thus enabling a functional analysis of the left ventricle and the cardiac valves.

To reduce the radiation dose delivered to the patient, a technique has been developed to modulate the mA according to the phase of the cardiac cycle. This technique is known as ECG pulsing and it allows the maximum current to be delivered during the phase of the cardiac cycle used in image reconstruction (end-diastolic phase), whereas during the rest of the cardiac cycle (not used in image reconstruction) the mA can be reduced by as much as 90% according to the scanner type. In line with the clinical indications, more mAs can be delivered during the phase of the cardiac cycle that is not needed for image reconstruction so as not to lose the data required for the functional study of the ventricles and valves.

The use of ECG pulsing can reduce the dose delivered to the patient by as much as 50%, according to the type of modulation and the scanner used.

### 4.2.5    ECG Editing

The presence of premature beats (extrasystole) during acquisition results in the incorrect synchronization of the volume to be reconstructed. ECG editing software can partly compensate for this type of artifact as it allows the position of the reconstruction time window to be arbitrarily shifted within the cardiac cycle or the data regarding the ectopic beat to be completely eliminated. Consequently, the reconstruction will not include the data acquired during the irregular beat. Extrasystoles do not constitute absolute contraindications to CT coronary angiography except when they are very frequent (> 1 for every 2 normal beats).

### 4.2.6    Multisegment Reconstructions

The precise temporal resolution of multislice scanners depends on the gantry rotation speed because the data acquired during half a rotation is

enough for the reconstruction of a single tomographic image. Therefore, with a gantry rotation time of 330 ms, a temporal resolution of 165 ms can be obtained.

The temporal resolution can be increased further by using multisegment reconstruction algorithms, which enable the combination of data from two or more cardiac cycles, thus requiring less information than obtained with a 180° projection. In multisegment reconstructions, data having the same relation to the ECG trace but derived from different heartbeats are combined in a single image. The resulting temporal resolution in this case will depend on the number and size of the segments used for the creation of the same image, but it will be higher than that deriving from a single segment. The temporal resolution is therefore increased by a factor equal to the number of segments used (n) for the reconstruction:

$$(\text{temporal resolution} = [\text{rotation time}/2]/n).$$

This technique can provide optimal temporal resolution only in a restricted range of HRs, and the image obtained is sensitive to variations in HR during the acquisition. Therefore, even slight changes in the HR during the examination can lead to a non-uniform temporal resolution and thus the appearance of artifacts.

## 4.3    Urinary System

In MDCT studies of the urinary tract, there is no need for special patient preparation other than oral hydration, which is aimed at increasing diuresis. This can be achieved by the intravenous administration of about 500 mL of saline solution or by the intravenous injection of a diuretic (low-dose furosemide: 0.1 mg/kg up to a maximum of 10 mg).

## 4.4    Small Bowel

MDCT of the small bowel requires the distention of bowel loops which, in physiologic conditions, are collapsed. Collapsed bowel loops may hide some pathologic findings or mimic others. To obtain a proper loops distention the administration of enteral CM is required which are usually classified in positive or neutral according to their density. The choice between one or the other type depends on radiologist's preferences.

In the case of occlusive or sub-occlusive bowel disease the administration of enteral CM is not required because the natural loops distention can be used.

The administration of enteral CM can be either oral (enterography) or through a naso-jejunal tube (enteroclysis).

### 4.4.1    Enteral Contrast Media

Different types of enteral contrast agents are used to obtain proper distension of the small-bowel loops. They are classified according to their density as positive, or high density, and neutral, or low density, contrast agents.

Neutral contrast agents, with X-ray attenuations similar to that of water, are preferred for most clinical indications. In particular, the association with intravenous iodinate contrast results in a better depiction of wall enhancement due to the higher attenuation difference with the hypodensity of the lumen. This is particularly important for the evaluation of inflammatory bowel disease (IBD) and neoplastic diseases or when angiography-like 3D reconstructions are required. Although water is the safest and cheapest agent, it suffers the limitation of intestinal absorption, which compromises an adequate distension of the distal ileum in a large number of patients. To minimize absorption, water is usually mixed with high molecular weight compounds that do not alter water density and taste. Thus, neutral contrast agents are mainly water-based solutions of osmotic compounds such as polyethylene glycol (PEG), mannitol, sugar alcohols, or sorbitol. Recently, a neutral oral contrast agent, a low concentration barium sulfate (0.1%) containing sorbitol, was expressly developed for CT enteral studies.

Positive contrast agents, which have high X-ray attenuation, are usually a mixture of barium sulfate (1–2%) or iodinate contrast agents (2–3%). These enteral agents are preferred for all situations in which a high intraluminal density is recommended, such as the evaluation of perforations or fistulas, complications of Crohn's disease, and for the evaluation of intraluminal masses, such as polyps or tumors. Because the high intraluminal density reduces contrast resolution with enhancing structures, positive contrast agents are contraindicated when the evaluation of wall enhancement patterns is required, as in IBD. On the other hand, positive CM can be used when intravenous contrast agents do not influence the conspicuity of the pathology or in the setting of difficult intravenous access or renal failure.

### 4.4.2    Enterography

In MDCT enterography, the oral administration of an adequate amount of contrast agent is required. Usually, for an average-size adult the dose of enteral contrast agent is around 1500–2000 mL. In addition, optimal timing of the administration is fundamental. Patients are likely to find it easier to ingest the oral volume over a longer period of time. However, if ingested over too long a period, the CM may be in the colon; if an insufficient volume is ingested, suboptimal small-bowel distension will limit the CT enterography examination. Consequently, contrast agent is usually divided into three aliquots administered starting around 60 min before CT scanning.

To minimize motion artifacts, a spasmolytic agent is administered intravenously immediately before the examination, i.e., while the patient is lying on the table inside the scanner room. The two agents mainly used in clinical routine are glucagon and hyoscine N-butylbromide. Their effects, following an intravenous injection, start approximately 30 s after administration. One milligram of glucagon is enough to reach the desired effect while around 40 mg of hyoscine N-butylbromide are needed to achieve the same results. Some reports in the literature claim that glucagon has a more reliable and longer effect.

### 4.4.3    Enteroclysis

MDCT enteroclysis was developed in the early 1990s and involves the infusion, by hand or by a peristaltic pump through a naso-jejunal tube, of variable amounts of low-density (methylcellulose or water) or high-density (4–5% sodium diatrizoate, 1% barium sulfate) CM prior to the CT scan. Manual infusion is limiting whereas better distension is achieved using the peristaltic pump, even if this does not always allow optimal distension of the entire bowel loops.

The naso-jejunal tube is placed under fluoroscopic guidance in order to avoid a time-consuming procedure inside the CT scanner. It is also advisable to use a tube with an anti-reflux balloon, which will prevent duodeno-gastric reflux.

Volume and infusion rate are crucial for the success of the examination, as in conventional enteroclysis. Volume varies among individuals, ranging between 1500 and 3000 mL, while the infusion rate varies in the range of 80–150 mL/min. The use of spasmolytics to reduce ab-

dominal discomfort is controversial, since higher infusion rates (in the order of 200 mL/min) induce natural small-bowel reflexive atony without the need for any pharmaceutical.

## 4.5    Colon

Bowel preparation is a critical step since excessive residual stools and/or fluid may mimic or hide a colonic lesion. Current recommendations for bowel preparation require full bowel cleansing in association with fecal/fluid tagging. But on-going research is dedicated to develop reduced bowel preparations and ultimately a preparation-free CTC, with the aim to minimize patient discomfort and to increase compliance to colo-rectal cancer screening; in the latter cases the use of fecal/fluid tagging is mandatory.

### 4.5.1    Full Bowel Cleansing and Faecal/Fluid Tagging

Patients referred for a colonic examination are required to follow a three-day low-residue diet in order to minimize fiber residues within the colon.

To achieve full bowel preparation several options are available, depending on local expertise.

In general purgative preparations are divided into "wet" and "dry", depending on the amount of residual fluids present in the colon. A typical example of "wet" preparation is that obtained by the administration of polyethylene glycol (PEG) 4000, an isosmotic agent, safe and effective, whose main limit is the volume to be ingested by the Patients (4 liters) and the saline taste, making up to 20% of patients unable to complete the preparation. New formula, delivering only two liters of PEG in association with bisacodyl, is now available and it has been demonstrated of being more efficient than and preferred to the conventional regimen. The main limitation of PEG in CTC is the amount of residual fluids left in the colon, which may impair a full evaluation of the colonic lumen.

"Dry" preparations can be obtained by using osmotic (sodium phosphate, magnesium citrate) or stimulant (sodium picosulfate) laxatives, which result in minimal or no fluid residue. Among the different agents, sodium phosphate has been questioned having a worse safety profile. Its use should be careful with full-dose cathartic preparation using, in-

cluding congestive heart failure, renal failure, electrolyte abnormalities, ascites, or ileus.

Magnesium citrate is known to be safer and it also has a more tolerable taste than sodium phosphate. Bisacodyl, stimulating parasympathetic reflexes, is often used in conjunction with sodium phosphate or magnesium citrate to induce evacuation of stool.

Independently of bowel cleansing, it is now considered to be mandatory the use of fluid/faecal tagging. Tagging consists in the oral administration of a positive contrast agent, either barium or iodine, to mark residual fluids and stool. The rationale is to improve sensitivity (detection of submerged lesions) and specificity (allowing a differential diagnosis between diminutive polyps and tiny stool residues) of CTC.

Even if it is known that the most successful trials to date have all used tagging, the optimal tagging protocol is still under investigation. Depending on the Authors, a combination of barium and iodine to tag respectively solid and fluid residues, barium alone or iodine alone has been suggested.

### 4.5.2 Reduced Bowel Cleansing

Bowel cleansing represents the most unpleasant part of CTC examination. This is the reason why reduced bowel preparation methods (using mild or no laxatives at all) have been implemented in order to make the examination more comfortable and less demanding for patients. Since fecal residues remain into the colon, the association of faecal tagging in these preparation schemes is mandatory. Among the different options, we optimized a protocol using diatrizoate/dimeglumine alone delivered to the patients without any other laxative agent on the day before the examination. The use of diatrizoate/dimeglumine, an hyperosmolar contrast agent, at relatively high doses (160 mL) makes the colon relatively clean and the residual stool completely and homogeneously tagged by the Iodine. This is not a completely diarrhea-free approach, but it minimizes patient discomfort in the majority of cases. Of course, other protocols for reduced bowel prep are available, all of them under clinical investigation.

The use of reduced bowel preparation, because of the large amount of faecal residues, is more challenging for readers. This is the reason why this approach is suggested only to radiologists with a consistent experience in CTC.

### 4.5.3 Patient Preparation

Patient preparation for scanning consists of air insufflation, administration of an anti-peristaltic drug, and, if necessary, intravenous injection of iodinated CM.

Air insufflation is a critical step since a collapsed bowel is a frequent cause of missed lesions at CT colonography. In the standard technique, with the patient in the left lateral decubitus position, a thin flexible rectal catheter is inserted and the colon is gently insufflated with room air to maximum patient tolerance. After insufflation, the patient is shifted to the prone position and a standard CT scout film of the abdomen and pelvis is acquired to evaluate the adequacy of colonic distention; further air insufflation is performed, if needed. A possible alternative to room air is $CO_2$, delivered by an automatic electronic pump, which provides better control of both the volume and the pressure of the enema. $CO_2$, although more expensive, is associated with better patient compliance especially after the examination, due to quick resorption through the colon wall and vessels, thus reducing abdominal distention.

The use of a spasmolytic agent (either hyoscine butylbromine, Buscopan, or glucagon) is particularly helpful in the case of colonic spasm, typically in the sigmoid colon, and in patients with severe diverticular disease.

The intravenous injection of CM is not necessary for lesion detection and is not routinely performed in screening examinations, which reduces both additional costs and the potential risk of allergic reactions.

For symptomatic patients, there is currently no consensus on whether CM should be given routinely or not. However, CM injection may be required in the evaluation of extracolonic findings, in patients with known colorectal cancer, or in those under surveillance for the disease.

## 4.6 Perfusion

Perfusion MDCT allows functional evaluation of tissue vascularity, measuring the temporal changes in tissue density after intravenous injection of a CM bolus through a series of dynamically acquired MDCT images. This enhancement depends on the tissue iodine concentration and is an indirect reflection of tissue vascularity and vascular physiology.

Perfusion is widely used in stroke, where the assessment of ischemic penumbra and necrotic areas guides the revascularization treatment,

especially in late-coming patients. In the field of oncology, perfusion MDCT has found applications in lesion characterization, the identification and diagnosis of occult malignancies, staging, prognostic information based on tumor vascularity, and monitoring of the therapeutic effects of the various treatment regimens, including chemoradiation and anti-angiogenic drugs.

The first-pass study for perfusion measurements comprises images acquired in the initial cine phase for a total of 40–60 s. For the typical first-pass study based on the deconvolution method, an image is acquired every 1 s, whereas for the compartmental method, image acquisition is every 3–5 s. In permeability measurements, a second phase, ranging from 2 to 10 min, is performed after the first-pass study. A contrast bolus of 40–70 mL and an injection rate 3.5–10 mL/s are typically adequate for optimal perfusion analysis.

A major concern of perfusion MDCT is the risk of patient exposure to ionizing radiation, especially in patients who require serial perfusion studies for monitoring treatment effects.

The main parameters that can be evaluated with perfusion MDCT are: blood flow, perfusion through the vasculature of various tissue regions (marker of tumor vascularity and grade); blood volume, volume of flowing blood within the vasculature in tissue regions (tumor vascularity); mean transit time, average time needed for flow from an artery to a vein (perfusion pressure); permeability surface area product, total flux from plasma to interstitial space (immature leaky vessels); time to peak, time from CM arrival in major arterial vessels to the peak enhancement (perfusion pressure); and peak enhancement intensity, maximum increase in tissue density after CM injection (tissue blood volume).

# 5    Essential References

ACCF/ACR/SCCT/SCMR/ASNC/NASCI/SCAI/SIR (2006) Appropriateness criteria for cardiac computed tomography and cardiac magnetic resonance imaging. A report of the American College of Cardiology Foundation Quality Strategic Directions Committee Appropriateness Criteria Working Group. J Am Coll Radiol 3:751-771

Awai K, Takada K, Onishi H et al (2002) Aortic and hepatic enhancement and tumor to liver contrast: analysis of the effect of different concentrations of contrast material at multi–detector row helical CT. Radiology 224:757–763

Bae KT, Seeck BA, Hildebolt CF et al (2008) Contrast enhancement in cardiovascular MDCT: effect of body weight, height, body surface area, body mass index, and obesity. AJR Am J Roentgenol 190:777-784

Budoff MJ, Dowe D, Jollis JG et al (2008) Diagnostic performance of 64-multidetector row coronary computed tomographic angiography for evaluation of coronary artery stenosis in individuals without known coronary artery disease: results from the prospective multicenter ACCURACY (Assessment by Coronary Computed Tomographic Angiography of Individuals Undergoing Invasive Coronary Angiography) trial. J Am Coll Cardiol 52:1724-3172

Busacker A, Newell JD Jr, Keefe T et al (2009) A multivariate analysis of risk factors for the air-trapping asthmatic phenotype as measured by quantitative CT analysis. Chest 135:48-56

Dodd JD, de Jong PA, Levy RD et al (2008) Conventional high-resolution CT versus contiguous multidetector CT in the detection of bronchiolitis obliterans syndrome in lung transplant recipients. J Thorac Imaging 23:235-243

Endo I, Shimada H, Sugita M et al (2007) Role of three-dimensional imaging in operative planning for hilar cholangiocarcinoma. Surgery 142:666-675

Erturk SM, Ichikawa T, Sou H et al (2008) Effect of duration of contrast material injection on peak enhancement times and values of the aorta, main portal vein, and liver at dynamic MDCT with the dose of contrast medium tailored to patient weight. Clin Radiol 63:263-271

Fleischmann D (2002) Present and future trends in multiple detector-row CT applications: CT angiography. Eur Radiol 12(Suppl 2):S11-S15

Fleischmann D (2003) High-concentration contrast media in MDCT angiography: principles and rationale. Eur Radiol 13 Suppl 3:N39-N43

Fleischmann D (2003) Use of high-concentration contrast media in multiple-detector-row CT: principles and rationale. Eur Radiol 13:M14-M20

Fleischmann D (2005) How to design injection protocols for multiple detector-row CT an- giography (MDCTA). Eur Radiol 15 Suppl 5:E60-E65

Fleischmann D (2010) CT angiography: injection and acquisition technique. Radiol Clin North Am 48:237-247

Fleischmann D, Kamaya A (2009) Optimal vascular and parenchymal contrast enhancement: the current state of the art. Radiol Clin North Am 47:13-26

Fleischmann D, Rubin GD (2005) Quantification of intravenously administered contrast medium transit through the peripheral arteries: implications for CT angiography. Radiology 236:1076-1082

Fletcher JG, Huprich J, Loftus EV Jr et al (2008) Computerized tomography enterography and its role in small-bowel imaging. Clin Gastroenterol Hepatol 6:283-289

Flohr TG, Stierstorfer K, Ulzheimer S et al (2005) Image reconstruction and image quality evaluation for a 64-slice CT scanner with z-flying focal spot. Med Phys 32:2536-2547

Funama Y, Awai K, Hatemura M et al (2008) Automatic tube current modulation technique for multidetector CT: is it effective with a 64-detector CT? Radiol Phys Technol 1:33-37

Funama Y, Awai K, Taguchi K et al (2009) Cone-beam technique for 64-MDCT of lung: image quality comparison with stepwise (step-and-shoot) technique. AJR Am J Roentgenol 192:273-278

Gomez D, Rahman SH, Won LF et al (2006) Characterization of malignant pancreatic cystic lesions in the background of chronic pancreatitis. JOP 7:465-472

Grierson C, Uthappa MC, Uberoi R, Warakaulle D (2007) Multidetector CT appearances of splanchnic arterial pathology. Clin Radiol 62:717-723

Groen JM, Greuter MJ, Schmidt B et al (2007). The influence of heart rate, slice thickness, and calcification density on calcium scores using 64-slice multidetector computed tomography: a systematic phantom study. Invest Radiol 42:848-855

Hirai N, Horiguchi J, Fujioka C et al (2008) Prospective versus retrospective ECG-gated 64-detector coronary CT angiography: assessment of image quality, stenosis, and radiation dose. Radiology 248:424-430

Huang JS, Pan HB, Chou CP et al (2008) Optimizing scanning phases in detecting small (<2 cm) hepatocellular carcinoma: whole-liver dynamic study with multidetector row CT. J Comput Assist Tomogr 32:341-346

Ichikawa T, Erturk SM, Araki T (2006) Multiphasic contrast-enhanced multidetector-row CT of liver: contrast-enhancement theory and practical scan protocol with a combination of fixed injection duration and patients' body-weight-tailored dose of contrast material. Eur J Radiol 58:165-176

Jankowski A, Martinelli T, Timsit JF et al (2007) Pulmonary nodule detection on MDCT images: evaluation of diagnostic performance using thin axial images, maximum intensity projections, and computer-assisted detection. Eur Radiol 17:3148-3156

Johnson PT, Fishman EK (2006) IV contrast selection for MDCT: current thoughts and practice. AJR Am J Roentgenol 186:406-415

Kakihara D, Yoshimitsu K, Irie H et al (2007) Usefulness of the long-axis and short-axis reformatted images of multidetector-row CT in evaluating T-factor of the surgically resected pancreaticobiliary malignancies. Eur J Radiol 63:96-104

Kalra MK, Maher MM, Toth TL et al (2004) Techniques and applications of automatic tube current modulation for CT. Radiology 233:649-657

Kamel IR, Liapi E, Fishman EK (2005) Liver and biliary system: evaluation by multidetector CT. Radiol Clin North Am 43:977-997

Kanamoto T, Matsuki M, Okuda J et al (2007) Preoperative evaluation of local invasion and metastatic lymph nodes of colorectal cancer and mesenteric vascular variations using multidetector-row computed tomography before laparoscopic surgery. J Comput Assist Tomogr 31:831-839

Kawel N, Seifert B, Luetolf M, Boehm T (2009) Effect of slab thickness on the CT detection of pulmonary nodules: use of sliding thin-slab maximum intensity projection and volume rendering. AJR Am J Roentgenol 192:1324-1329

Kim DH, Pickhardt PJ, Taylor AJ et al (2007) CT colonography versus colonoscopy for the detection of advanced neoplasia. N Engl J Med 357:1403-1412

Klauss M, Mohr A, von Tengg-Kobligk H et al (2008) A new invasion score for determining the resectability of pancreatic carcinomas with contrast-enhanced multidetector computed tomography. Pancreatology 8:204-210

Kobayashi T, Ikeda Y, Murakami M et al (2008) Computed tomographic angiography to evaluate the right gastroepiploic artery for coronary artery bypass grafting. Ann Thorac Cardiovasc Surg 14:166-171

Laghi A (2007) Multidetector CT (64 Slices) of the liver: examination techniques. Eur Radiol 17:675-683

Laghi A, Iannaccone R, Catalano C, Passariello R (2001) Multislice spiral computed tomography angiography of mesenteric arteries. Lancet 358:638-639

Laghi A, Passariello R (2008) La colonscopia virtuale. Springer, Milan

Maruyama T, Takada M, Hasuike T et al (2008) Radiation dose reduction and coronary as-sessability of prospective electrocardiogram-gated computed tomography coronary angiography: comparison with retrospective electrocardiogram-gated helical scan. J Am Coll Cardiol 52:1450-1455

Meijboom WB, Meijs MF, Schuijf JD et al (2008) Diagnostic accuracy of 64-slice computed tomography coronary angiography: a prospective, multicenter, multivendor study. J Am Coll Cardiol 52:2135-2144

Meijboom WB, van Mieghem CA, Mollet NR et al (2007). 64-slice computed tomography coronary angiography in patients with high, intermediate, or low pretest probability of significant coronary artery disease. J Am Coll Cardiol 50:1469-7514

Minordi LM, Vecchioli A, Poloni G, Bonomo L (2007) CT enteroclysis: multidetector technique (MDCT) versus single-detector technique (SDCT) in patients with suspected small-bowel Crohn's disease. Radiol Med 112:1188-1200

Mowatt G, Cummins E, Waugh N et al (2008). Systematic review of the clinical effectiveness and cost-effectiveness of 64-slice or higher computed tomography angiography as an alternative to invasive coronary angiography in the investigation of coronary artery disease. Health Technol Assess 12:iii-iv, ix-143

Mulkens TH, Bellinck P, Baeyaert M et al (2005) Use of an automatic exposure control mechanism for dose optimization in multi-detector row CT examinations: clinical evaluation. Radiology 237:213-223

NIMISCAD Study Group (2008) Italian multicenter, prospective study to evaluate the negative predictive value of 16- and 64-slice MDCT imaging in patients scheduled for coronary angiography. Eur Radiol PMID:19089430

Pandharipande PV, Krinsky GA, Rusinek H, Lee VS (2005) Perfusion imaging of the liver: current challenges and future goals. Radiology 234:661–673

Pickhardt PJ, Hassan C, Laghi A et al (2008) Small and diminutive polyps detected at screening CT colonography: a decision analysis for referral to colonoscopy. AJR 190:136-144

Platten D, Keat N, Lewis M, Edyvean S (2005) Report 05068. 32 to 64 slice CT scanner comparison report version 13. ImPACT, Purchasing and Supply Agency 1-23

Prokop M (2003) Multislice CT: technical principles and future trends. Eur Radiol 13:M3-M13

Reid JH et the International Atomic Energy Agency Consultants' Group (2009) Is the lung scan alive and well? Facts and controversies in defining the role of lung scintigraphy for the diagnosis of pulmonary embolism in the era of MDCT. Eur J Nucl Med Mol Imaging 36:505-521

Rogalla P, Kloeters C, Hein PA (2009) CT technology overview: 64-slice and beyond. Radiol Clin North Am 47:1-11

Romano S, Romano L, Grassi R (2007) Multidetector row computed tomography findings from ischemia to infarction of the large bowel. Eur J Radiol 61:433-441

Sahani DV, Soulez G, Chen KM et al (2007) Investigators of the IMPACT Study. A comparison of the efficacy and safety of iopamidol-370 and iodixanol-320 in patients undergoing multidetector-row computed tomography. Invest Radiol 42:856-861

Satoi S, Yamamoto H, Takai S et al (2007) Clinical impact of multidetector row computed tomography on patients with pancreatic cancer. Pancreas 34:175-179

Schroeder S, Achenbach S, Bengel F et al (2008) Cardiac computed tomography: indications, applications, limitations, and training requirements: report of a Writing Group deployed by the Working Group Nuclear Cardiology and Cardiac CT of the European Society of Cardiology and the European Council of Nuclear Cardiology. Eur Heart J 29:531-556

Smith RA, Cokkinides V, Brawley OW (2008) Cancer screening in the United States, 2008: a review of current American Cancer Society guidelines and cancer screening issues. CA Cancer J Clin 58:161-179

Strocchi S, Vite C, Callegari L et al (2006) Optimisation of multislice computed tomography protocols in angio-CT examinations. Radiol Med 11:238-244

Taylor SA, Laghi A, Lefere P et al (2007) European Society of Gastrointestinal and Abdominal Radiology (ESGAR): consensus statement on CT colonography. Eur Radiol 17:575-579

Wahidi MM, Govert JA, Goudar RK et al (2007) Evidence for the treatment of patients with pulmonary nodules: when is it lung cancer?: ACCP evidence-based clinical practice guidelines (2nd edition). Chest 132:94S-107S

Wang XP, Chen WX, Wu DS, Wang XD (2011) Whole-liver perfusion scans with 64-slice spiral CT in patients with liver cirrhosis. Sichuan Da Xue Xue Bao Yi Xue Ban 42:382-386

Xia D, Bian J, Han X et al (1997) An Investigation of Compressive-sensing Image Reconstruction from Flying-focal-spot CT Data. IEEE Nucl Sci Symp Conf Rec 2009:3458-3462

Yoneda K, Ueno J, Nishihara S et al (2007) Postprocessing technique with MDCT data improves the accuracy of the detection of lung nodules. Radiat Med 25:511-515

Yanaga Y, Awai K, Nakayama Y et al (2007) Optimal dose and injection duration (injection rate) of contrast material for depiction of hypervascular hepatocellular carcinomas by multidetector CT. Radiat Med 25:278-288

Zech CJ, Bruns C, Reiser MF, Herrmann KA (2008) [Tumor-like lesion of the pancreas in chronic pancreatitis : imaging characteristics of computed tomography]. Radiologe 48:777-784

# Clinical Cases

# NEURO – Aneurysm with Subarachnoid Hemorrhage
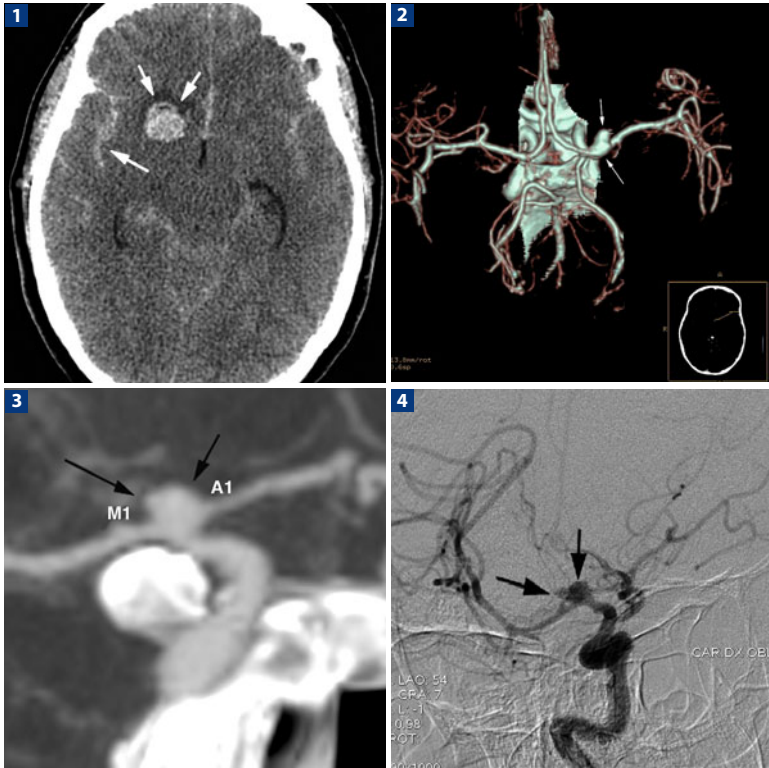


**1** Aneurysm of the bifurcation of the internal carotid artery in a patient with intraparenchymal and subarachnoid hemorrhage (*arrows*).   **2** Aneurysmatic dilatation of the internal carotid artery bifurcation (*arrows*) is seen in this volume rendering (VR) reconstruction overview.   **3** The relationships and dimensions are better identified in the maximum-intensity projection (MIP) reconstruction. **4** Digital angiography confirms the finding (*arrows*)

## Study Protocol

**Patient preparation:** As the examination is performed in an emergency situation, preparation is not possible.

**CM volume:** Determined according to the scan time (CM injection time = scan time + shortest [3 s] delay from the trigger).

**Iodine delivery rate:** 2 gI/s (vascular study)

| CM concentration (mgI/mL) | CM injection flow rate (mL/s) |
|---|---|
| 300 | 6.7 |
| 320 | 6.2 |
| 350 | 5.7 |
| 370 | 5.4 |
| 400 | 5.0 |

**Pre-contrast scan:** Performed in the context of an urgent evaluation.

**Post-contrast scan:** Acquisition time depends on the equipment available. We prefer the bolus-tracking technique, positioning the ROI at the level of the base of the skull, while trying to avoid possible artifacts from metallic orthodontic implants. The acquisition volume must extend from the foramen magnum to the top of the skull to identify all possible cerebral aneurysms (multiple aneurysms are seen in about 20% of patients).

**Scan delay:** It is important to minimize the delay between arterial opacification and the acquisition (this delay depends on the equipment available and the study protocol). Venous contamination should be minimized, as it can hinder identification of the relationship between the aneurysm and afferent and efferent vessels.

**Scan protocol:** Spiral caudate-cranial with a maximum value of thin collimation and pitch.

## References

Agid R, Willinsky RA, Farb RI, Terbrugge KG (2008) Life at the end of the tunnel: why emergent CT angiography should be done for patients with acute subarachnoid hemorrhage. AJNR Am J Neuroradiol 29:e45

Chen W, Wang J, Xing W et al (2009) Accuracy of 16-row multislice computerized tomography angiography for assessment of intracranial aneurysms. Surg Neuro l71:32-42

Fox AJ, Symons SP, Aviv RI (2008) CT angiography is state-of-the-art first vascular imaging for subarachnoid hemorrhage. AJNR Am J Neuroradiol 29:e41-42

Lubicz B, Levivier M, François O et al (2007) Sixty-four-row multisection CT angiography for detection and evaluation of ruptured intracranial aneurysms: interobserver and intertechnique reproducibility. AJNR Am J Neuroradiol 28:1949-1955

Tomandl BF, Köstner NC, Schempershofe M et al (2004) CT angiography of intracranial aneurysms: a focus on postprocessing. RadioGraphics 24:637-655

# NEURO – Arteriovenous Malformation in a Patient with Acute Cerebellar Hemorrhage
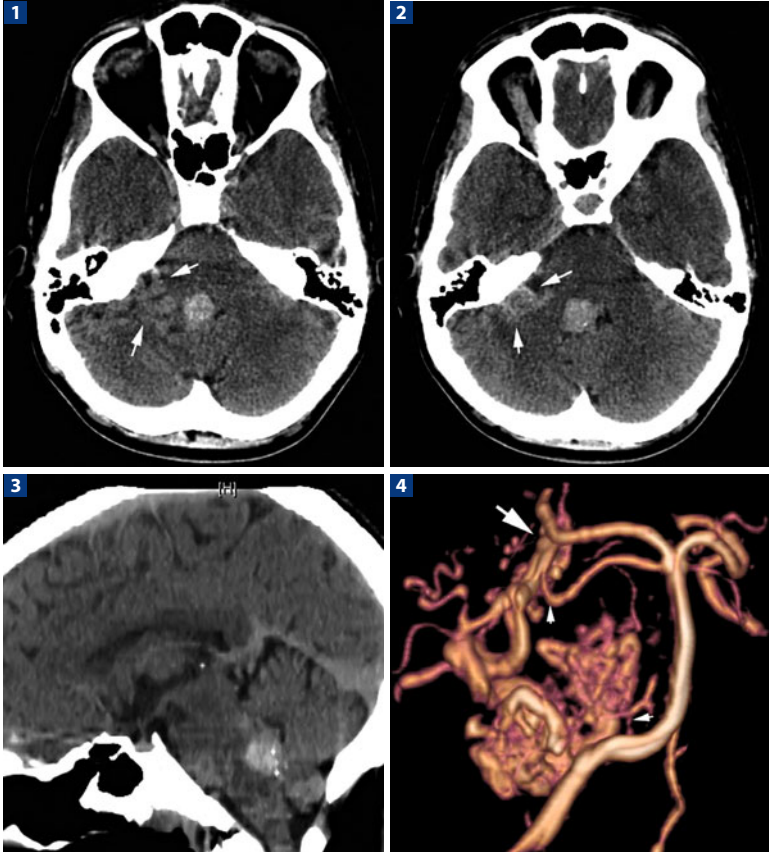


**1-3** Basal CT scan documents the presence of cerebellar hemorrhage, localized near the fourth ventricle. **2**, **3** In the cistern of the right pontocerebellar angle, there is a suspicious pathological vascular structure (*arrows*). **4** Angio-CT performed during the same session, which identified an AVM with predominant cerebellar afferents from the posterior-inferior arteries and right superior artery (*arrows*) and an efferent at the level of the straight sinus (*large arrow*)

## Study Protocol

**Patient preparation:** As the examination is performed in an emergency situation, preparation is not possible.

**CM volume:** Determined according to the scan time (CM injection time = scan time + variable delay from the trigger).

**Iodine delivery rate:** 2 gI/s (vascular study)

| CM concentration (mgI/mL) | CM injection flow rate (mL/s) |
|---|---|
| 300 | 6.7 |
| 320 | 6.2 |
| 350 | 5.7 |
| 370 | 5.4 |
| 400 | 5.0 |

**Pre-contrast scan:** Performed in the context of an urgent evaluation aimed at identifying the cerebral hemorrhage.

**Post-contrast scan:** Acquisition time depends on the equipment available. We prefer the bolus-tracking technique, positioning the ROI at the level of the base of the skull, while trying to avoid possible artifacts from metallic orthodontic implants. The acquisition volume must extend from the foramen magnum to the top of the skull.

**Scan delay:** In a suspected AVM, it is not essential to minimize the delay between arterial opacification and acquisition, unlike in aneurysm. "Complete" opacification of the malformation, in both the arterial and the venous components, is necessary. It is therefore preferable to start the acquisition, using a manual tracking technique, 2 s after the opacification of the internal carotid arteries in the distal exocranial segment.

**Scan protocol:** Spiral caudate-cranial with a maximum value of thin collimation and pitch.

## References

Gupta V, Chugh M, Walia BS et al (2008) Use of CT angiography for anatomic localization of arteriovenous malformation Nidal components. AJNR Am J Neuroradiol 29:1837-1840

Leclerc X, Gauvrit JY, Trystram D et al (2004) Cerebral arteriovenous malformations: value of the non invasive vascular imaging techniques. J Neuroradiol 31:349-358

Matsumoto M, Kodama N, Sakuma J et al (2005) 3D-CT arteriography and 3D-CT venography: the separate demonstration of arterial-phase and venous-phase on 3D-CT angiography in a single procedure. AJNR Am J Neuroradiol 26:635-641

# NEURO – Acute Pre-occlusive Stenosis of the Right Middle Cerebral Artery
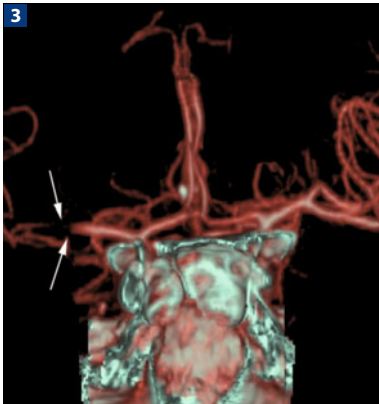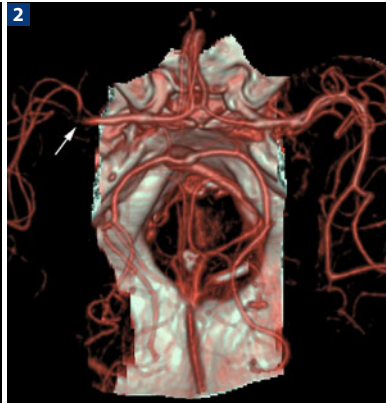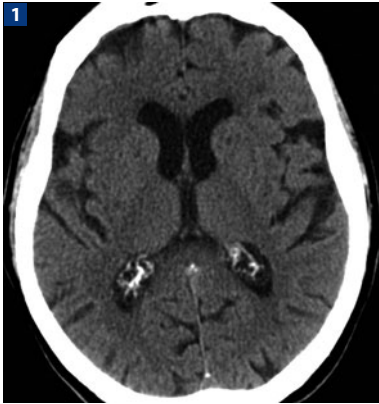










**1** Basal CT scan, performed in hyper-acute, 3 hours after the onset of left hemiparesis, is normal. **2**, **3** In the CT angiography with three-dimensional reconstructions, the tight stenosis is documented at the level of the middle cerebral artery bifurcation, M3, with the visualization of its distal branches (*arrows*). **4** The MIP reconstruction confirms the finding. **5** The CT scan at a distance of 30 days documents the ischemic lesion involving the temporo-parietal distribution area of the middle cerebral artery

## Study Protocol

**Patient preparation:** As the examination is performed in an emergency situation, preparation is not possible.

**CM volume:** Determined according to the scan time (CM injection time = scan time + shortest possible [less than 3 s] delay from the trigger).

**Iodine delivery rate:** 2 gI/s (vascular study)

| CM concentration (mgI/mL) | CM injection flow rate (mL/s) |
| --- | --- |
| 300 | 6.7 |
| 320 | 6.2 |
| 350 | 5.7 |
| 370 | 5.4 |
| 400 | 5.0 |

**Pre-contrast scan:** Performed in the context of an urgent evaluation of the patient. Patients with venous thrombosis have monolateral or bilateral areas of subcortical cerebral infarction, often complicated by hemorrhage.

**Post-contrast scan:** Acquisition time depends on the equipment available. We prefer the bolus-tracking technique, positioning the ROI at the level of the base of the skull, avoiding possible artifacts from metallic orthodontic implants. The acquisition volume must extend from the foramen magnum to the top of the skull.

**Scan delay:** Minimum possible.

**Scan protocol:** Spiral caudate-cranial with a maximum value of thin collimation and pitch.

## References

Camargo EC, Furie KL, Singhal AB et al (2007) Acute brain infarct: detection and delineation with CT angiographic source images versus nonenhanced CT scans. Radiology 244:541-548

Nguyen-Huynh MN, Wintermark M, English J et al (2008) How accurate is CT angiography in evaluating intracranial atherosclerotic disease? Stroke 39:1184-1188

Schaefer PW, Yoo AJ, Bell D et al (2008) CT angiography-source image hypo-attenuation predicts clinical outcome in posterior circulation strokes treated with intra-arterial therapy. Stroke 39:3107-3109

Sylaja PN, Puetz V, Dzialowski I et al (2008) Prognostic value of CT angiography in patients with  suspected vertebrobasilar ischemia. J Neuroimaging 18:46-49

# NEURO – Acute Thrombosis of the Left Transverse Sinus











**1** The basal CT scan, performed in emergency, documents the presence of hemorrhagic lesion in the left temporal area. **2** CT angiography study excludes the presence of arterial malformation but documents an alteration of the canalization of the omolateral transverse sinus (**3**, *arrows*). **4**, **5** MRI studies and Angio-MRI with gadolinium confirm the diagnosis of the left transverse sinus thrombosis. Despite the hemorrhagic lesion, treatment is based, in some cases, on the use of anticoagulants

## Study Protocol

**Patient preparation:** As the examination is performed in an emergency situation, preparation is not possible.

**CM volume:** Determined according to the scan time (CM injection time = scan time + variable delay from the trigger)

**Iodine delivery rate:** 2 gI/s (vascular study)

| CM concentration (mgI/mL) | CM injection flow rate (mL/s) |
|---|---|
| 300 | 6.7 |
| 320 | 6.2 |
| 350 | 5.7 |
| 370 | 5.4 |
| 400 | 5.0 |

**Pre-contrast scan:** Performed in the context of an urgent evaluation of the patient. Patients with venous thrombosis have monolateral or bilateral areas of subcortical cerebral infarction, often complicated by hemorrhage.

**Post-contrast scan:** Acquisition time depends on the equipment available. We prefer the bolus-tracking technique, positioning the ROI at the level of the base of the skull, avoiding possible artifacts from metallic orthodontic implants. The acquisition volume must extend from the foramen magnum to the top of the skull.

**Scan delay:** In suspected venous thrombotic disease, a pure arterial acquisition is not necessary, unlike in aneurysmal disease. Indeed, it is preferable to start the acquisition later, 3-4 s after opacification of the internal carotid arteries in the distal excranial segment, thereby allowing opacification of the venous sinuses.

**Scan protocol:** Spiral caudate-cranial with a maximum value of thin collimation and pitch.

## References

Gaikwad AB, Mudalgi BA, Patankar KB et al (2008) Diagnostic role of 64-slice multidetector row CT scan and CT venogram in cases of cerebral venous thrombosis. Emerg Radiol 15:325-333

Linn J, Ertl-Wagner B, Seelos KC et al (2007) Diagnostic value of multidetector-row CT angiography in the evaluation of thrombosis of the cerebral venous sinuses. AJNR Am J Neuroradiol 28:946-952

Wasay M, Azeemuddin M (2005) Neuroimaging of cerebral venous thrombosis. J Neuroimaging 15:118-128

# NEURO – Acute Thrombosis of the Right Rolandic Vein
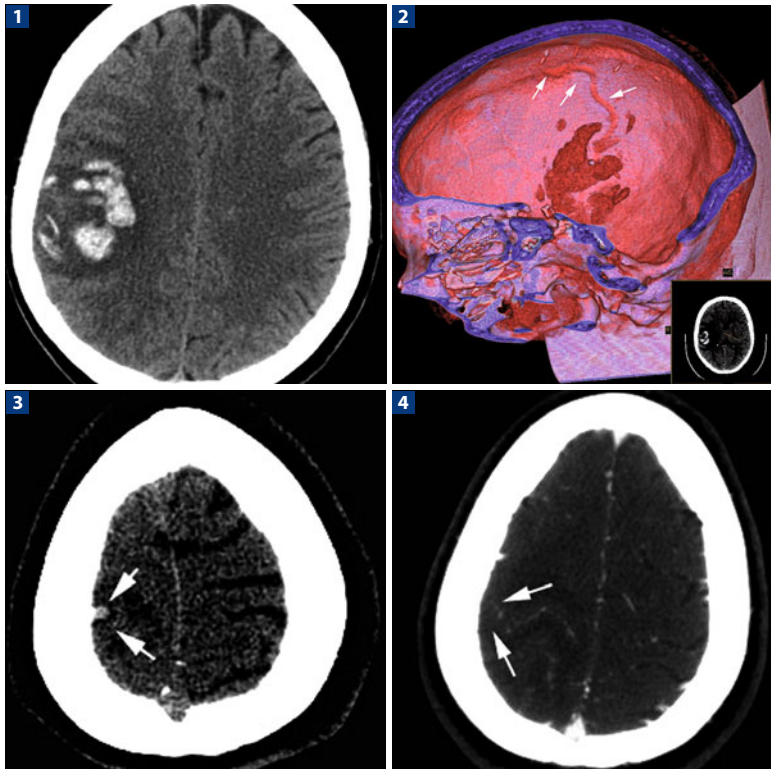








**1** Basal CT scan, performed in an emergency situation, documents a hemorrhagic lesion in the right parietal area.    **2** The same study identified a spontaneous hyperdensity along the rolandic sulcus, well-appreciated on 3D reconstruction.    **3**, **4** Angio-CT study confirms the lack of opacification of the right rolandic vein (*arrows*). Despite the hemorrhagic lesion, treatment is based, in some cases, on the use of anticoagulants

## Study Protocol

**Patient preparation:** As the examination is performed in an emergency situation, preparation is not possible.

**CM volume:** Determined according to the scan time (CM injection time = scan time + variable delay from the trigger).

**Iodine delivery rate:** 2 gl/s (vascular study)

| CM concentration (mgl/mL) | CM injection flow rate (mL/s) |
| --- | --- |
| 300 | 6.7 |
| 320 | 6.2 |
| 350 | 5.7 |
| 370 | 5.4 |
| 400 | 5.0 |

**Pre-contrast scan:** Performed in the context of an urgent evaluation of the patient. Patients with venous thrombosis have monolateral or bilateral areas of subcortical cerebral infarction, often complicated by hemorrhage. The presence of a spontaneous hyperdensity along the cerebral grooves at the top, cranial to the hemorrhagic lesion, should be considered as this may be indicative of venous thrombosis.

**Post-contrast scan:** Acquisition time depends on the equipment available. We prefer the bolus-tracking technique, positioning the ROI at the level of the base of the skull, avoiding possible artifacts from metallic orthodontic implants. The acquisition volume must extend from the foramen magnum to the top of the skull.
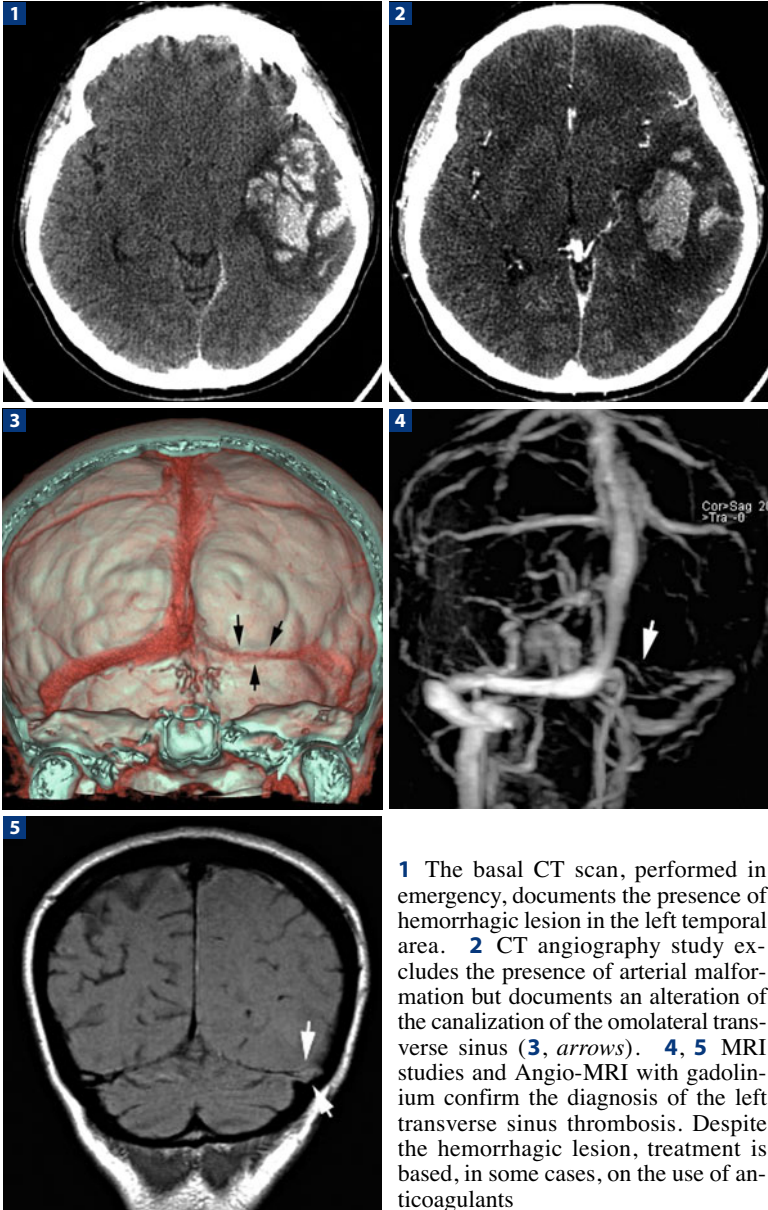
**Scan delay:** In suspected venous thrombotic disease, a pure arterial acquisition is not necessary, unlike in aneurysmal disease. Indeed, it is preferable to start the acquisition later, 3-4 s after opacification of the internal carotid arteries in the distal exocranial segment, to allow opacification of the venous sinuses.

**Scan protocol:** Spiral caudate-cranial with a maximum value of thin collimation and pitch.

## References

Gaikwad AB, Mudalgi BA, Patankar KB et al (2008) Diagnostic role of 64-slice multidetector row CT scan and CT venogram in cases of cerebral venous thrombosis. Emerg Radiol 15:325-333

Linn J, Ertl-Wagner B, Seelos KC et al (2007) Diagnostic value of multidetector-row CT angiography in the evaluation of thrombosis of the cerebral venous sinuses. AJNR Am J Neuroradiol 28:946-952

Wasay M, Azeemuddin M (2005) Neuroimaging of cerebral venous thrombosis. J Neuroimaging 15:118-128

**1** Basal CT scan documents the presence of a mildly hyperdense lesion in the left para-chiasmatic area. Angio-CT study, with partition images (**2**) and 3D overall (**3**) and detailed (**4**) reconstructions, respectively, clearly identifies the aneurysmal dilatation, where it is possible to define the size of the sac and the neck and the relationship with the artery of origin. This information may be sufficient for subsequent therapeutic deductions and, as needed, for eventual follow-up

## Study Protocol

**Patient preparation:** A 6-h fast before the exam.

**CM volume:** Determined according to the scan time (contrast medium injection time = scan time + shortest [less than 3 s] delay from the trigger).

**Iodine delivery rate:** 2 gl/s (vascular study)

| CM concentration (mgI/mL) | CM injection flow rate (mL/s) |
|---|---|
| 300 | 6.7 |
| 320 | 6.2 |
| 350 | 5.7 |
| 370 | 5.4 |
| 400 | 5.0 |

**Pre-contrast scan:** Useful to distinguish possible calcification.

**Post-contrast scan:** Acquisition time depends on the equipment available. We prefer the bolus-tracking technique, positioning the ROI at the level of the base of the skull, avoiding possible artifacts from metallic orthodontic implants. The acquisition volume must extend from the foramen magnum to the top of the skull.

**Scan delay:** It is important to minimize the delay between arterial opacification and the acquisition (this delay depends on the equipment available and the study protocol). Venous contamination must be kept to a minimum.

**Scan protocol:** Spiral caudate-cranial with a maximum value of thin collimation and pitch.

## References

Agid R, Willinsky RA, Farb RI, Terbrugge KG (2008) Life at the end of the tunnel: why emergent CT angiography should be done for patients with acute subarachnoid hemorrhage. AJNR Am J Neuroradiol 29:e45

Chen W, Wang J, Xing W et al (2009) Accuracy of 16-row multislice computerized tomography angiography for assessment of intracranial aneurysms. Surg Neuro l71:32-42

Fox AJ, Symons SP, Aviv RI (2008) CT angiography is state-of-the-art first vascular imaging for subarachnoid hemorrhage. AJNR Am J Neuroradiol 29:e41-42

Lubicz B, Levivier M, François O et al (2007) Sixty-four-row multisection CT angiography for detection and evaluation of ruptured intracranial aneurysms: interobserver and intertechnique reproducibility. AJNR Am J Neuroradiol 28:1949-1955

Tomandl BF, Köstner NC, Schempershofe M et al (2004) CT angiography of intracranial aneurysms: a focus on postprocessing. RadioGraphics 24:637-655

**1** Three-dimensional overall reconstruction of the intracranic circle that documents the presence of aneurysms of anterior communicating artery and middle cerebral artery (*arrows*).     **2** The three-dimensional digital angiography confirms the presence of aneurysms. The size of the bag and of the neck and and the relationship with the arteries of origin of the anterior communicating artery aneurysm are practically identical in the MIP reconstructions of Angio-CT (**3**) and angiography (**4**)

# Study Protocol

**Patient preparation:** A 6-h fast before the exam.

**CM volume:** Determined according to the scan time (CM injection time = scan time + shortest [less than 3 s] delay from the trigger).

**Iodine delivery rate:** 2 gI/s (vascular study)

| CM concentration (mgI/mL) | CM injection flow rate (mL/s) |
|---|---|
| 300 | 6.7 |
| 320 | 6.2 |
| 350 | 5.7 |
| 370 | 5.4 |
| 400 | 5.0 |

**Pre-contrast scan:** Useful to distinguish possible calcification.

**Post-contrast scan:** Acquisition time depends on the equipment available. We prefer the bolus-tracking technique, positioning the ROI at the level of the base of the skull, avoiding possible artifacts from metallic orthodontic implants. The acquisition volume must extend from the foramen magnum to the top of the skull.
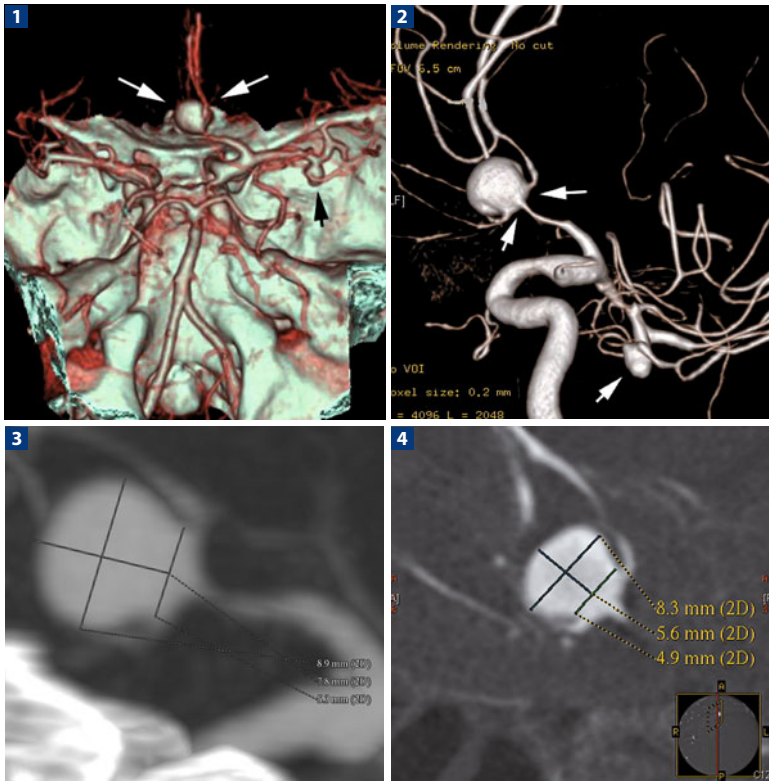
**Scan delay:** It is important to minimize the delay between arterial opacification and the acquisition (this delay depends on the equipment available and the study protocol). Venous contamination must be kept to a minimum.

**Scan protocol:** Spiral caudate-cranial with a maximum value of thin collimation and pitch.

## References

Agid R, Willinsky RA, Farb RI, Terbrugge KG (2008) Life at the end of the tunnel: why emergent CT angiography should be done for patients with acute subarachnoid hemorrhage. AJNR Am J Neuroradiol 29:e45

Chen W, Wang J, Xing W et al (2009) Accuracy of 16-row multislice computerized tomography angiography for assessment of intracranial aneurysms. Surg Neuro l71:32-42

Fox AJ, Symons SP, Aviv RI (2008) CT angiography is state-of-the-art first vascular imaging for subarachnoid hemorrhage. AJNR Am J Neuroradiol 29:e41-42

Lubicz B, Levivier M, François O et al (2007) Sixty-four-row multisection CT angiography for detection and evaluation of ruptured intracranial aneurysms: interobserver and intertechnique reproducibility. AJNR Am J Neuroradiol 28:1949-1955

Tomandl BF, Köstner NC, Schempershofe M et al (2004) CT angiography of intracranial aneurysms: a focus on postprocessing. RadioGraphics 24:637-655

# NEURO – Acute Occlusion of the Middle Cerebral Artery Frontal Branches
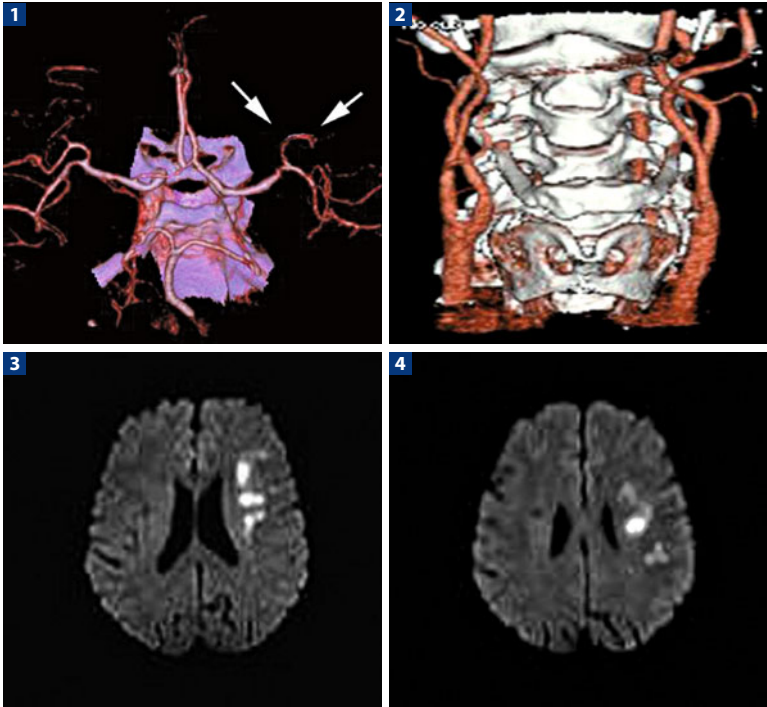


**1** Angio-CT scan, performed in a hyper-acute situation 3 h after the onset of left hemiparesis documents the lack of visualization of the frontal branches of the right middle cerebral artery (*arrows*). **2** Contextual evaluation of the epi-aortic vessels documents the normality of the internal carotid arteries. **3**, **4** MRI diffusion-weighted images performed 2 h later identify an acute ischemic lesion in the area of distribution of the frontal branches of the right middle cerebral artery

## Study Protocol

**Patient preparation:** As the examination is performed in an emergency situation, preparation is not possible.

**CM volume:** Determined according to the scan time (CM injection time = scan time + shortest [less than 3 s] delay from the trigger).

**Iodine delivery rate:** 2 gI/s (vascular study)

| CM concentration (mgI/mL) | CM injection flow rate (mL/s) |
| --- | --- |
| 300 | 6.7 |
| 320 | 6.2 |
| 350 | 5.7 |
| 370 | 5.4 |
| 400 | 5.0 |

**Pre-contrast scan:** Performed in the context of an urgent evaluation of the patient.

**Post-contrast scan:** Acquisition time depends on the equipment available. We prefer the bolus-tracking technique, positioning the ROI at the level of the aortic arch. The acquisition volume normally extends from the aortic arch to the intracranial circle, thereby providing an "overview" of the exo and intracranial vascular status.

**Scan delay:** Either manual or auto tracking is possible, starting the scan with initial opacification of the aortic arch.

**Scan protocol:** Spiral caudate-cranial.

## References

Camargo EC, Furie KL, Singhal AB et al (2007) Acute brain infarct: detection and delineation with CT angiographic source images versus nonenhanced CT scans. Radiology 244:541-548

Nguyen-Huynh MN, Wintermark M, English J et al (2008) How accurate is CT angiography in evaluating intracranial atherosclerotic disease? Stroke 39:1184-1188

Schaefer PW, Yoo AJ, Bell D et al (2008) CT angiography-source image hypoattenuation predicts clinical outcome in posterior circulation strokes treated with intra-arterial therapy. Stroke 39:3107-3109

Sylaja PN, Puetz V, Dzialowski I et al (2008) Prognostic value of CT angiography in patients with suspected vertebrobasilar ischemia. J Neuroimaging 18:46-49

# NEURO – Acute Occlusion of the Middle Cerebral Artery













**1** Basal CT scan, performed in a hyper-acute situation 4 h after the onset of left hemi-paresis, documents a hyperdensity at the right middle cerebral artery (*arrows*). **2** CT perfusion study generates a map of cerebral blood volume (CBV). **3** The identified hypoperfused area appears even larger in the MTT (mean transit time) map. **4** Microcatheters of the occluded artery with intra-arterial fibrinolysis. **5** Arter-ial patency as seen on angio-MRI performed 20 h later. **6** The size of the lesion in the MRI diffusion-weighted images is similar to that documented in the CBV maps

## Study Protocol

**Patient preparation:** As the examination is performed in an emergency situation, preparation is not possible.

**CM volume:** Determined according to the scan time (CM injection time = scan time + shortest [less than 3 s] delay from the trigger).

**Iodine delivery rate:** 2 gI/s (vascular study)

| CM concentration (mgI/mL) | CM injection flow rate (mL/s) |
| --- | --- |
| 300 | 6.7 |
| 320 | 6.2 |
| 350 | 5.7 |
| 370 | 5.4 |
| 400 | 5.0 |

**Pre-contrast scan:** Performed in the context of an urgent evaluation of the patient.

**Post-contrast scan:** The perfusion study is generally performed at the level of the basal ganglia. The acquisition volume depends on the rows available. Additional levels can be evaluated with a second administration of CM.

**Scan delay:** The images must be evaluated during the passage of CM, to obtain both pre-contrast images and arterial and venous phases. Processing involves the use of arterial input and venous output.

## References

de Lucas EM, Sánchez E, Gutiérrez A et al (2008) CT protocol for acute stroke: tips and tricks for general radiologists. RadioGraphics 28:1673-1687

Schaefer PW, Barak ER, Kamalian S et al (2008) Quantitative assessment of core/penumbra mismatch in acute stroke: CT and MR perfusion imaging are strongly correlated when sufficient brain volume is imaged. Stroke 39:2986-2992

Wintermark M (2005) Brain perfusion-CT in acute stroke patients. Eur Radiol 15 (Suppl 4): D28-D31
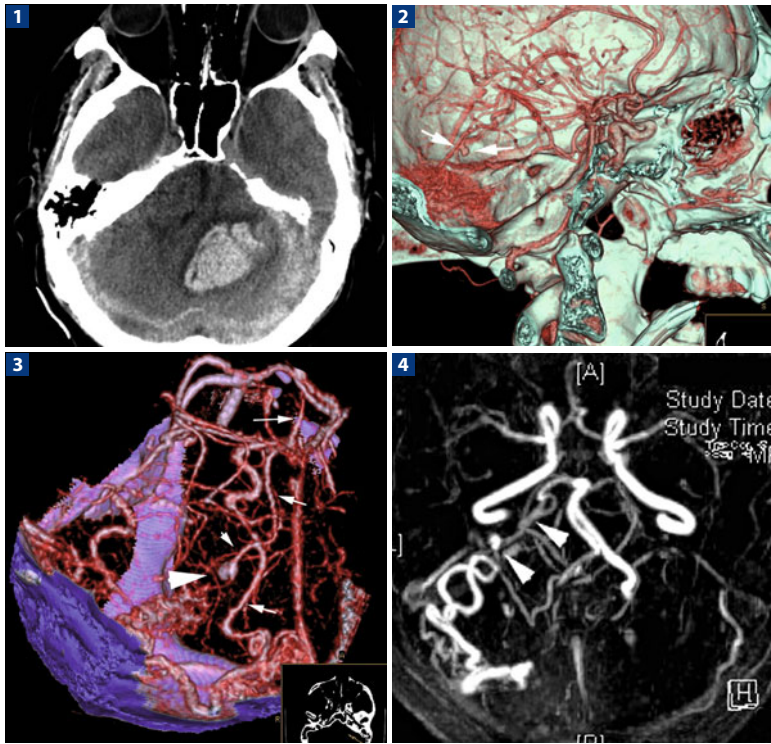
Patient with acute cerebellar hemorrhage. **1** Basal CT study documents the presence of cerebellar hemorrhage localized to the left cerebellar hemisphere. **2**, **3** Angio-CT study performed in the same session identifies an AVM with a predominant afferent from the left superior cerebellar artery, a hyperflow aneurysm along the course of the vasa (*large arrow*), and a predominant efferent at the level of the straight sinus. **4** Angio-MRI with gadolinium confirms the finding

## Study Protocol

**Patient preparation:** As the examination is performed in an emergency situation, preparation is not possible.

**CM volume:** Determined according to the scan time (CM injection time = scan time + variable delay from the trigger).

**Iodine delivery rate:** 2 gI/s (vascular study)

| CM concentration (mgI/mL) | CM injection flow rate (mL/s) |
| --- | --- |
| 300 | 6.7 |
| 320 | 6.2 |
| 350 | 5.7 |
| 370 | 5.4 |
| 400 | 5.0 |

**Pre-contrast scan:** Performed in the context of an urgent evaluation of the patient to define the cerebral hemorrhage.

**Post-contrast scan:** Acquisition time depends on the equipment available. We prefer the bolus-tracking technique, positioning the ROI at the level of the base of the skull, avoiding possible artifacts from metallic orthodontic implants. The acquisition volume must extend from the foramen magnum to the top of the skull.

**Scan delay:** In suspected AVM, it is not essential to minimize the delay between arterial opacification and acquisition, unlike in aneurysm. The acquisition is preferably started, using a manual tracking technique, 3-4 s after the opacification of the internal carotid arteries in the distal exocranial segment.

**Scan protocol:** Spiral caudate-cranial with a maximum value of thin collimation and pitch.

## References

Gupta V, Chugh M, Walia BS et al (2008) Use of CT angiography for anatomic localization of arteriovenous malformation Nidal components. AJNR Am J Neuroradiol 29:1837-1840

Leclerc X, Gauvrit JY, Trystram D et al (2004) Cerebral arteriovenous malformations: value of the non invasive vascular imaging techniques. J Neuroradiol 31:349-358

Matsumoto M, Kodama N, Sakuma J et al (2005) 3D-CT arteriography and 3D-CT venography: the separate demonstration of arterial-phase and venous-phase on 3D-CT angiography in a single procedure. AJNR Am J Neuroradiol 26:635-641

**1** MRI diffusion-weighted images document an acute ischemic area in the right frontal region. **2** On MRI TOF angiography there is a lack of visualization of the homolateral middle cerebral artery. **3** Angio-CT documents the effective arterial occlusion (*arrows*), but there are rich cortical anastomotic circles. **4** Digital angiography shows the arterial occlusion (*arrowhead*). **5** Compensation circles are visualized by the injection of the posterior circle (arrows) with the typical appearance of the disease (cloud of smoke, *arrows* in **4**)

## Study Protocol

**Patient preparation:** As the examination is performed in an emergency situation, preparation is not possible.

**CM volume:** Determined according to the scan time (CM injection time = scan time + shortest [less than 3 s] delay from the trigger).

**Iodine delivery rate:** 2 gI/s (vascular study)

| CM concentration (mgI/mL) | CM injection flow rate (mL/s) |
| --- | --- |
| 300 | 6.7 |
| 320 | 6.2 |
| 350 | 5.7 |
| 370 | 5.4 |
| 400 | 5.0 |

**Pre-contrast scan:** Performed in the context of an urgent evaluation of the patient to define the cerebral hemorrhage.

**Post-contrast scan:** Acquisition time depends on the equipment available. We prefer the bolus-tracking technique, positioning the ROI at the level of the base of the skull, avoiding possible artifacts from metallic orthodontic implants. The acquisition volume must extend from the foramen magnum to the top of the skull.

**Scan delay:** Since the aim is to document not only the vascular occlusion, but also the presence of compensation circles, it is preferable to start the acquisition 2-3 s after opacification of the internal carotid arteries, in the distal exocranial segment.

**Scan protocol:** Spiral caudate-cranial with a maximum value of thin collimation and pitch.

## References

Gazzola S, Aviv RI, Gladstone DJ et al (2008) Vascular and nonvascular mimics of the CT angiography "spot sign" in patients with secondary intracerebral hemorrhage. Stroke 39:1177-1183

# NEURO – Multiple Aneurysms in Subarachnoid Hemorrhage
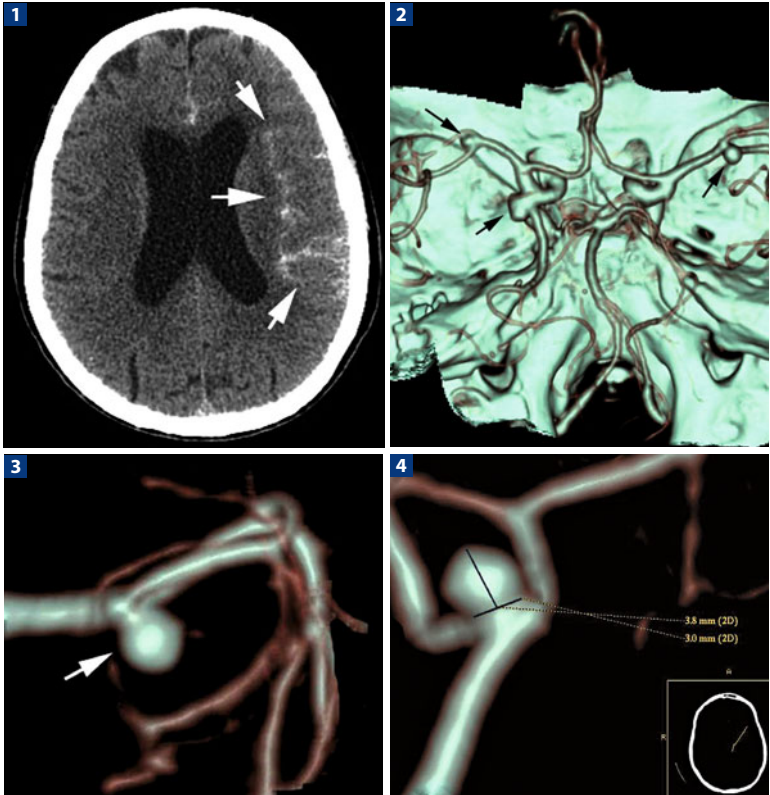








**1** Patient with subarachnoid hemorrhage. **2** VR reconstruction recognizes the presence of three aneurysmal dilatations localized at the level of the middle cerebral arteries and at the origin of the right posterior communicating artery. **3**, **4** Detailed reconstructions define the relationships and size of the aneurysm likely responsible for the bleeding

## Study Protocol

**Patient preparation:** As the examination is performed in an emergency situation, preparation is not possible.

**CM volume:** Determined according to the scan time (CM injection time = scan time + shortest [less than 3 s] delay from the trigger).

**Iodine delivery rate:** 2 gI/s (vascular study)

| CM concentration (mgI/mL) | CM injection flow rate (mL/s) |
| --- | --- |
| 300 | 6.7 |
| 320 | 6.2 |
| 350 | 5.7 |
| 370 | 5.4 |
| 400 | 5.0 |

**Pre-contrast scan:** Performed in the context of an urgent evaluation of the patient.

**Post-contrast scan:** Acquisition time depends on the equipment available. We prefer the bolus-tracking technique, positioning the ROI at the level of the base of the skull, avoiding possible artifacts from metallic orthodontic implants. The acquisition volume must extend from the foramen magnum to the top of the skull.
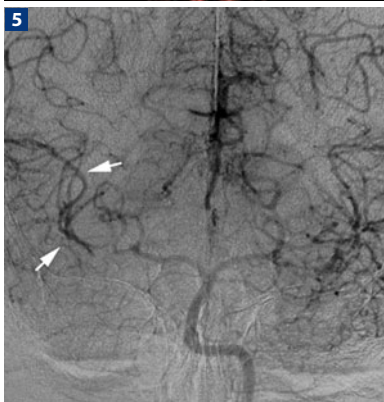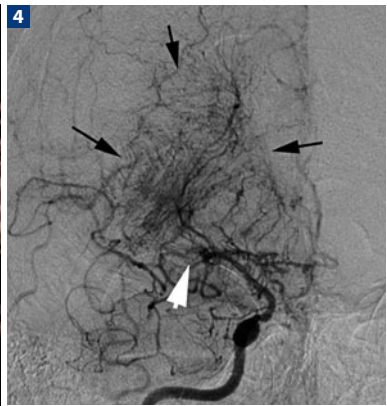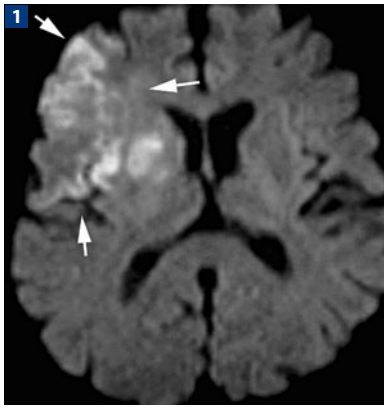
**Scan delay:** It is important to minimize the delay between arterial opacification and the acquisition (this delay depends on the equipment available and the study protocol). Venous contamination must be kept to a minimum. The acquisition is preferably started, using a manual tracking technique, at the initial opacification of the internal carotid arteries in the distal exocranial segment.

**Scan protocol:** Spiral caudate-cranial with a maximum value of thin collimation and pitch.

## References

Agid R, Willinsky RA, Farb RI, Terbrugge KG (2008) Life at the end of the tunnel: why emergent CT angiography should be done for patients with acute subarachnoid hemorrhage. AJNR Am J Neuroradiol 29:e45

Chen W, Wang J, Xing W et al (2009) Accuracy of 16-row multislice computerized tomography angiography for assessment of intracranial aneurysms. Surg Neuro l71:32-42

Fox AJ, Symons SP, Aviv RI (2008) CT angiography is state-of-the-art first vascular imaging for subarachnoid hemorrhage. AJNR Am J Neuroradiol 29:e41-42

Lubicz B, Levivier M, François O et al (2007) Sixty-four-row multisection CT angiography for detection and evaluation of ruptured intracranial aneurysms: interobserver and intertechnique reproducibility. AJNR Am J Neuroradiol 28:1949-1955

Tomandl BF, Köstner NC, Schempershofe M et al (2004) CT angiography of intracranial aneurysms: a focus on postprocessing. RadioGraphics 24:637-655

# NEURO – Dural Arteriovenous Fistula
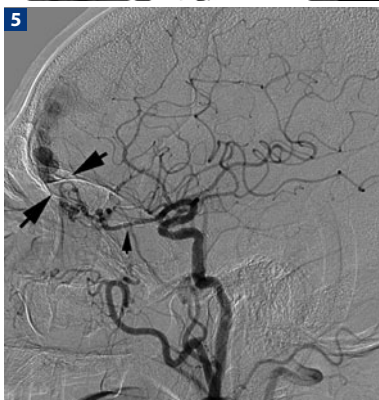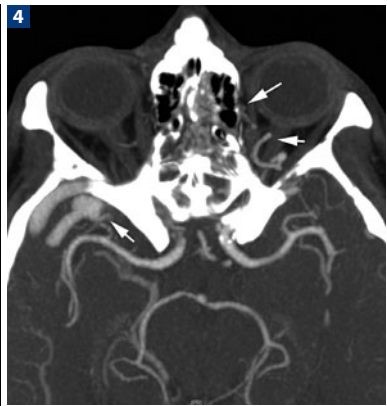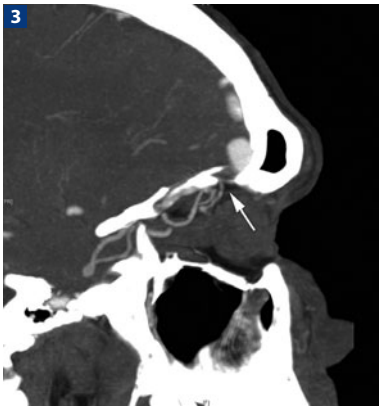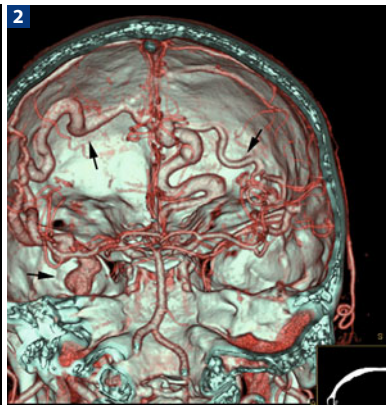










Patient with acute cerebral hemorrhage. **1** Basal CT study documents the presence of left frontal subcortical cerebral hemorrhage. **2** Angio-CT study performed in the same session reveals a complex vascular malformation likely attributable to an arteriovenous fistula (*arrows*). **3**, **4** The point of the fistula is best documented in the MIP images, which show its localization at the level of the base of the frontal skull, originating from the ophthalmic artery branches (*arrows*). **5** Digital angiography confirms the malformation and the point of the fistula (*arrows*)

## Study Protocol

**Patient preparation:** As the examination is performed in an emergency situation, preparation is not possible.

**CM volume:** Determined according to the scan time (CM injection time = scan time + variable delay from the trigger).

**Iodine delivery rate:** 2 gI/s (vascular study)

| CM concentration (mgI/mL) | CM injection flow rate (mL/s) |
| --- | --- |
| 300 | 6.7 |
| 320 | 6.2 |
| 350 | 5.7 |
| 370 | 5.4 |
| 400 | 5.0 |

**Pre-contrast scan:** Performed in the context of an urgent evaluation of the patient.

**Post-contrast scan:** Acquisition time depends on the equipment available. We prefer the bolus-tracking technique, positioning the ROI at the level of the base of the skull, avoiding possible artifacts from metallic orthodontic implants. The acquisition volume must extend from the foramen magnum to the top of the skull.

**Scan delay:** In suspected AVM, it is not essential to minimize the delay between arterial opacification and acquisition, unlike in aneurysm. The acquisition is preferably started, using a manual tracking technique, 2-3 s after opacification of the internal carotid arteries in the distal exocranial segment.

**Scan protocol:** Spiral caudate-cranial with a maximum value of thin collimation and pitch.

## References

Gupta V, Chugh M, Walia BS et al (2008) Use of CT angiography for anatomic localization of arteriovenous malformation Nidal components. AJNR Am J Neuroradiol 29:1837-1840

Leclerc X, Gauvrit JY, Trystram D et al (2004) Cerebral arteriovenous malformations: value of the non invasive vascular imaging techniques. J Neuroradiol 31:349-358

Matsumoto M, Kodama N, Sakuma J et al (2005) 3D-CT arteriography and 3D-CT venography: the separate demonstration of arterial-phase and venous-phase on 3D-CT angiography in a single procedure. AJNR Am J Neuroradiol 26:635-641

# NEURO – Pre-occlusive Stenosis of the Basilar Artery
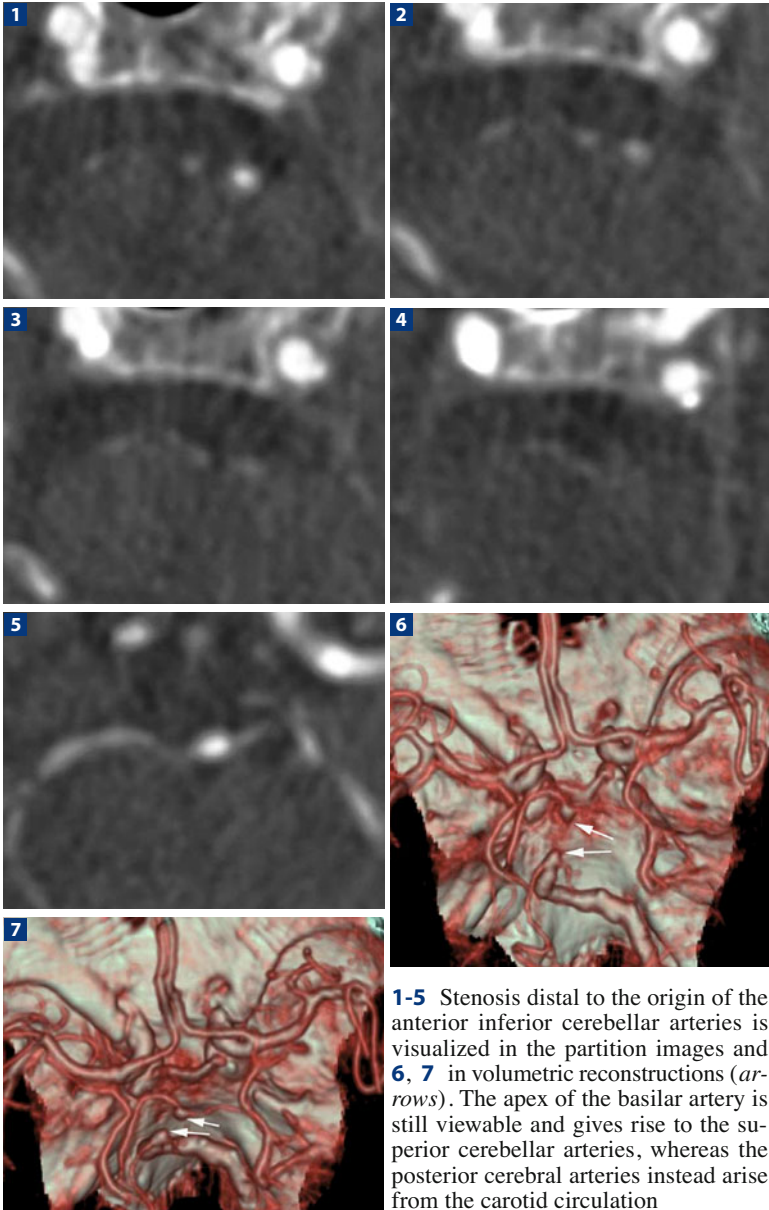














**1-5** Stenosis distal to the origin of the anterior inferior cerebellar arteries is visualized in the partition images and **6**, **7** in volumetric reconstructions (*arrows*). The apex of the basilar artery is still viewable and gives rise to the superior cerebellar arteries, whereas the posterior cerebral arteries instead arise from the carotid circulation

## Study Protocol

**Patient preparation:** A 6-h fast before the exam.

**CM volume:** Determined according to the scan time (CM injection time = scan time + shortest [less than 3 s] delay from the trigger).

**Iodine delivery rate:** 2 gI/s (vascular study)

| CM concentration (mgI/mL) | CM injection flow rate (mL/s) |
| --- | --- |
| 300 | 6.7 |
| 320 | 6.2 |
| 350 | 5.7 |
| 370 | 5.4 |
| 400 | 5.0 |

**Pre-contrast scan:** Used to identify possible calcifications, which are not infrequent in the vertebro-basilar circulation.

**Post-contrast scan:** Acquisition time depends on the equipment available. We prefer the bolus-tracking technique, positioning the ROI at the level of the base of the skull, avoiding possible artifacts from metallic orthodontic implants. The acquisition volume must extend from the foramen magnum to the top of the skull.

**Scan delay:** It is important to minimize the delay between arterial opacification and the acquisition (this delay depends on the equipment available and the study protocol). The acquisition is preferably started, using a manual tracking technique, at the initial opacification of the internal carotid arteries in the distal exocranial segment.

**Scan protocol:** Spiral caudate-cranial with a maximum value of thin collimation and pitch.

## References

Bash S, Villablanca JP, Jahan R et al (2005) Intracranial vascular stenosis and occlusive disease: evaluation with CT angiography, MR angiography, and digital subtraction angiography. AJNR Am J Neuroradiol 26:1012-1021

Hirai T, Korogi Y, Ono K et al (2002) Prospective evaluation of suspected stenoocclusive disease of the intracranial artery: combined MR angiography and CT angiography compared with digital subtraction angiography. AJNR Am J Neuroradiol 23:93-101

Nguyen-Huynh MN, Wintermark M, English J et al (2008) How accurate is CT angiography in evaluating intracranial atherosclerotic disease? Stroke 39:1184-1188

# NEURO – Pre-occlusive Stenosis of the Vertebral Arteries
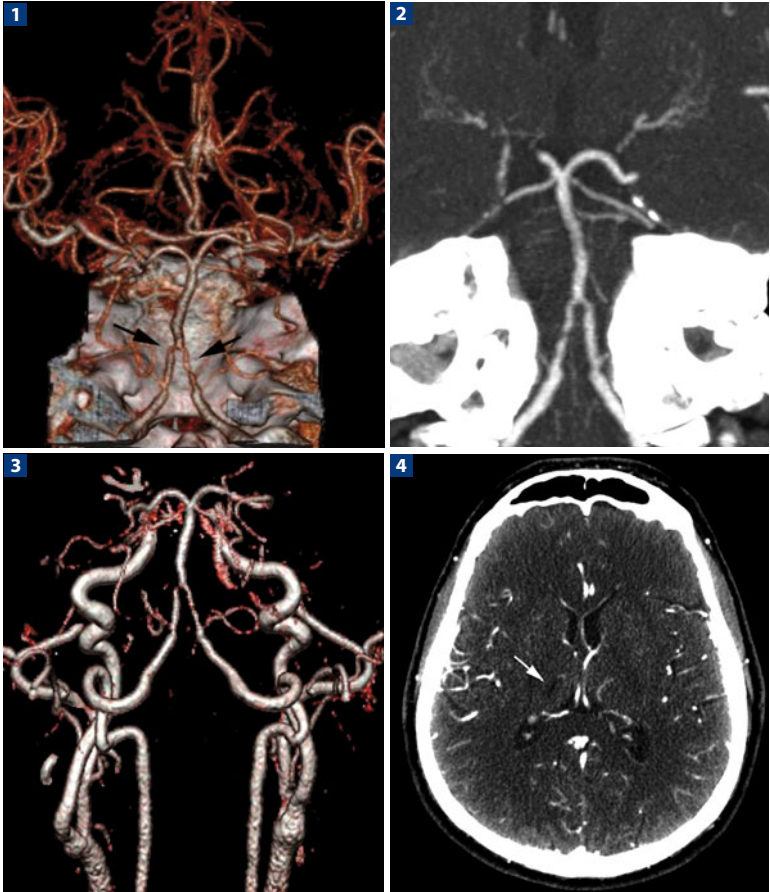


Patient with small lacunar ischemic stroke in the right thalamus. **1**, **2** The stenosis is visualized on volumetric and in MIP reconstructions, respectively, and confirmed (**3**) by angio-MRI. **4** The lacunar stroke is evident in the contrast-enhanced CT scan

## Study Protocol

**Patient preparation:** A 6-h fast before the exam.

**CM volume:** Determined according to the scan time (CM injection time = scan time + shortest [less than 3 s] delay from the trigger).

**Iodine delivery rate:** 2 gI/s (vascular study)

| CM concentration (mgI/mL) | CM injection flow rate (mL/s) |
| --- | --- |
| 300 | 6.7 |
| 320 | 6.2 |
| 350 | 5.7 |
| 370 | 5.4 |
| 400 | 5.0 |

**Pre-contrast scan:** Not necessary.

**Post-contrast scan:** Acquisition time depends on the equipment available. We prefer the bolus tracking technique, positioning the ROI at the level of the base of the skull, while trying to avoid possible artifacts from metallic orthodontic implants. The acquisition volume must extend from 2 cm caudal to the foramen magnum to the top of the skull.

**Scan delay:** The acquisition is preferably started, using a manual tracking technique, at initial opacification of the internal carotid arteries in the distal exocranial segment. The acquisition starts when the carotid arteries are well opacified, thereby allowing good opacification of the vertebral arteries.

**Scan protocol:** Spiral caudate-cranial with a maximum value of thin collimation and pitch.

## References

Bash S, Villablanca JP, Jahan R et al (2005) Intracranial vascular stenosis and occlusive disease: evaluation with CT angiography, MR angiography, and digital subtraction angiography. AJNR Am J Neuroradiol 26:1012-1021

Hirai T, Korogi Y, Ono K et al (2002) Prospective evaluation of suspected stenoocclusive disease of the intracranial artery: combined MR angiography and CT angiography compared with digital subtraction angiography. AJNR Am J Neuroradiol 23:93-101

Nguyen-Huynh MN, Wintermark M, English J et al (2008) How accurate is CT angiography in evaluating intracranial atherosclerotic disease? Stroke 39:1184-1188

# NEURO – Acute Thrombosis of the Superior Sagittal Sinus
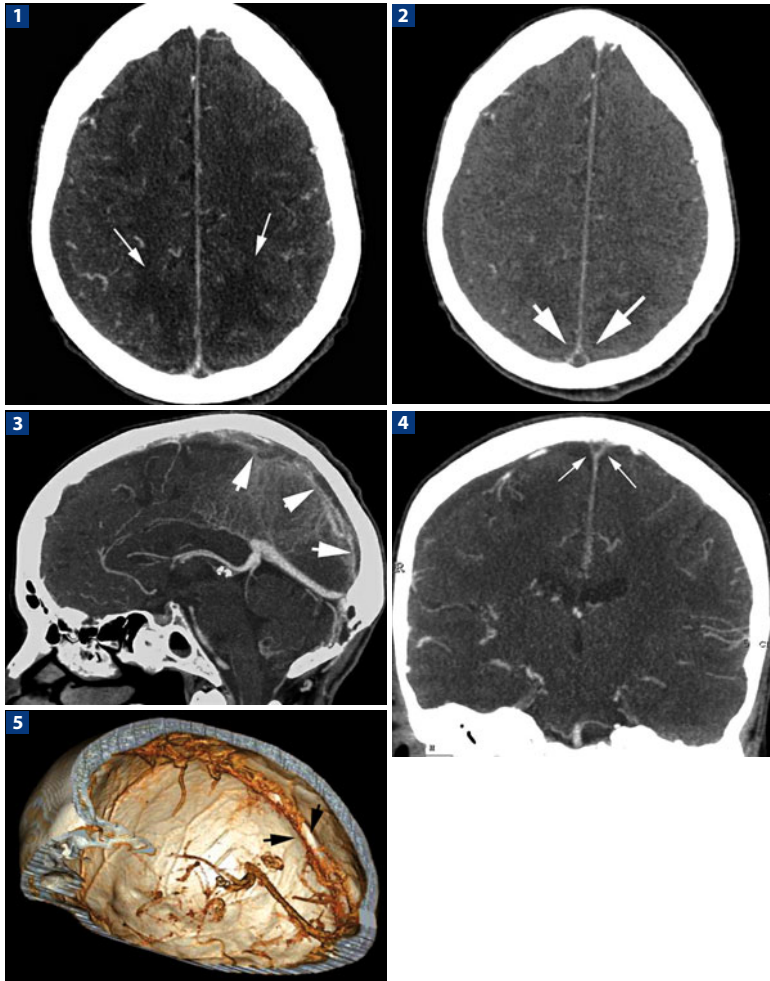










**1** CT scan with contrast, performed in an emergency, documents the presence of subcortical parietal bilateral hypodense lesions. **2-4** Angio CT study documents an alteration in the canalization of the superior sagittal sinus, with the typical delta sign. **5** In the 3D reconstruction, the sinus (*arrows*), when normal, is not observable

## Study Protocol

**Patient preparation:** As the examination is performed in an emergency situation, preparation is not possible.

**CM volume:** Determined according to the scan time (CM injection time = scan time + variable delay from the trigger).

**Iodine delivery rate:** 2 gI/s (vascular study)

| CM concentration (mgI/mL) | CM injection flow rate (mL/s) |
| --- | --- |
| 300 | 6.7 |
| 320 | 6.2 |
| 350 | 5.7 |
| 370 | 5.4 |
| 400 | 5.0 |

**Pre-contrast scan:** In the context of the patient evaluation.

**Post-contrast scan:** Acquisition time depends on the equipment available. We prefer the bolus-tracking technique, positioning the ROI at the level of the base of the skull, while trying to avoid possible artifacts from metallic orthodontic implants. The acquisition volume must extend from the foramen magnum to the top of the skull.

**Scan delay:** In suspected venous thrombotic disease, a pure arterial acquisition is not necessary, unlike in aneurysmal disease. Indeed, the acquisition is preferably started later, 3-4 s after the opacification of the internal carotid arteries in the distal extraocranial segment, to allow opacification of the venous sinuses.

**Scan protocol:** Spiral caudate-cranial with a maximum value of thin collimation and pitch. MIP thin reconstructions on orthogonal and three-dimensional planes (less useful and more difficult to interpret).

## References

Gaikwad AB, Mudalgi BA, Patankar KB et al (2008) Diagnostic role of 64-slice multidetector row CT scan and CT venogram in cases of cerebral venous thrombosis. Emerg Radiol 15:325-333

Linn J, Ertl-Wagner B, Seelos KC et al (2007) Diagnostic value of multidetector-row CT angiography in the evaluation of thrombosis of the cerebral venous sinuses. AJNR Am J Neuroradiol 28:946-952

Wasay M, Azeemuddin M (2005) Neuroimaging of cerebral venous thrombosis. J Neuroimaging 15:118-128

# NEURO – Arteriovenous Malformation (AVM) in a Patient with Acute Intraventricular Hemorrhage
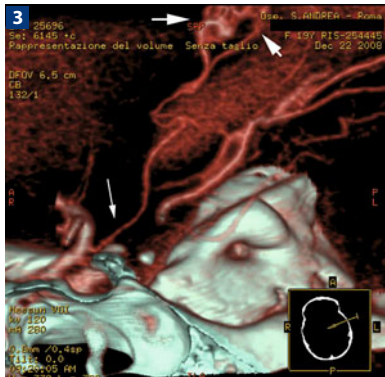








**1** Basal CT study documents the presence of intraventricular hemorrhage. **2**, **3** Angio CT study performed in the same session identifies an AVM (*arrows*) arising from the right anterior choroidal artery, **4** subsequently documented by digital angiography

## Study Protocol

**Patient preparation:** As the examination is performed in an emergency situation, preparation is not possible.

**CM volume:** Determined according to the scan time (CM injection time = scan time + variable delay from the trigger).

**Iodine delivery rate:** 2 gI/s (vascular study)

| CM concentration (mgI/mL) | CM injection flow rate (mL/s) |
|---|---|
| 300 | 6.7 |
| 320 | 6.2 |
| 350 | 5.7 |
| 370 | 5.4 |
| 400 | 5.0 |

**Pre-contrast scan:** In the context of the patient evaluation.

**Post-contrast scan:** Acquisition time depends on the equipment available. We prefer the bolus-tracking technique, positioning the ROI at the level of the base of the skull, while trying to avoid possible artifacts from metallic orthodontic implants. The acquisition volume must extend from the foramen magnum to the top of the skull.

**Scan delay:** In suspected AVM, it is not essential to minimize the delay between arterial opacification and acquisition, unlike in aneurysm. The acquisition is preferably started, using a manual tracking technique, 2–3 s after opacification of the internal carotid arteries in the distal exocranial segment.

**Scan protocol:** Spiral caudate-cranial with a maximum value of thin collimation and pitch.

## References

Gupta V, Chugh M, Walia BS et al (2008) Use of CT angiography for anatomic localization of arteriovenous malformation Nidal components. AJNR Am J Neuroradiol 29:1837-1840

Leclerc X, Gauvrit JY, Trystram D et al (2004) Cerebral arteriovenous malformations: value of the non invasive vascular imaging techniques. J Neuroradiol 31:349-358

Matsumoto M, Kodama N, Sakuma J et al (2005) 3D-CT arteriography and 3D-CT venography: the separate demonstration of arterial-phase and venous-phase on 3D-CT angiography in a single procedure. AJNR Am J Neuroradiol 26:635-641

**1, 2** Comparison between inspiratory and expiratory scans: the trachea in the expiratory scan is collapsed (*arrow*) and the density decreased. Comparison between inspiratory (**3**) and expiratory (**4**) CT scans shows multiple areas with a less than normal increase in attenuation (*arrowheads*). These areas correspond to secondary lobules

## Study Protocol

**Patient preparation:** It is important to ensure that the patient can maintain a breath-hold long enough to allow the images to be obtained. The patient must be able to stop breathing and hold his or her breath at full inspiration and full expiration when instructed to do so. Expiratory scans should be obtained with a medium breath, followed by complete exhalation and a breath-hold at full expiration. The patient should be instructed to take 2 normal breaths, followed by a medium breath, then exhale completely, with a breath-hold at full expiration.

**Pre-contrast scan:** This can be the only phase acquired; a comparison between inspiratory and expiratory CT scans is helpful when air trapping is subtle or diffuse.

**Inspiratory scan:** Helical mode, 0.5-s gantry rotation time, pitch 1.4, 120 kVp, 64 × 0.6-mm (Sensation 64) or 16 × 0.75-mm (Sensation 16) detector configuration CARE-Dose on*.

**Expiratory scan:** Non-contiguous axial (non-helical) mode, 0.5-s gantry rotation time, 120 kVp, 2 × 1-mm detector configuration with a 20-mm slice interval, CAREDose on*.

**Post-contrast scan:** Usually not necessary.

**Comments:** Air trapping is the retention of air in the lung at a site distal to an obstruction (usually partial). It is seen on end-expiration CT scans as parenchymal areas with a less than normal increase in attenuation and a lack of volume reduction. Differentiation from areas of decreased attenuation resulting from hypoperfusion as a consequence of an occlusive vascular disorder (e.g., chronic thromboembolism) may be problematic on the inspiratory scan; however in hypoperfusion, the vascular network is often decreased in inspiratory as well as in expiratory phase.

## References

Teel GS, Engeler CE, Tashijian J H, duCret RP (1996) Imaging of small airways disease. Radiographics 16(1):1627-1641

Bankier AA, Mehrain S, Kienzl D et al (2008) Regional heterogeneity of air trapping at expiratory thin-section CT of patients with bronchiolitis: potential implications for dose reduction and CT protocol planning. Radiology 247(3):862-870

Bankier AA, Schaefer-Prokop C, De Maertelaer V et al (2007) Air trapping: comparison of standard-dose and simulated low-dose thin-section CT techniques. Radiology 242(3):898-906

Müller NL, Thurlbeck WM (1996) Thin-section CT, emphysema, air trapping, and airway obstruction. Radiology 199(3):621-622

# THORAX – Mosaic Oligoemia
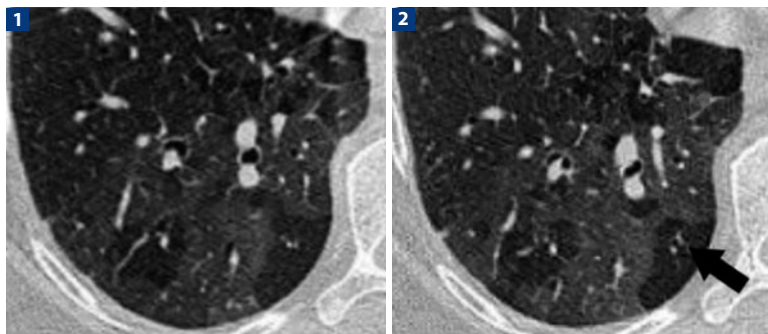


**1**, **2** Mosaic pattern: a comparison between the inspiratory (**1**) and expiratory (**2**) scans shows areas with the same attenuation (occlusive vascular disease). Note the decreased vessel density within those areas (*arrow*)

## Study Protocol

**Patient preparation:** It is important to be sure that the patient can maintain a breath-hold long enough to allow the images to be obtained. The patient must be able to stop breathing and hold his or her breath at full inspiration and full expiration when instructed to do so. Expiratory scans should be obtained with a medium breath, followed by complete exhalation and a breath-hold at full expiration. The patient should be instructed to take 2 normal breaths, followed by a medium breath, then to exhale completely, with a breath-hold at full expiration.

**Pre-contrast scan:** This can be the only phase acquired; a comparison between inspiratory and expiratory CT scans can be helpful when air trapping is subtle or diffuse.

**Inspiratory scan:** Helical mode, 0.5-s gantry rotation time, pitch 1.4, 120 kVp, 64 × 0.6-mm (Sensation 64) or 16 × 0.75-mm (Sensation 16) detector configuration CARE-Dose on*.

**Expiratory scan:** Non-contiguous axial (non-helical) mode, 0.5-s gantry rotation time, 120 kVp, 2 × 1-mm detector configuration with a 20-mm slice interval, CAREDose on*.

**Post-contrast scan:** Usually not necessary.

**Comments:** Differentiation from air trapping is achieved by comparing inspiratory and expiratory scans. In oligoemia, multiple patchy areas of hypolucency are seen in both phases, whereas in air trapping a loss in density is seen only during expiration. Moreover, the density loss in oligoemia can easily be seen as mainly due to a decrease of vessel density.
Different disorders, such as primitive pulmonary hypertension, left to right cardiac shunt, thrombo-embolic disease, peripheral vascular malformation (AVM, anomalous pulmonary venous return, Botallo's duct) may be responsible for the mosaic pattern. However, other causes mimicking the disease include: patchy interstitial disease and obliterative small-airways disease. An accurate evaluation of inspiratory and expiratory phases as well as vascular and bronchial density within the patchy areas may be helpful in the final diagnosis.

## References

Hansell DM, Bankier AA, MacMahon H et al (2008) Fleischner Society glossary of terms for thoracic imaging. Radiology 246(3):697-722. Epub 2008 Jan 14

Stern EJ, Müller NL, Swensen SJ, Hartman TE (1995) CT mosaic pattern of lung attenuation: etiologies and terminology. J Thorac Imaging 10(4):294-297

Martin KW, Sagel SS, Siegel BA (1986) Mosaic oligemia simulating pulmonary infiltrates on CT. AJR Am J Roentgenol 147(4):670-673

Eber CD, Stark P, Bertozzi P (1993) Bronchiolitis obliterans on high-resolution CT: a pattern of mosaic oligemia. J Comput Assist Tomogr 17(6):853-856
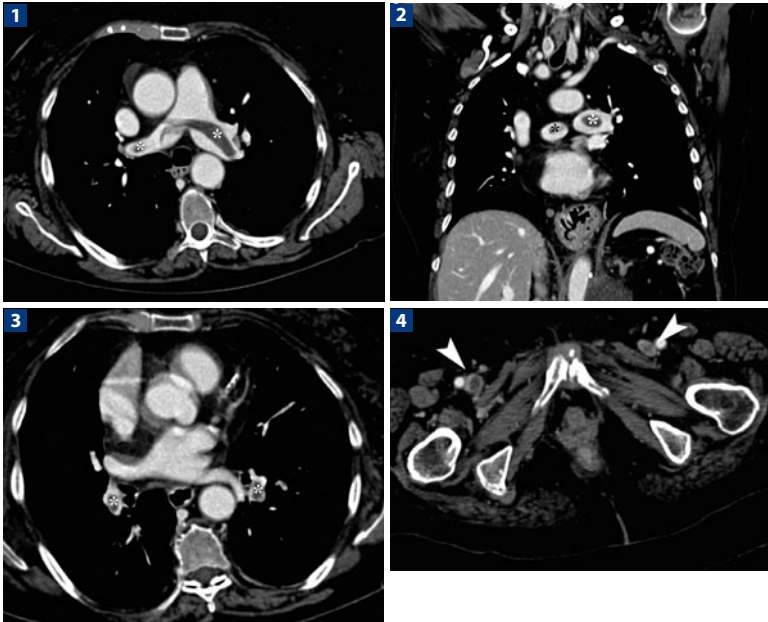
**1** Axial reconstruction after contrast medium administration shows a "straddle" thrombotic apposition (*asterisks*) in the pulmonary artery bifurcation.   **2** Coronal MPR reconstruction after contrast medium administration. Note the emboli's extent (*asterisks*) at the level of the main pulmonary artery branches.   **3** Axial reconstruction after contrast medium administration shows the presence of thrombosis (*asterisks*) of the pulmonary artery branches of the lower lobe bilaterally.   **4** Axial venous phase reconstruction demonstrates the presence of a thrombosis in the iliac-femoral vein axis bilaterally (*arrowheads*)

## Study Protocol

**Patient preparation:** A 6-h fast prior to the examination; 18G cannula placed on the right side.

**CM volume:** According to scan time.

| Patient weight (kg) | < 60 | < 80 | > 80 |
|---|---|---|---|
| **CM concentration (mgl/mL)** | | | |
| 300 | 100 | 130 | 150 |
| 320 | 95 | 125 | 140 |
| 350 | 85 | 115 | 130 |
| 370 | 80 | 110 | 120 |
| 400 | 75 | 100 | 110 |
| **CM injection flow rate (mL/s)** | **1.6 gl/s** | **1.8 gl/s** | **2.0 gl/s** |
| **CM concentration (mgl/mL)** | | | |
| 300 | 5.3 | 6.0 | 6.7 |
| 320 | 5.0 | 5.6 | 6.2 |
| 350 | 4.6 | 5.1 | 5.7 |
| 370 | 4.3 | 4.8 | 5.4 |
| 400 | 4.0 | 4.5 | 5.0 |

**Pre-contrast scan:** Not indispensable.

**Post-contrast scan:**
Arterial phase: 7 s (4-s scan + 3-s delay).
Bolus-tracking technique: 3 s after the threshold of 100 HU is reached, with the ROI in the lumen of the pulmonary artery.
Venous phase: 180 s from the start of CM injection to evaluate deep-vein thrombosis.

**Scan delay:**
The bolus-tracking monitoring technique is used.
Arterial phase: 3 s after the threshold of 100 HU is reached.
Venous phase: 180 s from the start of CM injection.

## References

Pruszczyk P, Torbicki A, Pacho R et al (1997) Noninvasive diagnosis of suspected severe pulmonary embolism: transesophageal echocardiography vs spiral CT. Chest 112:722-728

Remy-Jardin M, Remy J, Deschildre F (1996) Diagnosis of pulmonary embolism with spiral CT: comparison with pulmonary angiography and scintigraphy. Radiology 200:699-706

Winer-Muram HT, Rydberg J, Johnson MS (2004) Suspected acute pulmonary embolism: evaluation with multi-detector row CT versus digital subtraction pulmonary arteriography. Radiology 233:806-815

# THORAX – Pulmonary Embolism, CT Perfusion
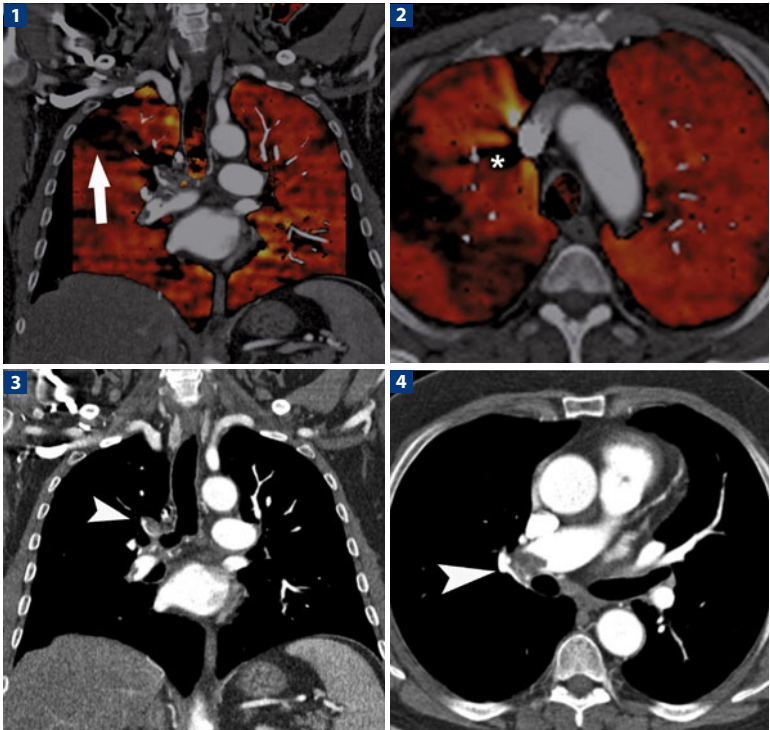


Lung perfusion CT with dual-energy analysis in a patient with lung embolism. **1**, **2** A segmental perfusion defect (*arrow*) is evident in the superior lobe of the right lung, due to a thrombus in the lumen of the right pulmonary artery (*arrow heads*, in **3** and **4**). The *asterisk* (**2**) shows the cone-beam artifact from the high-density contrast material throughout the superior vena cava

## Study Protocol

**Patient preparation:** A 6-h fast prior to the examination; 18G cannula placed on the right side.

**CM volume:** Adapted to the patient's body weight, at 1.35 mL/kg.

| Patient weight (kg) | < 60 | < 80 | > 80 |
|---|---|---|---|
| **CM concentration (mgl/mL)** | | | |
| 300 | 100 | 130 | 150 |
| 320 | 95 | 125 | 140 |
| 350 | 85 | 115 | 130 |
| 370 | 80 | 110 | 120 |
| 400 | 75 | 100 | 110 |
| **CM injection flow rate (mL/s)** | **1.6 gl/s** | **1.8 gl/s** | **2.0 gl/s** |
| **CM concentration (mgl/mL)** | | | |
| 300 | 5.3 | 6.0 | 6.7 |
| 320 | 5.0 | 5.7 | 6.2 |
| 350 | 4.6 | 5.0 | 5.7 |
| 370 | 4.3 | 4.8 | 5.4 |
| 400 | 4.0 | 4.5 | 5.0 |

**Pre-contrast scan:** Images are acquired in a single breath-hold in the caudo-cranial direction from the costophrenic angle to the lung apex. This may be important to reduce diaphragmatic movement at the end of the scan (uncooperative patients) and to reduce cone-beam artifacts within the superior vena cava.

**Post-contrast scan:** Two simultaneous helical scans are acquired with two tube voltages, 140 and 80 kV.

**Scan delay:**
The delay is usually longer than in the standard pulmonary embolism protocol in order to reduce possible artifacts from the flowing of CM. High IDR is recommended, as well as saline bolus chaser. A bolus tracking technique should be used starting the acquisition 11 seconds after the threshold of 100 HU in the main pulmonary artery.

## References

Nazaroğlu H, Ozmen CA, Akay HO et al (2009) 64-MDCT Pulmonary angiography and CT venography in the diagnosis of thromboembolic disease. AJR Am J Roentgenol 192(3):654-661

Stein PD, Yaekoub AY, Matta F et al (2010) Resolution of pulmonary embolism on CT pulmonary angiography. AJR Am J Roentgenol 194(5):1263-1268

Wildberger JE, Schoepf UJ, Mahnken AH et al (2005) Approaches to CT perfusion imaging in pulmonary embolism. Semin Roentgenol 40(1):64-73

Herzog P, Wildberger JE, Niethammer M et al (2003) CT perfusion imaging of the lung in pulmonary embolism. Acad Radiol 10(10):1132-1146
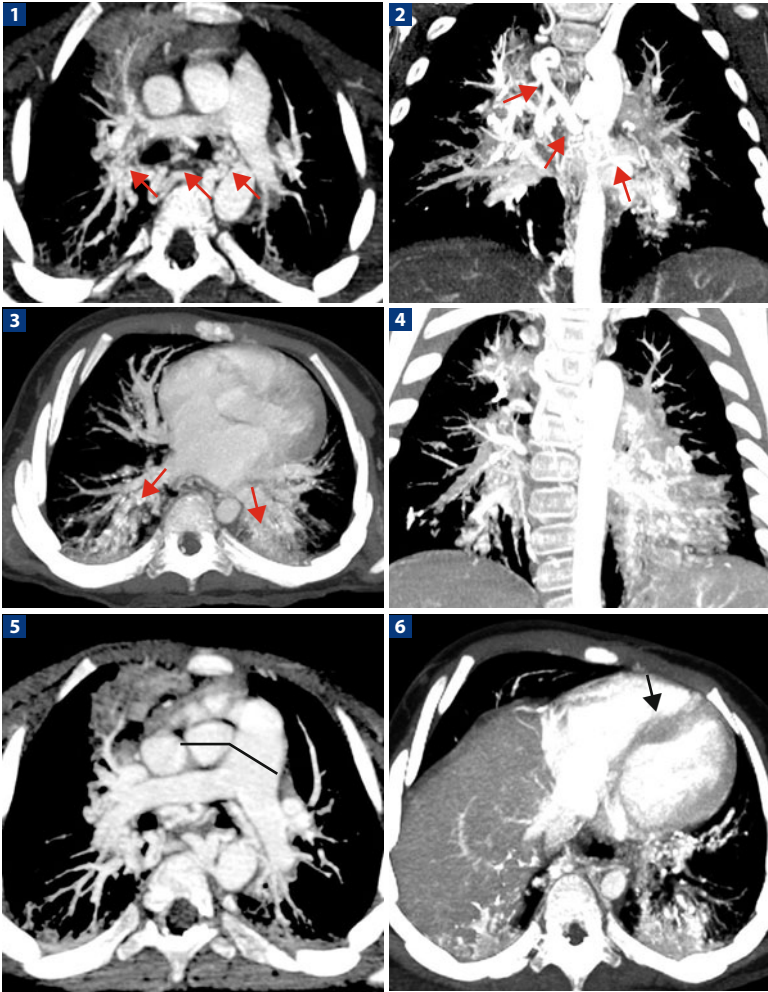
**1** Marked ectasia in the bronchial arteries in the peri-esophageal space and around both main bronchi (*arrows*). **2** Coronal MIP reconstruction documents enlargement of the bronchial arteries originating from the descending aorta and heading toward both pulmonary hila (*arrows*). **3** Axial scan of the base of the lungs shows marked ectasia of the anastomosis between the pulmonary and bronchial arteries, which is not seen under normal conditions (*arrows*). **4** Coronal reformatted images document congestion of the pulmonary arterial circulation. **5** Axial scan shows that the transverse diameter of the pulmonary trunk is greater than the diameter of the ascending aorta. **6** Interventricular septal deviation (*arrow*) as seen on an axial scan performed through the ventricular cavities

## Study Protocol

| | | | |
|---|---|---|---|
| **Patient preparation:** A 6-h fast prior to the examination. | | | |
| **Study volume:** From the pulmonary apex to the diaphragm. | | | |
| **CM volume:** 500-600 mgI (iodine dose) per kg body weight. | | | |
| **Patient weight (kg)** | **< 60** | **< 80** | **> 80** |
| **CM concentration (mgI/mL)** | | | |
| 300 | 100 | 130 | 150 |
| 320 | 95 | 125 | 140 |
| 350 | 85 | 115 | 130 |
| 370 | 80 | 110 | 120 |
| 400 | 75 | 100 | 110 |
| **CM injection flow rate (mL/s)** | **1.6 gI/s** | **1.8 gI/s** | **2.0 gI/s** |
| **CM concentration (mgI/mL)** | | | |
| 300 | 5.3 | 6.0 | 6.7 |
| 320 | 5.0 | 5.6 | 6.2 |
| 350 | 4.6 | 5.1 | 5.7 |
| 370 | 4.3 | 4.8 | 5.4 |
| 400 | 4.0 | 4.5 | 5.0 |

**Pre-contrast scan:** Not necessary.

**Post-contrast scan:**
Arterial phase: Bolus-tracking technique, with two ROIs, one in the ascending thoracic aorta and one in the pulmonary trunk; this is necessary to evaluate the entire pulmonary circulation.

**Comments:** Normally, the caliber of the bronchial arteries does not exceed 1–1.5 mm; values above that are responsible for an increase in the pressure gradient at the level of the thin anastomosis between the pulmonary and the bronchial circulation, resulting in hemoptysis. In the case presented here (pediatric patient with recurrent episodes of hemoptysis), there was congenital enlargement of the bronchial arteries and their anastomoses with the pulmonary circulation. An arterio-arterial shunt caused pulmonary hypertension, with the diameter of the pulmonary artery trunk greater than the diameter of the ascending aorta, and with interventricular septal deviation to the left.

## References

Adelman M, Haponik EF, Bleecker ER et al (1985) Cryptogenetic hemoptysis: clinical features, bronchoscopic findings and natural history in 67 patients. Ann Int Med 102:829-834

Khail A, Fartoukh M, Tassart M et al (2007) Role of MDCT in identification of the bleeding site and the vessels causing hemoptysis. AJR Am J Roentgenol 188:117-125

Peacock AJ (1999) Primary pulmonary hypertension. Thorax 54:1107-1118

# THORAX – Arteriovenous Pulmonary Malformation
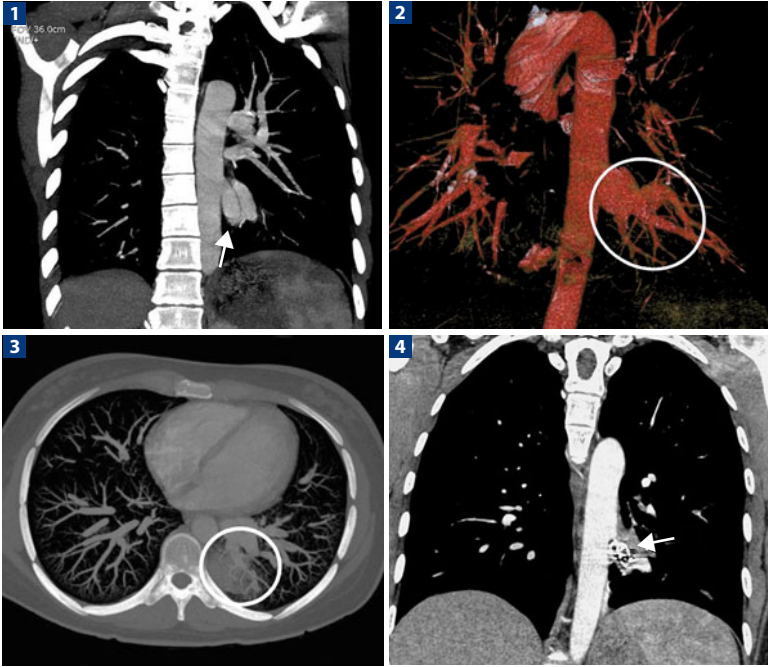


**1** Coronal MIP reconstruction shows a large aberrant vessel (*arrow*) originating from the left profile of the descending thoracic aorta.   **2** Coronal oblique VR reconstruction shows the arterial anastomosis with the left lower pulmonary vein (AVM); this confluence gives rise to the intraparenchymal branches (*oval*). **3** Axial MIP image: vessels that lead from the AVM cause extensive alveolar hemorrhage in the medial segment of the left lower lobe (*oval*).   **4** Coronal MIP reconstruction: evaluation of the AVM after embolization, with exclusion of the abnormal arterial branch (*arrow*)

## Study Protocol

| **Patient preparation:** A 6-h fast prior to the examination. | | | |
|---|---|---|---|

**Study volume:** From the pulmonary apex to the diaphragm.

**CM volume:** 500-600 mgI (iodine dose) per kg body weight.

| Patient weight (kg) | < 60 | < 80 | > 80 |
|---|---|---|---|
| **CM concentration (mgI/mL)** | | | |
| 300 | 100 | 130 | 150 |
| 320 | 95 | 125 | 140 |
| 350 | 85 | 115 | 130 |
| 370 | 80 | 110 | 120 |
| 400 | 75 | 100 | 110 |
| **CM injection flow rate (mL/s)** | **1.6 gI/s** | **1.8 gI/s** | **2.0 gI/s** |
| **CM concentration (mgI/mL)** | | | |
| 300 | 5.3 | 6.0 | 6.7 |
| 320 | 5.0 | 5.6 | 6.2 |
| 350 | 4.6 | 5.1 | 5.7 |
| 370 | 4.3 | 4.8 | 5.4 |
| 400 | 4.0 | 4.5 | 5.0 |

**Pre-contrast scan:** Useful but not necessary.

**Post-contrast scan:**
Arterial phase: Bolus-tracking technique, placing the ROI in the aortic arch.
Portal phase: 50 s after the arterial phase, necessary to evaluate the pulmonary parenchyma and venous vessels.

**Comments:** Patients who have recurrent episodes of hemoptysis should undergo CT angiography of the thoracic aorta, which will highlight or exclude vascular abnormalities of the bronchial vessels and/or vascular lesions, such as malformations and arteriovenous shunts (AVMs). The case illustrated is that of a young patient with recurrent episodes of hemoptysis. Biphasic angio-CT scan, with the aid of volumetric multiplanar reconstructions, revealed an AVM with high arterial flow between the aorta and pulmonary vein, associated with alveolar hemorrhage. This finding guided an appropriate therapeutic approach, i.e., embolization of the AVM.

## References

Bruzzi JF, Martine RJ, Delhaye D et al (2006) Multi-detector row CT of hemoptysis. RadioGraphics 26:3-22

Coulier B (2003) Detection of pulmonary arteriovenous malformations by multislice spiral CT angiography. JBR-BTR 86:28

Nawaz A, Litt HI, Stavropoulos SW et al (2008) Digital subtraction pulmonary arteriography versus multidetector CT in the detection of pulmonary arteriovenous malformations. J Vasc Interv Radiol 19:S1582-S1588

# THORAX – Pulmonary Nodules
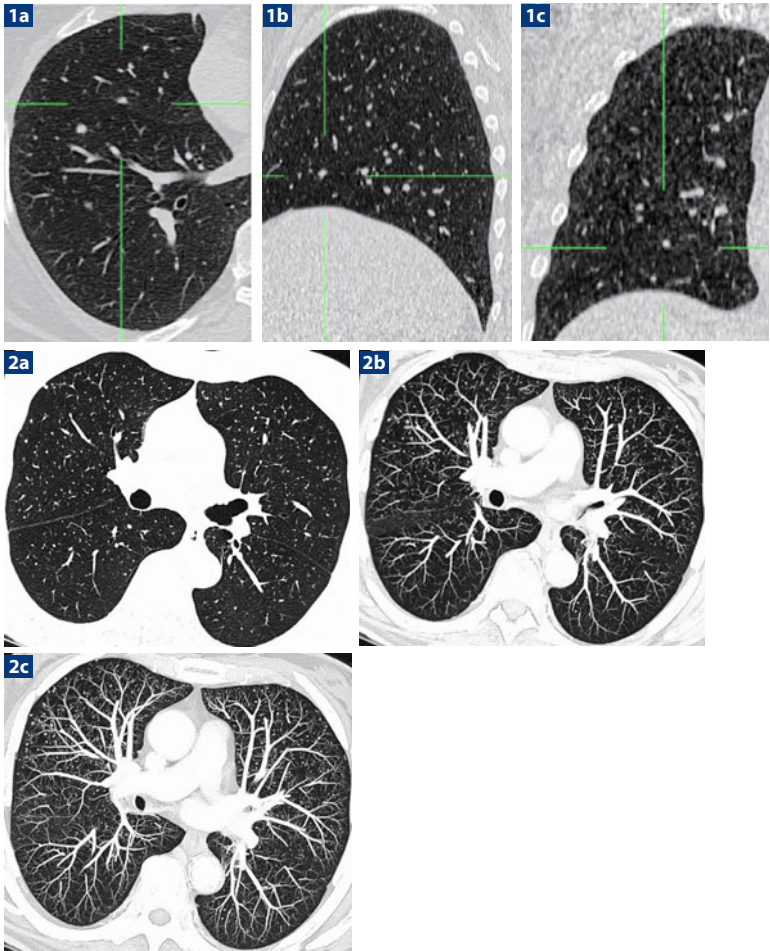
The detection and characterization of pulmonary nodules continues to improve with technological advancements. The increasing use of MDCT has resulted in the more frequent detection of solitary pulmonary nodules. Although the majority of these lesions are benign, lung cancer is an important consideration in the differential diagnosis of solitary pulmonary nodules. The goal of management is to correctly differentiate malignant from benign nodules in order to ensure appropriate treatment.     **1** Multiplanar reconstructions (MPRs): CT scans show a sub-scissural nodule (*arrow*) in the middle lobe in axial (**a**), saggital (**b**) and coronal (**c**) images.     **2** Maximum intensity projections (MIP) scans: 1-mm (**a**), 5-mm (**b**), and 10-mm (**c**) slices for the detection of pulmonary nodules are helpful to differentiate a perivascular nodule from the vessel

## Study Protocol During Follow-up

Recommendations for follow-up and management of nodules < 8 mm detected incidentally at non-screening CT [modified from MacMahon et al. (2005) and Brandman and Ko (2011)]

| Nodule size (mm)[a] | Low-risk patient[b] | High-risk patient[c] |
|---|---|---|
| < 4 | No follow-up needed[d] | Follow-up CT at 12 months; if unchanged, no further follow-up[e] |
| 4–6 | Follow-up CT at 12 months; if unchanged, no further follow-up[e] | Initial follow-up CT at 6–12 months then at 18–24 months if no change[e] |
| 6–8 | Initial follow-up CT at 6–12 months then at 18–24 months if no change | Initial follow-up CT at 3–6 months then at 9–12 and 24 months if no change |
| > 8 | Follow-up CT at around 3, 9, and 24 months, dynamic contrast-enhanced CT, PET, and/or biopsy | Same as for low-risk patient |

**Note:** Newly detected indeterminate nodule in persons 35 years of age or older.
[a] Average of length and width. [b] Minimal or absent history of smoking and other known risk factors. [c] History of smoking or other known risk factors. [d] The risk of malignancy in this category (< 1%) is substantially less than that of an asymptomatic smoker, as evaluated in a baseline CT scan. [e] Non-solid (ground-glass) or partly solid nodules may require longer follow-up to exclude indolent adenocarcinoma.

## References

MacMahon H, Austin JH, Gamsu G et al (2005) Guidelines for management of small pulmonary nodules detected on CT scans: a statement from the Fleischner Society. Radiology 237(2):395-400

Brandman S, Ko J (2011) Pulmonary nodule detection, characterization, and management with multidetector computed tomography. J Thorac Imaging 26(2):90-105

Truong MT, Sabloff BS, Ko JP (2010) Multidetector CT of solitary pulmonary nodules. Radiol Clin North Am 48(1):141-155

Wormanns D, Diederich S (2004) Characterization of small pulmonary nodules by CT. Eur Radiol 14(8):1380-1391

# THORAX – Computer-assisted Detection (CAD)



**1**

Study: 2003-06-23
Img-Num 39 - C1
Diam 2D 11.6/7.2 mm
Av 8.4 mm
Dens Av -46 HU
Max 313 HU
Vol 305.2 cu.mm



**2**

Study: 2004-03-02
Img-Num 46 - C1
Diam 2D 18.9/11.5 mm
Av 10.8 mm
Dens Av -35 HU
Max 299 HU
Vol 658.5 cu.mm
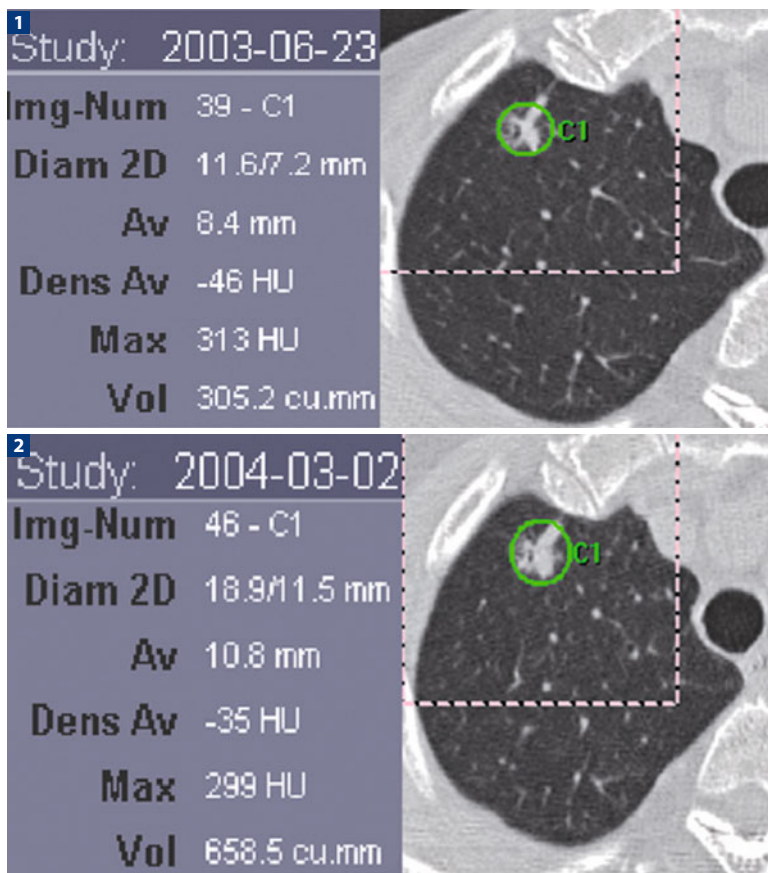
**1**, **2** Although very similar in source images and despite the difficulty in determining and comparing their axial maximum diameters, these two lesions are easily identified using computer-aided detection (CAD). In fact, with computerized schemes the dimensions, volumes, and modifications between baseline and follow-up studies can be better evaluated

# Study Protocol

**General information:** The lung CAD CT device is a CAD tool designed to assist radiologists in the detection of solid pulmonary nodules. Early detection of lung nodules is extremely important for the diagnosis and clinical management of lung cancer. CAD CT allows the computer-guided localization of lesions, close-up inspection of suspected lesions by applying MPR, automatic segmentation and volumetric measurements of lung lesions, visualization of the segmented lesions with perspective volume-rendering (VR) displays or MPR techniques, and the dedicated and flexible reporting of all findings.

## References

Hansell DM, Bankier AA, MacMahon H et al (2008) Fleischner Society: glossary of terms for thoracic imaging. Radiology 246(3):697-722. Epub 2008 Jan 14

Laurent F (2010) Role of CAD for the detection of lung nodules on CT. J Radiol 91(3 Pt 1):259-260

Fraioli F, Serra G, Passariello R (2010) CAD (computed-aided detection) and CADx (computer aided diagnosis) systems in identifying and characterising lung nodules on chest CT: overview of research, developments and new prospects. Radiol Med 115(3):385-402

Sahiner B, Chan HP, Hadjiiski LM et al (2009) Effect of CAD on radiologists' detection of lung nodules on thoracic CT scans: analysis of an observer performance study by nodule size. Acad Radiol 16(12):1518-1530

# THORAX – Lung Cancer, CT Perfusion
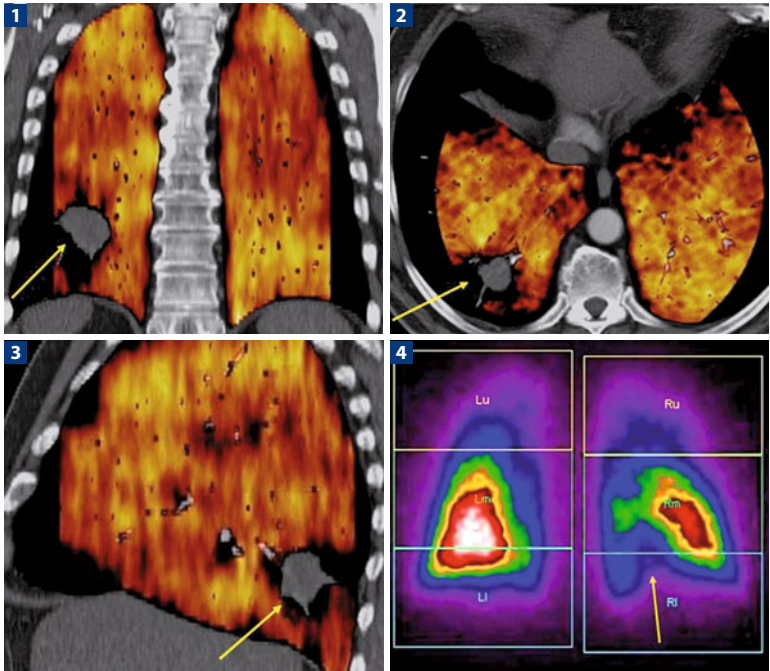


Lung perfusional evaluation by dual-source CT and scintigraphy in a patient with lung cancer (*arrow*). Both methods show a segmental perfusional defect surrounding the neoplasm (localized in a low-posterior region of the right lung). CT findings obtained in coronal (**1**), axial (**2**), and lateral (**3**) planes, respectively. The defect is seen in a posterior projection in the scintigraphic evaluation (**4**)

## Study Protocol

| Patient weight (kg) | < 60 | < 80 | > 80 |
|---|---|---|---|
| **Patient preparation:** A 6-h fast prior to the examination; 18G cannula on the right side. | | | |
| **CM volume:** 500–600 mgI (iodine dose) per kg body weight. | | | |
| **Patient weight (kg)** | **< 60** | **< 80** | **> 80** |
| **CM concentration (mgI/mL)** | | | |
| 300 | 100 | 130 | 150 |
| 320 | 95 | 125 | 140 |
| 350 | 85 | 115 | 130 |
| 370 | 80 | 110 | 120 |
| 400 | 75 | 100 | 110 |
| **CM injection flow rate (mL/s)** | **1.6 gI/s** | **1.8 gI/s** | **2.0 gI/s** |
| **CM concentration (mgI/mL)** | | | |
| 300 | 5.3 | 6.0 | 6.7 |
| 320 | 5.0 | 5.6 | 6.2 |
| 350 | 4.6 | 5.1 | 5.7 |
| 370 | 4.3 | 4.8 | 5.4 |
| 400 | 4.0 | 4.5 | 5.0 |

**Pre-contrast scan:** Images are acquired in a single breath-hold in the caudo-cranial direction from the costophrenic angles to the lung apex. This is important to reduce both diaphragmatic movement at the end of the scan (uncooperative patients) and cone-beam artifacts within the superior vena cava.

**Post-contrast scan:** Two simultaneous helical scans are acquired with two tube voltages, 140 and 80 kV.

**Scan delay:** The scan is initiated with a bolus-tracking technique, in which the arrival of the contrast bolus in the pulmonary trunk is detected at a threshold of 100 HU. Based on common experience, with dual-energy iodine maps, a 7-s scan delay after the threshold should be used.

**Comments:** Lung dual-energy may be useful in the pre-operative evaluation of lung cancer patients. Indeed, perfusional scintigraphy is often necessary before lung surgery to evaluate the outcome of residual status in patients who have undergone pneumonectomy or enlarged lobectomy. Dual-energy CT may be able to obtain similar information, correlating with the results of NMR.

## References

Nazaroğlu H, Ozmen CA, Akay HO et al (2009) 64-MDCT Pulmonary angiography and CT venography in the diagnosis of thromboembolic disease. AJR Am J Roentgenol 192(3):654-661

Stein PD, Yaekoub AY, Matta F et al (2010) Resolution of pulmonary embolism on CT pulmonary angiography. AJR Am J Roentgenol 194(5):1263-1268

Xiong Z, Liu JK, Hu CP et al (2010) Role of immature microvessels in assessing the relationship between CT perfusion characteristics and differentiation grade in lung cancer. Arch Med Res 41(8):611-617

# THORAX – Whole-Thorax Perfusion
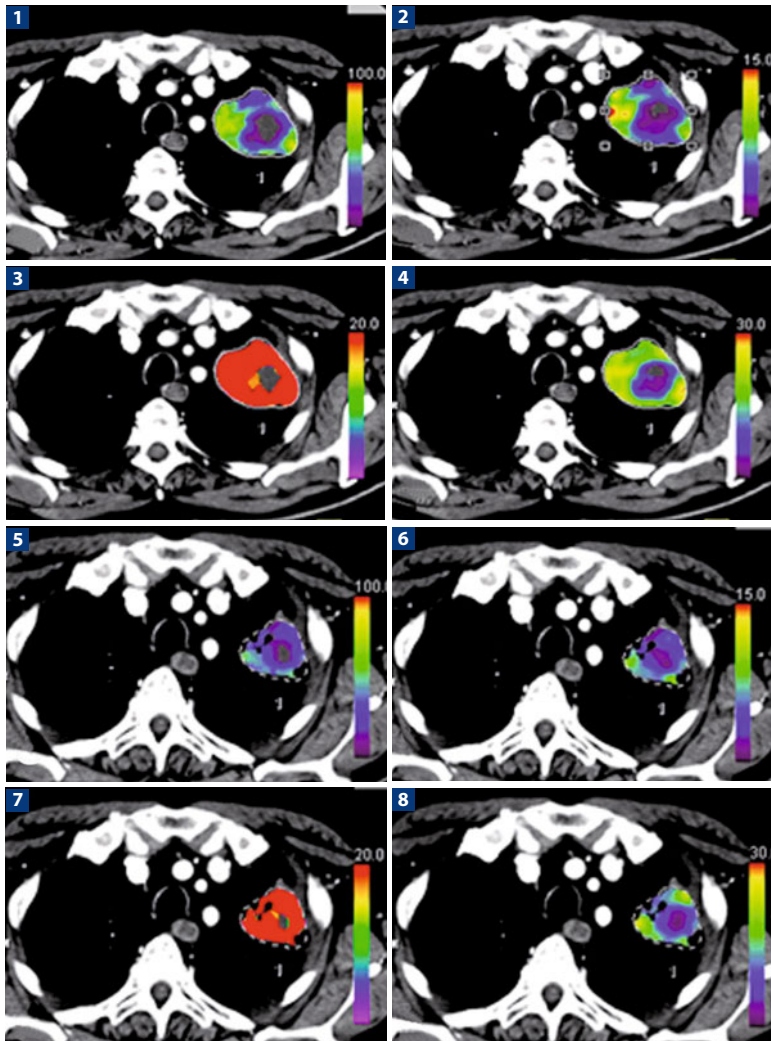


A 66-year-old man with a diagnosis of stage IV adenocarcinoma of the left upper lobe. Axial images show color-coded maps of blood-flow (BF), blood volume (BV), time to peak (TTP), and permeability (PS) before (**1**, **2**, **3**, **4**) and after (**5**, **6**, **7**, **8**) therapy. At follow-up, RECIST (response evaluation criteria in solid tumors) measurements demonstrated a 30% decrease in size (partial response), while CT-p (perfusion CT) evaluation showed a 20% decrease of BF, a 5% increase of BV, a 4% increase in TTP, and a 14% decrease in PS

## Study Protocol

**Patient preparation:** A 6-h fast prior to the examination.

**CM volume:** 60–80 mL of CM according to patient weight.

| Patient weight (kg) | < 60 | < 80 | > 80 |
|---|---|---|---|
| **CM concentration (mgI/mL)** | | | |
| 300 | 100 | 130 | 150 |
| 320 | 95 | 125 | 140 |
| 350 | 85 | 115 | 130 |
| 370 | 80 | 110 | 120 |
| 400 | 75 | 100 | 110 |
| **CM injection flow rate (mL/s)** | **1.6 gI/s** | **1.8 gI/s** | **2.0 gI/s** |
| **CM concentration (mgI/mL)** | | | |
| 300 | 5.3 | 6.0 | 6.7 |
| 320 | 5.0 | 5.6 | 6.2 |
| 350 | 4.6 | 5.1 | 5.7 |
| 370 | 4.3 | 4.8 | 5.4 |
| 400 | 4.0 | 4.5 | 5.0 |

**Scanning protocols:** CM is injected with a single, sharp bolus administered at high injection speed. The rationale of administrating a small amount of contrast at high flow is mainly related to the assumption that immediate tumor enhancement is largely due to the presence of the iodine molecules within the intravascular space and subsequent modifications of the contrast distribution to the first-pass extraction in the extravascular space from the leaking vessels of the neoplastic environment. Thus, as time progresses, iodine accumulation into the extravascular space continues, and the observed tumor enhancement reflects the presence of CM in the intravascular and extravascular spaces. The 65-s acquisition is a technical compromise to enable imaging of both the vascular phase and part of the interstitial phase.
Tube voltage: 100 kV with an automated current modulation system (quality reference set at 120 mAs); effective dose 21.7 ± 1.6 mSv.

**Comments:** CT-p is one of the most interesting tools in the field of oncologic imaging. It is aimed at monitoring disease response or progression after therapy. Its use is based on the assumption that many drugs inhibit the proliferation of neoplastic cells by acting on the vascular network, as increasingly evidenced by the development of therapy protocols that include anti-angiogenic molecules to inhibit blood-vessel growth.

## References

Fraioli F, Anzidei M, Zaccagna F et al (2011) Whole-tumor perfusion CT in patients with advanced lung adenocarcinoma treated with conventional and antiangiogenetic chemotherapy: initial experience. Radiology 259(2):574-582. Epub 2011 Feb 25

Li Y, Yang ZG, Chen TW et al (2008) Whole tumour perfusion of peripheral lung carcinoma: evaluation with first-pass CT perfusion imaging at 64-detector row CT. Clin Radiol 63(6):629-635

# THORAX – COPD, Dual-Energy
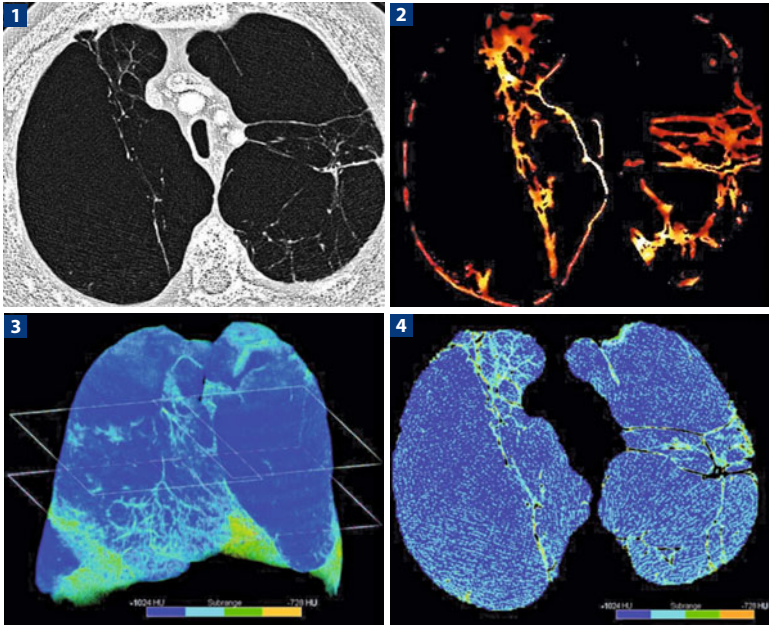


**1** Analysis of air volume and emphysema using dual-source CT. The morphological image in B60 is compared with the results obtained from the automatic assessment of air volumes and emphysematous areas within the lungs on the same axial projection (**3**) and in volume-rendering (**4**). **2** Perfusional analysis of the same case

# Study Protocol

**Patient preparation:** The patient must be able to maintain a breath-hold long enough for the images to be obtained. The patient must be able to stop breathing and to perform a breath-hold at full inspiration and full expiration when instructed to do so. Expiratory scans should be obtained with a medium breath, followed by complete exhalation and a breath-hold at full expiration. The patient should be instructed to take 2 normal breaths, followed by a medium breath, then to exhale completely with a breath-hold at full expiration.

**CM volume:** 500-600 mgI (iodine dose) per kg body weight.

| Patient weight (kg) | < 60 | < 80 | > 80 |
|---|---|---|---|
| **CM concentration (mgI/mL)** | | | |
| 300 | 100 | 130 | 150 |
| 320 | 95 | 125 | 140 |
| 350 | 85 | 115 | 130 |
| 370 | 80 | 110 | 120 |
| 400 | 75 | 100 | 110 |

| CM injection flow rate (mL/s) | 1.6 gI/s | 1.8 gI/s | 2.0 gI/s |
|---|---|---|---|
| **CM concentration (mgI/mL)** | | | |
| 300 | 5.3 | 6.0 | 6.7 |
| 320 | 5.0 | 5.6 | 6.2 |
| 350 | 4.6 | 5.1 | 5.7 |
| 370 | 4.3 | 4.8 | 5.4 |
| 400 | 4.0 | 4.5 | 5.0 |

**Pre-contrast scan:** This can be the only phase acquired. Comparisons between inspiratory and expiratory CT scans can be helpful when air trapping is subtle or diffuse.

**Inspiratory scan:** Helical mode, 0.5-s gantry rotation time, pitch 1.4, 120 kVp, 64 × 0.6-mm (Sensation 64) or 16 × 0.75-mm (Sensation 16) detector configuration CAREDose on*.

**Expiratory scan:** Non-contiguous axial (non-helical) mode, 0.5-s gantry rotation time, 120 kVp, 2 × 1-mm detector configuration with a 20-mm slice interval, CAREDose on*.

**Post-contrast scan:** When lung perfusion is required.

**Scan delay:** Double quantification (pulmonary destruction and CT-p quantification of COPD have been improved over the years, yielding a good method of quantification and allowing appropriate follow-up. Densitometry has been recognized as the most important scheme to quantify pulmonary emphysema.
Recently, different commercial software packages have been used in the determination of lung emphysematous areas, allowing the preoperative evaluation of candidates for lung surgery aimed at volume reduction, or simply for a more accurate follow-up to evaluate the response to bronchodilator therapy.

## References

Hansell DM, Bankier AA, MacMahon H et al (2008) Fleischner Society: glossary of terms for thoracic imaging. Radiology 246(3):697-722. Epub 2008 Jan 14
Bafadhel M, Umar I, Gupta S et al (2011) The Role of CT scanning in multidimensional phenotyping of COPD. Chest 140(3):634-642
Dirksen A (2008) Is CT a new research tool for COPD? Clin Respir J 2(Suppl 1):76-83

# ABDOMEN – Liver. Hemangioma
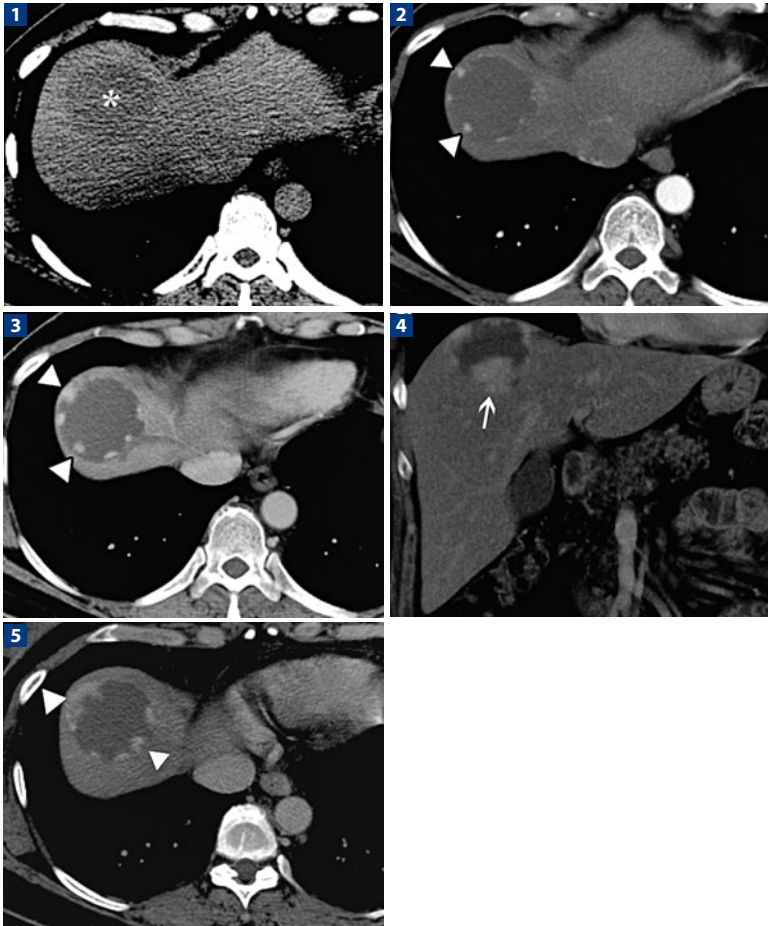


**1** Pre-contrast image shows a hypodense focal hepatic lesion (*asterisk*). **2** In the late arterial phase, areas of peripheral enhancement can be appreciated within the lesion, with a globular appearance (*arrowheads*). Note that the density of the enhanced areas can be superimposed on that of the abdominal aorta in relation to the vascular nature of the angiomatous lesion. **3** Portal phase: centrifugal filling of the lesion with contrast medium (*arrowheads*). **4, 5** Late phase: tendency towards homogeneous filling (*arrow* and *arrowheads*, respectively). In large hemangiomas, internal areas with hypodensities may persist. Wash-out of the enhanced areas is never noted, and the density of these elements is always identical to that of the vessels. The sign most useful for characterizing the lesion is the peripheral and globular enhancement in the arterial phase

## Study Protocol

| Patient preparation: A 6-h fast prior to the examination. | | | |
|---|---|---|---|
| CM volume: 500–600 mgl (iodine dose) per kg body weight. | | | |
| Patient weight (kg) | < 60 | < 80 | > 80 |
| CM concentration (mgl/mL) | | | |
| 300 | 100 | 130 | 150 |
| 320 | 95 | 125 | 140 |
| 350 | 85 | 115 | 130 |
| 370 | 80 | 110 | 120 |
| 400 | 75 | 100 | 110 |
| CM injection flow rate (mL/s) | 1.6 gl/s | 1.8 gl/s | 2.0 gl/s |
| CM concentration (mgl/mL) | | | |
| 300 | 5.3 | 6.0 | 6.7 |
| 320 | 5.0 | 5.6 | 6.2 |
| 350 | 4.6 | 5.1 | 5.7 |
| 370 | 4.3 | 4.8 | 5.4 |
| 400 | 4.0 | 4.5 | 5.0 |
| Pre-contrast scan: Useful. | | | |
| Post-contrast scan: Three phases (late arterial, portal, equilibrium). | | | |
| Scan delay: A bolus-tracking monitoring technique is used. Late arterial phase: 18-23 s after a threshold of 100 HU is reached. Portal phase: 60-70 s from the start of the CM injection. Equilibrium phase: 180 s from the start of the CM injection. | | | |

## References

Kebapci M, Kaya T, Gurbuz E et al (2003) Differentiation of adrenal adenomas (lipid rich and lipid poor) from nonadenomas by use of washout characteristics on delayed enhanced CT. Abdom Imaging 28:709-715

Mayo-Smith WW, Boland GW, Noto RB et al (2001) Sate of the art of adrenal imaging. RadioloGraphics 4:995-1012

Park BK, Kim B, Ko K et al (2006) Adrenal masses falsely diagnosed as adenomas on unenhanced and delayedcontrast-enhanced computed tomography: pathological correlation. Eur Radiol 16:642-647

# ABDOMEN – Liver. Adenoma
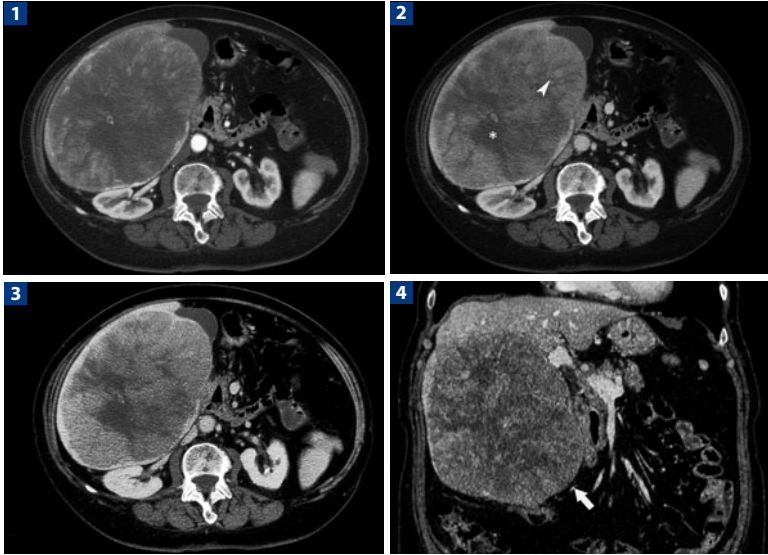


**1** Hepatic arterial phase shows a large, solid, focal hepatic lesion containing a hypervascular component with marked inhomogeneity due to the presence of internal necrotic areas. **2** Portal phase: solid enhancing components (*arrowhead*) can be better differentiated from the hypodense necrotic areas (*asterisk*). **3** Late phase: evident wash-out of the contrast medium. **4** Coronal reformation better demonstrates the size of the lesion and the partly exophytic growth pattern (*arrow*). The remaining liver parenchyma shows no sign of chronic liver disease

## Study Protocol

| Patient preparation: A 6-h fast prior to the examination. | | | |
|---|---|---|---|
| CM volume: 500–600 mgI (iodine dose) per kg body weight. | | | |
| **Patient weight (kg)** | **< 60** | **< 80** | **> 80** |
| **CM concentration (mgI/mL)** | | | |
| 300 | 100 | 130 | 150 |
| 320 | 95 | 125 | 140 |
| 350 | 85 | 115 | 130 |
| 370 | 80 | 110 | 120 |
| 400 | 75 | 100 | 110 |
| **CM injection flow rate (mL/s)** | **1.6 gI/s** | **1.8 gI/s** | **2.0 gI/s** |
| **CM concentration (mgI/mL)** | | | |
| 300 | 5.3 | 6.0 | 6.7 |
| 320 | 5.0 | 5.6 | 6.2 |
| 350 | 4.6 | 5.1 | 5.7 |
| 370 | 4.3 | 4.8 | 5.4 |
| 400 | 4.0 | 4.5 | 5.0 |
| Pre-contrast scan: Useful. | | | |
| Post-contrast scan: 3 phases (late arterial, portal, equilibrium). | | | |
| Scan delay: A bolus-tracking monitoring technique is used. Late arterial phase: 18-23 s after a threshold of 100 HU is reached. Portal phase: 60-70 s from the start of the CM injection. Equilibrium phase: 180 s from the start of the CM injection. | | | |

## References

Brancatelli G, Federle MP, Vullierme MP et al (2006) CT and MR imaging evaluation of hepatic adenoma. J Comput Assist Tomogr 30(5):745-750

Lim AK, Patel N, Gedroyc WM et al (2002) Hepatocellular adenoma: diagnostic difficulties and novel imaging techniques. Br J Radiol 75(896):695-699

Ichikawa T, Federle MP, Grazioli L, Nalesnik M (2000) Hepatocellular adenoma: multiphasic CT and histopathologic findings in 25 patients. Radiology 214(3):861-868

# ABDOMEN – Liver. Focal Nodular Hyperplasia (FNH)
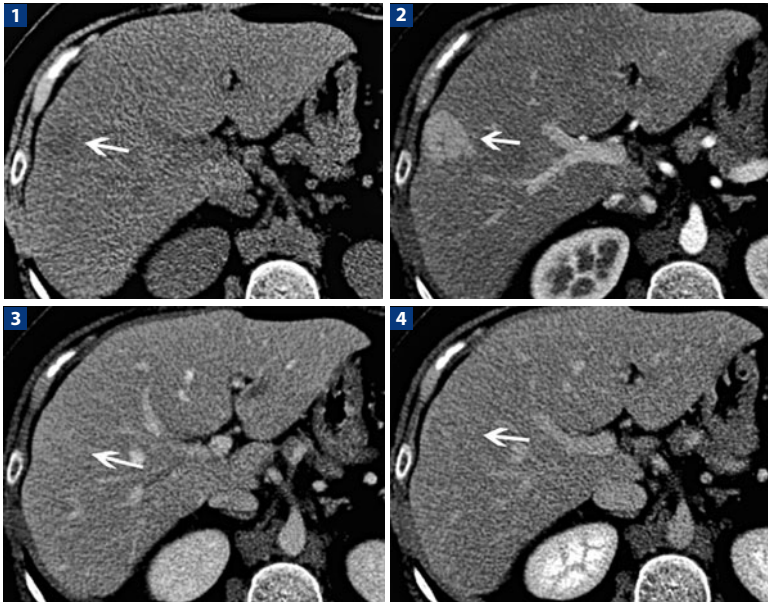


**1** Pre-contrast image shows a slightly hypodense nodular formation compared to the liver parenchyma (*arrow*). **2** Late arterial phase: a solid focal lesion with a lobulated morphology and homogeneous and intense enhancement (*arrow*). **3** Portal-phase: wash-out of the lesion, which is isodense to the liver parenchyma (*arrow*). **4** Late-phase confirms the isodensity of the lesion compared to the liver parenchyma (*arrow*). This aspect is characteristic of benign hypervascular hepatocellular lesions, such as FNH. The absence of a central scar is not an indispensable sign for the diagnosis of FNH, particularly in lesions of small dimensions

## Study Protocol

| Patient preparation: A 6-h fast prior to the examination. | | | |
|---|---|---|---|
| **CM volume:** 500–600 mgI (iodine dose) per kg body weight. | | | |
| **Patient weight (kg)** | **< 60** | **< 80** | **> 80** |
| **CM concentration (mgI/mL)** | | | |
| 300 | 100 | 130 | 150 |
| 320 | 95 | 125 | 140 |
| 350 | 85 | 115 | 130 |
| 370 | 80 | 110 | 120 |
| 400 | 75 | 100 | 110 |
| **CM injection flow rate (mL/s)** | **1.6 gI/s** | **1.8 gI/s** | **2.0 gI/s** |
| **CM concentration (mgI/mL)** | | | |
| 300 | 5.3 | 6.0 | 6.7 |
| 320 | 5.0 | 5.6 | 6.2 |
| 350 | 4.6 | 5.1 | 5.7 |
| 370 | 4.3 | 4.8 | 5.4 |
| 400 | 4.0 | 4.5 | 5.0 |
| **Pre-contrast scan:** Useful. | | | |
| **Post-contrast scan:** 3 phases (late arterial, portal, equilibrium). | | | |
| **Scan delay:** The bolus-tracking monitoring technique is used. Late arterial phase: 18-23 s after a threshold of 100 HU is reached. Portal phase: 60-70 s from the start of the CM injection. Equilibrium phase: 180 s from the start of the CM injection. | | | |

## References

Brancatelli G, Federle MP, Katyal S, Kapoor V (2002) Hemodynamic characterization of focal nodular hyperplasia using three-dimensional volume-rendered multidetector CT angiography. AJR Am J Roentgenol 179:81-85

Lin MC, Tsay PK, Ko SF et al (2008) Triphasic dynamic CT findings of 63 hepatic focal nodular hyperplasia in 46 patients: correlation with size and pathological findings. Abdom Imaging 33:301-307

Xu AM, Cheng HY, Chen D et al (2002) Plane and weighted tri-phase helical CT findings in the diagnosis of liver focal nodular hyperplasia. Hepatobiliary Pancreat Dis Int 1:219-223

# ABDOMEN – Liver. Hepatocellular Carcinoma (HCC)
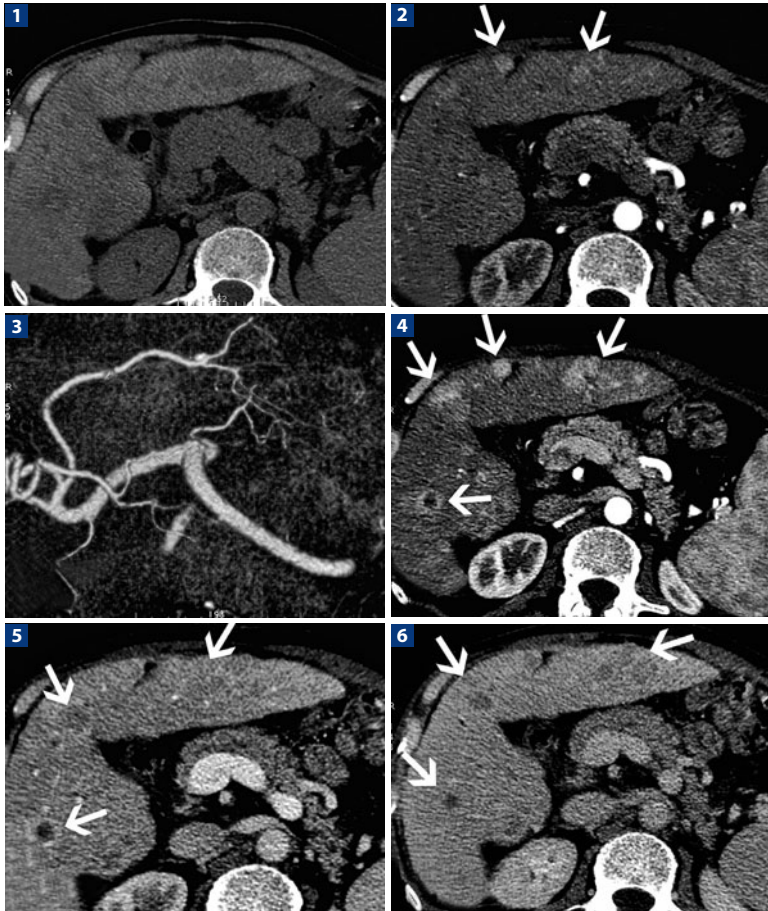


**1** Pre-contrast study: cirrhotic alterations of the liver, with widespread irregularities of the margins due to the presence of multiple nodularities. **2** Post-contrast study: early arterial phase shows optimal vascular enhancement, with only a slight enhancement of the multiple hypervascular HCC nodules (*arrows*). **3** Three-dimensional vascular reconstruction using a MIP algorithm demonstrates pathologic circles in segment II, site of a large HCC nodule. **4** Post-contrast study: late arterial phase provides the best visualization of the multiple HCC nodules, which display an intense hypervascularity. The number of nodules identified is markedly greater than in the early arterial phase. **5** Post-contrast study: portal phase demonstrates the typical wash-out of the HCC nodules, although not complete in all nodules. **6** Post-contrast study: late phase provides better evidence of the wash-out typical of malignant neoplastic lesions, with an increase in contrast between the lesion and the adjacent hepatic parenchyma

## Study Protocol

| Patient weight (kg) | < 60 | < 80 | > 80 |
|---|---|---|---|

**Patient preparation:** A 6-h fast prior to the examination.

**CM volume:** 500–600 mgI (iodine dose) per kg body weight.

| Patient weight (kg) | < 60 | < 80 | > 80 |
|---|---|---|---|
| **CM concentration (mgI/mL)** | | | |
| 300 | 100 | 130 | 150 |
| 320 | 95 | 125 | 140 |
| 350 | 85 | 115 | 130 |
| 370 | 80 | 110 | 120 |
| 400 | 75 | 100 | 110 |
| **CM injection flow rate (mL/s)** | **1.6 gI/s** | **1.8 gI/s** | **2.0 gI/s** |
| **CM concentration (mgI/mL)** | | | |
| 300 | 5.3 | 6.0 | 6.7 |
| 320 | 5.0 | 5.6 | 6.2 |
| 350 | 4.6 | 5.1 | 5.7 |
| 370 | 4.3 | 4.8 | 5.4 |
| 400 | 4.0 | 4.5 | 5.0 |

**Pre-contrast scan:** Useful.

**Post-contrast scan:** 3 phases (late arterial, portal, equilibrium).
Early arterial phase: Useful only for the analysis of vascular anatomy.

**Scan delay:** The bolus-tracking monitoring technique is used.
Early arterial phase: 10 s after a threshold of 100 HU is reached.
Late arterial phase: 18-23 s after the 100-HU threshold of 100 HU.
Portal phase: 60-70 s from the start of the CM injection.
Equilibrium phase: 180 s from the start of the CM injection.

## References

Iannaccone R, Laghi A, Catalano C et al (2005) Hepatocellular carcinoma: role of unenhanced and delayed phase multi-detector row helical CT in patients with cirrhosis. Radiology 234:460-467

Laghi A, Iannaccone R, Rossi P et al (2003) Hepatocellular carcinoma: detection with triple-phase multi-detector row helical CT in patients with chronic hepatitis. Radiology 226:543-549

Mori K, Yoshioka H, Takahashi N et al (2005) Triple arterial phase dynamic MRI with sensitivity encoding for hypervascular hepatocellular carcinoma: comparison of the diagnostic accuracy among the early, middle, late, and whole triple arterial phase imaging. AJR Am J Roentgenol 184:63-69
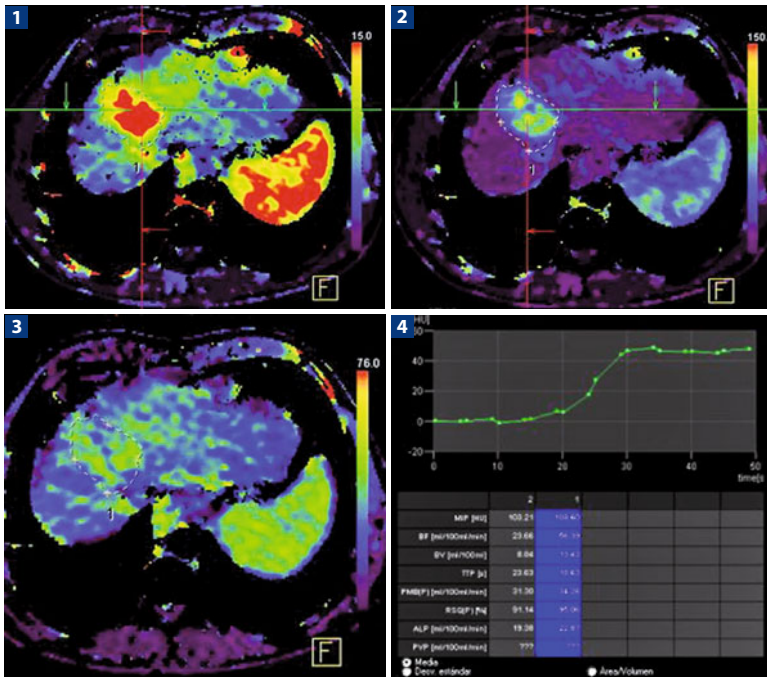
Hepatocellular carcinoma treated with anti-angiogenic inhibitors does not correlate well with RECIST criteria for tumoral response. Perfusion imaging can visualize the anti-angiogenic effect, assessing shrinkage of the tumoral tissue. **1** Perfusion analysis (color map: blood volume, ml/100 ml, axial plane) in this BV map, obtained with a dedicated software application, shows an increase in volume (*reference lines*) as expected in a neoplastic angiogenesis. **2** Perfusion analysis (color map: blood flow, axial plane) shows a large increase in blood flow (*green areas*) in the tumor with respect to the adjacent tissue. **3** Perfusion analysis (color map: permeability surface area product, axial plane) shows a large increase in permeability (*green areas*) in the peripheral tumor area, as expected for inflammation tissues (arterial angiogenesis behavior; note similar values to spleen). The center core of the tumor shows lower permeability values, as expected for well-shaped vessels. **4** Perfusion parameters: quantitative evaluation. (Courtesy of Jordie Rimola MD, Department of Radiology, Hospital Clinic, Barcelona, Spain)

## Study Protocol

**CT scan parameters:**
kV: 80
mAs: 145
Thickness: 4 mm
Acquisition length: 28 cm

**Patient preparation:** A 6-h fast prior to the examination.
Before scanning: 20 mg butyl scopolamine (Buscopan, Boehringer, Ingelheim, Germany) is injected to suppress peristalsis.

**CM volume:** 60-80 mL of CM according to patient weight.

| CM injection flow rate (mL/s) | 1.6 gI/s | 1.8 gI/s | 2.0 gI/s |
|---|---|---|---|
| **CM concentration (mgI/mL)** | | | |
| 300 | 5.3 | 6.0 | 6.7 |
| 320 | 5.0 | 5.6 | 6.2 |
| 350 | 4.6 | 5.1 | 5.7 |
| 370 | 4.3 | 4.8 | 5.4 |
| 400 | 4.0 | 4.5 | 5.0 |

**Pre-contrast scan:** Baseline CT images without CM and with a thickness of 2.5–5.0 mm are acquired to locate liver lesion and to select the volume for the perfusion scans.

**Post-contrast scan:** 40 contiguous sections with 5-s delay are obtained at 2.2 s during the first 30 s and at 5 s during the last 30 s (80 kV, 145 mAs, 4-cm scanning field of view, 512 × 512 mm matrix).

## References

Petralia G, Fazio N, Bonello L et al (2011) Perfusion computed tomography in patients with hepatocellular carcinoma treated with thalidomide: initial experience. J Comput Assist Tomogr 35(2):195-201. PubMed PMID: 21412089

Ng CS, Chandler AG, Wei W et al (2011) Reproducibility of CT Perfusion parameters in liver tumors and normal liver. Radiology Jul 25. [Epub ahead of print] PubMed PMID: 21788525

Spira D, Schulze M, Sauter A et al (2011) Volume perfusion-CT of the liver: Insights and applications. Eur J Radiol May 2. [Epub ahead of print] PubMed PMID: 21543180
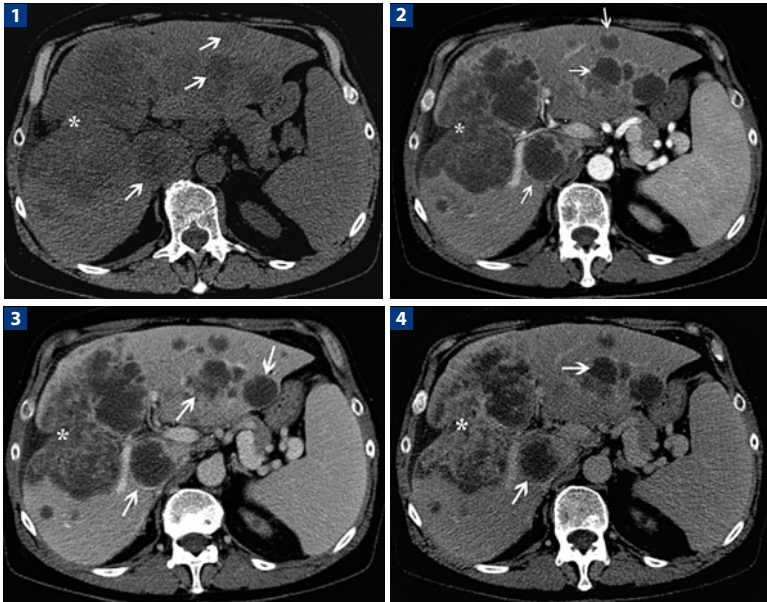
**1** Pre-contrast study highlights numerous hypodense focal hepatic lesions (*arrows*). A lesion with larger dimensions shows an associated capsular retraction (*asterisk*), a typical sign of malignancy and in this case highly suggestive of cholangiocarcinoma. **2** Arterial phase: all lesions (*arrows*) appear frankly hypovascular with respect to the surrounding hepatic parenchyma. **3** Portal phase: improved demarcation of the lesions from the hepatic parenchyma, with evidence of enhancement of the solid components (*arrows*). **4** Late phase: late enhancement of the lesions (more evident in the lesion of greater dimensions), which is characteristic of the stromal nature of the tumor (*arrows* and *asterisk*)

## Study Protocol

| Patient preparation: A 6-h fast prior to the examination. | | | |
|---|---|---|---|
| **CM volume:** 500–600 mgI (iodine dose) per kg body weight. | | | |
| **Patient weight (kg)** | **< 60** | **< 80** | **> 80** |
| **CM concentration (mgI/mL)** | | | |
| 300 | 100 | 130 | 150 |
| 320 | 95 | 125 | 140 |
| 350 | 85 | 115 | 130 |
| 370 | 80 | 110 | 120 |
| 400 | 75 | 100 | 110 |
| **CM injection flow rate (mL/s)** | **1.6 gI/s** | **1.8 gI/s** | **2.0 gI/s** |
| **CM concentration (mgI/mL)** | | | |
| 300 | 5.3 | 6.0 | 6.7 |
| 320 | 5.0 | 5.6 | 6.2 |
| 350 | 4.6 | 5.1 | 5.7 |
| 370 | 4.3 | 4.8 | 5.4 |
| 400 | 4.0 | 4.5 | 5.0 |
| **Pre-contrast scan:** Useful. | | | |
| **Post-contrast scan:** 3 phases (late arterial, portal, equilibrium). | | | |
| **Scan delay:** The bolus-tracking monitoring technique is used.<br>Late arterial phase: 18-23 s after the threshold of 100 HU is reached.<br>Portal phase: 60–70 s from the start of the CM injection.<br>Equilibrium phase: 180 s from the start of the CM injection. | | | |

## References

Choi YH, Lee JM, Lee JY et al (2008) Biliary malignancy: value of arterial, pancreatic, and hepatic phase imaging with multidetector-row computed tomography. J Comput Assist Tomogr 32(3):362-368

Kim NR, Lee JM, Kim SH et al (2008) Enhancement characteristics of cholangiocarcinomas on mutiphasic helical CT: emphasis on morphologic subtypes. Clin Imaging 32(2):114-120

Uchida M, Ishibashi M, Tomita N et al (2005) Hilar and suprapancreatic cholangiocarcinoma: value of 3D angiography and multiphase fusion images using MDCT. AJR Am J Roentgenol 184(5):1572-1577
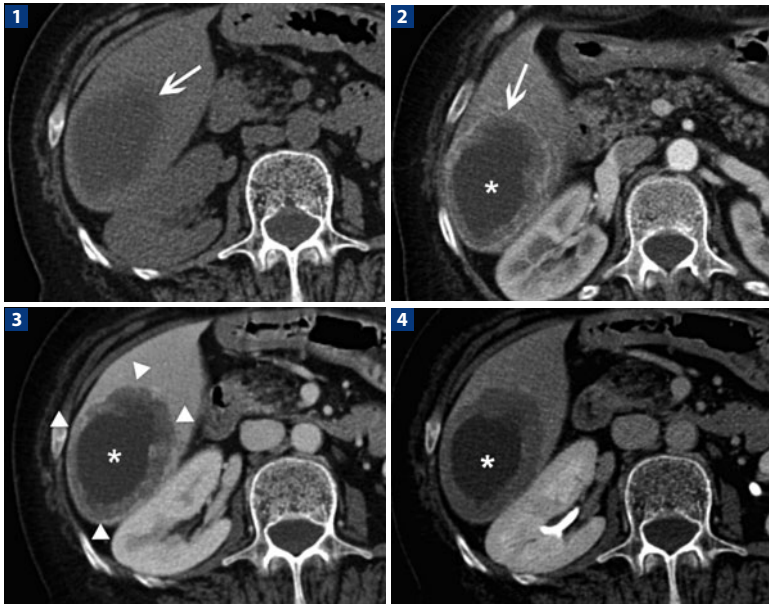
**1** Pre-contrast study: a hypodense nodular lesion in hepatic segment VI, with poorly defined margins (*arrow*). **2** Late arterial phase shows a hypovascular metastasis but with peripheral enhancement demarcating the vital neoplastic tissue (*arrow*) from the necrotic center (*asterisk*). **3** Portal phase demonstrates enhancement of the peripheral vital tissue (*arrowheads*) and the hypodensity of the necrotic central portion. **4** In the equilibrium phase, enhancement of the peripheral portion becomes more homogeneous; the central necrotic portion appears more evident (*asterisk*)

## Study Protocol

| Patient weight (kg) | < 60 | < 80 | > 80 |
|---|---|---|---|

**Patient preparation:** A 6-h fast prior to the examination.

**CM volume:** 500–600 mgI (iodine dose) per kg body weight.

| Patient weight (kg) | < 60 | < 80 | > 80 |
|---|---|---|---|
| **CM concentration (mgI/mL)** | | | |
| 300 | 100 | 130 | 150 |
| 320 | 95 | 125 | 140 |
| 350 | 85 | 115 | 130 |
| 370 | 80 | 110 | 120 |
| 400 | 75 | 100 | 110 |
| **CM injection flow rate (mL/s)** | **1.6 gI/s** | **1.8 gI/s** | **2.0 gI/s** |
| **CM concentration (mgI/mL)** | | | |
| 300 | 5.3 | 6.0 | 6.7 |
| 320 | 5.0 | 5.6 | 6.2 |
| 350 | 4.6 | 5.1 | 5.7 |
| 370 | 4.3 | 4.8 | 5.4 |
| 400 | 4.0 | 4.5 | 5.0 |

**Pre-contrast scan:** Useful to detect dystrophic calcification (mucinous tumor).

**Post-contrast scan:** Phases: Only 2 phases (venous and equilibrium), since late arterial phase is unnecessary in the characterization of hypovascular liver metastasis. However, if surgical intervention is needed, late arterial phase may be useful to depict the vascular anatomy (surgical planning or interventional radiology). Since oncology patients undergo several follow-up examinations, it is advisable to use arterial phase only at the first evaluation, optimizing the number of CT scans for subsequent follow-up.

**Scan delay:** The bolus-tracking monitoring technique is used.
Late arterial phase: 18–23 s after a threshold of 100 HU is reached.
Portal phase: 60–70 s from the start of the CM injection.
Equilibrium phase: 180 s from the start of the CM injection.

## References

Dawson P, Blomley M (2002) The value of mathematical modelling in understanding contrast enhancement in CT with particular reference to the detection of hypovascular liver metastases. Eur J Radiol 41:222-236

Silverman PM (2006) Liver metastases: imaging considerations for protocol development with multislice CT (MSCT). Cancer Imaging 6:175-181

Soyer P, Poccard M, Boudiaf M et al (2004) Detection of hypovascular hepatic metastases at triple-phase helical CT: sensitivity of phases and comparison with surgical and histopathologic findings. Radiology 231:413-420

# ABDOMEN – Liver. Hypervascular Metastases from Renal Cell Carcinoma



**1** In the baseline study: the lesion is not evident due to the absence of contrast with the surrounding hepatic parenchyma.  **2** Late arterial phase shows marked enhancement of the metastatic lesion (*arrow*) located in segment VI, now clearly differentiated from the surrounding parenchyma.  **3** Partial wash-out of the central portion of the lesion (*asterisk*), indicative of malignancy.  **4** In the equilibrium phase, a complete wash-out of the lesion, of which the peripheral portion is still moderately hypodense compared to the surrounding hepatic parenchyma, can be appreciated

## Study Protocol

| **Patient preparation:** A 6-h fast prior to the examination. | | | |
| --- | --- | --- | --- |
| **CM volume:** 500–600 mgI (iodine dose) per kg body weight. | | | |
| **Patient weight (kg)** | **< 60** | **< 80** | **> 80** |
| **CM concentration (mgI/mL)** | | | |
| 300 | 100 | 130 | 150 |
| 320 | 95 | 125 | 140 |
| 350 | 85 | 115 | 130 |
| 370 | 80 | 110 | 120 |
| 400 | 75 | 100 | 110 |
| **CM injection flow rate (mL/s)** | **1.6 gI/s** | **1.8 gI/s** | **2.0 gI/s** |
| **CM concentration (mgI/mL)** | | | |
| 300 | 5.3 | 6.0 | 6.7 |
| 320 | 5.0 | 5.6 | 6.2 |
| 350 | 4.6 | 5.1 | 5.7 |
| 370 | 4.3 | 4.8 | 5.4 |
| 400 | 4.0 | 4.5 | 5.0 |
| **Pre-contrast scan:** Useful. | | | |
| **Post-contrast scan:** At least 3 phases (arterial, venous, and equilibrium); in oncology patients with hypervascular tumors (renal neoplasia, carcinoids, colon cancer, corio carcinoma, breast cancer, melanoma, neuroendocrine tumors, ovarian cystadenocarcinoma, sarcoma, pheochromocytoma) all three phases must be performed because, as in the example, the lesion may be homogenous with the surrounding liver parenchyma. | | | |
| **Scan delay:** The bolus-tracking monitoring technique is used. Late arterial phase: 18-23 s after a threshold of 100 HU is reached. Portal phase: 60–70 s from the start of the CM injection. Equilibrium phase: 180 s from the start of the CM injection. | | | |

## References

Ascenti G, Visalli C, Genitori A et al (2004) Multiple hypervascular pancreatic metastases from renal cell carcinoma: dynamic MR and spiral CT in three cases. Clin Imaging 28:349-352

Meyer BC, Frericks BB, Voges M et al (2008) Visualization of hypervascular liver lesions during TACE: comparison of angiographic C-arm CT and MDCT. AJR Am J Roentgenol 190:W263-269

Namasivayam S, Salman K, Mittal PK et al (2007) Hypervascular hepatic focal lesions: spectrum of imaging features. Curr Probl Diagn Radiol 36:107-123
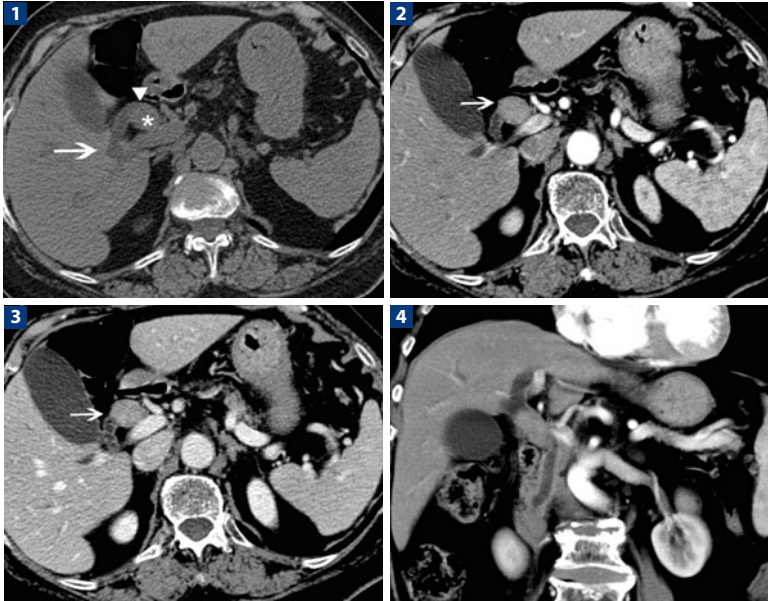
**1** Non-enhanced axial scan at the level of the hepatic hilum highlights a dilatation of the main bile duct (*arrowhead*) and the first intrahepatic branches (*arrow*). Distal to the dilatation of the main bile duct, a rounded mass with well-defined margins and soft-tissue density can be appreciated (*asterisk*). **2** Late arterial phase shows enhancement of the solid tissue (*arrow*) located within the lumen of the main bile duct, consistent with intraductal carcinoma. **3** Portal phase shows persistent enhancement of the intraductal lesion (*arrow*); this scan demonstrates intraluminal growth without infiltration of the surrounding adipose tissue. **4** The coronal MPR in the portal phase shows the longitudinal extension of the intraductal lesion and proximal dilatation of the biliary tract

## Study Protocol

| Patient preparation: A 6-h fast prior to the examination. | | | |
|---|---|---|---|
| **CM volume:** 500–600 mgI (iodine dose) per kg body weight. | | | |
| **Patient weight (kg)** | **< 60** | **< 80** | **> 80** |
| **CM concentration (mgI/mL)** | | | |
| 300 | 100 | 130 | 150 |
| 320 | 95 | 125 | 140 |
| 350 | 85 | 115 | 130 |
| 370 | 80 | 110 | 120 |
| 400 | 75 | 100 | 110 |
| **CM injection flow rate (mL/s)** | **1.6 gI/s** | **1.8 gI/s** | **2.0 gI/s** |
| **CM concentration (mgI/mL)** | | | |
| 300 | 5.3 | 6.0 | 6.7 |
| 320 | 5.0 | 5.6 | 6.2 |
| 350 | 4.6 | 5.1 | 5.7 |
| 370 | 4.3 | 4.8 | 5.4 |
| 400 | 4.0 | 4.5 | 5.0 |
| **Pre-contrast scan:** Useful. | | | |
| **Post-contrast scan:** 3 phases (late arterial, portal, equilibrium). | | | |
| **Scan delay:** The bolus-tracking monitoring technique is used. Late arterial phase: 18-23 s after a threshold of 100 HU is reached. Portal phase: 60-70 s from the start of the CM injection. Equilibrium phase: 180 s from the start of the CM injection. | | | |

## References

Itatsu K, Fujii T, Sasaki M et al (2007) Intraductal papillary cholangiocarcinoma and atypical biliary epithelial lesions confused with intrabiliary extension of metastatic colorectal carcinoma. Hepatogastroenterology 54:677-680

Ji Y, Fan J, Zhou J et al (2008) Intraductal papillary neoplasms of bile duct. A distinct entity like its counterpart in pancreas. Histol Histopathol 23:41-50

Kim NR, Lee JM, Kim SH et al (2008) Enhancement characteristics of cholangiocarcinomas on mutiphasic helical CT: emphasis on morphologic subtypes. Clin Imaging 32:114-120
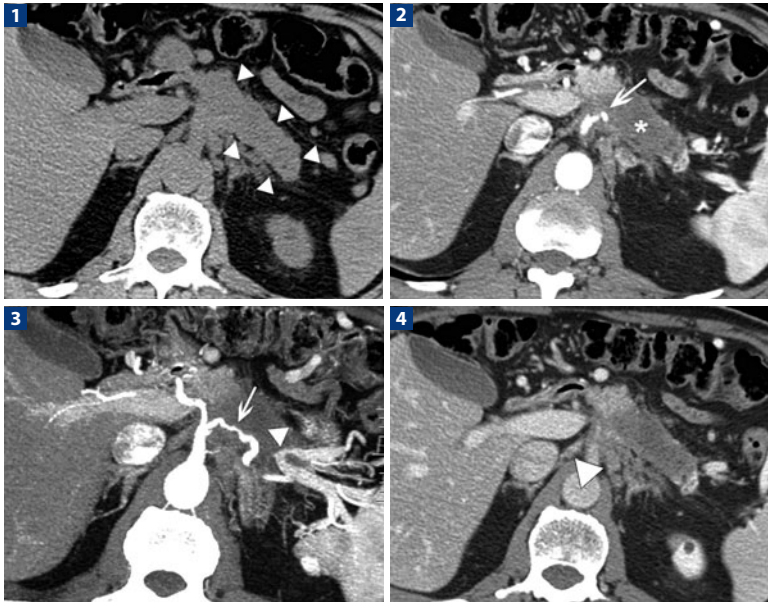
**1** Pre-contrast axial scan shows a solid lesion with irregular margins (*arrowheads*) in the body of the pancreas. While alteration of the anterior peri-pancreatic adipose tissue can be appreciated, posteriorly it is impossible to define the relationship with the vascular structure.   **2** Post-contrast axial image in the pancreatic phase evidences a voluminous, newly formed, solid tissue (*asterisk*) moderately hypovascular compared to the surrounding pancreatic parenchyma, at the level of the pancreas body-head. Signs of infiltration of the peri-pancreatic adipose tissue anteriorly and of the anterior pararenal fascia posteriorly can be seen; there is also encasement of the celiac tripod and of the origin of the splenic artery (*arrow*).   **3** Axial MIP reconstruction in the pancreatic phase shows infiltration of the celiac tripod and the splenic artery, with a reduced diameter of the pancreas and diffuse parietal irregularity (*arrow*). In this phase, there is already complete occlusion of the splenic vein (*arrowhead*), with evidence of collateral circulation.   **4** Post-contrast axial scan in the portal phase confirms a mass in the body of the pancreas, with infiltration of the peri-pancreatic adipose tissue anteriorly and of the anterior pararenal fascia posteriorly; para-aortic lymphadenopathies are also evident (*arrowhead*)

## Study Protocol

| Patient weight (kg) | < 60 | < 80 | > 80 |
|---|---|---|---|

**Patient preparation:** A 6-h fast prior to the examination.

**CM volume:** 500–600 mgI (iodine dose) per kg body weight.

| Patient weight (kg) | < 60 | < 80 | > 80 |
|---|---|---|---|
| **CM concentration (mgI/mL)** | | | |
| 300 | 100 | 130 | 150 |
| 320 | 95 | 125 | 140 |
| 350 | 85 | 115 | 130 |
| 370 | 80 | 110 | 120 |
| 400 | 75 | 100 | 110 |
| **CM injection flow rate (mL/s)** | **1.6 gI/s** | **1.8 gI/s** | **2.0 gI/s** |
| **CM concentration (mgI/mL)** | | | |
| 300 | 5.3 | 6.0 | 6.7 |
| 320 | 5.0 | 5.6 | 6.2 |
| 350 | 4.6 | 5.1 | 5.7 |
| 370 | 4.3 | 4.8 | 5.4 |
| 400 | 4.0 | 4.5 | 5.0 |

**Pre-contrast scan:** Useful.

**Post-contrast scan:** 2 phases (pancreatic phase, portal phase).

**Scan delay:** The bolus-tracking monitoring technique is used.
Pancreatic phase: 28-33 s after the threshold of 100 HU is reached.
Portal phase: 60–70 s from the start of the CM injection.

## References

Brennan DD, Zamboni GA, Raptopoulos VD, Kruskal JB (2007) Comprehensive preoperative assessment of pancreatic adenocarcinoma with 64-section volumetric CT. RadioGraphics 27:1653-1666

Chaudhari VV, Raman SS, Vuong NL et al (2007) Pancreatic cystic lesions: discrimination accuracy based on clinical data and high resolution CT features. J Comput Assist Tomogr 31:860-867

Gomez D, Rahman SH, Won LF et al (2006) Characterization of malignant pancreatic cystic lesions in the background of chronic pancreatitis. JOP 7:465-472

# ABDOMEN – Pancreas. Serous Cystic Neoplasm
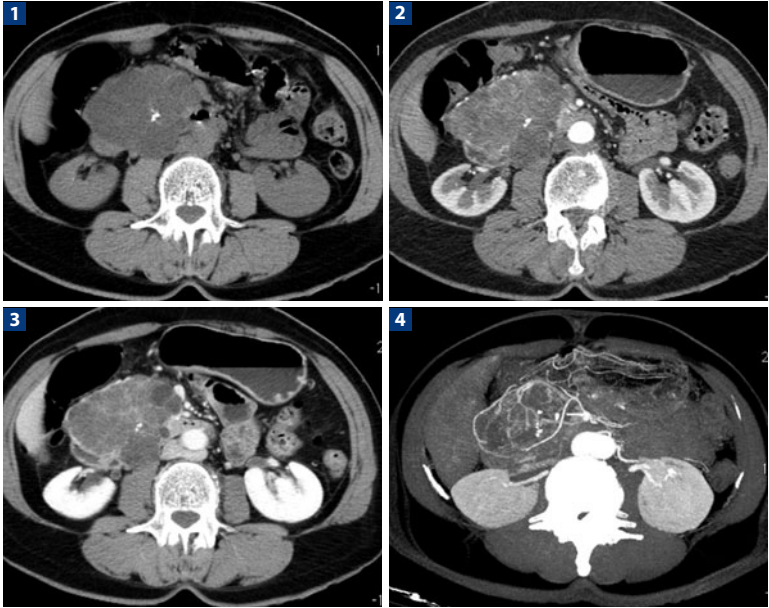


**1** Pre-contrast axial scan shows a round inhomogeneous mass encapsulated by the fibrous tissue of the head of the pancreas, with associated calcification of the cyst wall. **2** Post-contrast axial image in the pancreatic phase: a voluminous and inhomogeneous mass with diffuse parietal irregularity can be seen. The mass is moderately hypovascular compared with the pancreatic parenchymal enhancement, as seen at the level of the pancreas body-head. **3** Post-contrast axial scan in the portal phase: the mass in the head of the pancreas shows enhancement of the cystic wall and internal septa, and the presence of another associated peripheral cyst. **4** Axial MIP reconstruction in the pancreatic phase shows the distribution of the pancreatic and peri-pancreatic vessels surrounding the voluminous pancreatic mass

## Study Protocol

| Patient preparation: A 6-h fast prior to the examination. | | | |
|---|---|---|---|
| **CM volume:** 500–600 mgI (iodine dose) per kg body weight. | | | |
| **Patient weight (kg)** | **< 60** | **< 80** | **> 80** |
| **CM concentration (mgI/mL)** | | | |
| 300 | 100 | 130 | 150 |
| 320 | 95 | 125 | 140 |
| 350 | 85 | 115 | 130 |
| 370 | 80 | 110 | 120 |
| 400 | 75 | 100 | 110 |
| **CM injection flow rate (mL/s)** | **1.6 gI/s** | **1.8 gI/s** | **2.0 gI/s** |
| **CM concentration (mgI/mL)** | | | |
| 300 | 5.3 | 6.0 | 6.7 |
| 320 | 5.0 | 5.6 | 6.2 |
| 350 | 4.6 | 5.1 | 5.7 |
| 370 | 4.3 | 4.8 | 5.4 |
| 400 | 4.0 | 4.5 | 5.0 |
| **Pre-contrast scan:** Useful. | | | |
| **Post-contrast scan:** 2 phases (pancreatic, portal). | | | |
| **Scan delay:** The bolus-tracking monitoring technique is used. Pancreatic phase: 28–33 s after a threshold of 100 HU is reached. Portal phase: 60-70 s from the start of the CM injection. | | | |

## References

Edirimanne S, Connor SJ (2008) Incidental pancreatic cystic lesions. World J Surg 32(9):2028-2037

Garcea G, Ong SL, Rajesh A et al (2008) Cystic lesions of the pancreas. A diagnostic and management dilemma. Pancreatology 8(3):236-251

Sahani D, Prasad S, Saini S et al (2002) Cystic pancreatic neoplasms evaluation by CT and magnetic resonance cholangiopancreatography. Gastrointest Endosc Clin N Am 12(4):657-672

# ABDOMEN – Pancreas. Intraductal Papillary Mucinous Neoplasm (IPMN)
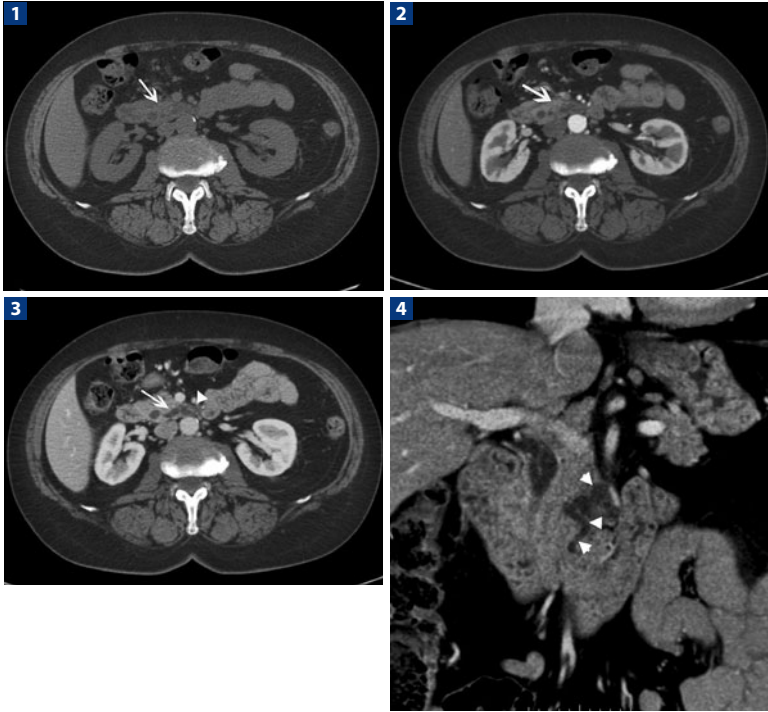


**1** Pre-contrast axial scan shows a swelling of the uncinate process (*arrow*), which appears mildly hypodense to the surrounding pancreatic parenchyma.    **2** Post-contrast axial scan in the pancreatic phase: evident enhancement of the normal pancreatic parenchyma is sharply contrasted with the hypodensity of the region of the uncinate process, which has a cystic-like appearance (*arrow*).    **3** Post-contrast axial scan in the portal phase: the cystic-like ectasia (*arrowhead*) of a secondary ventral duct (*arrow*) draining the region of the uncinate process is compatible with a diagnosis of intraductal mucinous tumor.    **4** Coronal reformation in the portal phase: the entire course of the secondary dilated ventral duct and the cystic-like appearance of the distal tract are shown

## Study Protocol

| Patient preparation: A 6-h fast prior to the examination. | | | |
|---|---|---|---|
| **CM volume:** 500–600 mgI (iodine dose) per kg body weight. | | | |
| **Patient weight (kg)** | **< 60** | **< 80** | **> 80** |
| **CM concentration (mgI/mL)** | | | |
| 300 | 100 | 130 | 150 |
| 320 | 95 | 125 | 140 |
| 350 | 85 | 115 | 130 |
| 370 | 80 | 110 | 120 |
| 400 | 75 | 100 | 110 |
| **CM injection flow rate (mL/s)** | **1.6 gI/s** | **1.8 gI/s** | **2.0 gI/s** |
| **CM concentration (mgI/mL)** | | | |
| 300 | 5.3 | 6.0 | 6.7 |
| 320 | 5.0 | 5.6 | 6.2 |
| 350 | 4.6 | 5.1 | 5.7 |
| 370 | 4.3 | 4.8 | 5.4 |
| 400 | 4.0 | 4.5 | 5.0 |
| **Pre-contrast scan:** Useful. | | | |
| **Post-contrast scan:** 2 phases (pancreatic, portal). | | | |
| **Scan delay:** The bolus-tracking monitoring technique is used. Pancreatic phase: 28-33 s after a threshold of 100 HU is reached. Portal phase: 60-70 s from the start of the CM injection. | | | |

## References

Kawamoto S, Lawler LP, Horton KM et al (2006) MDCT of intraductal papillary mucinous neoplasm of the pancreas: evaluation of features predictive of invasive carcinoma. AJR Am J Roentgenol 186(3):687-695

Takada A, Itoh S, Suzuki K et al (2005) Branch duct-type intraductal papillary mucinous tumor: diagnostic value of multiplanar reformatted images in multislice CT. Eur Radiol 15(9):1888-1897

Takeshita K, Kutomi K, Takada K et al (2008) Differential diagnosis of benign or malignant intraductal papillary mucinous neoplasm of the pancreas by multidetector row helical computed tomography: evaluation of predictive factors by logistic regression analysis. J Comput Assist Tomogr 32(2):191-197

# ABDOMEN – Spleen. Post-traumatic Arteriovenous Intrasplenic Fistulas
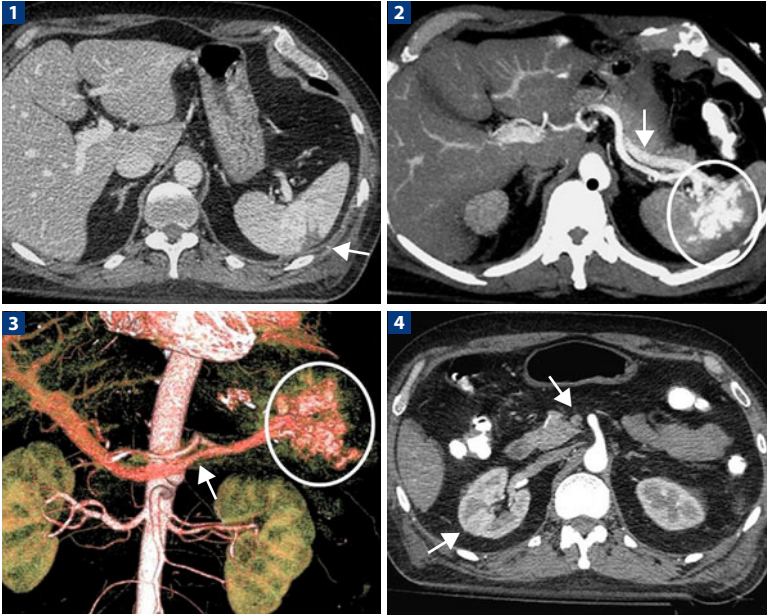


**1** Axial image in portal phase documents a small hypodense region (*arrow*) in the absence of hemoperitoneum.   **2**, **3**  Axial MIP and coronal VR reconstructions in arterial phase show multiple vascular intrasplenic formations (*oval*) with arteriovenous shunting documented by retrograde enhancement through the spleno-portal axis, in pure arterial phase.   **4**  Lack of contrast enhancement of the superior mesenteric vein (*arrows*)

## Study Protocol

| Patient preparation: A 6-h fast prior to the examination. | | | |
|---|---|---|---|
| **CM volume:** 500–600 mgI (iodine dose) per kg body weight. | | | |
| **Patient weight (kg)** | **< 60** | **< 80** | **> 80** |
| **CM concentration (mgI/mL)** | | | |
| 300 | 100 | 130 | 150 |
| 320 | 95 | 125 | 140 |
| 350 | 85 | 115 | 130 |
| 370 | 80 | 110 | 120 |
| 400 | 75 | 100 | 110 |
| **CM injection flow rate (mL/s)** | **1.6 gI/s** | **1.8 gI/s** | **2.0 gI/s** |
| **CM concentration (mgI/mL)** | | | |
| 300 | 5.3 | 6.0 | 6.7 |
| 320 | 5.0 | 5.6 | 6.2 |
| 350 | 4.6 | 5.1 | 5.7 |
| 370 | 4.3 | 4.8 | 5.4 |
| 400 | 4.0 | 4.5 | 5.0 |
| **Pre-contrast scan:** Useful to detect hemoperitoneum or sentinel clots. | | | |
| **Post-contrast scan:**<br>The bolus-tracking monitoring technique is used.<br>Arterial phase: 10-18 s after a threshold of 100 HU is reached.<br>Portal phase: 60-70 s from the start of the CM injection.<br>Equilibrium phase: 180 s from the start of the CM injection. | | | |

## References

Anderson SW (2006) Sixty-four multi-detector row computed tomography in multitrauma patient imaging: early experience. Curr Probl Diagn Radiol 35:188-198

Anderson SW, Varghese JC, Lucey BC et al (2007) Blunt splenic trauma: delayed-phase CT for differentiation of active hemorrhage from contained vascular injury in patients. Radiology 243:88-95

Shanmuganathan K, Mirvis SE, Boyd-Kranis R et al (2000) Nonsurgical management of blunt splenic injury: use of CT criteria to select patients for splenic arteriography and potential endovascular therapy. Radiology 217:75-82

# ABDOMEN – Stomach. Adenocarcinoma
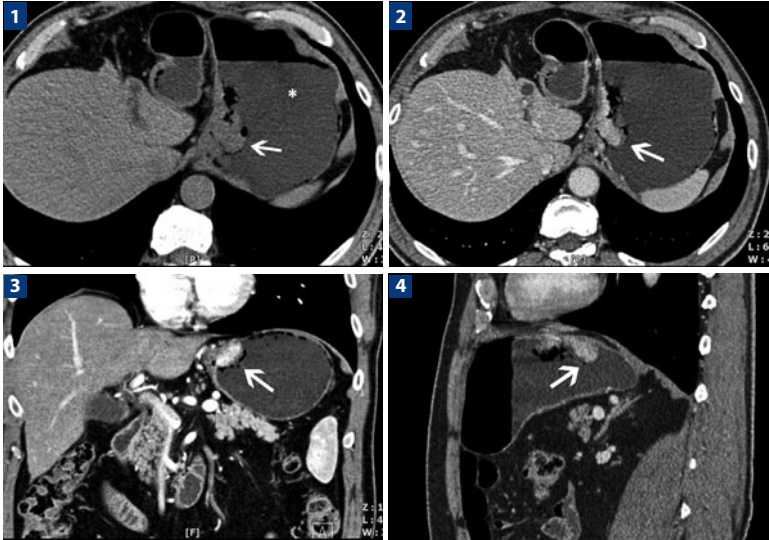


**1** Axial images of the pre-contrast scan show an optimal distension of the stomach by water, used like an oral contrast agent (*asterisk*); there is a slightly hyperdense mass (*arrow*) arising from the gastric wall. **2** Study in the portal venous phase with prior distension of the stomach with water. Optimal distension of the stomach facilitates identification of the hyperdense and partially pedunculated mass of the lesser curvature of the stomach (*arrow*). **3** Coronal and **4** sagittal MPR images provide a better evaluation of the extension of the lesion (*arrow*). Evaluation of the peri-visceral adipose tissue of interest is particularly important as it allows infiltration to be ruled out. In this case, the peri-visceral adipose tissue appears normal. The study with coronal and sagittal reformatted images is also useful for the identification of lymphadenopathies

## Study Protocol

**Patient preparation:** Gastric distension is mandatory for a proper evaluation of the visceral walls. For proper distension, 600 ml of water should be administrated orally immediately before the scan. The administration of anti-spasmolytic drugs is recommended.

**CM volume:** 500–600 mgI (iodine dose) per kg body weight.

| Patient weight (kg) | < 60 | < 80 | > 80 |
|---|---|---|---|
| **CM concentration (mgI/mL)** | | | |
| 300 | 100 | 130 | 150 |
| 320 | 95 | 125 | 140 |
| 350 | 85 | 115 | 130 |
| 370 | 80 | 110 | 120 |
| 400 | 75 | 100 | 110 |
| **CM injection flow rate (mL/s)** | **1.6 gI/s** | **1.8 gI/s** | **2.0 gI/s** |
| **CM concentration (mgI/mL)** | | | |
| 300 | 5.3 | 6.0 | 6.7 |
| 320 | 5.0 | 5.6 | 6.2 |
| 350 | 4.6 | 5.1 | 5.7 |
| 370 | 4.3 | 4.8 | 5.4 |
| 400 | 4.0 | 4.5 | 5.0 |

**Pre-contrast scan:** Useful.

**Post-contrast scan:** Portal phase, equilibrium phase (only in case of liver disease).

**Scan delay:** The bolus-tracking monitoring technique is used if arterial phase is required.
Portal phase: 60-70 s from the start of the CM injection.
Equilibrium phase: 180 s from the start of the CM injection (in case of liver disease).

## References

Chen CY, Hsu JS, Wu DC et al (2007) Gastric cancer: preoperative local staging with 3D multi-detector row CT-correlation with surgical and histopathologic results. Radiology 242(2):472-482

Kim AY, Kim HJ, Ha HK (2005) Gastric cancer by multidetector row CT: preoperative staging. Abdom Imaging 30(4):465-472

Lee SM, Kim SH, Lee JM et al (2008) Usefulness of CT volumetry for primary gastric lesions in predicting pathologic response to neoadjuvant chemotherapy in advanced gastric cancer. Abdom Imaging PMID: 18546037
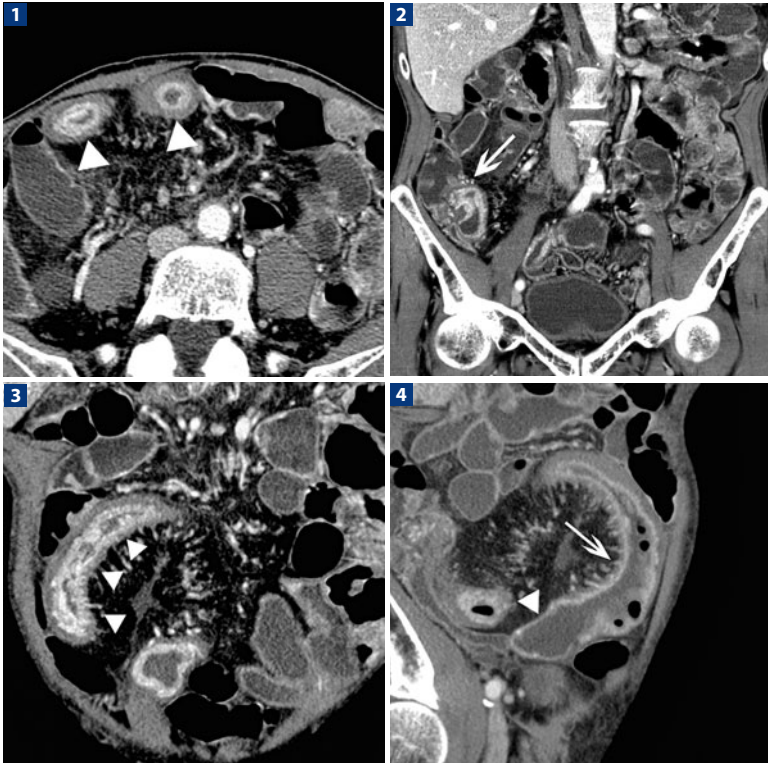
**1** CT enterography study in the enterographic phase shows diffuse concentric wall thickening involving several loops of the terminal ileum (*arrowheads*). The enhanced wall has a pseudo-stratified appearance, with hyperdensity of the internal parietal layers and relative hypodensity of the external layers. This appearance is typical of the recurrence of active inflammatory disease. **2** Coronal MPR image shows the involvement of the terminal ileum up to the ileocecal valve (*arrow*). **3** Wall thickening causes marked and extensive reduction of the visceral lumen, where there are several ulcers and pseudopolyps producing the typical cobblestone appearance (*arrowheads*). **4** Sagittal MPR image shows the transition zone between the distal diseased loop (*arrow*) and the proximal healthy loop (*arrowhead*), which appears slightly distended

## Study Protocol

**Patient preparation:** A 6-h fast prior to the examination.
Bowel distention is mandatory. The use of low-attenuation oral CM is recommended to better evaluate the bowel walls. Either of two approaches is recommended: (a) 1500 ml of PEG 4000, 20 min before exam; (b) 900 ml of a solution containing sorbitol, 30 min before the exam.

**CM volume:** 500–600 mgI (iodine dose) per kg body weight.

| Patient weight (kg) | < 60 | < 80 | > 80 |
|---|---|---|---|
| **CM concentration (mgI/mL)** | | | |
| 300 | 100 | 130 | 150 |
| 320 | 95 | 125 | 140 |
| 350 | 85 | 115 | 130 |
| 370 | 80 | 110 | 120 |
| 400 | 75 | 100 | 110 |
| **CM injection flow rate (mL/s)** | **1.6 gI/s** | **1.8 gI/s** | **2.0 gI/s** |
| **CM concentration (mgI/mL)** | | | |
| 300 | 5.3 | 6.0 | 6.7 |
| 320 | 5.0 | 5.6 | 6.2 |
| 350 | 4.6 | 5.1 | 5.7 |
| 370 | 4.3 | 4.8 | 5.4 |
| 400 | 4.0 | 4.5 | 5.0 |

**Pre-contrast scan:** Useful, not indispensable.

**Post-contrast scan:** 2 phases (late arterial, enteric).
Arterial phase: Useful for the evaluation of splanchnic vessels.
Enteric phase: Allows better evaluation of wall enhancement.

**Scan delay:** The bolus-tracking monitoring technique is used.
Late arterial phase: 18-23 s after a threshold of 100 HU is reached.
Enteric phase: 75 s from the start of the CM injection.

## References

Hara AK, Alam S, Heigh RI et al (2008) Using CT enterography to monitor Crohn's disease activity: a preliminary study. AJR Am J Roentgenol 190:1512-1516

Hara AK, Leighton JA, Heigh RI et al (2006) Crohn disease of the small bowel: preliminary comparison among CT enterography, capsule endoscopy, small-bowel follow-through, and ileoscopy. Radiology 238:128-134

Bodily KD, Fletcher JG, Solem CA et al (2006) Crohn disease: mural attenuation and thickness at contrast-enhanced CT enterography-correlation with endoscopic and histologic findings of inflammation. Radiology 238:505-516
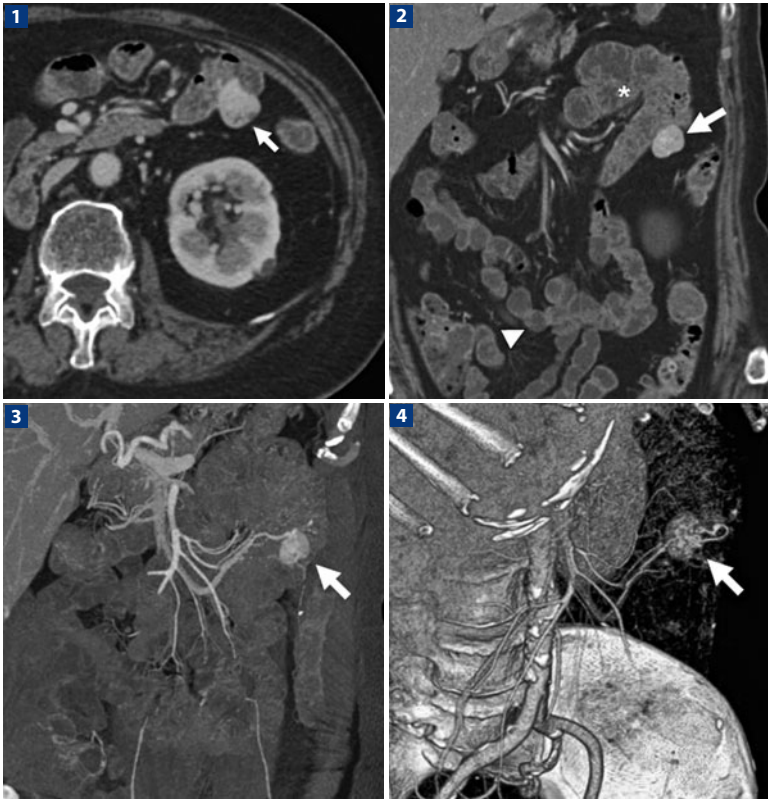
**1** CT enterography in the arterial phase: neutral contrast medium distends the lumen of the jejunal and ileal loops; the normal intestinal wall shows moderate enhancement. In this setting, a solid expansive lesion with nodular morphology (*arrow*) and exophytic growth is clearly seen adjacent to a group of jejunal loops. **2** Coronal reconstruction provides a more panoramic view of the small bowel; note the normal appearance of: the jejunal mucosa, as indicated by the presence of mucosal folds (*asterisk*), the ileal mucosa, with its smooth appearance and the absence of folds (*arrowhead*), and the bowel wall (< 3 mm). The coronal reformatted image provides a more detailed visualization of the anatomic relations between the solid lesion (*arrow*) and the bowel wall, with the solid nodule adhering to the latter but with a prevalently extra-parietal growth pattern. There are no signs of intestinal occlusion. **3** MIP and (**4**) VR reconstructions are useful for demonstrating the intense vascularity of the nodule and the feeding vessels. Indeed, both show the branches of the dilated jejunal arteries, with one artery clearly reaching the nodule. In this case, the most useful signs for the diagnostic evaluation include evidence of a solid extramucosal hypervascular nodule of the jejunum

## Study Protocol

**Patient preparation:** A 6-h fast prior to the examination.
Bowel distention is mandatory. The use of low-attenuation oral CM is recommended to better evaluate the bowel walls. Either of two approaches is recommended: (a) 1500 ml of PEG 4000, 20 min before exam; (b) 900 ml of solutions containing sorbitol, 30 min before the exam.

**CM volume:** 500–600 mgI (iodine dose) per kg body weight.

| Patient weight (kg) | < 60 | < 80 | > 80 |
|---|---|---|---|
| **CM concentration (mgI/mL)** | | | |
| 300 | 100 | 130 | 150 |
| 320 | 95 | 125 | 140 |
| 350 | 85 | 115 | 130 |
| 370 | 80 | 110 | 120 |
| 400 | 75 | 100 | 110 |
| **CM injection flow rate (mL/s)** | **1.6 gI/s** | **1.8 gI/s** | **2.0 gI/s** |
| **CM concentration (mgI/mL)** | | | |
| 300 | 5.3 | 6.0 | 6.7 |
| 320 | 5.0 | 5.6 | 6.2 |
| 350 | 4.6 | 5.1 | 5.7 |
| 370 | 4.3 | 4.8 | 5.4 |
| 400 | 4.0 | 4.5 | 5.0 |

**Pre-contrast scan:** Useful, not indispensable.

**Post-contrast scan:** 2 phases (late arterial phase, enteric phase).
Arterial phase: Useful for the evaluation of the splanchnic vessel.
Enteric phase: Allows better evaluation of wall enhancement.

**Scan delay:** The bolus-tracking monitoring technique is used.
Late arterial phase: 18-23 s after a threshold of 100 HU is reached.
Enteric phase: 75 s from the start of the CM injection.

## References

Da Ronch T, Modesto A, Bazzocchi M et al (2006) Gastrointestinal stromal tumour: spiral computed tomography features and pathologic correlation. Radiol Med 111:661-673

De Leo C, Memeo M, Spinelli F, Angeletti G (2006) Gastrointestinal stromal tumours: experience with multislice CT. Radiol Med 111:1103-1114

Rimondini A, Belgrano M, Favretto G et al (2007) Contribution of CT to treatment planning in patients with GIST. Radiol Med 112:691-702
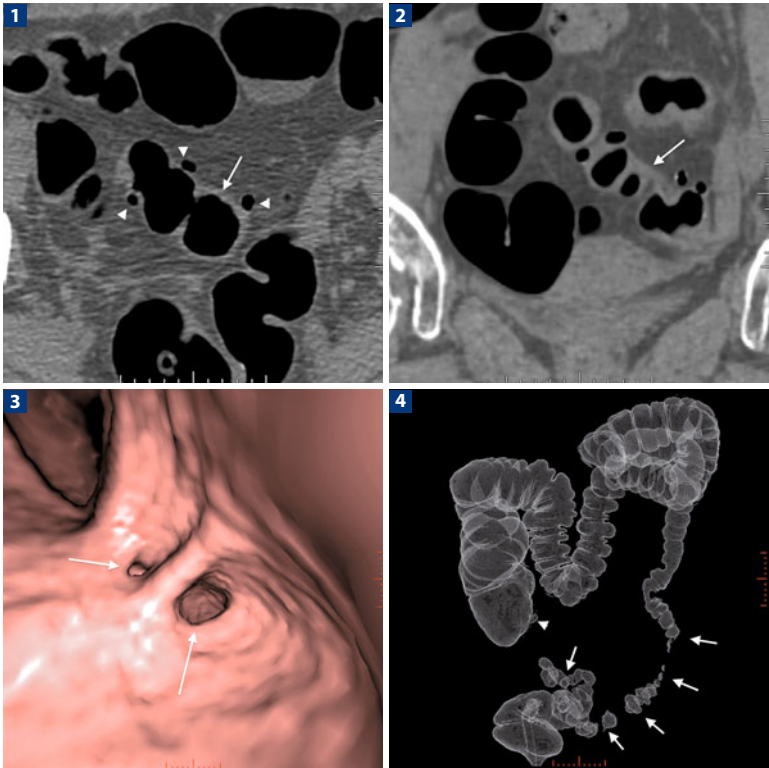
**1** Focal wall thickening in the sigmoid colon (*arrow*) and diverticula (*arrowheads*) as seen on axial two-dimensional CT colonography: pre-contrast scan with the patient in the prone position. **2** Post-contrast scan, coronally reformatted, shows a thickened segment of sigmoid colon without surrounding inflammatory changes in the peri-colonic fat; there are no signs of diverticulitis or perforation. **3** Three-dimensional intraluminal VR reconstruction shows two diverticula of the sigmoid colon (*arrows*). **4** Tissue transition projection reconstruction simulates a double-contrast enema and is extremely useful in demonstrating the location of narrowing. In this case, a reduction of the colonic lumen from the rectum to the ascending colon (*arrows*) and a diverticulum of the cecum (*arrowhead*) are seen

## Study Protocol

**Patient preparation:** Patients have to be adequately prepared: liquid diet the evening before the exam, fasting the day of exam, cathartic preparation, PEG (70 mg in 4 l of water the day before the exam).
Alternatively, either of two different fecal tagging techniques, with less cathartic effect and better patient compliance, can be used: (a) 200 ml of amidotrizoate meglumine the day before the exam, 100 ml in the morning and 100 in the afternoon; (b) same-day preparation: two bags of macrogol solution (20 mg), before meals, 2 days before the exam. Administration of 100 ml of a solution containing meglumine 3 h before the exam.

**Pre-contrast scan:** Acquired in prone and supine position, with low mAs.

**Post-contrast scan:** Not necessary.

## References

Halligan S, Saunders B (2002) Imaging diverticular disease. Best Practice Res Clinical Gastroenterol 16(4):595-610

Lawrimore T, Rhea JT (2004) Computed tomography evaluation of diverticulitis. J Intensive Care Med 19(4):194-204

# ABDOMEN – Colon. Adenocarcinoma of the Sigmoid Colon
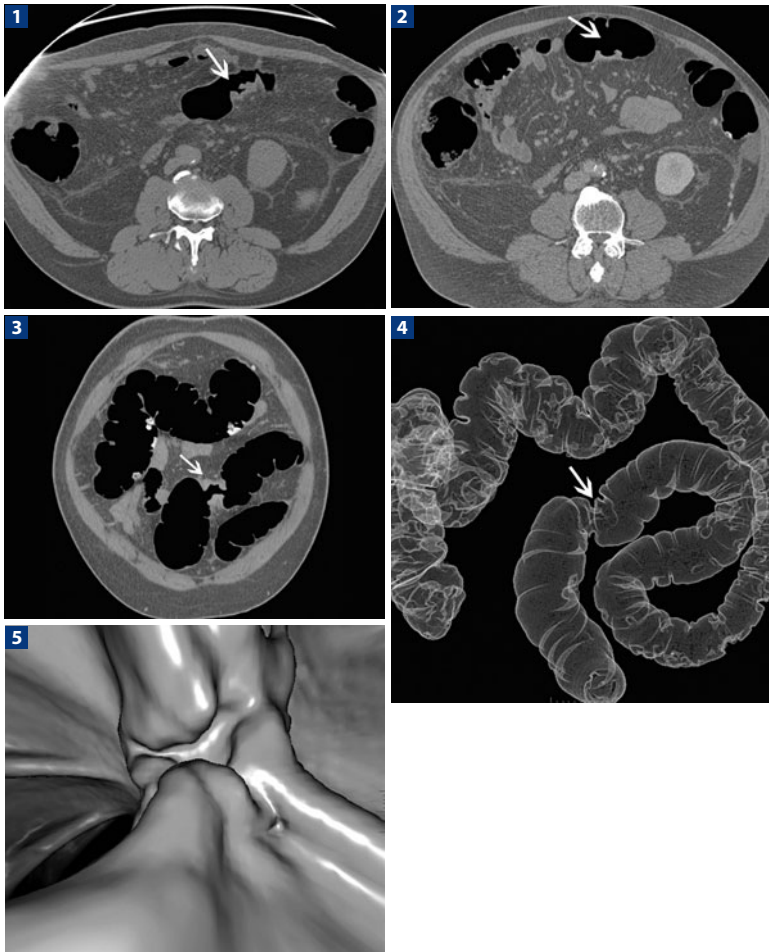










**1** Pre-contrast scan with the patient in the prone position shows a stenosing lesion within the lumen (*arrow*) of the sigmoid colon. **2** Post-contrast scan in the supine position: the lesion is easily identifiable (*arrow*) and displays contrast enhancement. **3** Post-contrast coronal reformatted image with patient in the supine position shows the stenosing appearance of the mass (*arrow*). **4** Tissue transition projection reconstruction, which simulates a double-contrast enema and is extremely useful in demonstrating the location of the lesion. The "apple-core" sign, typical of malignancies of the colon, can be appreciated (*arrow*). **5** Three-dimensional intraluminal VR reconstruction shows marked distortion of the normal morphology of the haustra coli

## Study Protocol

**Patient preparation:** Patients have to be prepared adequately: liquid diet the evening before the exam, fasting the day of exam, cathartic preparation, PEG (70 mg in 4 l of water the day before the exam).

Alternatively, two different fecal tagging techniques, with less cathartic effect and better patient compliance can be used: (a) 200 ml of amidotrizoate meglumine the day before the exam, 100 ml in the morning and 100 in the afternoon; (b) same-day preparation: two bags of macrogol solution (20 mg) before meals in 2 days before the exam. Administration of 100 ml of a solution containing meglumine 3 h before the exam.

**CM volume:** 500–600 mgI (iodine dose) per kg body weight.

| Patient weight (kg) | < 60 | < 80 | > 80 |
|---|---|---|---|
| CM concentration (mgI/mL) | | | |
| 300 | 100 | 130 | 150 |
| 320 | 95 | 125 | 140 |
| 350 | 85 | 115 | 130 |
| 370 | 80 | 110 | 120 |
| 400 | 75 | 100 | 110 |

**Pre-contrast scan:** Patient in prone position, low mAs.

**Post-contrast scan:** Patient in supine position, single portal phase.

**Scan delay:** Portal phase: 60-70 s from the start of the CM injection.

## References

Kim DH, Pickhardt PJ, Hoff G, Kay CL (2007) Computed tomographic colonography for colorectal screening. Endoscopy 39:545-549

Mang T, Graser A, Schima W, Maier A (2007) CT colonography: techniques, indications, findings. Eur J Radiol 61:388-399

Taylor SA, Laghi A, Lefere P et al (2007) European Society of Gastrointestinal and Abdominal Radiology (ESGAR): consensus statement on CT colonography. Eur Radiol 17:575-579
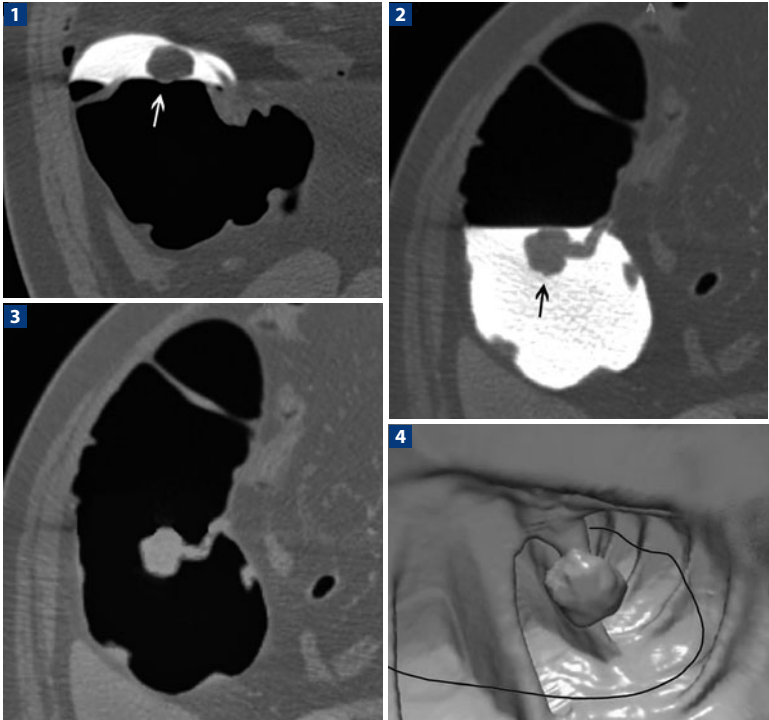
**1** Scan with patient in the prone position shows the presence of a pedunculated polyp in the ascending colon (*arrow*), covered by luminal fluid opacified by the oral iodinated contrast medium.　**2** Scan with patient in the supine position: the large pedunculated polyp (*arrow*) is still completely covered by the luminal fluid and is visible due to the opacification effect of the fluid (oral contrast medium). **3** Coronal MPR image obtained after electronic cleansing: electronic removal of the opacified fluid, which enables virtual cleansing of the colon by electronically subtracting the opacified fluid, shows the polypoid lesion with the peduncle.　**4** Intraluminal VR reconstruction after electronic cleansing: the polypoid lesions is well visualized within the lumen of the colon

## Study Protocol

**Patient preparation:** Patients have to be prepared adequately: liquid diet the evening before the exam, fasting the day of exam, cathartic preparation, PEG (70 mg in 4 l of water the day before the exam).
Alternatively, two different fecal tagging techniques, with less cathartic effect and better patient compliance, can be used: (a) 200 ml of amidotrizoate meglumine the day before the exam, 100 ml in the morning and 100 in the afternoon; (b) same-day preparation: two bags of macrogol solution (20 mg), before the meals, in 3 days before the exam. Administration of 100 ml of a solution containing meglumine 3 h before the exam.

**CM volume:** 500–600 mgI (iodine dose) per kg body weight is suggested only for staging of an accidental cancer.

| Patient weight (kg) | < 60 | < 80 | > 80 |
|---|---|---|---|
| CM concentration (mgI/mL) | | | |
| 300 | 100 | 130 | 150 |
| 320 | 95 | 125 | 140 |
| 350 | 85 | 115 | 130 |
| 370 | 80 | 110 | 120 |
| 400 | 75 | 100 | 110 |

**Pre-contrast scan:** Patient in prone and supine position, with 100 mAs if injection is not required.

**Post-contrast scan:** Patient in supine position, 200 mAs.

## References

Kim DH, Pickhardt PJ, Hoff G, Kay CL (2007) Computed tomographic colonography for colorectal screening. Endoscopy 39:545-549

Mang T, Graser A, Schima W, Maier A (2007) CT colonography: techniques, indications, findings. Eur J Radiol 61:388-399

Taylor SA, Laghi A, Lefere P et al (2007) European Society of Gastrointestinal and Abdominal Radiology (ESGAR): consensus statement on CT colonography. Eur Radiol 17:575-579

**1** Axial image in portal phase: foci of vascular hyperdensity in the wall of the sigmoid colon (*arrows*).   **2** Coronal MIP image in portal phase: a vascular tangle of sigmoid wall (*arrow*).   **3** Axial image shows hyperdense sigmoid-wall thickening caused by multiple vascular ectasias (*red and white arrows*); the bowel lumen is distended by hypodense corpuscular fluid.   **4** Sagittal MIP reconstruction in venous phase: angiodysplasia of the sigmoid wall (*arrow*)

## Study Protocol

| Patient weight (kg) | < 60 | < 80 | > 80 |
|---|---|---|---|

**Patient preparation:** A 6-h fast prior to the examination.

**CM volume:** 500–600 mgI (iodine dose) per kg body weight.

| CM concentration (mgI/mL) | | | |
|---|---|---|---|
| 300 | 100 | 130 | 150 |
| 320 | 95 | 125 | 140 |
| 350 | 85 | 115 | 130 |
| 370 | 80 | 110 | 120 |
| 400 | 75 | 100 | 110 |

| CM injection flow rate (mL/s) | 1.6 gI/s | 1.8 gI/s | 2.0 gI/s |
|---|---|---|---|

| CM concentration (mgI/mL) | | | |
|---|---|---|---|
| 300 | 5.3 | 6.0 | 6.7 |
| 320 | 5.0 | 5.6 | 6.2 |
| 350 | 4.6 | 5.1 | 5.7 |
| 370 | 4.3 | 4.8 | 5.4 |
| 400 | 4.0 | 4.5 | 5.0 |

**Pre-contrast scan:** Useful to detect intraluminal bleeding and clots.

**Post-contrast scan:** The bolus-tracking monitoring technique is used.
Late arterial phase: 18-23 s after a treshold of 100 HU is reached.
Portal phase: 60-70 s from the start of the CM injection.
Delay phase: 100 s after arterial phase, necessary to distinguish CM extravasation from active bleeding.

## References

Hammerstingl RM, Vogl TJ (2005) Abdominal MDCT: protocols and contrast considerations. Eur Radiol (15 Suppl) 5:E78-E90

Jaeckle T, Stuber G, Hoffmann MH et al (2008) Detection and localization of acute upper and lower gastrointestinal (GI) bleeding with arterial phase multi-detector row helical CT. Eur Radiol 18:1406-1413

Yoon W, Jeong YY, Kim JK (2006) Acute gastrointestinal bleeding: contrast-enhanced MDCT. Abdom Imaging 31:1-8

# ABDOMEN – Rectum. Carcinoma
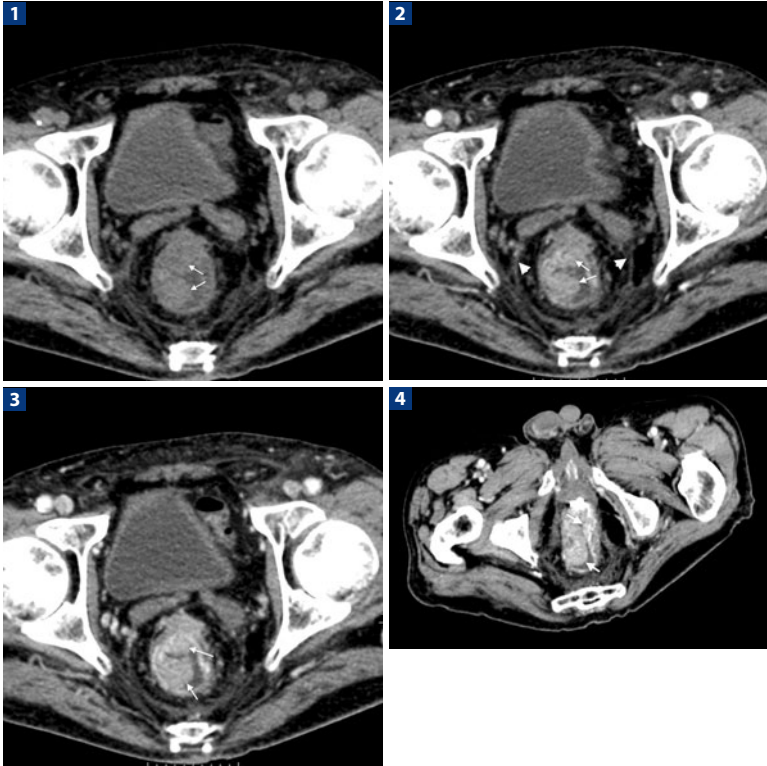


**1** Axial image obtained in pre-contrast phase shows a solid mass as bowel-wall thickening in the right side of the rectal ampulla (*arrows*). **2** In the arterial phase of the study, the tissue shows moderate contrast enhancement suggestive of a neoplastic exophytic lesion (*arrows*). Although stratification of the bowel wall cannot be distinguished, the absence of pathology in the mesorectal adipose tissue is clear. The mesorectal fascia can be easily identified as a thin and hyperdense structure (*arrowheads*). **3** Portal phase shows enhancement growth (*arrows*). **4** Axial-oblique MPR shows a stenosing morphology of the lesion (*arrows*)

## Study Protocol

**Patient preparation:** A 6-h fast prior to the examination; a cleaning enema of the rectum the morning of the exam is useful. Some centers prefer to perform rectal distension with air or water; excessive distension is not recommended..

**CM volume:** 500–600 mgI (iodine dose) per kg body weight.

| Patient weight (kg) | < 60 | < 80 | > 80 |
|---|---|---|---|
| **CM concentration (mgI/mL)** | | | |
| 300 | 100 | 130 | 150 |
| 320 | 95 | 125 | 140 |
| 350 | 85 | 115 | 130 |
| 370 | 80 | 110 | 120 |
| 400 | 75 | 100 | 110 |
| **CM injection flow rate (mL/s)** | **1.6 gI/s** | **1.8 gI/s** | **2.0 gI/s** |
| **CM concentration (mgI/mL)** | | | |
| 300 | 5.3 | 6.0 | 6.7 |
| 320 | 5.0 | 5.6 | 6.2 |
| 350 | 4.6 | 5.1 | 5.7 |
| 370 | 4.3 | 4.8 | 5.4 |
| 400 | 4.0 | 4.5 | 5.0 |

**Pre-contrast scan:** Useful.

**Post-contrast scan:** 2 phases (late arterial and portal).

**Scan delay:** The bolus-tracking monitoring technique is used.
Late arterial phase: 18-23 s after a treshold of 100 HU is reached.
Portal phase: 60-70 s from the start of the CM injection.

## References

Kanamoto T, Matsuki M, Okuda J et al (2007) Preoperative evaluation of local invasion and metastatic lymph nodes of colorectal cancer and mesenteric vascular variations using multidetector-row computed tomography before laparoscopic surgery. J Comput Assist Tomogr 31:831-839

Sinha R, Verma R, Rajesh A, Richards CJ (2006) Diagnostic value of multidetector row CT in rectal cancer staging: comparison of multiplanar and axial images with histopathology. Clin Radiol 61:924-931

Vliegen R, Dresen R, Beets G et al (2008) The accuracy of multi-detector row CT for the assessment of tumor invasion of the mesorectal fascia in primary rectal cancer. Abdom Imaging 33(5):604-610
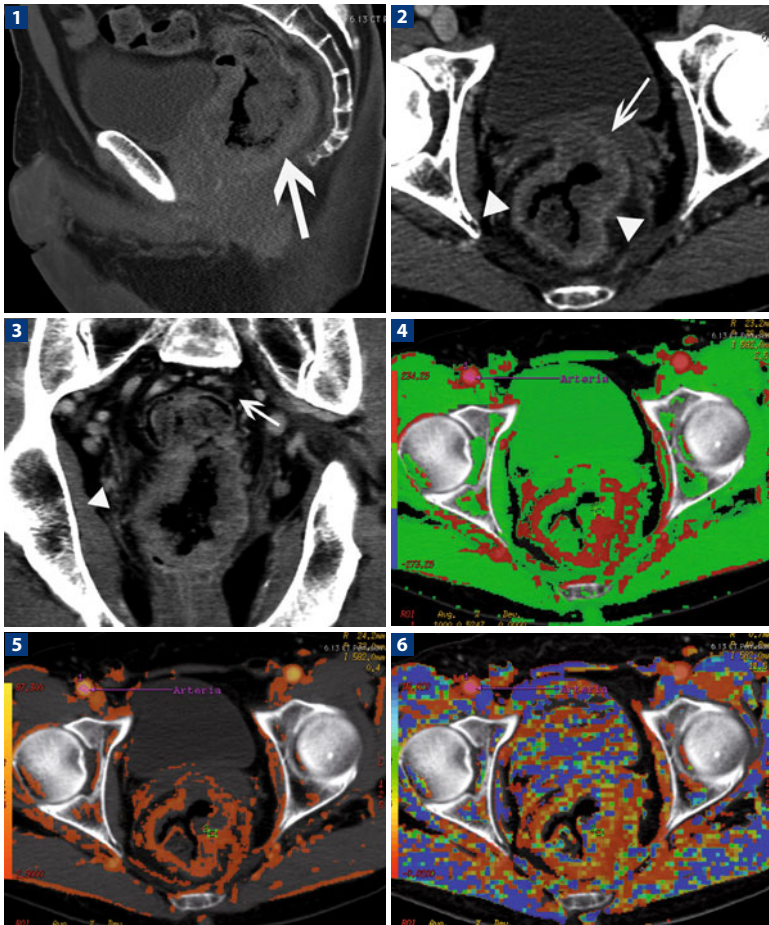
**1** Pre-contrast sagittal MPR image. Note the marked thickening of the rectal wall (*arrow*), due to the presence of a large neoplastic parietal lesion. Sagittal scan shows the exact longitudinal extension of the tumor, which is necessary for volume placement in the perfusion study. **2** Post-contrast axial scan in the venous phase: enhancement of the lesion involving the circumference of the rectum (*arrowheads*), with sparing only of the right posterolateral wall. Note the neoplastic infiltration of the mesorectum (*arrow*). **3** Post-contrast coronal MPR image in the venous phase: the tumor is shown in its entire longitudinal extension as are the bands of tumor infiltration in the mesorectum (*arrowhead*). Locoregional lymphadenopathies can also be appreciated (*arrow*). Perfusion analysis carried out with dedicated software shows: **4** (color map: blood flow) an increase in flow (red areas) as expected in a neoplastic lesion; **5** (color map: blood volume) an increase ▶

## Study Protocol

| Patient preparation: A 6-h fast prior to the examination. | | | |
|---|---|---|---|
| **CM volume:** 60-80 mL according to patient weight. | | | |
| **CM injection flow rate (mL/s)** | **1.6 gl/s** | **1.8 gl/s** | **2.0 gl/s** |
| **CM concentration (mgl/mL)** | | | |
| 300 | 5.3 | 6.0 | 6.7 |
| 320 | 5.0 | 5.6 | 6.2 |
| 350 | 4.6 | 5.1 | 5.7 |
| 370 | 4.3 | 4.8 | 5.4 |
| 400 | 4.0 | 4.5 | 5.0 |

**Pre-contrast scan:** Baseline CT images without CM and with a thickness of 2.5–5.0 mm must be acquired to locate the cancer and select the volume on which perfusion scans are to be done.

**Post-contrast scan:** Cine mode acquisition with no table movement, anatomical coverage of 4 cm, 1 volume/1 × 40 s.

**Scan delay:** Perfusion CT scan start 10 s after the injection of CM.

## References

Bellomi M, Petralia G, Sonzogni A et al (2007) CT perfusion for the monitoring of neoadjuvant chemotherapy and radiation therapy in rectal carcinoma: initial experience. Radiology 244:486-493

Goh V, Padhani AR, Rasheed S (2007) Functional imaging of colorectal cancer angiogenesis. Lancet Oncol 8:245-255

Sahani DV, Kalva SP, Hamberg LM et al (2005) Assessing tumor perfusion and treatment response in rectal cancer with multisection CT: initial observations. Radiology 234:785-792

◀ in blood volume (*orange areas*) in the tumor with respect to the adjacent tissue; **6** (color map: mean transit time) a reduction in the values in the tumor (*red areas*). The latter finding reflects the presence of multiple arteriovenous shunts in the pathologic tissue with respect to normal tissue

**1**, **2** and **3**. A pelvic nodule of carcinomatosis from ovarian cancer (*arrow*). The enhancement of the nodule is progressive from the arterial (**1**) to the delayed phase (**3**). In the delayed phase, acquired after 5 minutes from the injection of the CM, the conspicuity of the nodule is significantly higher. The acquisition of the delayed phase is mandatory for the detection of diaphragmatic nodules (*arrow* in **4**, **5** and **6**). The diaphragmatic nodule is not appreciable in the portal phase (**4**) while is clearly visible in the delayed phase (*arrow* in **5** and **6**)

## Study Protocol

**Patient preparation:** A 6-h fast prior to the examination.

**CM volume:** 500–600 mgI (iodine dose) per kg body weight.

| Patient weight (kg) | < 60 | < 80 | > 80 |
|---|---|---|---|
| **CM concentration (mgI/mL)** | | | |
| 300 | 100 | 130 | 150 |
| 320 | 95 | 125 | 140 |
| 350 | 85 | 115 | 130 |
| 370 | 80 | 110 | 120 |
| 400 | 75 | 100 | 110 |
| **CM injection flow rate (mL/s)** | **1.6 gI/s** | **1.8 gI/s** | **2.0 gI/s** |
| **CM concentration (mgI/mL)** | | | |
| 300 | 5.3 | 6.0 | 6.7 |
| 320 | 5.0 | 5.6 | 6.2 |
| 350 | 4.6 | 5.1 | 5.7 |
| 370 | 4.3 | 4.8 | 5.4 |
| 400 | 4.0 | 4.5 | 5.0 |

**Pre-contrast scan:** Useful.

**Post-contrast scan:** 3 phases (late arterial, portal and delayed phase).

**Scan delay:** The bolus-tracking monitoring technique is used.
Late arterial phase: 18-23 s after a treshold of 100 HU is reached.
Portal phase: 60-70 s from the start of the CM injection.
Delayed phase: five minutes from the start of the CM injection.

## References

Pannu HK, Bristow RE, Montz FJ et al (2003) Multidetector CT of peritoneal carcinomatosis from ovarian cancer. Radiographics 23(3):687-701
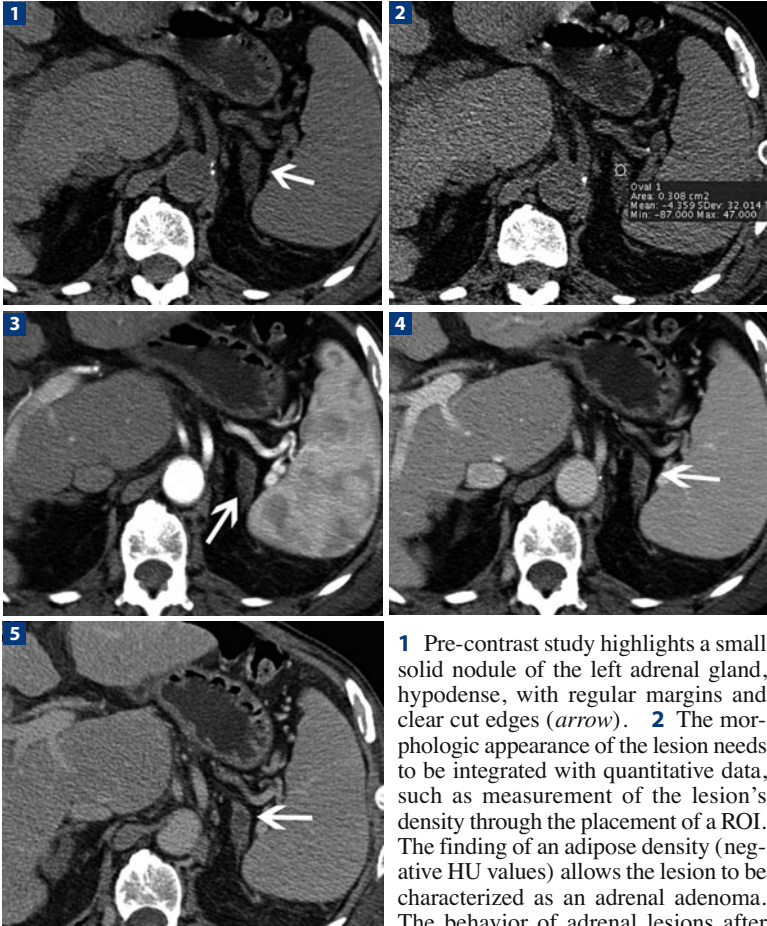
**1** Pre-contrast study highlights a small solid nodule of the left adrenal gland, hypodense, with regular margins and clear cut edges (*arrow*). **2** The morphologic appearance of the lesion needs to be integrated with quantitative data, such as measurement of the lesion's density through the placement of a ROI. The finding of an adipose density (negative HU values) allows the lesion to be characterized as an adrenal adenoma. The behavior of adrenal lesions after the intravenous administration of contrast medium, evaluated qualitatively, is not pathognomonic, either (**3**) in the arterial phase (*arrow*) or (**4**) in the portal phase (*arrow*). **5** In the late phase at 10 min, benign adrenal lesions tend to display a marked wash-out compared to earlier phases. Late wash-out should also be evaluated quantitatively by measuring the density in the portal phase and in the late phase using the formula: $(1 - \text{HU late phase}/\text{HU portal phase}) \times 100$. A late wash-out > 50% is suggestive of a benign adrenal lesion, as are absolute values < 30 HU in the late phase

## Study Protocol

| Patient weight (kg) | < 60 | < 80 | > 80 |
|---|---|---|---|

**Patient preparation:** A 6-h fast prior to the examination.

**CM volume:** 500–600 mgI (iodine dose) per kg body weight.

| Patient weight (kg) | < 60 | < 80 | > 80 |
|---|---|---|---|
| **CM concentration (mgI/mL)** | | | |
| 300 | 100 | 130 | 150 |
| 320 | 95 | 125 | 140 |
| 350 | 85 | 115 | 130 |
| 370 | 80 | 110 | 120 |
| 400 | 75 | 100 | 110 |
| **CM injection flow rate (mL/s)** | **1.6 gI/s** | **1.8 gI/s** | **2.0 gI/s** |
| **CM concentration (mgI/mL)** | | | |
| 300 | 5.3 | 6.0 | 6.7 |
| 320 | 5.0 | 5.6 | 6.2 |
| 350 | 4.6 | 5.1 | 5.7 |
| 370 | 4.3 | 4.8 | 5.4 |
| 400 | 4.0 | 4.5 | 5.0 |

**Pre-contrast scan:** Indispensable.

**Post-contrast scan:** 3 phases (late arterial, portal, late).

**Scan delay:** The bolus-tracking monitoring technique is used.
Late arterial phase: 10 s after a threshold of 100 HU is reached.
Portal phase: 60-70 s from the start of the CM injection.
Late phase: 10 min from the start of the CM injection; useful to characterize pre-contrast phase lesions > 10 HU.

## References

Bae KT, Fuangtharnthip P, Prasad SR et al (2003) Adrenal masses: CT characterization with histogram analysis method. Radiology 228:735-742

Korobkin M, Brodeur FJ, Yutzy GG et al (1996) Differentiation of adrenal adenomas from nonadenomas using CT attenuation values. AJR Am J Roentgenol 166:531-536

Yamada T, Ishibashi T, Saito H et al (2003) Adrenal adenomas: relationship between histologic lipid-rich cells and CT attenuation number. Eur J Radiol 48:198-202

# ABDOMEN – Adrenal Glands. Metastases from Lung Cancer



**1** Pre-contrast study shows an increase in the size of the left adrenal gland with pseudonodular morphology (*arrow*). Numerous large hepatic lesions can also be appreciated. The pre-contrast phase is crucial for the characterization of adrenal lesions. The imaging characteristics are based not only on morphological and size criteria (lesions > 4 cm are more probably malignant) but also on quantitative criteria. The density of the adrenal lesion needs to be measured with the placement of a ROI. Benign lesions (adrenal adenomas) are characterized by the presence of intracellular adipose tissue that produces low-density characteristics (negative HU values). Adrenal lesions with density > 10 HU cannot be interpreted as benign and are at risk of being metastatic. The qualitative evaluation of the behavior of adrenal lesions after the intravenous administration of contrast medium is not pathognomonic, as shown in **2** the arterial phase and **3** the portal phase.   **4** In the late phase at 10 min, malignant adrenal lesions tend to display poor wash-out with respect to the earlier phases. Late wash-out should also be quantitatively evaluated by measuring the density in the portal and late phases using the formula: (1 – HU late phase/HU portal phase) × 100. A late wash-out < 50% is suggestive of a malignant adrenal lesion, as are absolute values > 30 HU in the late phase

## Study Protocol

| **Patient preparation:** A 6-h fast prior to the examination. | | | |
|---|---|---|---|

| **CM volume:** 500–600 mgI (iodine dose) per kg body weight. | | | |
|---|---|---|---|

| **Patient weight (kg)** | **< 60** | **< 80** | **> 80** |
|---|---|---|---|
| **CM concentration (mgI/mL)** | | | |
| 300 | 100 | 130 | 150 |
| 320 | 95 | 125 | 140 |
| 350 | 85 | 115 | 130 |
| 370 | 80 | 110 | 120 |
| 400 | 75 | 100 | 110 |
| **CM injection flow rate (mL/s)** | **1.6 gI/s** | **1.8 gI/s** | **2.0 gI/s** |
| **CM concentration (mgI/mL)** | | | |
| 300 | 5.3 | 6.0 | 6.7 |
| 320 | 5.0 | 5.6 | 6.2 |
| 350 | 4.6 | 5.1 | 5.7 |
| 370 | 4.3 | 4.8 | 5.4 |
| 400 | 4.0 | 4.5 | 5.0 |

| **Pre-contrast scan:** Useful, not indispensable. |
|---|

| **Post-contrast scan:** 3 phases (late arterial, portal, late). |
|---|

| **Scan delay:** The bolus-tracking monitoring technique is used.<br>Late arterial phase: 10 s after a threshold of 100 HU is reached.<br>Portal phase: 60-70 s from the start of the CM injection.<br>Late phase: 10 min from the start of the CM injection; useful to characterize pre-contrast phase lesions >10 HU. |
|---|

## References

Kebapci M, Kaya T, Gurbuz E et al (2003) Differentiation of adrenal adenomas (lipid rich and lipid poor) from nonadenomas by use of washout characteristics on delayed enhanced CT. Abdom Imaging 28:709-715

Mayo-Smith WW, Boland GW, Noto RB et al (2001) Sate of the art of adrenal imaging. RadioloGraphics 4:995-1012

Park BK, Kim B, Ko K et al (2006) Adrenal masses falsely diagnosed as adenomas on unenhanced and delayedcontrast-enhanced computed tomography: pathological correlation. Eur Radiol 16:642-647

**1** Pre-contrast coronal reformatted image highlights an alteration of the superior capsular profile due to the presence of a solid nodular lesion (*arrow*). Another mass, with a partially exophytic growth pattern and prevalently adipose density, can be seen at the level of the middle to inferior third (*curved arrow*). **2** Coronal reformatted image in the late arterial phase shows marked enhancement of the lesion located at the level of the right upper renal pole, compatible with primary heteroplasia (*arrow*). The lesion located at the level of the middle-inferior third displays only moderate enhancement of the solid, non-adipose areas (*curved arrow*), typical of angiomyolipomas. **3** Coronal MIP reconstruction in the later arterial phase enables better evaluation of the relations of the lesion with the vascular structures and the identification of anomalies of the renal vessels. **4** Coronal reformatted image in the portal phase shows wash-out of the lesion located in the right upper pole (*arrow*). This lesion appears capsulated, without signs of infiltration of the peri-renal adipose tissue, while the lesion at the middle inferior third shows late enhancement (*curved arrow*). **5** Post-contrast coronal MIP reconstruction in the urographic phase shows normal calices and the normal course and diameter of the ureters

## Study Protocol
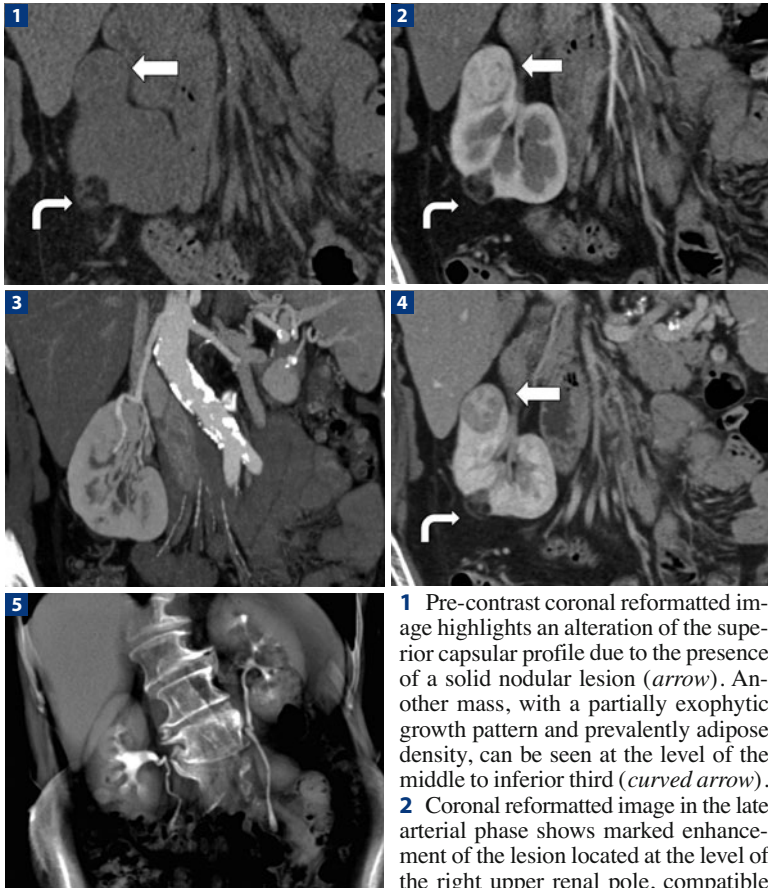
| Patient weight (kg) | < 60 | < 80 | > 80 |
|---|---|---|---|

**Patient preparation:** A 6-h fast prior to the examination.

**CM volume:** 500–600 mgI (iodine dose) per kg body weight.

| Patient weight (kg) | < 60 | < 80 | > 80 |
|---|---|---|---|
| **CM concentration (mgI/mL)** | | | |
| 300 | 100 | 130 | 150 |
| 320 | 95 | 125 | 140 |
| 350 | 85 | 115 | 130 |
| 370 | 80 | 110 | 120 |
| 400 | 75 | 100 | 110 |
| **CM injection flow rate (mL/s)** | **1.6 gI/s** | **1.8 gI/s** | **2.0 gI/s** |
| **CM concentration (mgI/mL)** | | | |
| 300 | 5.3 | 6.0 | 6.7 |
| 320 | 5.0 | 5.6 | 6.2 |
| 350 | 4.6 | 5.1 | 5.7 |
| 370 | 4.3 | 4.8 | 5.4 |
| 400 | 4.0 | 4.5 | 5.0 |

**Pre-contrast scan:** Useful.

**Post-contrast scan:** 3 phases (late arterial, portal, equilibrium).

**Scan delay:** The bolus-tracking monitoring technique is used.
Late arterial phase: 18-23 s after a threshold of 100 HU is reached.
Portal phase: 60-70 s from the start of the CM injection.
Excretory phase: 7 min from the start of the CM injection.

## References

Sheir KZ, El-Azab M, Mosbah A et al (2005) Differentiation of renal cell carcinoma subtypes by multislice computerized tomography. J Urol 174:451-455; discussion 455

Zhang J, Lefkowitz RA, Ishill NM et al (2007) Solid renal cortical tumors: differentiation with CT. Radiology 244:494-504

Zhang J, Lefkowitz RA, Wang L et al (2007) Significance of peritumoral vascularity on CT in evaluation of renal cortical. tumor. J Comput Assist Tomogr 31:717-723
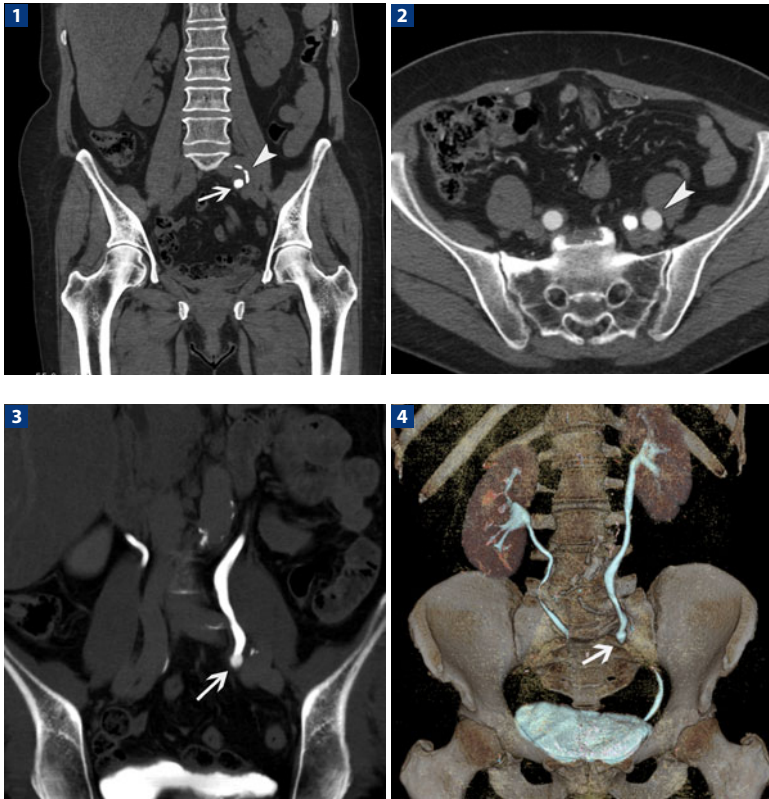
**1** Pre-contrast axial scan, coronal MPR image. A large calcific structure can be seen at the level of the renal pelvis (*arrow*); above it a tubular structure with partially calcified walls is visible (*arrowhead*). **2** Post-contrast axial scan in the arterial phase shows enhancement of the tubular structure referable to the left common iliac artery (*arrowhead*). **3** Post-contrast axial scan in the urographic phase: the calcified structure (*arrow*) is located within the left upper urinary tract, with proximal dilatation of the ureter. **4** Post-contrast scan: the three-dimensional VR image shows the ureter in its proximal course, with stenosis caused by the calcified stone (*arrow*)

## Study Protocol

**Patient preparation:** A 6-h fast prior to the examination; fluid administration (oral or i.v.) to stimulate diuresis.

**CM volume:** 500-600 mgI (iodine dose) per kg body weight.

| Patient weight (kg) | < 60 | < 80 | > 80 |
|---|---|---|---|
| **CM concentration (mgI/mL)** | | | |
| 300 | 100 | 130 | 150 |
| 320 | 95 | 125 | 140 |
| 350 | 85 | 115 | 130 |
| 370 | 80 | 110 | 120 |
| 400 | 75 | 100 | 110 |
| **CM injection flow rate (mL/s)** | **1.6 gI/s** | **1.8 gI/s** | **2.0 gI/s** |
| **CM concentration (mgI/mL)** | | | |
| 300 | 5.3 | 6.0 | 6.7 |
| 320 | 5.0 | 5.6 | 6.2 |
| 350 | 4.6 | 5.1 | 5.7 |
| 370 | 4.3 | 4.8 | 5.4 |
| 400 | 4.0 | 4.5 | 5.0 |

**Pre-contrast scan:** Indispensable for the detection of radio-opaque structures.

**Post-contrast scan:** 3 phases (arterial, portal, excretory).

**Scan delay:** The bolus-tracking monitoring technique is used.
Arterial phase: 10 s after a threshold of 100 HU is reached.
Portal phase: 60-70 s from the start of the CM injection.
Excretory phase: 7 min from the start of the CM injection.

## References

Memarsadeghi M, Schaefer-Prokop C, Prokop M et al (2007) Unenhanced MDCT in patients with suspected urinary stone disease: do coronal reformations improve diagnostic performance? AJR Am J Roentgenol 189:W60-W64

Paulson EK, Weaver C, Ho LM et al (2008) Conventional and reduced radiation dose of 16-MDCT for detection of nephrolithiasis and ureterolithiasis. AJR Am J Roentgenol 190:151-157

Poletti PA, Platon A, Rutschmann OT et al (2007) Low-dose versus standard-dose CT protocol in patients with clinically suspected renal colic. AJR Am J Roentgenol 188:927-933

**1, 2** Non-enhanced scan: in this study, acquired with a low-dose protocol, there is a calcified stone at the level of the distal third of the left ureter (*arrowhead*). **1** Images obtained with 0.6-mm slice thickness are very noisy. **2** The reformatted image, with 3-mm slice thickness, results in significant noise reduction. **3, 4** Non-enhanced scan, coronal reformatted image. **3** Thin-slice (0.9 mm) images are very noisy and do not allow correct localization of the stone (*arrowhead*). **4** Image reconstruction to 5 mm produces a marked reduction in noise and enables a more precise localization of the stone (*arrowhead*)

## Study Protocol

**Patient preparation:** None.

**Post-contrast scan:** To rule out the presence of calcified urinary tract stones, a low-dose (mAs, 50; kVp, 100) scan is sufficient.

## References

Kalra MK, Maher MM, D'Souza RV et al (2005) Detection of urinary tract stones at low-radiation-dose CT with z-axis automatic tube current modulation: phantom and clinical studies. Radiology 235:523-529. Epub 2005 Mar 15

Kim BS, Hwang IK, Choi YW et al (2005) Low-dose and standard-dose unenhanced helical computed tomography for the assessment of acute renal colic: prospective comparative study. Acta Radiol 46:756-763

Poletti PA, Platon A, Rutschmann OT et al (2007) Low-dose versus standard-dose CT protocol in patients with clinically suspected renal colic. AJR Am J Roentgenol 188:927-933

# ABDOMEN – Bladder. Carcinoma



**1** Non-enhanced CT image shows neoplastic tissue bulging from the right lateral wall of the bladder (*arrow*).    **2** In arterial phase, bladder carcinoma is clearly visible (*arrow*).    **3** Portal phase shows mild enhancement of the neoplastic mass (*arrow*).    **4** Excretory phase with the patient in supine decubitus does not clearly depict neoplastic margins due to high-density iodinated urine shading the bladder wall.    **5** Excretory phase, acquired with the patient in prone decubitus (optional phase for selected patients), shows clearly neoplastic margins (*arrow*). Note blood clots as hypodense inclusions in the bladder lumen (*arrowhead*). **6** In arterial phase, a metastatic lymph node, enlarged, round, with homogeneous enhancement, is evident near the anterior wall of the bladder

## Study Protocol

**Patient preparation:** A 6-h fast prior to the examination; fluid administration (oral or i.v.) to stimulate diuresis.

**CM volume:** 500–600 mgI (iodine dose) per kg body weight.

| Patient weight (kg) | < 60 | < 80 | > 80 |
|---|---|---|---|
| **CM concentration (mgI/mL)** | | | |
| 300 | 100 | 130 | 150 |
| 320 | 95 | 125 | 140 |
| 350 | 85 | 115 | 130 |
| 370 | 80 | 110 | 120 |
| 400 | 75 | 100 | 110 |
| **CM injection flow rate (mL/s)** | **1.6 gI/s** | **1.8 gI/s** | **2.0 gI/s** |
| **CM concentration (mgI/mL)** | | | |
| 300 | 5.3 | 6.0 | 6.7 |
| 320 | 5.0 | 5.6 | 6.2 |
| 350 | 4.6 | 5.1 | 5.7 |
| 370 | 4.3 | 4.8 | 5.4 |
| 400 | 4.0 | 4.5 | 5.0 |

**Pre-contrast scan:** Indispensable for the detection of radio-opaque structures.

**Post-contrast scan:** 3 phases (arterial, portal, excretory).

**Scan delay:** The bolus-tracking monitoring technique is used.
Arterial phase: 10 s after a threshold of 100 HU is reached.
Portal phase: 60-70 s from the start of the CM injection.
Excretory phase supine: 7 min from the start of the CM injection.
Excretory phase prone (optional): 7 min from the start of the CM injection.

## References

Memarsadeghi M, Schaefer-Prokop C, Prokop M et al (2007) Unenhanced MDCT in patients with suspected urinary stone disease: do coronal reformations improve diagnostic performance? AJR Am J Roentgenol 189:W60-W64

Paulson EK, Weaver C, Ho LM et al (2008) Conventional and reduced radiation dose of 16- MDCT for detection of nephrolithiasis and ureterolithiasis. AJR Am J Roentgenol 190:151-157

Poletti PA, Platon A, Rutschmann OT et al (2007) Low-dose versus standard-dose CT protocol in patients with clinically suspected renal colic. AJR Am J Roentgenol 188:927-933

# ABDOMEN – Prostate. CT Perfusion
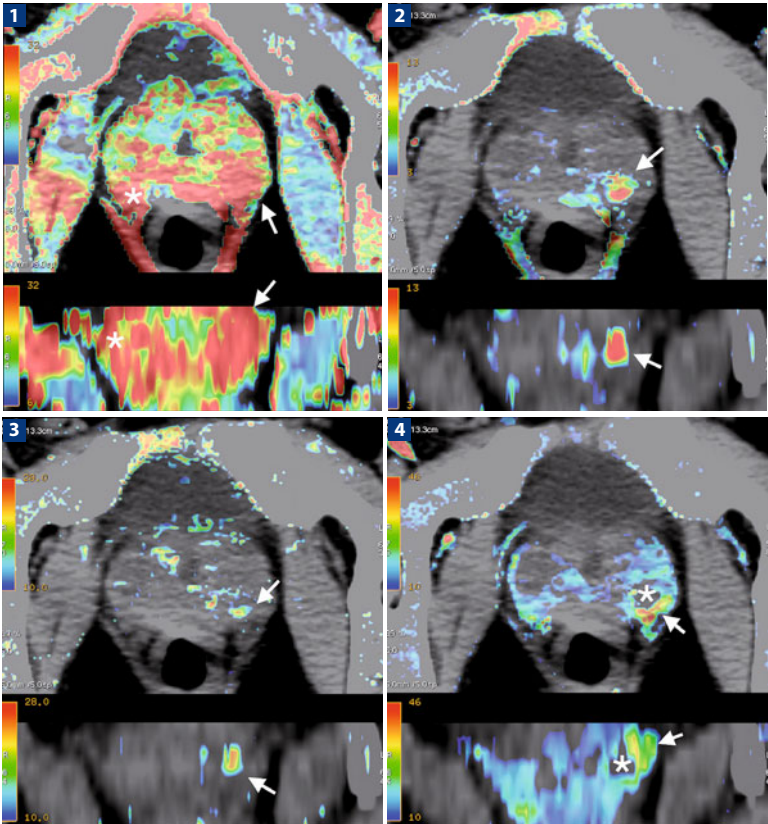


**1** Perfusion analysis (color map: blood flow), axial (*upper image*) and coronal (*lower image*) planes. The map, obtained with a dedicated software application, shows an increase in flow (*arrow*) as expected in a neoplastic lesion. In this map, a focal hotspot was absent but a diffuse increase in flow values may be see also in the contralateral region (*asterisk*). **2** Perfusion analysis (color map: blood volume), axial (*upper image*) and coronal (*lower image*) planes. The map shows an increase in blood volume (*red areas, arrow*) in the tumor with respect to the adjacent tissue. **3** Perfusion analysis (color map: mean transit time), axial (*upper image*) and coronal (*lower image*) planes. The map shows a reduction in the values in the tumor (*blue area*); this finding reflects the presence of multiple arteriovenous shunts in the pathologic tissue with respect to normal tissue. **4** Perfusion analysis (color map: permeability surface area product), axial (*upper image*) and coronal (*lower image*) planes. The map shows an increase in permeability (*red areas, arrow*) in the peripheral tumor area, as expected with inflammation tissues (angiogenesis behavior). The tumor's center shows lower permeability values, as expected for well-shaped vessels (*asterisk*)

## Study Protocol

**Patient preparation:** A 6-h fast prior to the examination. Before scanning, 20 mg butyl scopolamine (Buscopan, Boehringer, Ingelheim, Germany) is injected to suppress peristalsis.

**CM volume:** 60-80 mL according to patient weight.

| CM injection flow rate (mL/s) | 1.6 gI/s | 1.8 gI/s | 2.0 gI/s |
|---|---|---|---|
| CM concentration (mgI/mL) | | | |
| 300 | 5.3 | 6.0 | 6.7 |
| 320 | 5.0 | 5.6 | 6.2 |
| 350 | 4.6 | 5.1 | 5.7 |
| 370 | 4.3 | 4.8 | 5.4 |
| 400 | 4.0 | 4.5 | 5.0 |

**Pre-contrast scan:** Baseline CT images without CM and with a thickness of 2.5–5.0 mm must be acquired to locate the prostate gland and to select the volume on which perfusion scans are to be done.

**Post-contrast scan:** Eight contiguous sections, each collimated to 5 mm, obtained at 1-s intervals by using a cine mode acquisition with no table movement for 45 s during CM first pass, assuming that CM is only in the vascular compartment.
This acquisition should be followed by three 1-s scans separated by 10-s intervals from each other according to deconvolution CT analysis. On the basis of St. Lawrence and Lee's adiabatic approximation, passage of CM into the interstitial compartment can be quantified, and the permeability surface product (PS) count determined according to the equation: $PS = -BF [\ln(1-E)]$, where BF is blood flow and E is the fraction of CM that leaks into the interstitium from the vascular space.
The dynamic CT examination may be optionally followed by a staging abdominal-pelvic examination.

**Scan delay:**
Perfusion first-pass CT scan starts 10 s after the injection of CM.
Perfusion interstitial phase CT scan starts at the end of the first pass with 10 s of temporal resolution.
Optional staging scan starts 85 s after the injection of CM (equilibrium phase).

## References

Bellomi M, Viotti S, Preda L et al (2010) Perfusion CT in solid body-tumours part II. Clinical applications and future development. Radiol Med 115:858-874

Petralia G, Preda L, D'Andreas G et al (2010) In: Bellomi M (ed) La Radiologia Medica. CT perfusion in solid-body tumours. Part I: technical issues. Radiol Med, pp 843-857

Sahani DV, Kalva SP, Hamberg LM et al (2005) Assessing tumor perfusion and treatment response in rectal cancer with multisection CT: initial observations. Radiology 234:785-792

# HEART – Dilated Cardiomyopathy
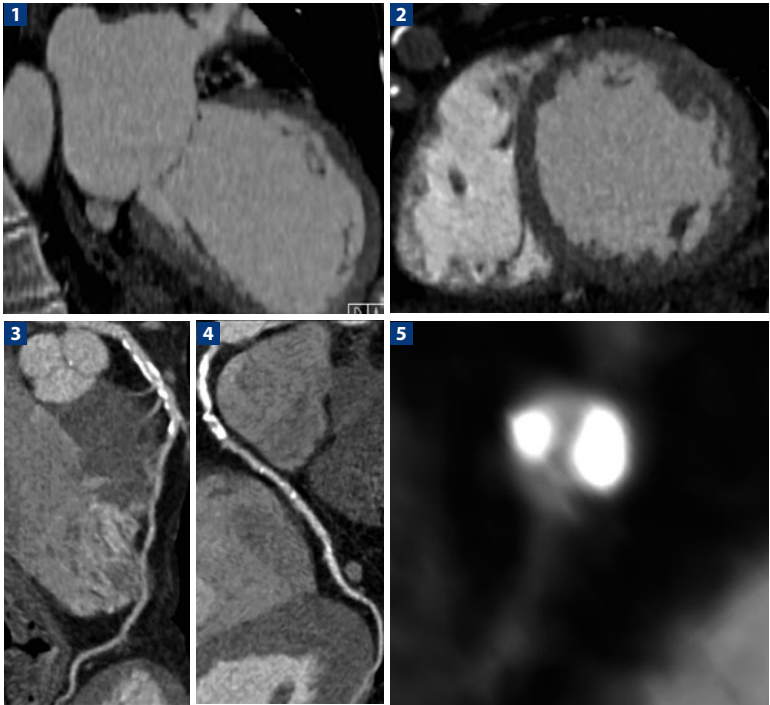










A 67-year-old patient with ischemic dilated cardiomyopathy. **1** Vertical long-axis and **2** short-axis MPR images of the heart show ventricular dilatation with wall thinning. **3**, **4** Curved MPR images show diffuse and severe vascular disease of the coronary arteries. **5** MPR image in a plane orthogonal to the longitudinal axis of the vessel identifies diffuse calcified plaques along the vessel. (Reproduced with the kind permission of Dr. Gorka Bastarrika, University Clinic of Navarra, Pamplona, Spain)

## Study Protocol

**Patient preparation:** A 6-h fast prior to the examination; 18G intravenous catheter in the right antecubital vein. Contraindications to the administration of negative chronotropic drugs and nitrates should be carefully investigated. The administration of negative chronotropic drugs, such as beta blockers and calcium antagonists, is mandatory to reduce and to stabilize heart rate (HR). Control of HR should be decided according to the technology used. For a 64-slice CT scanner, the HR should be < 65 bpm. The administration of nitrates is recommended to dilate the coronary arteries.

**Iodine flow rate:** 2.0 gI/s.

| CM concentration (mgI/mL) | Flow rate (mL/s) |
| --- | --- |
| 300 | 6.7 |
| 320 | 6.2 |
| 350 | 5.7 |
| 370 | 5.4 |
| 400 | 5.0 |

**CM volume:** (Scan time + trigger delay)*flow rate.

**Saline flush:** 50 ml of saline or 10 ml of CM + 40 ml of saline at the same flow rate.

**Pre-contrast scan (calcium score):** Useful for the quantification of coronary calcium.

**Post-contrast scan:**
CM injection protocol with injection time = scan time + 7-s trigger delay.
Trigger delay: 7 s after the threshold of 100 HU is reached in the ascending aorta using a bolus-tracking technique.
Gating: Retrospective or prospective (according to patient's HR and the technology available).
Scan region: From the ascending aorta to the heart apex.

## References

Andreini D, Pontone G, Pepi M et al (2007) Diagnostic accuracy of multidetector computed tomography coronary angiography in patients with dilated cardiomyopathy. J Am Coll Cardiol 49:2044-2050

Butler J (2007) The emerging role of multi-detector computed tomography in heart failure. J Card Fail 13:215-226

Williams TJ, Manghat NE, McKay-Ferguson A et al (2008) Cardiomyopathy: appearances on ECG-gated 64-detector row computed tomography. Clin Radiol 63:464-474

# HEART – Hypertrophic Cardiomyopathy
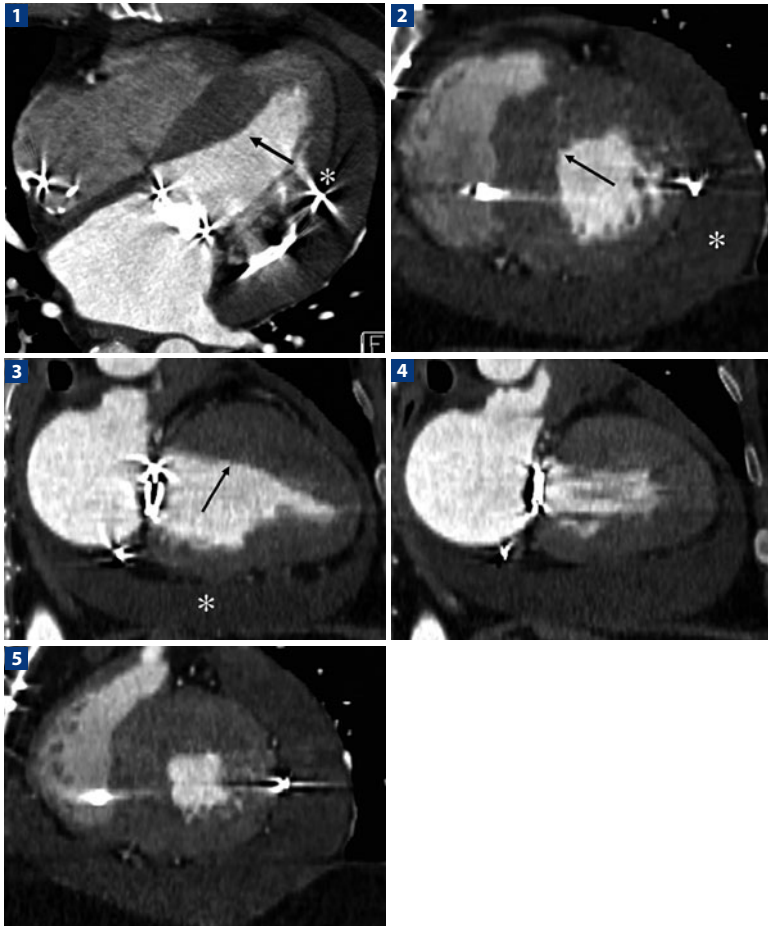


A 52-year-old patient with hypertrophic cardiomyopathy treated with mitral valve replacement and pacemaker implantation. **1-3** Four-chamber, short-axis and vertical long-axis MPR images, respectively. In diastole, note the marked eccentric hypertrophy of the interventricular septum (*arrow*), with associated hypertrophy of the remaining cardiac segments resulting from systemic hypertension. Marked concentric pericardial effusion can also be appreciated (*asterisk*). **4**, **5** Short-axis and vertical long-axis MPR images, respectively. In systole, note the concentric hypertrophy and the overall reduction in heart-wall motion. The ventricular diameters should be measured in diastole. (Reproduced with the kind permission of Dr. Gorka Bastarrika, University Clinic of Navarra, Pamplona, Spain)

## Study Protocol

**Patient preparation:** A 6-h fast prior to the examination; 18G intravenous catheter in the right antecubital vein. Contraindications to the administration of negative chronotropic drugs and nitrates should be carefully investigated. The administration of negative chronotropic drugs, such as beta blockers and calcium antagonists, is mandatory to reduce and to stabilize heart rate (HR). Control of HR should be decided according to the technology used. For a 64-slice CT scanner, the HR should be < 65 bpm. The administration of nitrates is recommended to dilate the coronary arteries.

**Iodine flow rate:** 2.0 gI/s.

| CM concentration (mgI/mL) | Flow rate (mL/s) |
|---|---|
| 300 | 6.7 |
| 320 | 6.2 |
| 350 | 5.7 |
| 370 | 5.4 |
| 400 | 5.0 |

**CM volume:** (Scan time + trigger delay)*flow rate.

**Saline flush:** 50 ml of saline or 10 ml of CM + 40 ml of saline at the same flow rate.

**Pre-contrast scan (calcium score):** Useful for the quantification of coronary calcium.

**Post-contrast scan:**
CM injection protocol with the injection time = scan time + 7-s trigger delay.
Trigger delay: 7 s after the threshold of 100 HU is reached in the ascending aorta using a bolus-tracking technique.
Gating: Retrospective or prospective (according to patient HR and technology available).
Scan region: From the ascending aorta to the heart apex.

## References

Ghersin E, Lessick J, Litmanovich D et al (2006) Comprehensive multidetector CT assessment of apical hypertrophic cardiomyopathy. Br J Radiol 79:e200-204

Mitsutake R, Miura S, Sako H et al (2008) Usefulness of multi-detector row computed tomography for the management of percutaneous transluminal septal myocardial ablation in patient with hypertrophic obstructive cardiomyopathy. Int J Cardiol 129:e61-63

Sparrow P, Merchant N, Provost Y et al (2009) Cardiac MRI and CT features of inheritable and congenital conditions associated with sudden cardiac death. Eur Radiol 19:259-270. PMID: 18795295

# HEART – Non-compaction Cardiomyopathy
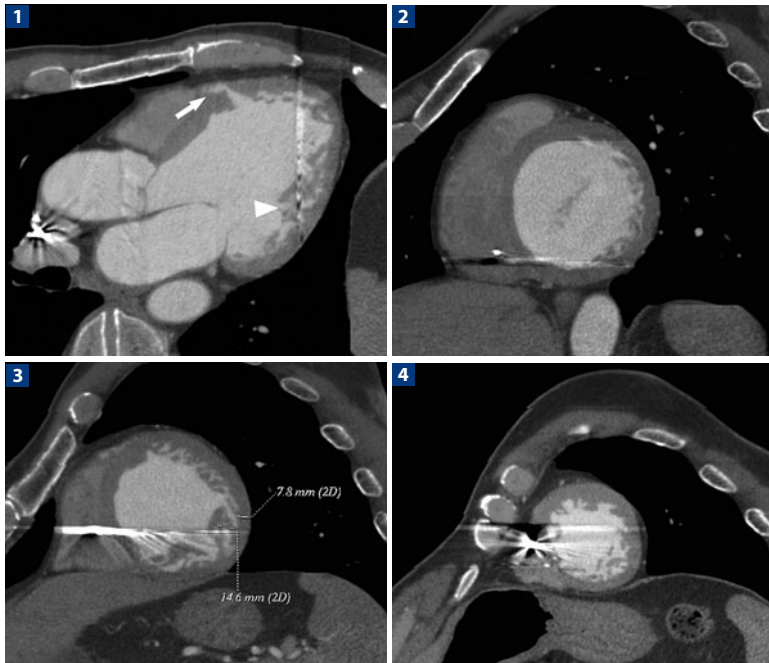


A 49-year-old patient with a history of cardiac arrest and automatic defibrillator implantation underwent CT coronary angiography to rule out the presence of coronary artery disease. The examination showed no significant alterations of the coronary arteries. **1** Three-chamber MPR image shows an accentuation of the trabecular meshwork of the ventricular myocardium (*arrowhead*). A deep intratrabecular recess (*arrow*) seems to cross the interventricular septum up to the right ventricle. **2**, **3**, **4** Short- and long-axis MPR images. An accentuation of the trabecular meshwork of the entire ventricular myocardium can be appreciated at the **2** valvular, **3** middle, and **4** apical levels. The "non-compact" trabecular myocardium is thicker than the "compact" nontrabecular myocardium. Such beam-hardening artifacts are caused by the automatic defibrillator catheter

## Study Protocol

**Patient preparation:** A 6-h fast prior to the examination; 18G catheter in the right antecubital vein. Contraindications to the administration of negative chronotropic drugs and nitrates should be carefully investigated. The administration of negative chronotropic drugs, such as beta blockers and calcium antagonists, is mandatory to reduce and to stabilize heart rate (HR). The control of HR should be decided according to the technology used. For a 64-slice CT scanner, the patient's HR should be < 65 bpm. The administration of nitrates is recommended to dilate the coronary arteries.

**Iodine flow rate:** 2.0 gI/s.

| CM concentration (mgI/mL) | Flow rate (mL/s) |
|---|---|
| 300 | 6.7 |
| 320 | 6.2 |
| 350 | 5.7 |
| 370 | 5.4 |
| 400 | 5.0 |

**CM volume:** (Scan time + trigger delay)*flow rate.

**Saline flush:** 50 ml of saline or 10 ml of CM + 40 ml of saline at the same flow rate.

**Pre-contrast scan (calcium score):** Useful for the quantification of coronary calcium.

**Post-contrast scan:**
CM injection protocol with injection time = scan time + 7-s trigger delay.
Trigger delay: 7 s after the threshold of 100 HU is reached in the ascending aorta using a bolus-tracking technique.
Gating: Retrospective or prospective (according to patient HR and technology available).
Scan region: From the ascending aorta to the heart apex.

## References

Eilen D, Peterson N, Karkut C et al (2008) Isolated noncompaction of the left ventricular myocardium: a case report and literature review. Echocardiography 25:755-761

Jacquier A, Revel D, Saeed M (2008) MDCT of the myocardium: a new contribution to ischemic heart disease. Acad Radiol 15:477-487

Orakzai SH, Orakzai RH, Nasir K et al (2006) Assessment of cardiac function using multidetector row computed tomography. J Comput Assist Tomogr 30:555-563
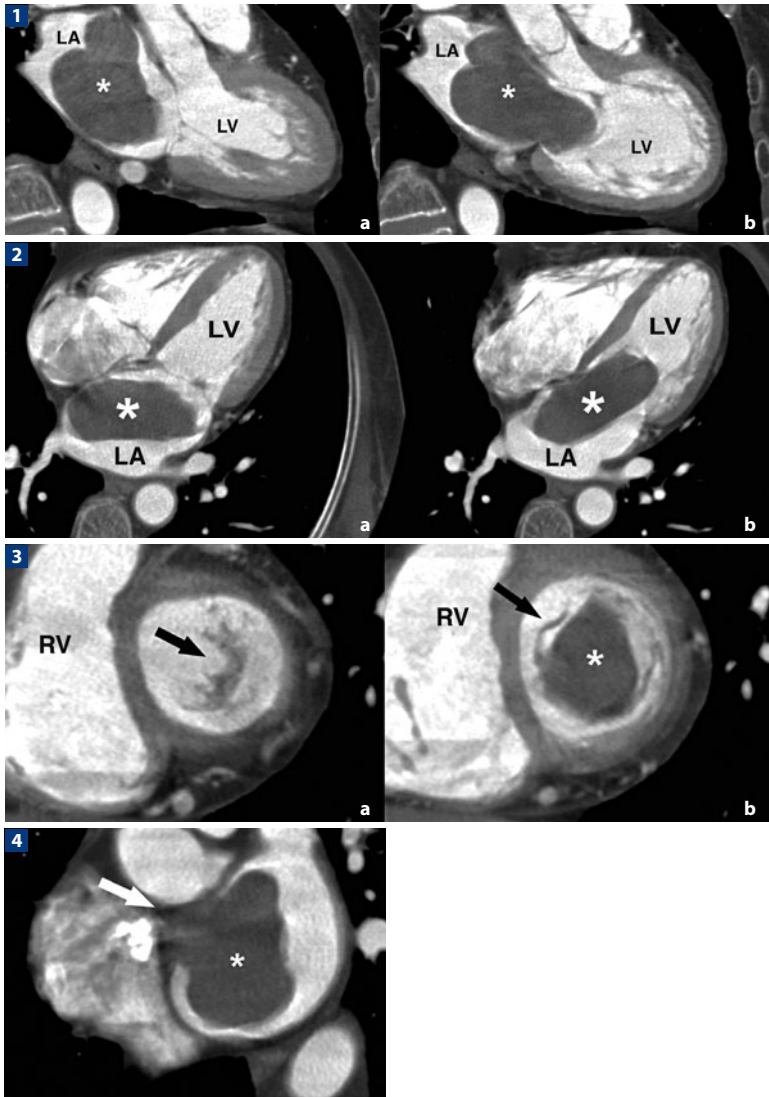
A 77-year-old patient with dyspnea, palpitations, and chest pain but with no ECG or enzymatic changes underwent echocardiography, which revealed the presence of a mobile mass within the atrium. As the relationship of the mass with the heart chamber could not be correctly visualized, an MDCT examination was requested.

**1, 2** Three- and four-chamber MPR images of the heart during systole (**a**) and ▶

## Study Protocol

**Patient preparation:** A 6-h fast prior to the examination; 18G intravenous catheter in the right antecubital vein. Contraindications to the administration of negative chronotropic drugs and nitrates should be carefully investigated. The administration of negative chronotropic drugs, such as beta blockers and calcium antagonists, is mandatory to reduce and to stabilize heart rate (HR). The control of HR should be decided according to the technology used. For a 64-slice CT scanner, the HR should be < 65 bpm. The administration of nitrates is recommended to dilate the coronary arteries.

**Iodine flow rate:** 2.0 gI/s.

| CM concentration (mgI/mL) | Flow rate (mL/s) |
|---|---|
| 300 | 6.7 |
| 320 | 6.2 |
| 350 | 5.7 |
| 370 | 5.4 |
| 400 | 5.0 |

**CM volume:** (Scan time + trigger delay)*flow rate.

**Saline flush:** 50 ml of saline or 10 ml of CM + 40 ml of saline at the same flow rate.

**Pre-contrast scan (calcium score):** Useful for the quantification of coronary calcium.

**Post-contrast scan:**
CM injection protocol is calculated with injection time = scan time + 7-s trigger delay.
Trigger delay: 7 s after the threshold of 100 HU is reached in the ascending aorta using a bolus-tracking technique.
Gating: Retrospective or prospective (according to patient HR and technology available).
Scan region: From the ascending aorta to the heart apex.

## References

Grebenc ML, Rosado-de-Christenson ML, Green CE et al (2002) Cardiac myxoma: imaging features in 83 patients. RadioGraphics 22:673-689

Neragi-Miandoab S, Kim J, Vlahakes GJ (2007) Malignant tumours of the heart: a review of tumour type, diagnosis and therapy. Clin Oncol (R Coll Radiol) 19:748-756

Yuan SM, Shinfeld A, Lavee J et al (2009) Imaging morphology of cardiac tumours. Cardiol J 16:26-35

◀ diastole (**b**). Note the presence of a mass (*asterisk*) within the left atrium (*LA*) that during diastole (**b**) migrates within the left ventricle (*LV*).   **3** Short-axis MPR image of the heart. The reconstruction shows the relations between the mass (asterisk) and the mitral valve (*arrow*).   **4** Axial MPR image shows the insertion (*arrow*) of the atrial mass (*asterisk*) at the level of the interatrial septum
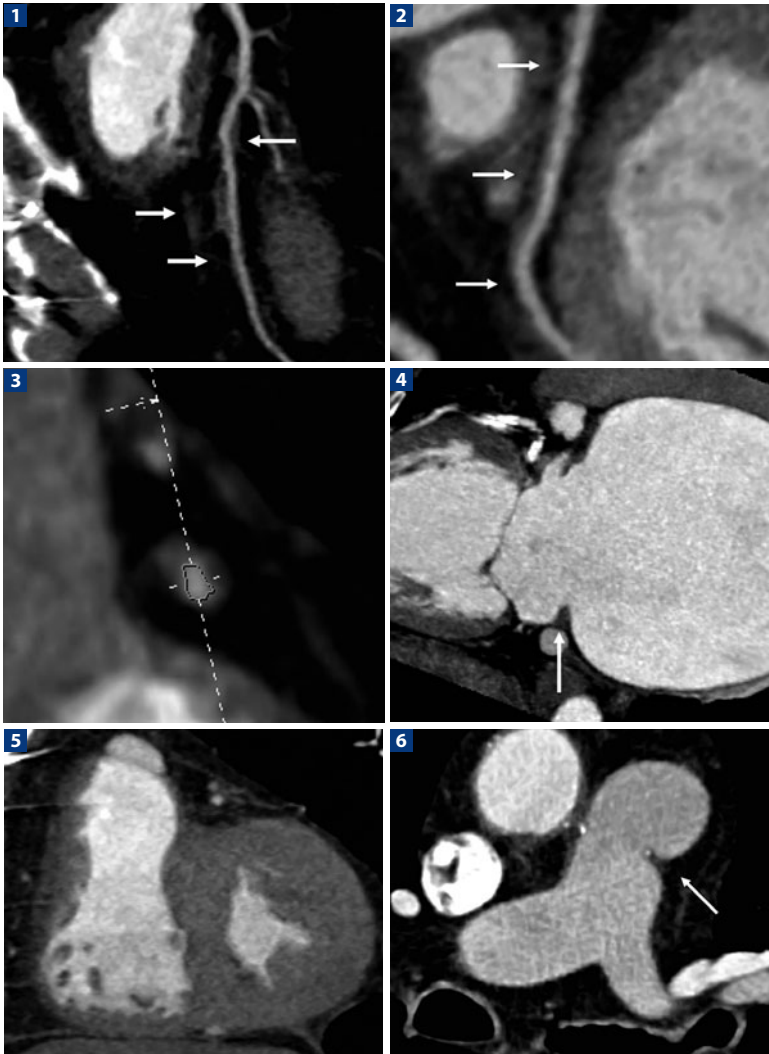
A 62-year-old patient underwent an orthotopic heart transplant with biatrial technique 7 years earlier. **1**, **2** Curved MPR image shows transplant vasculopathy and rejection, with diffuse thickening of the vessel wall due to intimal hyperplasia. The finding can be distinguished from classic atheromatous disease by the concentric thickening, beginning from the distal vessels and progressing proximally (*arrows*). **3** MPR image in a plane orthogonal to the longitudinal axis of the vessel shows diffuse concentric thickening of the vessel wall. **4** Vertical long-axis MPR image ▶

## Study Protocol

**Patient preparation:** A 6-h fast prior to the examination. 18G intravenous catheter in the right antecubital vein. The administration of negative chronotropic drugs is useless because of the denervation of the transplanted heart.

**Iodine flow rate:** 2.0 gI/s.

| CM concentration (mgI/mL) | Flow rate (mL/s) |
| --- | --- |
| 300 | 6.7 |
| 320 | 6.2 |
| 350 | 5.7 |
| 370 | 5.4 |
| 400 | 5.0 |

**CM volume:** (Scan time + trigger delay)*flow rate.

**Saline flush:** 50 ml of saline or 10 ml of CM + 40 ml of saline at the same flow rate.

**Pre-contrast scan (calcium score):** Unnecessary.

**Post-contrast scan:**
CM injection protocol with injection time = scan time + 7-s trigger delay.
Trigger delay: 7s after the threshold of 100 HU is reached in the ascending aorta using a bolus-tracking technique.
Gating: Retrospective or prospective (according to patient HR and technology available).
Scan region: From the ascending aorta to the heart apex.

## References

Ferencik M, Gregory SA, Butler J et al (2007) Analysis of cardiac dimensions, mass and function in heart transplant recipients using 64-slice multi-detector computed tomography. J Heart Lung Transplant 26:478-484

Gregory SA, Ferencik M, Achenbach S et al (2006) Comparison of sixty-four-slice multidetector computed tomographic coronary angiography to coronary angiography with intravascular ultrasound for the detection of transplant vasculopathy. Am J Cardiol 98:877-884

Iyengar S, Feldman DS, Cooke GE et al (2006) Detection of coronary artery disease in orthotopic heart transplant recipients with 64-detector row computed tomography angiography. J Heart Lung Transplant 25:1363-1366

◀ of the heart: massive left atrial dilatation, characteristic of the transplant particularly when done with biatrial technique. Note the site of the anastomosis (*arrow*). **5** Short-axis MPR image of the heart identifies concentric ventricular hypertrophy; this finding is common in transplant patients and results from the immunosuppressive treatment and systemic hypertension. **6** Axial MPR image shows anastomosis of the pulmonary artery (*arrow*). (Reproduced with the kind permission of Dr. Gorka Bastarrika, University Clinic of Navarra, Pamplona, Spain)
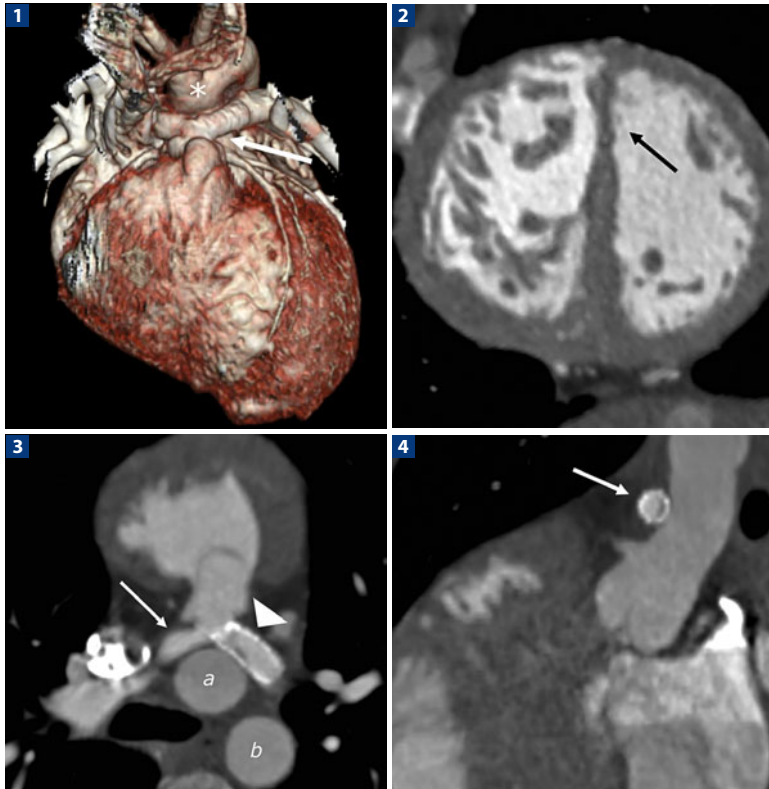
Evaluation of a left pulmonary artery stent due to frequent stenosis after the procedure. Following the Jatene procedure, the coronary arteries were excised from the aorta, which was sectioned and then inverted together with the pulmonary artery. Before the vessels are anastomosed, the pulmonary artery is positioned in front of the aorta. This maximizes the length of the neo-aorta and minimizes the risk of kinking or compression of the coronary arteries. The coronary arteries are then re-implanted on the neo-aorta. In patients undergoing the arterial switch procedure, there is a substantial risk of early or late coronary stenosis or occlusion. **1** VR reconstruction shows the pulmonary artery (*arrow*) running in front of the aorta (*asterisk*). **2** Short-axis MPR image of the heart highlights concentric hypertrophy of the right ventricle with thinning of the interventricular septum (*arrow*). **3** Axial MIP reconstruction shows the left pulmonary stent with initial intimal hyperplasia (*arrowhead*). Note the pulmonary artery running in front of the aorta (*arrow*) and the anomalous position of the ascending aorta (**a**) with respect to the descending aorta (**b**). **4** On oblique MPR image, the left pulmonary stent with initial intimal hyperplasia (*arrow*) is seen. Note the compression of the ▶

## Study Protocol

**Patient preparation:** A 6-h fast prior to the examination; 18G intravenous catheter in the right antecubital vein. Contraindications to the administration of negative chronotropic drugs and nitrates should be carefully investigated. The administration of negative chronotropic drugs, such as beta blockers and calcium antagonists, is mandatory to reduce and to stabilize heart rate (HR). The control of HR should be decided according to the technology used. For a 64-slice CT scanner, the HR should be < 65 bpm. The administration of nitrates is recommended to dilate the coronary arteries.

**Iodine flow rate:** 2.0 gI/s.

| CM concentration (mgI/mL) | Flow rate (mL/s) |
|---|---|
| 300 | 6.7 |
| 320 | 6.2 |
| 350 | 5.7 |
| 370 | 5.4 |
| 400 | 5.0 |

**CM volume:** (Scan time + trigger delay)*flow rate.

**Saline flush:** 50 ml of saline or 10 ml of CM + 40 ml of saline at the same flow rate.

**Pre-contrast scan (calcium score):** Unnecessary.

**Post-contrast scan:**
CM injection protocol with injection time = scan time + 7-s trigger delay.
Trigger delay: 7s after the threshold of 100 HU is reached in the ascending aorta using a bolus-tracking technique.
Gating: Retrospective or prospective (according to patient HR and technology available.
Scan region: from the ascending aorta to the heart apex.

## References

Eichhorn JG, Long FR, Hill SL et al (2006) Assessment of in-stent stenosis in small children with congenital heart disease using multi-detector computed tomography: a validation study. Catheter Cardiovasc Interv 68:11-20

Lee T, Tsai IC, Fu YC et al (2006) Using multidetector-row CT in neonates with complex congenital heart disease to replace diagnostic cardiac catheterization for anatomical investigation: initial experiences in technical and clinical feasibility. Pediatr Radiol 36:1273-1282

Leschka S, Oechslin E, Husmann L et al (2007) Pre- and postoperative evaluation of congenital heart disease in children and adults with 64-section CT. Radio-Graphics 27:829-846

◀ pulmonary artery on the ascending aorta, which predisposes the pulmonary arteries to stenosis. (Reproduced with the kind permission of Dr. Gorka Bastarrika, University Clinic of Navarra, Pamplona, Spain)

# HEART – Bicuspid Aortic Valve
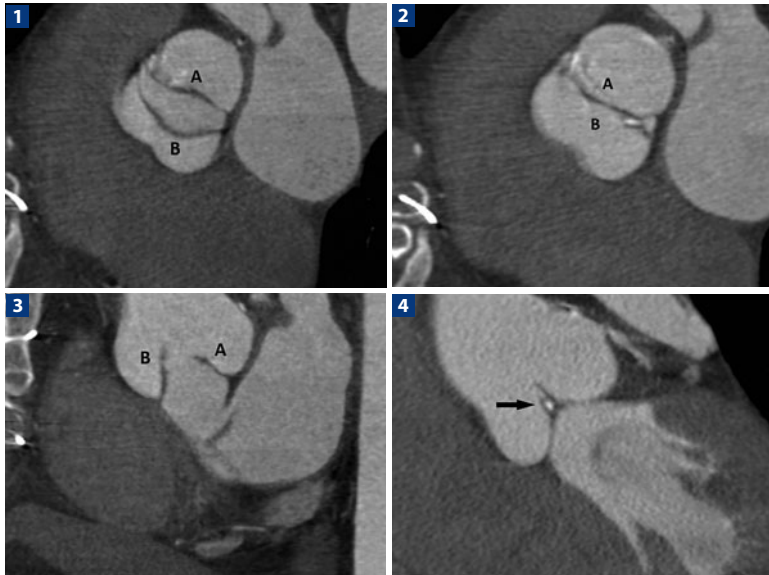


A 64-year-old patient underwent CT coronary angiography after an episode of chest pain. CT examination reveals the presence of a bicuspid aortic valve. **1, 2** MPR images in a plane parallel to the valve in the systolic and diastolic phases. The aortic valve consists of only two leaflets, the right (**b**) and the left (**a**). In systole, reduced excursion of the valve leaflets can be appreciated (stenosis). **3, 4** MPR images on an axis perpendicular to the valve in the systolic and diastolic phases. Note the presence of calcifications (*arrow*) on the valve leaflets (**a**, **b**), which have a slightly thickened appearance

## Study Protocol

**Patient preparation:** A 6-h fast prior to the examination; 18G intravenous catheter in the right antecubital vein. The administration of negative chronotropic drugs, such as beta blockers and calcium antagonists, is mandatory to reduce and to stabilize heart rate (HR). The administration of nitrates is recommended to dilate the coronary arteries.

**Iodine flow rate:** 2.0 gI/s.

| CM concentration (mgI/mL) | Flow rate (mL/s) |
| --- | --- |
| 300 | 6.7 |
| 320 | 6.2 |
| 350 | 5.7 |
| 370 | 5.4 |
| 400 | 5.0 |

**CM volume:** Scan time + trigger delay)*flow rate.

**Saline flush:** 50 ml of saline or 10 ml of CM + 40 ml of saline at the same flow rate.

**Pre-contrast scan (calcium score):** Useful for the quantification of coronary calcium.

**Post-contrast scan:**
CM injection protocol with injection time= scan time + 7-s trigger delay.
Trigger delay: 7 s after the threshold of 100 HU is reached in the ascending aorta using a bolus-tracking technique.
Scan protocol:
Gating: Retrospective or prospective (according to patient HR and technology available).
Scan region: From the ascending aorta to the heart apex.

## References

Gilkeson RC, Markowitz AH, Balgude A et al (2006) MDCT evaluation of aortic valvular disease. AJR Am J Roentgenol 186:350-360
Ryan R, Abbara S, Colen RR et al (2008) Cardiac valve disease: spectrum of findings on cardiac 64-MDCT. AJR Am J Roentgenol 190:W294-303

# HEART – Iatrogenic Coronary Dissection
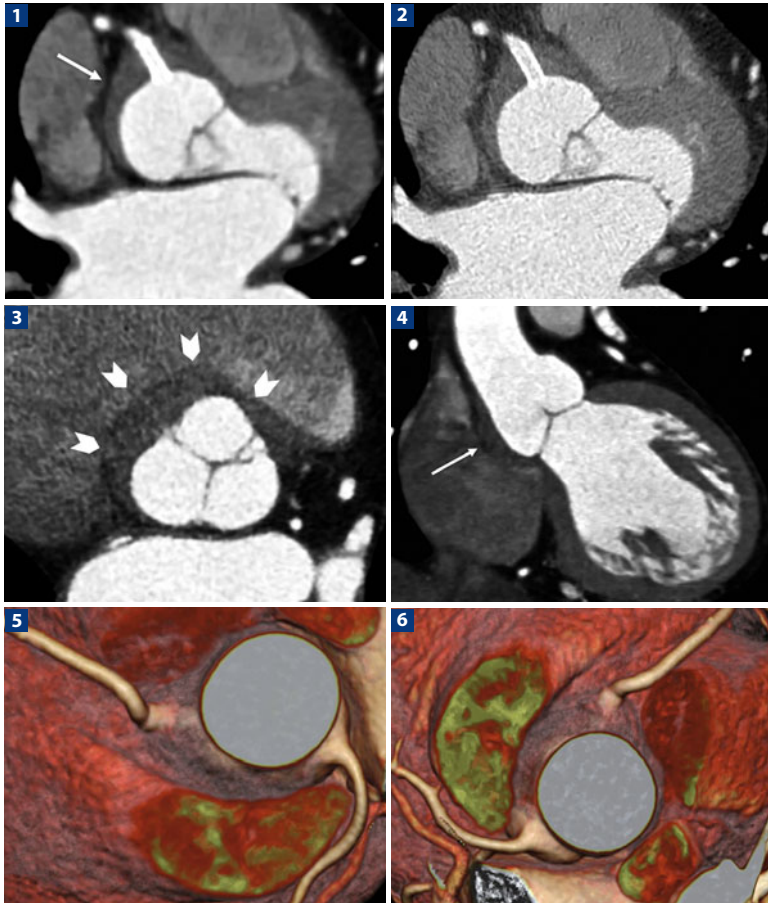












A 54-year-old patient underwent coronary angiography prior to aortic valve replacement. Following iatrogenic dissection and perforation of the right coronary artery with stent deployment, a second CT coronary angiography was performed the day after the procedure to evaluate the stent and the hematoma. **1** Axial MPR image shows the well positioned stent. Note the peri-coronary hematoma (*arrow*) surrounding the proximal tract of the right coronary artery. **2** Axial MPR image with reconstruction using the Bf46 filter better evaluates stent patency. **3** MPR image in the aortic valve plane reveals the hematoma, concentrically surrounding the aortic valve (*arrowheads*). **4** Coronal MPR image demonstrates the coronary hematoma (*arrow*) located along the coronary sinus for its entire length. **5**, **6** On VR reconstruction, the peri-coronary hematoma appears as a thin band of intermediate density involving the origin of both coronary sinuses. (Reproduced with the kind permission of Dr. Gorka Bastarrika, University Clinic of Navarra, Pamplona, Spain)

## Study Protocol

**Patient preparation:** A 6-h fast prior to the examination; 18G intravenous catheter in the right antecubital vein. The administration of negative chronotropic drugs, such as beta blockers and calcium antagonists, is mandatory to reduce and to stabilize HR. The administration of nitrates is recommended to dilate the coronary arteries.

**Iodine flow rate:** 2.0 gI/s.

| CM concentration (mgI/mL) | Flow rate (mL/s) |
|---|---|
| 300 | 6.7 |
| 320 | 6.2 |
| 350 | 5.7 |
| 370 | 5.4 |
| 400 | 5.0 |

**CM volume:** (Scan time + trigger delay)*flow rate.

**Saline flush:** 50 ml of saline or 10 ml of CM + 40 ml of saline at the same flow rate.

**Pre-contrast scan (calcium score):** Unnecessary.

**Post-contrast scan:**
CM injection protocol with injection time = scan time + 7-s trigger delay.
Trigger delay: 7 s after the threshold of 100 HU is reached in the ascending aorta using a bolus-tracking technique.
Scan protocol:
Gating: Retrospective or prospective (according to patient HR and technology available).
Scan region: From the ascending aorta to the heart apex.

## References

Cheng CC, Tsao TP, Tzeng BH et al (2008) Stenting for coronary intervention-related dissection of the left main coronary artery with extension to the aortic root: a case report. South Med J 101:1165-1167

Kantarci M, Ceviz N, Sevimli S et al (2007) Diagnostic performance of multidetector computed tomography for detecting aorto-ostial lesions compared with catheter coronary angiography: multidetector computed tomography coronary angiography is superior to catheter angiography in detection of aorto-ostial lesions. J Comput Assist Tomogr 31:595-599

Yoshikai M, Ikeda K, Itoh M et al (2008) Detection of coronary artery disease in acute aortic dissection: the efficacy of 64-row multidetector computed tomography. J Card Surg 23:277-279
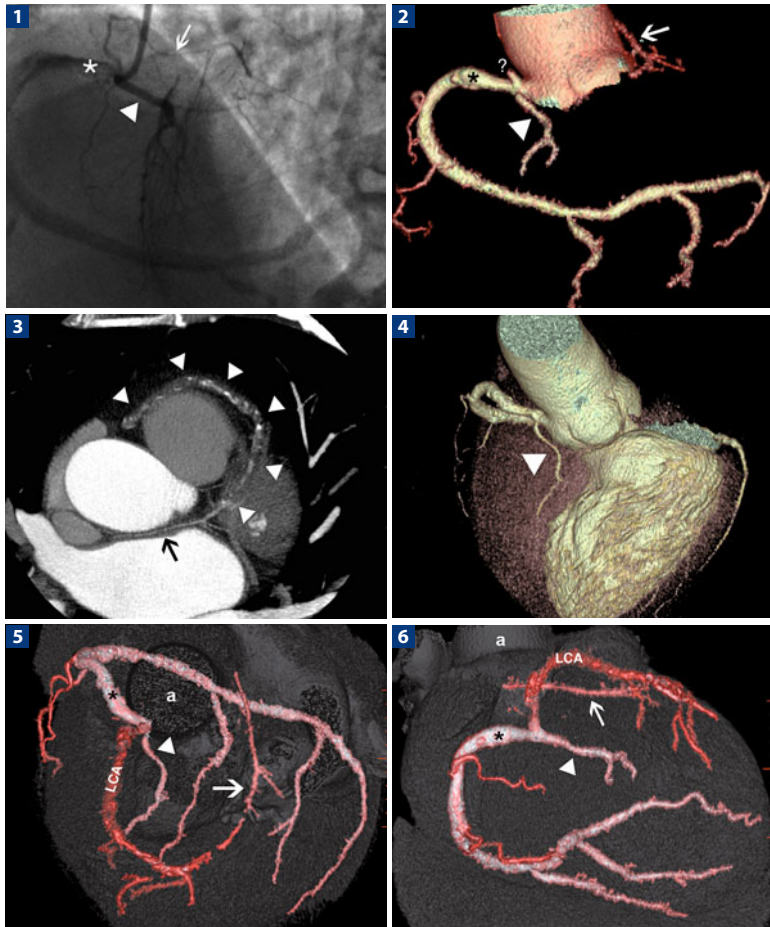
Following an episode of angina due to myocardial ischemia, a 49-year-old patient underwent conventional coronary angiography, which was unable to identify the left coronary ostium. CT coronary angiography was performed to search for an anomalous origin of the left coronary circulation. **1** Angiography examination reveals the right coronary ostium as the origin of the right coronary artery (*asterisk*), a large branch (*arrowhead*) running anteriorly, and another smaller branch running posteriorly (*arrow*). **2** VR reconstruction reveals the same findings as seen on conventional coronary angiography and an additional vessel of which only the origin can be appreciated (*question mark*). **3** Axial MIP reconstruction highlights the anastomotic circulation anterior to the origin of the pulmonary artery (*arrowheads*). This circulation apparently consists of the branch identified at coronary angiography (*arrow*) and a larger branch originating ▶

## Study Protocol

**Patient preparation:** A 6-h fast prior to the examination; 18G catheter in the right antecubital vein. The administration of negative chronotropic drugs, such as beta blockers and calcium antagonists, is mandatory to reduce and to stabilize HR. The administration of nitrates is recommended to dilate the coronary arteries.

**Iodine flow rate:** 2.0 gl/s.

| CM concentration (mgl/mL) | Flow rate (mL/s) |
| --- | --- |
| 300 | 6.7 |
| 320 | 6.2 |
| 350 | 5.7 |
| 370 | 5.4 |
| 400 | 5.0 |

**CM volume:** (Scan time + trigger delay)*flow rate.

**Saline flush:** 50 ml of saline or 10 ml of CM + 40 ml of saline at the same flow rate.

**Pre-contrast scan (calcium score):** Useful for the evaluation of the coronary anatomy in case of anomalous origin.

**Post-contrast scan:**
CM injection protocol with injection time = scan time + 7-s trigger delay.
Trigger delay: 7 s after the threshold of 100 HU is reached in the ascending aorta using a bolus-tracking technique.
Scan protocol:
Gating: Retrospective or prospective (according to patient HR and technology available).
Scan region: From the ascending aorta to the heart apex.

## References

Cademartiri F, Runza G, Luccichenti G et al (2006) Coronary artery anomalies: incidence, pathophysiology, clinical relevance and role of diagnostic imaging. Radiol Med 111:376-391

Dodd JD, Ferencik M, Liberthson RR et al (2007) Congenital anomalies of coronary artery origin in adults: 64-MDCT appearance. AJR Am J Roentgenol 188:W138-146

Kacmaz F, Ozbulbul NI, Alyan O et al (2008) Imaging of coronary artery anomalies: the role of multidetector computed tomography. Coron Artery Dis 19:203-209

◀ from the right, and appears completely occluded (*arrowheads*).  **4**  VR reconstruction shows the branch (*arrowhead*), arising from the right coronary ostium and running towards the apex, with an intramyocardial course within the interventricular septum.  **5**, **6**  VR reconstructions identifies a single coronary ostium on the right, from which arises the right coronary artery (*asterisk*), an interventricular branch (*arrowhead*), the left coronary artery (LCA), and a small branch that anastomizes anteriorly with the left coronary artery (*arrow*)
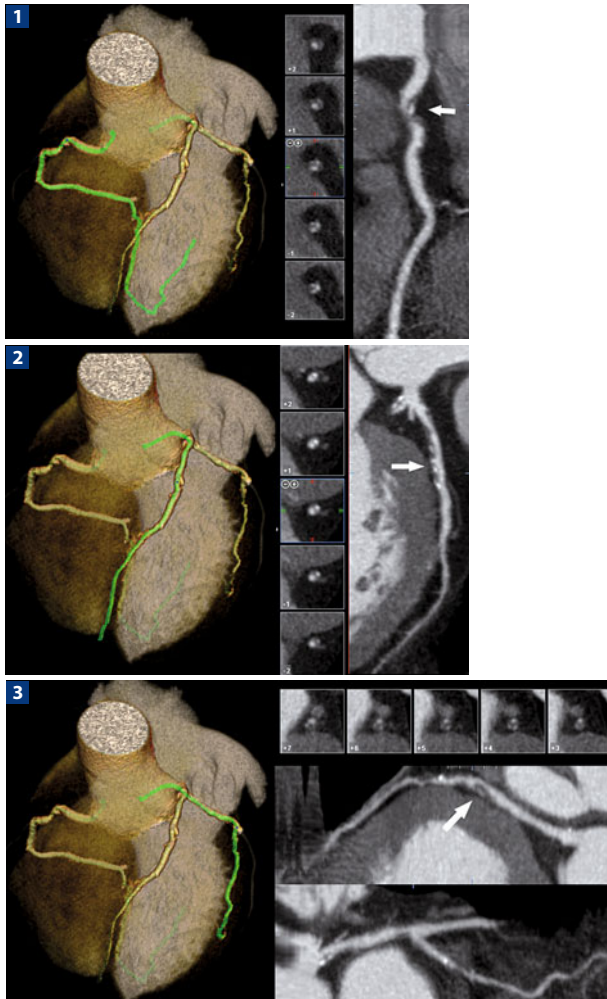
A 63-year-old patient with no family history or risk factors for coronary artery disease reported an episode of angina; ECG signs of myocardial ischemia were absent. VR reconstruction and curved MPR image show: **1** a fibrocalcific plaque at the level of the proximal segment of the right coronary artery (*arrow*); **2** a large fibrocalcific plaque extending for the entire length of the proximal tract of the left anterior descending coronary artery (*arrow*); **3** an extensive fibrocalcific plaque at the level of the circumflex artery (*arrow*) and corresponding with the first marginal branch

## Study Protocol

**Patient preparation:** A 6-h fast prior to the examination; 18G intravenous catheter in the right antecubital vein. The administration of negative chronotropic drugs, such as beta blockers and calcium antagonists, is mandatory to reduce and to stabilize heart rate (HR). The administration of nitrates is recommended to dilate the coronary arteries.

**Iodine flow rate:** 2.0 gI/s.

| CM concentration (mgI/mL) | Flow rate (mL/s) |
|---|---|
| 300 | 6.7 |
| 320 | 6.2 |
| 350 | 5.7 |
| 370 | 5.4 |
| 400 | 5.0 |

**CM volume:** (Scan time + trigger delay)*flow rate.

**Saline flush:** 50 ml of saline or 10 ml of CM + 40 ml of saline at the same flow rate.

**Pre-contrast scan (calcium score):** Useful for the quantification of coronary calcium.

**Post-contrast scan:**
CM injection protocol: Injection time = scan time + 7-s trigger delay.
Trigger delay: 7s after the threshold of 100 HU is reached in the ascending aorta using a bolus-tracking technique.
Scan protocol:
Gating: Retrospective or prospective (according to patient HR and technology available).
Scan region: From the ascending aorta to the heart apex.

## References

Cademartiri F, Romano M, Seitun S et al (2008) Prevalence and characteristics of coronary artery disease in a population with suspected ischemic heart disease using CT coronary angiography: correlations with cardiovascular risk factors and clinical presentation. Radiol Med 113:363-372

Meijboom WB, van Mieghem CA, Mollet NR et al (2007) 64-slice computed tomography coronary angiography in patients with high, intermediate, or low pretest probability of significant coronary artery disease. J Am Coll Cardiol 50:1469-1475

Meijboom WB, van Mieghem CA, van Pelt N et al (2008) Comprehensive assessment of coronary artery stenoses: computed tomography coronary angiography versus conventional coronary angiography and correlation with fractional flow reserve in patients with stable angina. J Am Coll Cardiol 52:636-643

# HEART – Chronic Total Occlusion of the Left Anterior Descending Artery with Associated Apical Infarction
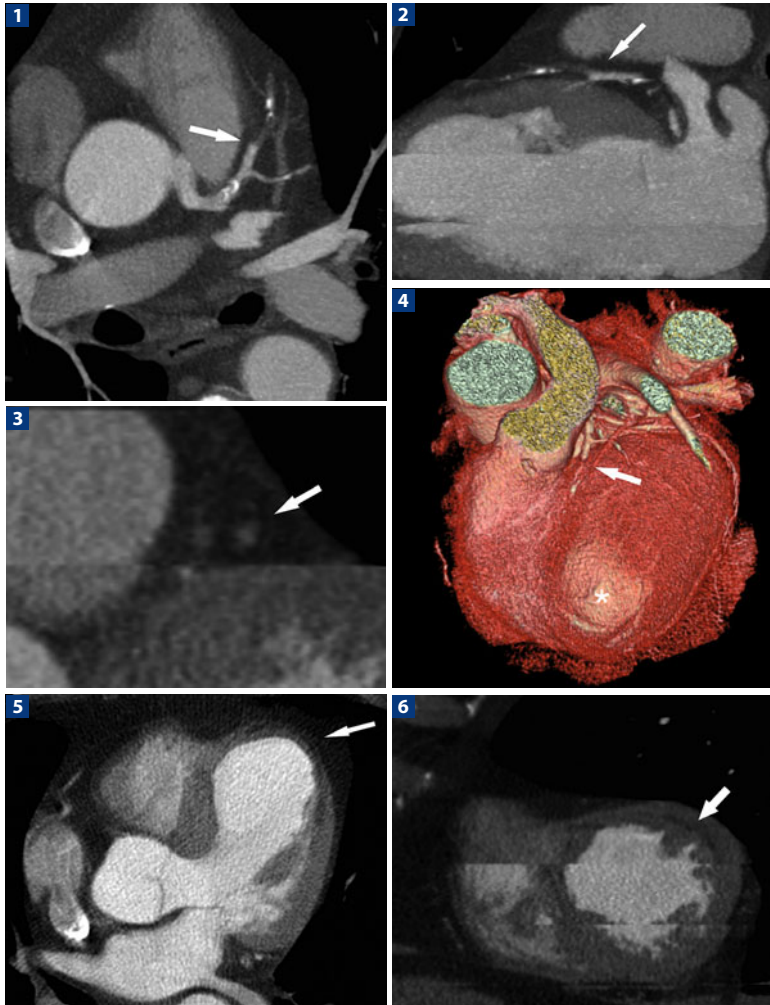












A 73-year-old patient with a prior episode of chest pain (3 years earlier) was treated pharmacologically but undergoes CT coronary angiography at the return of symptoms. **1** Axial MPR image shows the occluded left anterior descending artery (*arrow*) distal to the origin of the first diagonal branch. **2** Vertical long-axis MPR image of the heart shows the extension of the occlusion (*arrow*), which involves the entire vessel. **3** MPR image in a plane orthogonal to the ▶

## Study Protocol

**Patient preparation:** A 6-h fast prior to the examination; 18G catheter in the right antecubital vein. The administration of negative chronotropic drugs, such as beta blockers and calcium antagonists, is mandatory to reduce and to stabilize HR. The administration of nitrates is recommended to dilate the coronary arteries.

**Iodine flow rate:** 2.0 gI/s.

| CM concentration (mgI/mL) | Flow rate (mL/s) |
|---|---|
| 300 | 6.7 |
| 320 | 6.2 |
| 350 | 5.7 |
| 370 | 5.4 |
| 400 | 5.0 |

**CM volume:** (Scan time + trigger delay)*flow rate.

**Saline flush:** 50 ml of saline or 10 ml of CM + 40 ml of saline at the same flow rate.

**Pre-contrast scan (calcium score):** Useful for the quantification of coronary calcium.

**Post-contrast scan:**
CM injection protocol: Injection time= scan time + 7-strigger delay.
Trigger delay: 7s after the threshold of 100 HU is reached in the ascending aorta using a bolus-tracking technique.
Scan protocol:
Gating: Retrospective or prospective (according to patient HR and technology available).
Scan region: From the ascending aorta to the heart apex.

## References

Hecht HS (2008) Applications of multislice coronary computed tomographic angiography to percutaneous coronary intervention: how did we ever do without it? Catheter Cardiovasc Interv 71:490-503

Otsuka M, Sugahara S, Umeda K et al (2008) Utility of multislice computed tomography as a strategic tool for complex percutaneous coronary intervention. Int J Cardiovasc Imaging 24:201-210

Yokoyama N, Yamamoto Y, Suzuki S et al (2006) Impact of 16-slice computed tomography in percutaneous coronary intervention of chronic total occlusions. Catheter Cardiovasc Interv 68:1-7

◀ longitudinal axis of the vessel. Note the complete absence of contrast material within the vessel (*arrow*). **4** VR reconstruction demonstrates complete occlusion of the vessel (*arrow*). **5**, **6** Three-chamber short-axis MPR images show diffuse hypoattenuation indicating the ischemic area, which resulted from the occlusion of the left anterior descending artery. (Reproduced with the kind permission of Dr. Nico R. Mollet, Erasmus Medical Center, Rotterdam, Netherlands)

# HEART – Plaque with Positive Remodeling
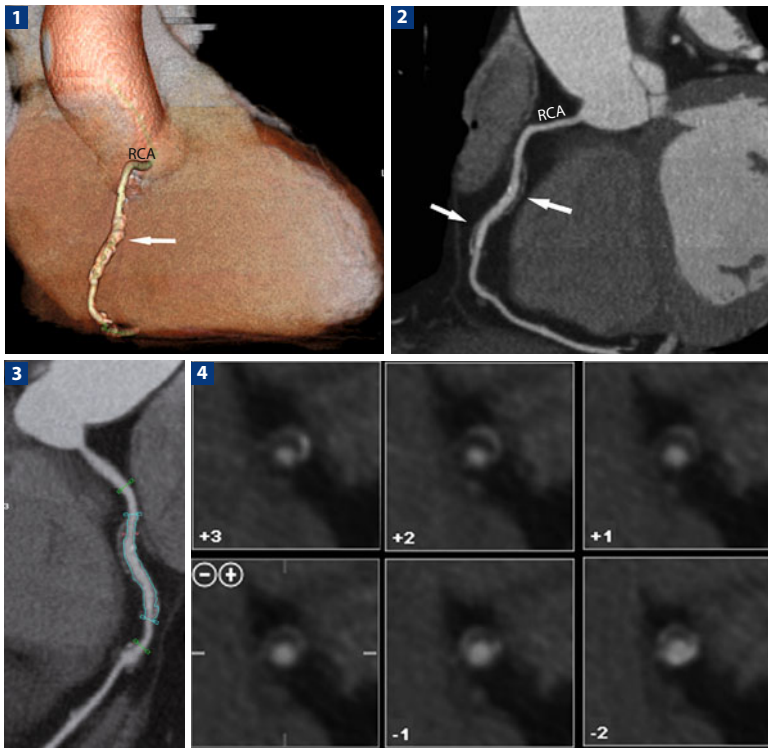


A 68-year-old hypertensive patient with a history of smoking and hypercholesterolemia reported chest pain after intense physical activity. The ECG was normal and there were no enzymatic changes.   **1**  VR reconstruction shows the right coronary artery (*RCA*) all along its course, with diffuse irregularities in the middle part of the vessel (*arrow*).   **2**, **3**  Curved MPR reconstruction highlights the extensive low-density plaque (*arrows*) at the middle third of the RCA. The caliber of the lumen is constant all along its course.   **4**  MPR reconstruction perpendicular to the longitudinal axis of the vessel identifies a plaque that is eccentric, with centrifugal growth (positive remodeling) but without causing stenosis of the lumen

## Study Protocol

**Patient preparation:** A 6-h fast prior to the examination; 18G catheter in the right antecubital vein. The administration of negative chronotropic drugs, such as beta blockers and calcium antagonists, is mandatory to reduce and to stabilize HR. The administration of nitrates is recommended to dilate the coronary arteries.

**Iodine flow rate:** 2.0 gI/s.

| CM concentration (mgI/mL) | Flow rate (mL/s) |
| --- | :---: |
| 300 | 6.7 |
| 320 | 6.2 |
| 350 | 5.7 |
| 370 | 5.4 |
| 400 | 5.0 |

**CM volume:** (Scan time + trigger delay)*flow rate.

**Saline flush:** 50 ml of saline or 10 ml of CM + 40 ml of saline at the same flow rate.

**Pre-contrast scan (calcium score):** Useful for the quantification of coronary calcium.

**Post-contrast scan:**
CM injection protocol: Injection time = scan time + 7-s trigger delay.
Trigger delay: 7s after the threshold of 100 HU is reached in the ascending aorta using a bolus-tracking technique.
Scan protocol:
Gating: Retrospective or prospective (according to patient HR and technology available).
Scan region: From the ascending aorta to the heart apex.

## References

Mowatt G, Cummins E, Waugh N et al (2008) Systematic review of the clinical effectiveness and cost-effectiveness of 64-slice or higher computed tomography angiography as an alternative to invasive coronary angiography in the investigation of coronary artery disease. Health Technol Assess 12(17):iii-iv, ix-143

Narula J, Garg P, Achenbach S et al (2008) Arithmetic of vulnerable plaques for non-invasive imaging. Nat Clin Pract Cardiovasc Med (5 Suppl) 2:S2-10

Schmid M, Pflederer T, Jang IK et al (2008) Relationship between degree of remodeling and CT attenuation of plaque incoronary atherosclerotic lesions: an in-vivo analysis by multi-detector computed tomography. Atherosclerosis 197:457-464

# HEART – Stenosis of the Left Anterior Descending Artery
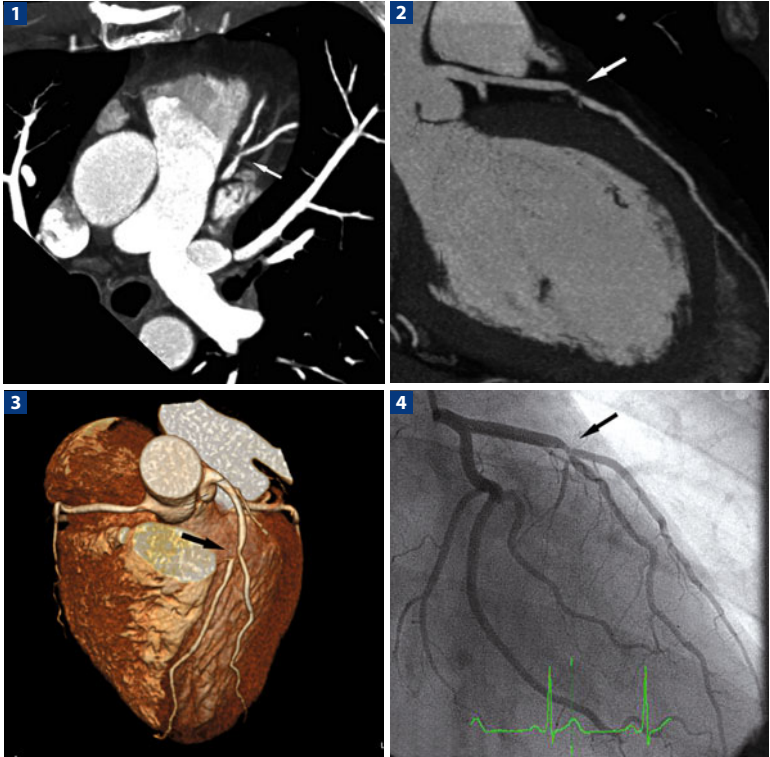


A 58-year-old patient with a family history of coronary artery disease reported an episode of angina. A stress test was carried out but was interrupted due to the patient's inability to complete the test. **1**, **2** Axial MIP reconstruction and curved MPR image show a low-density plaque in the middle segment of the left anterior descending artery and the first diagonal branch (*arrow*). **3** VR reconstruction identifies the presence of significant stenosis at the level of the middle segment of the left anterior descending artery (*arrow*), **4** which was confirmed on angiography (*arrow*). (Reproduced with the kind permission of Dr. Nico R. Mollet, Erasmus Medical Center, Rotterdam, Netherlands)

## Study Protocol

**Patient preparation:** A 6-h fast prior to the examination; 18G intravenous catheter in the right antecubital vein. The administration of negative chronotropic drugs, such as beta blockers and calcium antagonists, is mandatory to reduce and to stabilize HR. The administration of nitrates is recommended to dilate the coronary arteries.

**Iodine flow rate:** 2.0 gI/s.

| CM concentration (mgI/mL) | Flow rate (mL/s) |
|---|---|
| 300 | 6.7 |
| 320 | 6.2 |
| 350 | 5.7 |
| 370 | 5.4 |
| 400 | 5.0 |

**CM volume:** (Scan time + trigger delay)*flow rate.

**Saline flush:** 50 ml of saline or 10 ml of CM + 40 ml of saline at the same flow rate.

**Pre-contrast scan (calcium score):** Useful for the quantification of coronary calcium.

**Post-contrast scan:**
CM injection protocol: Injection time = scan time + 7-s trigger delay.
Trigger delay: 7s after the threshold of 100 HU is reached in the ascending aorta using a bolus-tracking technique.
Scan protocol:
Gating: Retrospective or prospective (according to patient HR and technology available).
Scan region: From the ascending aorta to the heart apex.

## References

Foster G, Shah H, Sarraf G et al (2009) Detection of noncalcified and mixed plaque by multirow detector computed tomography. Expert Rev Cardiovasc Ther 7:57-64

Schmid M, Achenbach S, Ropers D et al (2008) Assessment of changes in non-calcified atherosclerotic plaque volume in the left main and left anterior descending coronary arteries over time by 64-slice computed tomography. Am J Cardiol 101:579-584

Schuijf JD, Jukema JW, van der Wall EE et al (2007) Multi-slice computed tomography in the evaluation of patients with acute chest pain. Acute Card Care 9:214-221

# HEART – Right Coronary Artery Stent
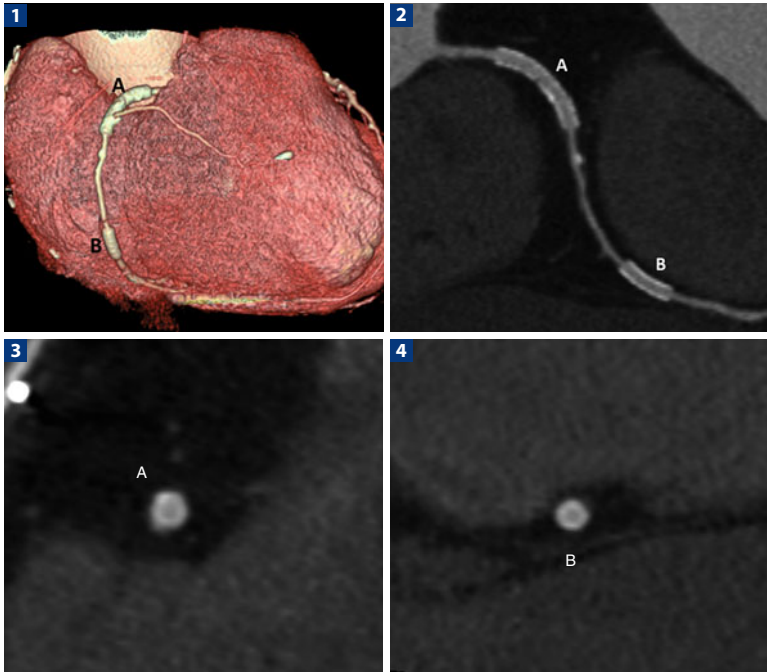


A 73-year-old patient underwent double stenting of the right coronary artery.
**1** VR reconstruction shows the presence of the 4-mm stent in the proximal segment (**a**) and the 3-mm stent in the distal segment (**b**) of the right coronary artery. Both stents show distal passage of the contrast material. **2** Curved MPR image obtained with the appropriate filter demonstrates the patency of both stents, which show no signs of intimal hyperplasia. **3**, **4** MPR images perpendicular to the axis of the vessel confirm the absence of intimal hyperplasia of both stents (**a**, **b**)

## Study Protocol

**Patient preparation:** A 6-h fast prior to the examination; 18G intravenous catheter in the right antecubital vein. The administration of negative chronotropic drugs, such as beta blockers and calcium antagonists, is mandatory to reduce and to stabilize HR. The administration of nitrates is recommended to dilate the coronary arteries.

**Iodine flow rate:** 2.0 gI/s.

| CM concentration (mgI/mL) | Flow rate (mL/s) |
|---|---|
| 300 | 6.7 |
| 320 | 6.2 |
| 350 | 5.7 |
| 370 | 5.4 |
| 400 | 5.0 |

**CM volume:** (Scan time + trigger delay)*flow rate.

**Saline flush:** 50 ml of saline or 10 ml of CM + 40 ml of saline at the same flow rate.

**Pre-contrast scan (calcium score):** Useful for the quantification of coronary calcium.

**Post-contrast scan:**
CM injection protocol: Injection time = scan time + 7-s trigger delay.
Trigger delay: 7s after the threshold of 100 HU is reached in the ascending aorta using a bolus-tracking technique.
Scan protocol:
Gating: Retrospective or prospective (according to patient HR and technology available).
Scan region: From the ascending aorta to the heart apex.

## References

Maintz D, Seifarth H, Raupach R et al (2006) 64-slice multidetector coronary CT angiography: in vitro evaluation of 68 different stents. Eur Radiol 16:818-826

Mitsutake R, Miura S, Nishikawa H et al (2008) Usefulness of the evaluation of stent fracture by 64-multi-detector row computed tomography. J Cardiol 51:135-138

Pugliese F, Cademartiri F, van Mieghem C et al (2006) Multidetector CT for visualization of coronary stents. Radiographics 26:887-904

# HEART – Aneurysm of an Aorto-coronary Venous Graft
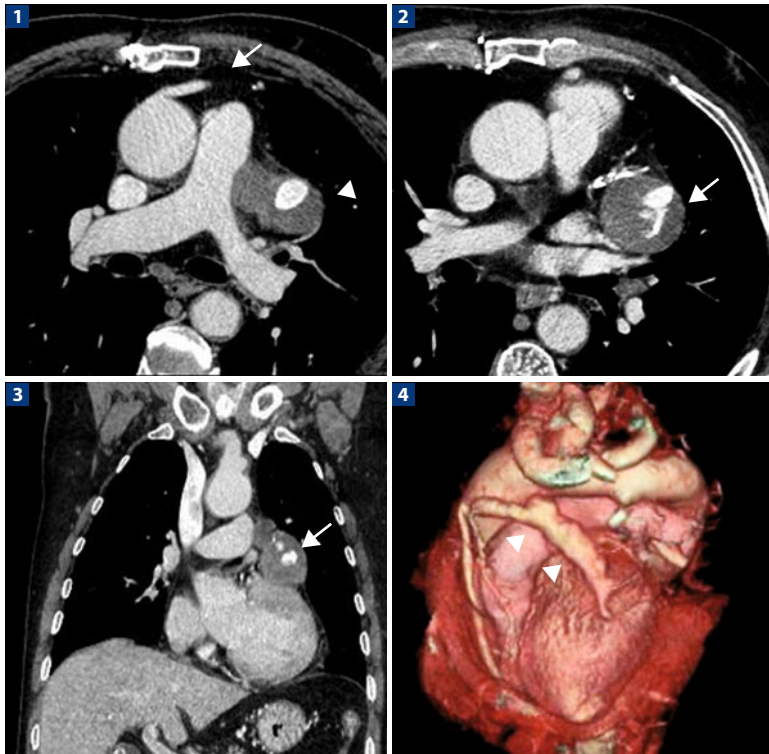


A 73-year-old patient underwent triple bypass surgery. Revascularization was done with the left internal thoracic artery, anastomized with the left anterior descending artery (LAD), and three venous grafts (VG) anastomized with the circumflex (CX) and right coronary arteries (RCA). **1** Axial scan shows the origin of the aorto-coronary graft (*arrow*), in which a saphenous vein segment was used, and the cranial portion of the aneurysm (arrowhead). **2** Evidence of the maximum diameter of the by-pass aneurysm and the structural irregularity of the parietal thrombus. **3** Coronal MPR reconstruction shows the anatomic relationships of the aneurysm with vascular structures (pulmonary artery trunk) and the left ventricle. **4** VR reconstruction shows the course of the coronary artery bypass (*arrowheads*) and its aneurysmal lumen

## Study Protocol

**Patient preparation:** A 6- h fast prior to the examination; 18G intravenous catheter in the right antecubital vein. The administration of negative chronotropic drugs, such as beta blockers and calcium antagonists, is mandatory to reduce and to stabilize HR. The administration of nitrates is recommended to dilate the coronary arteries.

**Iodine flow rate:** 2.0 gI/s.

| CM concentration (mgI/mL) | Flow rate (mL/s) |
|---|---|
| 300 | 6.7 |
| 320 | 6.2 |
| 350 | 5.7 |
| 370 | 5.4 |
| 400 | 5.0 |

**CM volume:** (Scan time + trigger delay)*flow rate.

**Saline flush:** 50 ml of saline or 10 ml of CM + 40 ml of saline at the same flow rate.

**Pre-contrast scan (calcium score):** Unnecessary.

**Post-contrast scan:**
CM injection protocol: Injection time = scan time + 7-s trigger delay.
Trigger delay: 7s after the threshold of 100 HU is reached in the ascending aorta using a bolus-tracking technique.
Scan protocol:
Gating: Retrospective or prospective (according to patient HR and technology available).
Scan region: From the lungs apex to the heart apex.

## References

Abbasi M, Soltani G, Somali A, Javan H (2009) A large saphenous vein graft aneurysm one year after coronary artery bypass graft surgery presenting as a left lung mass. Interact CardioVasc Thorac Surg 8:691-693

Trop I, Samson L, Cordeau MP (1999) Anterior mediastinal mass in a patient with prior saphenous vein coronary artery bypass grafting. Chest 115:572–576

Williams ML, Rampresaud E, Wolfe WG (2004) A man with saphenous vein graft aneu- rysm after bypass surgery. Ann Thorac Surg 77:1815-1817
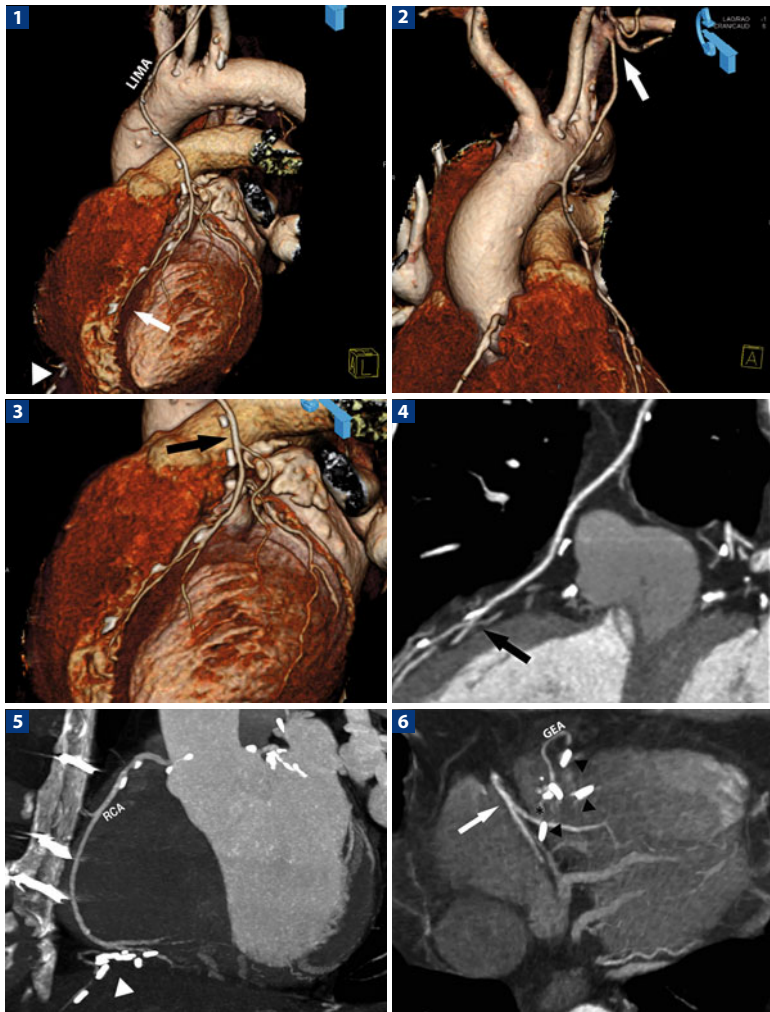
An 85-year-old patient underwent double bypass surgery. Revascularization was done with the left internal thoracic artery (anastomized with the left anterior descending artery) and the right gastroepiploic artery (anastomized with the posterior descending artery). **1** VR reconstruction clearly shows the presence of an arterial graft (left internal mammary artery, *LIMA*) mobilized and anastomized at the level of the distal tract of the left anterior descending artery (*arrow*). Note the presence of the metal clips at the base, following the course of a vessel originating from the abdomen (*arrowhead*). **2** VR reconstruction shows the origin of the left internal mammary artery (*arrow*). **3** Distal anastomosis of the ▶

## Study Protocol

**Patient preparation:** A 6- h fast prior to the examination; 18G intravenous catheter in the right antecubital vein. The administration of negative chronotropic drugs, such as beta blockers and calcium antagonists, is mandatory to reduce and to stabilize HR. The administration of nitrates is recommended to dilate the coronary arteries.

**Iodine flow rate:** 2.0 gI/s.

| CM concentration (mgI/mL) | Flow rate (mL/s) |
| --- | --- |
| 300 | 6.7 |
| 320 | 6.2 |
| 350 | 5.7 |
| 370 | 5.4 |
| 400 | 5.0 |

**CM volume:** (Scan time + trigger delay)*flow rate.

**Saline flush:** 50 ml of saline or 10 ml of CM + 40 ml of saline at the same flow rate.

**Pre-contrast scan (calcium score):** Unnecessary.

**Post-contrast scan:**
CM injection protocol: Injection time = scan time + 7-s trigger delay.
Trigger delay: 7s after the threshold of 100 HU is reached in the ascending aorta using a bolus-tracking technique.
Scan protocol:
Gating: Retrospective or prospective (according to patient HR and technology available).
Scan region: From the lungs apex to the heart apex.

## References

Jones CM, Chin KY, Yang GZ et al (2008) Coronary artery bypass graft imaging with 64-slice multislice computed tomography: literature review. Semin Ultrasound CT MR 29:204-213

Marano R, Liguori C, Rinaldi P et al (2007) Coronary artery bypass grafts and MD-CT imaging: what to know and what to look for. Eur Radiol 17:3166-3178

Nabuchi A, Kurata A, Okuyama H et al (2008) Three-dimensional images of extra-routine grafts in CABG by multi detector computed tomography. Ann Thorac Cardiovasc Surg 14:333-335

◀ arterial graft (*arrow*) is seen on VR reconstruction. Note the presence of multiple clips along the course of the vessel, necessary for the closure of side branches. **4** Curved MPR reconstruction along the course of the arterial graft shows the distal anastomosis of the graft (*arrow*), which appears patent. **5** MIP reconstruction shows the metal clips placed along the right gastroepiploic artery (*arrowhead*), mobilized and anastomosed with the posterior descending artery. **6** MIP reconstruction demonstrates the anastomosis (*asterisk*) between the posterior descending artery (*arrow*) and the gastroepiploic artery (*GEA*). The anastomosis cannot be assessed due to the presence of multiple metal clips (*arrowheads*)
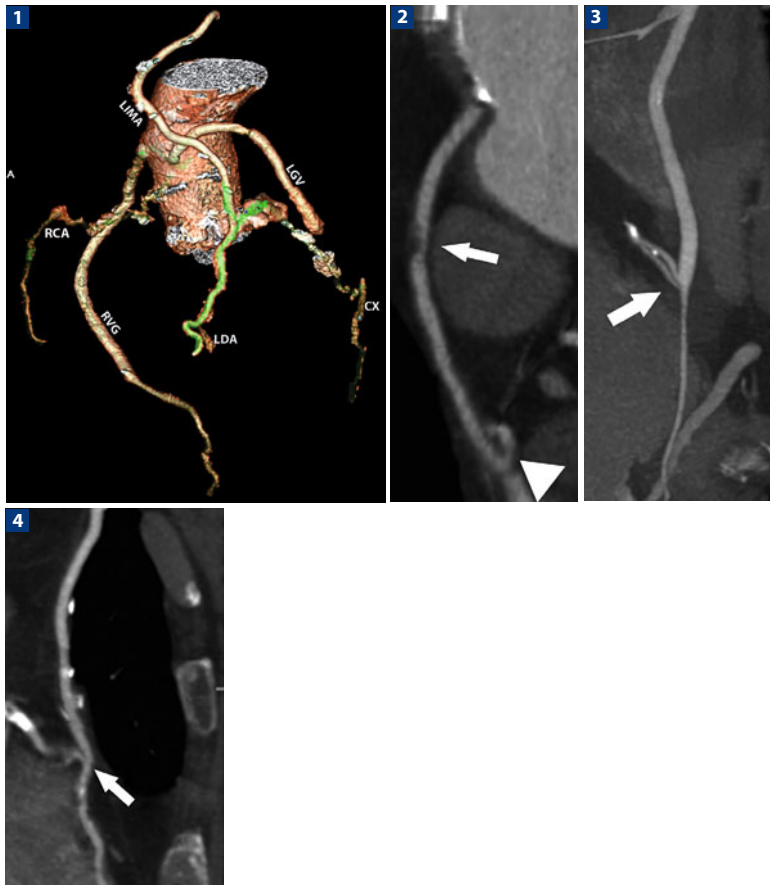
A 75-year-old patient underwent triple bypass surgery. Revascularization was done with the left internal thoracic artery, anastomized with the left anterior descending artery (LAD), and two venous grafts (VG) anastomized with the circumflex (CX) and posterior descending arteries. **1** VR reconstruction shows the course of the native coronary arteries (LAD, CX and right coronary artery), which present diffuse calcifications and numerous stenoses. The three grafts used for the revascularization, i.e., left internal mammary artery (LIMA), and VG, can also be appreciated. **2** Curved MPR image allows evaluation of the left VG. A low-density plaque (*arrow*) causing significant stenosis of the lumen is seen at the level of the middle tract of the graft. The distal anastomosis of the graft (*arrowhead*) appears patent. **3** Curved MPR image, used to evaluate the right VG, shows no significant alterations in the graft and its distal anastomosis appears patent (*arrow*). **4** In this curved MPR image, the LIMA shows no significant alterations and the distal anastomosis of the graft appears patent (*arrow*)

## Study Protocol

**Patient preparation:** A 6-h fast prior to the examination; 18G intravenous catheter in the right antecubital vein. The administration of negative chronotropic drugs, such as beta blockers and calcium antagonists, is mandatory to reduce and to stabilize HR. The administration of nitrates is recommended to dilate the coronary arteries.

**Iodine flow rate:** 2.0 gI/s.

| CM concentration (mgI/mL) | Flow rate (mL/s) |
| --- | --- |
| 300 | 6.7 |
| 320 | 6.2 |
| 350 | 5.7 |
| 370 | 5.4 |
| 400 | 5.0 |

**CM volume:** (Scan time + trigger delay)*flow rate.

**Saline flush:** 50 ml of saline or 10 ml of CM + 40 ml of saline at the same flow rate.

**Pre-contrast scan (calcium score):** Useful for the quantification of coronary calcium.

**Post-contrast scan:**
CM injection protocol: Injection time = scan time + 7-s trigger delay.
Trigger delay: 7s after the threshold of 100 HU is reached in the ascending aorta using a bolus-tracking technique.
Scan protocol:
Gating: Retrospective or prospective (according to patient HR and technology available).
Scan region: From the lungs apex to the heart apex.

## References

Crusco F, Antoniella A, Papa V et al (2007) Evidence based medicine: role of multidetector CT in the follow-up of patients receiving coronary artery bypass graft. Radiol Med 112:509-525

Jabara R, Chronos N, Klein L et al (2007) Comparison of multidetector 64-slice computed tomographic angiography to coronary angiography to assess the patency of coronary artery bypass grafts. Am J Cardiol 99:1529-1534

Mueller J, Jeudy J, Poston R et al (2007) Cardiac CT angiography after coronary bypass surgery: prevalence of incidental findings. AJR Am J Roentgenol 189:414-419

# VASCULAR – Whole-Body Angiography
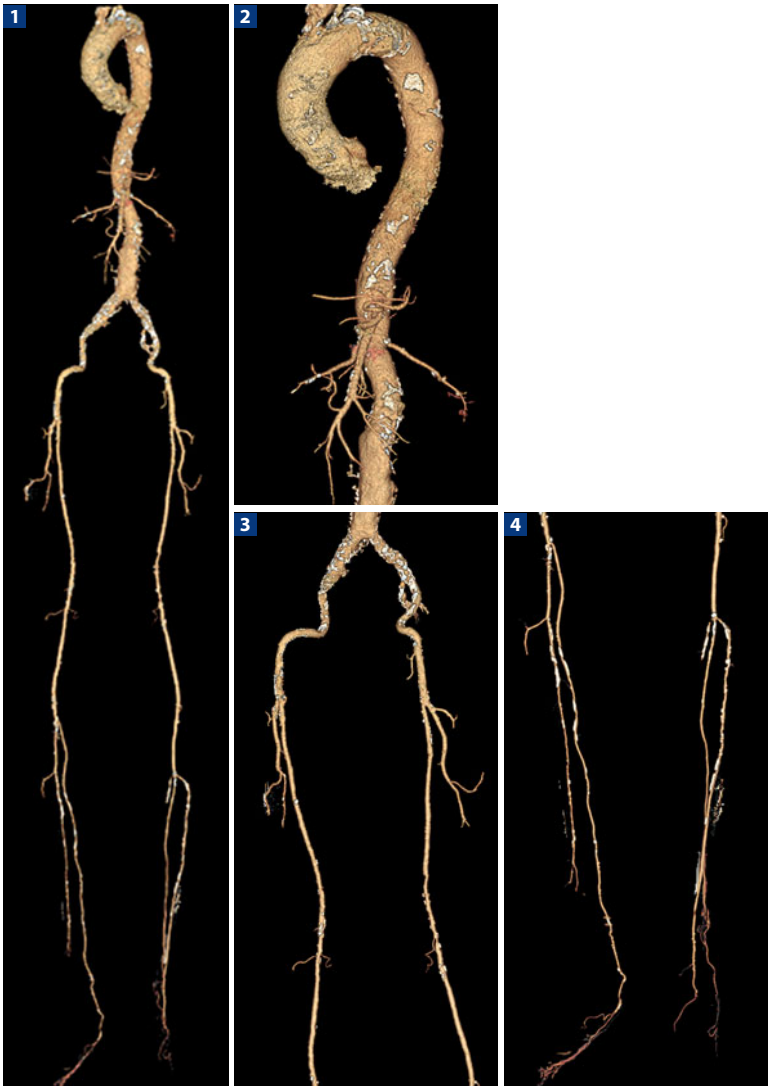


Images reconstructed with a VR algorithm of a whole-body angiography study in a diabetic patient. **1** Note the excellent representation of the entire aorta, the mesenteric vessels, and the vascular regions of the lower limbs and the feet. **2** Detail of the thoraco-abdominal aorta and the mesenteric vessels. Note the diffuse parietal calcifications. **3** Detail of the iliac-femoral region. **4** Detail of the distal run-off and the circulation of the feet

## Study Protocol

**Patient preparation:** A 6-h fast prior to the examination; 18G intravenous catheter in the right antecubital vein and 1.2 gI/s.

**Iodine flow rate:** 2.0 gI/s and 1.2 gI/s.

| CM concentration (mgI/mL) | Flow rate (mL/s) |
|---|---|
| 300 | 6.7/4 |
| 320 | 6.2/3.7 |
| 350 | 5.7/3.4 |
| 370 | 5.4/3.2 |
| 400 | 5.0/3 |

**Pre-contrast scan:** Unnecessary.

**Post-contrast scan:**
CM injection protocol:
Fixed injection time: 35 s (for patients between 60 and 90 kg).
Biphasic protocol: 1/3 of CM at 2 gI/s followed by 2/3 of CM at 1.2 gI/s every s after the threshold of 100 HU is reached in the ascending aorta using a bolus-tracking technique.
Saline flush: 50 ml of saline at the same flow rate.
Scan protocol: An arterial phase is mandatory. The diagnostic protocol provides lower kV values (80–100 kV) with fixed mA (200 mA); alternatively, automated techniques to reduce mA can be used.
Scan region: From the aortic arch to the foot.

## References

Jackowski C, Persson A, Thali MJ et al (2008) Whole body postmortem angiography with a high viscosity contrast agent solution using poly ethylene glycol as contrast agent dissolver. J Forensic Sci 53:465-468

Napoli A, Anzidei M, Francone M et al (2008) 64-MDCT imaging of the coronary arteries and systemic arterial vascular tree in a single examination: optimisation of the scan protocol and contrast-agent administration. Radiol Med 113:799-816

Ross S, Spendlove D, Bolliger S et al (2008) Postmortem whole-body CT angiography: evaluation of two contrast media solutions. AJR Am J Roentgenol 190:1380-1389

# VASCULAR – Carotid Arteries-Carotid Stenosis with Ulcerated Plaque
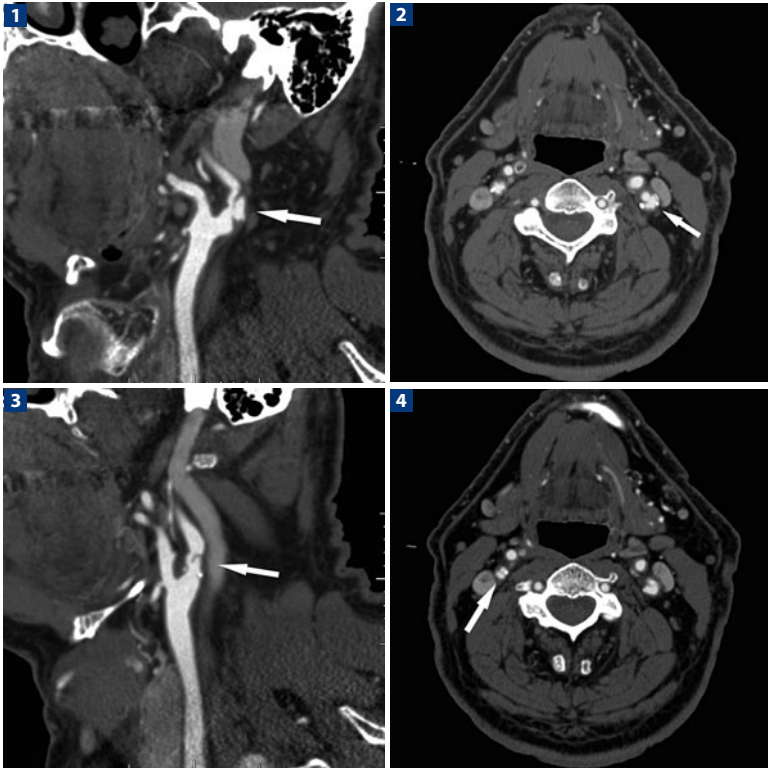


Patient with bilateral carotid stenosis. **1** Sagittal reformation image shows an ulcerated fibrotic plaque of the left internal carotid artery (*arrow*). **2** Stenosis of the left internal carotid artery by a fibrotic plaque with extensive ulceration (*arrow*) is seen in this axial image. **3** Sagittal reformation image reveals a partial intimal dissection at the level of the internal carotid artery (*arrow*). **4** Axial image shows partial intimal dissection (*arrow*)

## Study Protocol

**Patient preparation:** A 6-h fast pior to the examination; 18G intravenous catheter in the right antecubital vein.

**Iodine flow rate:** 2.0 gI/s.

| CM concentration (mgI/mL) | Flow rate (mL/s) |
|---|---|
| 300 | 6.7 |
| 320 | 6.2 |
| 350 | 5.7 |
| 370 | 5.4 |
| 400 | 5.0 |

**CM volume:** (Scan time + trigger delay)*flow rate.

**Saline flush:** 50 ml of saline at the same flow rate.

**Pre-contrast scan:** Unnecessary.

**Post-contrast scan:**
CM injection protocol: Injection time = scan time + 3-s delay.
Diagnostic delay: 3 s after the value of 100 HU is reached, with the ROI in the ascending thoracic aorta.
Scan protocol: Spiral, caudate-cranial with maximum values of pitch and thin collimation.
Scan region: From the aortic arch to the skull base.

## References

Forsting M (2005) CTA of the ICA bifurcation and intracranial vessels. Eur Radiol 15 Suppl 4:D25-D27

Koelemay MJ, Nederkoorn PJ, Reitsma JB et al (2004) Systematic review of computed tomographic angiography for assessment of carotid artery disease. Stroke 35:2306-2312

Saba L, Sanfilippo R, Pirisi R et al (2007) Multidetector-row CT angiography in the study of atherosclerotic carotid arteries. Neuroradiology 49:623-637

# VASCULAR – Evaluation of Carotid Stent
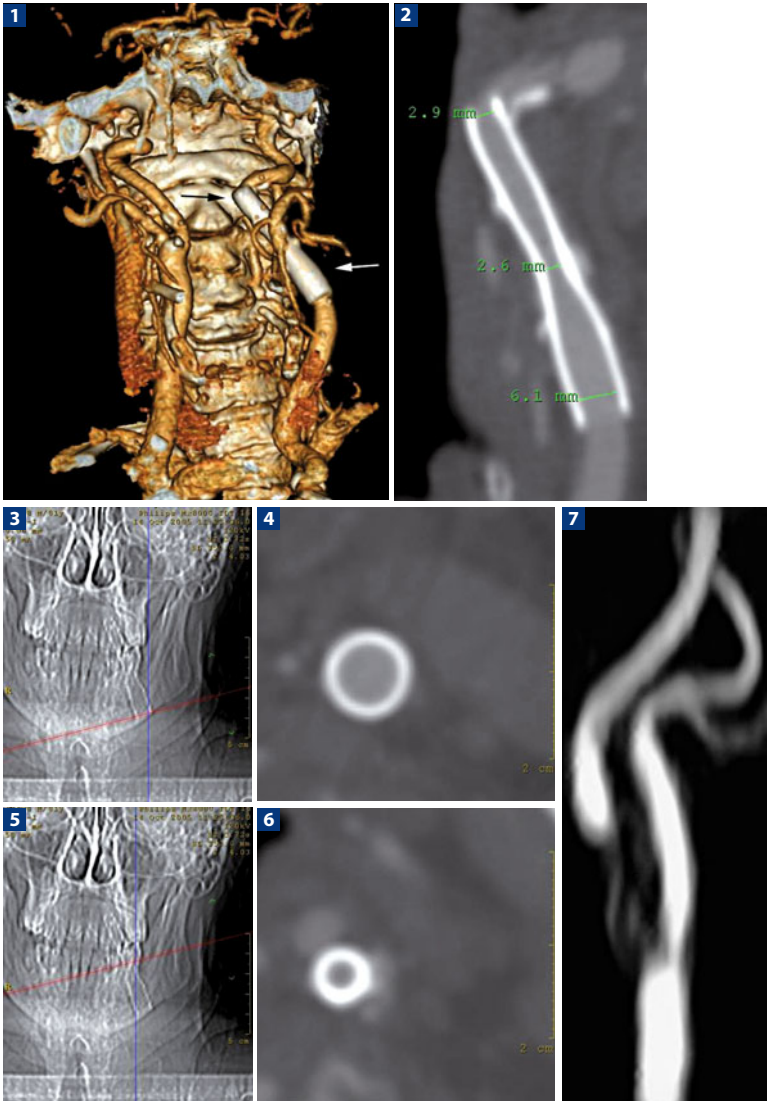














**1** The stent is evident in volumetric images (*arrow*), which do not provide information about its patency.   **2** Data obtained through the analysis of longitudinal axial-oblique reconstructions of the stent axis.   **3-6** The condition of the stent is seen on the anterior-posterior scanogram.   **7** No information was obtained from the angio-MRI study with gadolinium

## Study Protocol

**Patient preparation:** A 6-h fast pior to the examination; 18G intravenous catheter in the right antecubital vein.

**Iodine flow rate:** 2.0 gl/s.

| CM concentration (mgl/mL) | Flow rate (mL/s) |
| --- | --- |
| 300 | 6.7 |
| 320 | 6.2 |
| 350 | 5.7 |
| 370 | 5.4 |
| 400 | 5.0 |

**CM volume:** (Scan time + trigger delay)*flow rate.

**Saline flush:** 50 ml of saline at the same flow rate.

**Pre-contrast scan:** Unnecessary.

**Post-contrast scan:**
CM injection protocol: Injection time = scan time + 3-s delay.
Diagnostic delay: 3 s after the value of 100 HU is reached, with the ROI in the ascending thoracic aorta.
Scan protocol: Spiral, caudate-cranial with maximum values of pitch and thin collimation.
Scan region: From the aortic arch to the skull base.

## References

Kwon BJ, Jung C, Sheen SH et al (2007) CT angiography of stented carotid arteries: comparison with Doppler ultrasonography. J Endovasc Ther 14:489-497

Orbach DB, Pramanik BK, Lee J et al (2006) Carotid artery stent implantation: evaluation with multi-detector row CT angiography and virtual angioscopy-initial experience. Radiology 238:309-320

# VASCULAR – Lusory Artery
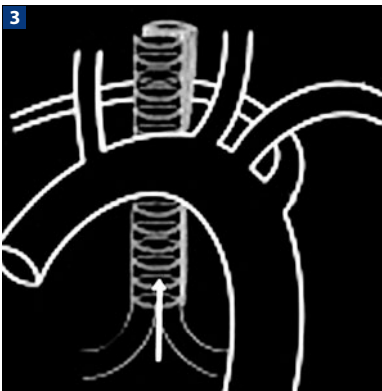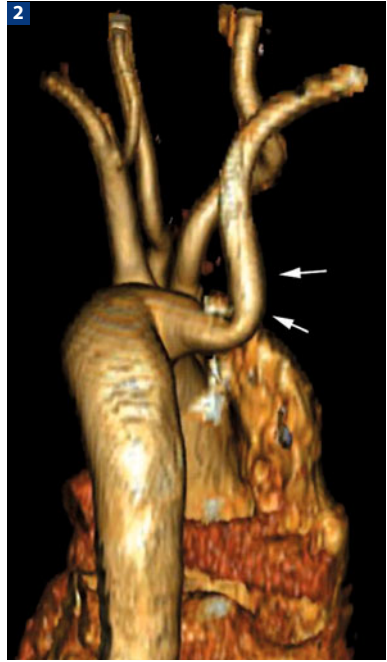






**1, 2** Anatomical variation consisting of a direct origin of the right subclavian artery which has a retro-esophageal course (lusory artery). The schema is shown in **3**. The patient was asymptomatic; the anomaly was observed during a chest CT

## Study Protocol

**Patient preparation:** A 6-h fast prior to the examination; 18G intravenous catheter in the right antecubital vein.

**Iodine flow rate:** 2.0 gI/s.

| CM concentration (mgI/mL) | Flow rate (mL/s) |
|---|---|
| 300 | 6.7 |
| 320 | 6.2 |
| 350 | 5.7 |
| 370 | 5.4 |
| 400 | 5.0 |

**CM volume:** (Scan time + trigger delay)*flow rate.

**Saline flush:** 50 ml of saline at the same flow rate.

**Pre-contrast scan:** Unnecessary.

**Post-contrast scan:**
CM injection protocol: Injection time = scan time + 7-s trigger delay.
Trigger delay: 7s after the threshold of 100 HU is reached in the ascending aorta using a bolus-tracking technique.
Scan protocol:
Scan region: From the aortic arch to the heart apex.
Spiral with maximum values of pitch and thin collimation.

## References

Dursun M, Yilmaz S, Sayin OA et al (2007) Combination of unicuspid aortic valve, aortic coarctation, and aberrant right subclavian artery in a child: MR imaging and CTA findings. Cardiovasc Intervent Radiol 30:547-549

# VASCULAR – Post-traumatic Thoracic Aorta Aneurysm (with Cardiac Gating)
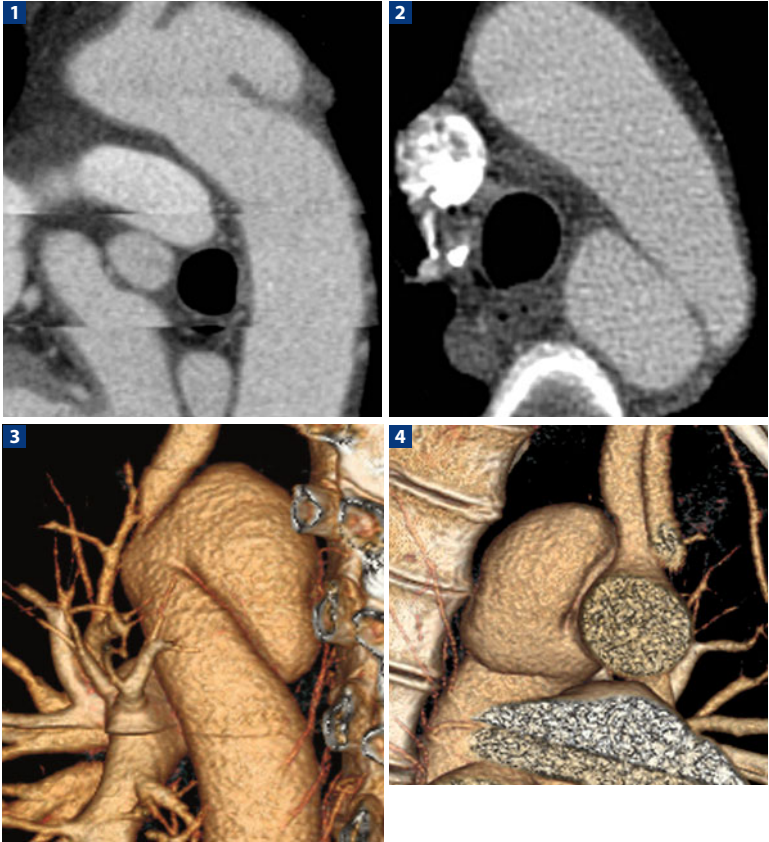








Post-traumatic pseudoaneurysm at the level of the isthmus, the area of the aorta most frequently involved by traumatic lesions. In this study of the thoracic aorta with cardiac gating, note the presence of artifacts produced by ectopic heart beats. **1** Sagittal MIP reconstruction. **2** The 2D axial image shows a detail of the neck of the pseudoaneurysm. Note the close relation with the esophageal wall, a risk factor for possible fistula formation. **3** VR reconstruction identifies the pseudoaneurysm, highlighting its atypical morphology, which is quite different from the saccular or spindle-like morphology of true aneurysms. **4** VR reconstruction shows the aneurysm and its anatomical relations

## Study Protocol

**Patient preparation:** A 6-h fast prior to the examination; 18G intravenous catheter in the right antecubital vein.

**Iodine flow rate:** 2.0 gI/s.

| CM concentration (mgI/mL) | Flow rate (mL/s) |
|---|---|
| 300 | 6.7 |
| 320 | 6.2 |
| 350 | 5.7 |
| 370 | 5.4 |
| 400 | 5.0 |

**CM volume:** (Scan time + trigger delay)*flow rate.

**Saline flush:** 50 ml of saline at the same flow rate.

**Pre-contrast scan:** Unnecessary.

**Post-contrast scan:**
CM injection protocol: Injection time = scan time + 7-s trigger delay.
Trigger delay: 7 s after the threshold of 100 HU is reached in the ascending aorta using a bolus-tracking technique.
Scan protocol:
Gating: Retrospective or prospective (according to patient HR and technology available).
Scan region: From the aortic arch to the heart apex.

## References

Ledbetter S, Stuk JL, Kaufman JA et al (1999) Helical (spiral) CT in the evaluation of emergent thoracic aortic syndromes. Traumatic aortic rupture, aortic aneurysm, aortic dissection, intramural hematoma, and penetrating atherosclerotic ulcer. Radiol Clin North Am 37:575-589

Manghat NE, Morgan-Hughes GJ, Roobottom CA et al (2005) Multi-detector row computed tomography: imaging in acute aortic syndrome. Clin Radiol 60:1256-1267

Salvolini L, Renda P, Fiore D et al (2008) Acute aortic syndromes: role of multi-detector row CT. Eur J Radiol 65:350-358

# VASCULAR – Perforating Ulcer of the Thoracic Aorta (without Cardiac Gating)
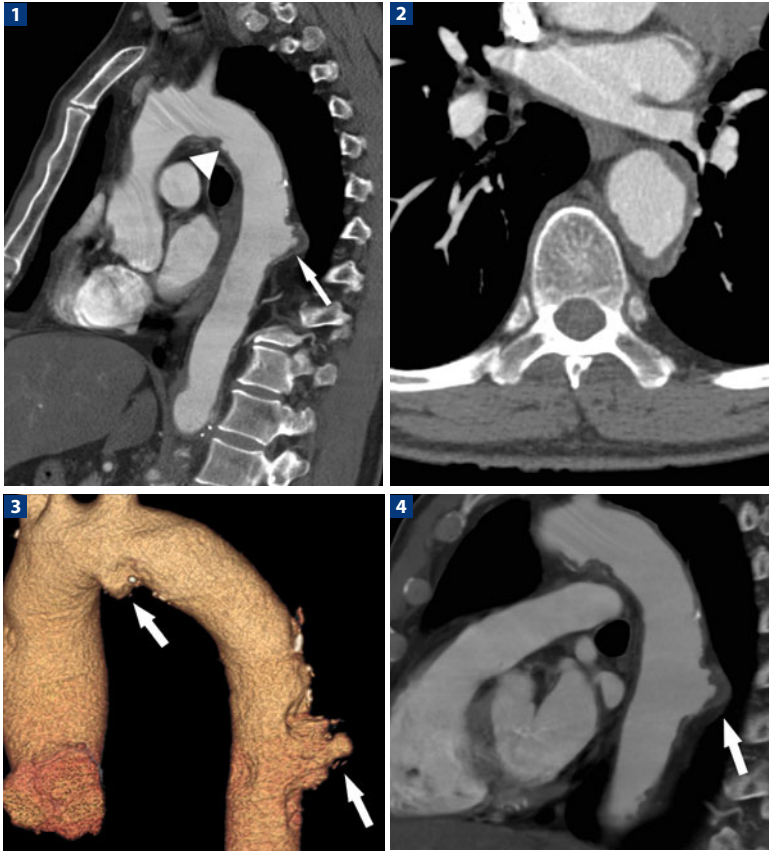


Study of the thoracic aorta without cardiac gating. **1** Sagittal MPR image shows a large perforating ulcer of the posterior wall of the thoracic aorta (*arrow*) and a small ulcer of the inferior wall of the aortic arch (*arrowhead*). **2** The 2D axial image shows a detail of the perforating ulcer of the thoracic aorta. Note the thrombotic apposition within the ulcer itself. **3** VR reconstruction demonstrates the spindle-shaped aneurysm of the ascending aorta and the two "plus" images (*arrows*) corresponding to the two parietal ulcers. **4** Oblique MIP reconstruction shows the perforating ulcer of the thoracic aorta, highlighting its marked retro-aortic extension

## Study Protocol

**Patient preparation:** A 6-h fast prior to the examination; 18G intravenous catheter in the right antecubital vein.

**Iodine flow rate:** 2.0 gI/s.

| CM concentration (mgI/mL) | Flow rate (mL/s) |
| --- | --- |
| 300 | 6.7 |
| 320 | 6.2 |
| 350 | 5.7 |
| 370 | 5.4 |
| 400 | 5.0 |

**CM volume:** (Scan time + trigger delay)*flow rate.

**Saline flush:** 50 ml of saline at the same flow rate.

**Pre-contrast scan:** Unnecessary.

**Post-contrast scan:**
CM injection protocol: Injection time = scan time + 7-s trigger delay.
Trigger delay: 7s after the threshold of 100 HU is reached in the ascending aorta using a bolus-tracking technique.
Scan protocol:
Scan region: From the aortic arch to the heart apex.
Spiral with maximum values of pitch and thin collimation.

## References

Hayashi H, Matsuoka Y, Sakamoto I et al (2000) Penetrating atherosclerotic ulcer of the aorta: imaging features and disease concept. RadioGraphics 20:995-1005

Johnson TR, Nikolaou K, Wintersperger BJ et al (2007) Optimization of contrast material administration for electrocardiogram-gated computed tomographic angiography of the chest. J Comput Assist Tomogr 31:265-271

Takahashi K, Stanford W (2005) Multidetector CT of the thoracic aorta. Int J Cardiovasc Imaging 21:141-153

# VASCULAR – Aortic Dissection Type A
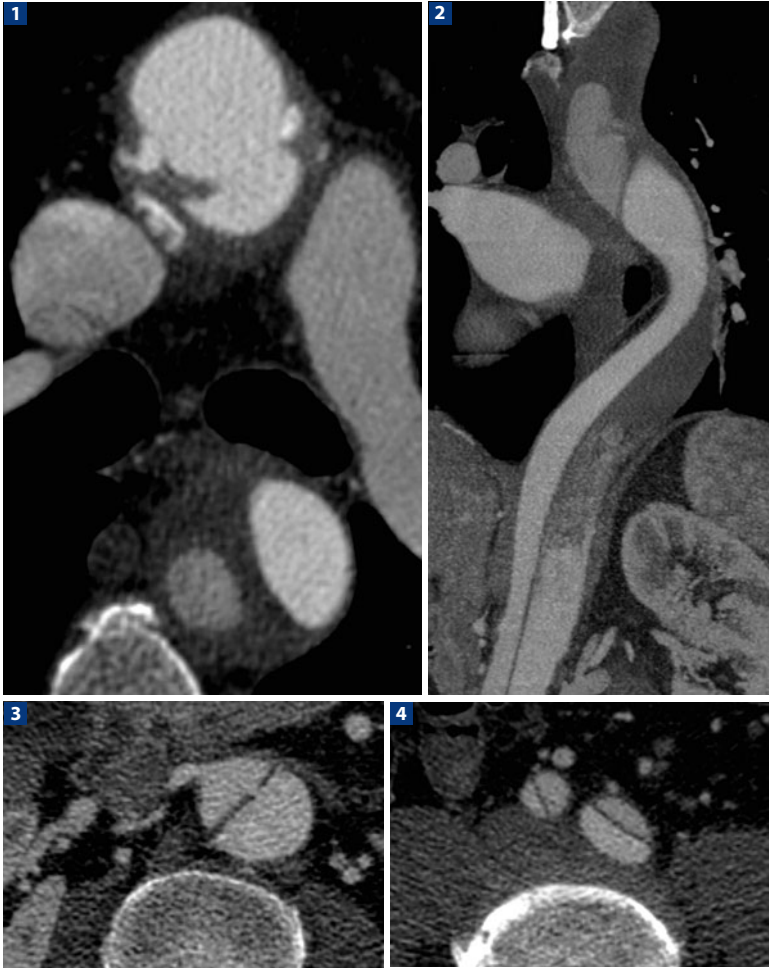








**1** Two-dimensional axial image shows the dissection arising at the level of the ascending aorta and the double lumen at the level of the descending thoracic aorta, with less enhancement of the false lumen.   **2** On oblique MPR image, the dissection can be seen extending along the thoraco-abdominal aorta up to the iliac arteries.   **3** Detail of the entry site at the level of the origin of the right renal artery, which arises from the true lumen.   **4** The dissection involves both common iliac arteries

## Study Protocol

**Patient preparation:** A 6-h fast prior to the examination; 18G intravenous catheter in the right antecubital vein.

**Iodine flow rate:** 2.0 gl/s.

| CM concentration (mgl/mL) | Flow rate (mL/s) |
|---|---|
| 300 | 6.7 |
| 320 | 6.2 |
| 350 | 5.7 |
| 370 | 5.4 |
| 400 | 5.0 |

**CM volume:** (Scan time + trigger delay)*flow rate.

**Saline flush:** 50 ml of saline at the same flow rate.

**Pre-contrast scan:** Unnecessary.

**Post-contrast scan:**
CM injection protocol: Injection time = scan time + 7-s trigger delay.
Trigger delay: 7 s after the threshold of 100 HU is reached in the ascending aorta using a bolus-tracking technique.
Scan protocol:
Gating: Retrospective or prospective (according to patient HR and technology available) to best evaluate the aortic arch.
Scan region: From the aortic arch to the pelvis.
Spiral with maximum values of pitch and thin collimation.

## References

Chirillo F, Salvador L, Bacchion F et al (2007) Clinical and anatomical characteristics of subtle-discrete dissection of the ascending aorta. Am J Cardiol 15:1314-1319

Heye T, Karck M, Richter G et al (2007) Visualization of entry and re-entry tears in a complex type A aortic dissection by 64-slice dual-source computer tomography. Eur J Cardiothorac Surg 32:935

Theisen D, von Tengg-Kobligk H, Michaely H et al (2007) CT angiography of the aorta. Radiologe 47:982-992
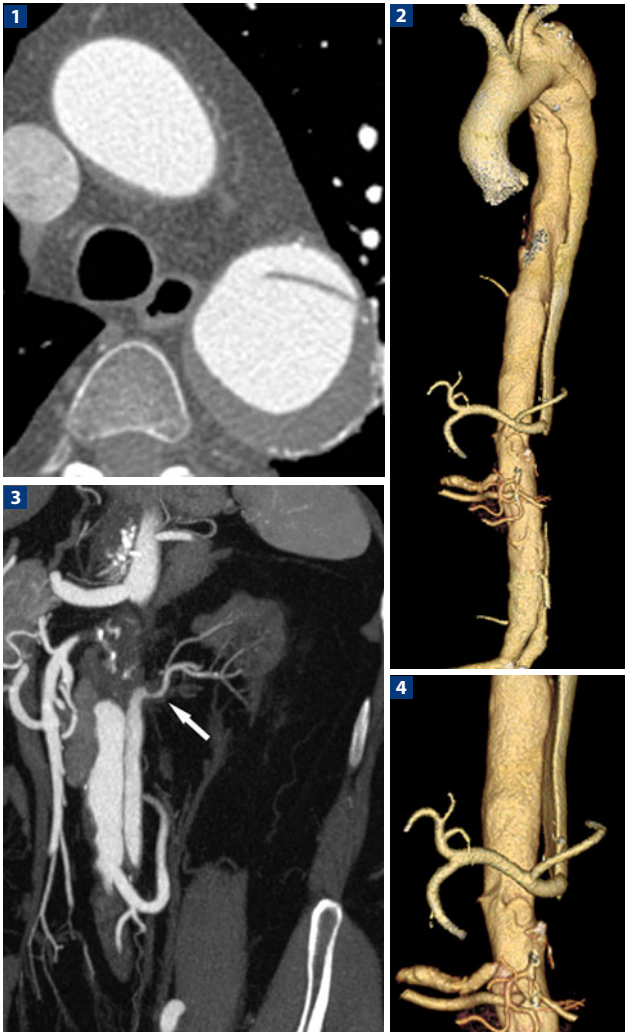
Spindle-shaped aneurysmal dilatation of the thoracic aorta after the origin of the left subclavian artery. Note the lamellar thrombotic apposition of the posterior wall and the point of entry of the intimal dissection. **1** Two-dimensional axial image. **2** VR reconstruction shows the extension of the dissection above the common iliac bifurcation. **3** On oblique MIP reconstruction, the dissection can be seen extending along the thoraco-abdominal aorta. The left renal artery arises from the false lumen (*arrow*). **4** VR reconstruction shows the origin of the left main artery from the false lumen

## Study Protocol

**Patient preparation:** A 6-h fast prior to the examination; 18G intravenous catheter in the right antecubital vein.

**Iodine flow rate:** 2.0 gl/s.

| CM concentration (mgl/mL) | Flow rate (mL/s) |
| --- | --- |
| 300 | 6.7 |
| 320 | 6.2 |
| 350 | 5.7 |
| 370 | 5.4 |
| 400 | 5.0 |

**CM volume:** (Scan time + trigger delay)*flow rate.

**Saline flush:** 50 ml of saline at the same flow rate.

**Pre-contrast scan:** Unnecessary.

**Post-contrast scan:**
CM injection protocol: Injection time = scan time + 7-s trigger delay.
Trigger delay: 7s after the threshold of 100 HU is reached in the ascending aorta using a bolus-tracking technique.
Scan protocol:
Scan region: From the aortic arch to the pelvis.
Spiral with maximum values of pitch and thin collimation.

## References

Mosquera VX, Marini M, Rodríguez F et al (2007) Complicated acute type B aortic dissection with involvement of an aberrant right subclavian artery and rupture of a thoracoabdominal aortic aneurysm, Crawford type I: successful emergency endovascular treatment. J Thorac Cardiovasc Surg 134:1055-1057

Romano L, Pinto A, Gagliardi N et al (2007) Multidetector-row CT evaluation of nontraumatic acute thoracic aortic syndromes. Radiol Med 112:1-20

Salvolini L, Renda P, Fiore D et al (2007) Acute aortic syndromes: role of multidetector row CT. Eur J Radiol 65:350-358
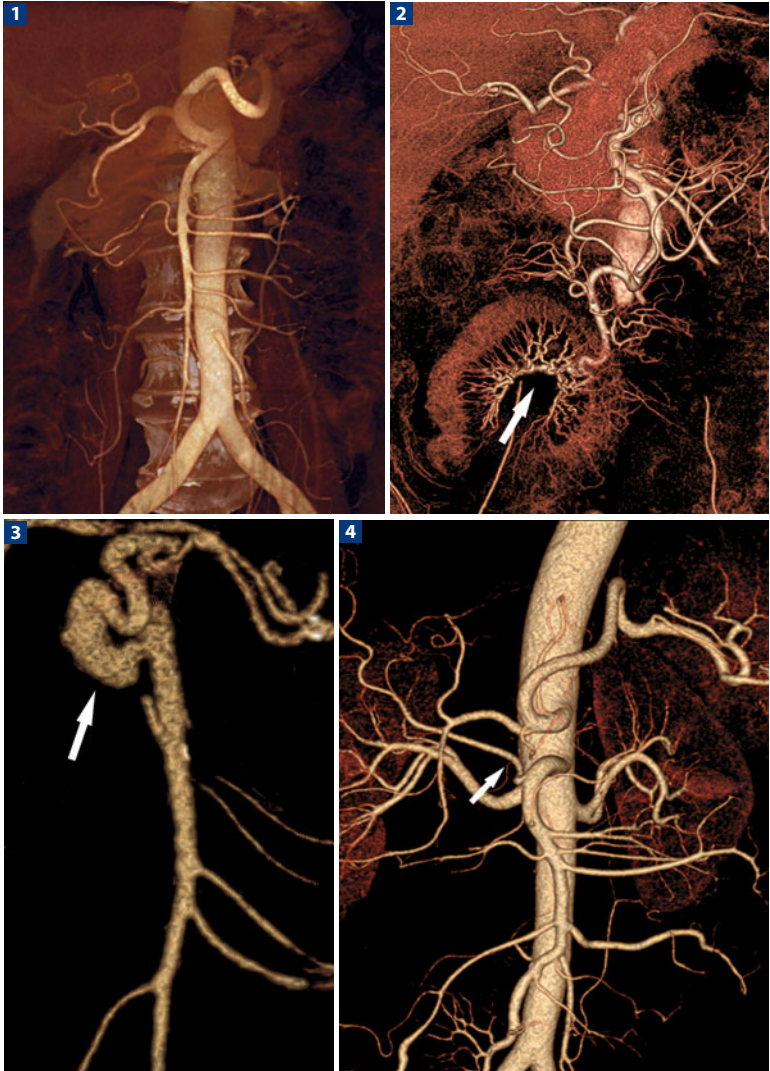
These VR reconstructions show: **1** the celiac trunk, with the common origin of the splenic artery, common hepatic artery and the superior mesenteric artery; **2** Crohn's disease, with hypertrophy of the vasa recta of the last ileal loop affected by the disease (*arrow*); **3** an aneurysm of the inferior pancreaticoduodenal artery (*arrow*); **4** the right hepatic artery arising from the superior mesenteric artery (*arrow*)

## Study Protocol

**Patient preparation:** A 6-h fast prior to the examination; 18G intravenous catheter in an antecubital vein.

**Iodine flow rate:** 2.0 gI/s.

| CM concentration (mgl/mL) | Flow rate (mL/s) |
| --- | --- |
| 300 | 6.7 |
| 320 | 6.2 |
| 350 | 5.7 |
| 370 | 5.4 |
| 400 | 5.0 |

**CM volume:** (Scan time + trigger delay)*flow rate.

**Saline flush:** 50 ml of saline at the same flow rate.

**Pre-contrast scan:** Unnecessary.

**Post-contrast scan:**
CM injection protocol: Injection time= scan time + 8-s trigger delay.
Trigger delay: 8 s after the value of 100 HU is reached, with the ROI in the abdominal aorta, using a bolus-tracking technique.
Scan protocol:
Arterial phase is mandatory. The diagnostic protocol provides lower kV values (80–100 kV) with fixed mA (200 mA); alternatively automated techniques to reduce mA can be used.
Spiral with maximum values of pitch and thin collimation.
Scan region: From the diaphragmatic dome to the pelvis.

## References

Capuñay C, Carrascosa P, Martín López E et al (2009) Multidetector CT angiography and virtual angioscopy of the abdomen. Abdom Imaging 34:81-93. PMID: 18709405

Ofer A, Abadi S, Nitecki S et al (2009) Multidetector CT angiography in the evaluation of acute mesenteric ischemia. Eur Radiol 19:24-30. PMID:18690454

Saba L, Mallarini G (2008) Multidetector row CT angiography in the evaluation of the hepatic artery and its anatomical variants. Clin Radiol 63:312-321

# VASCULAR – Aneurysm of the Subrenal Abdominal Aorta
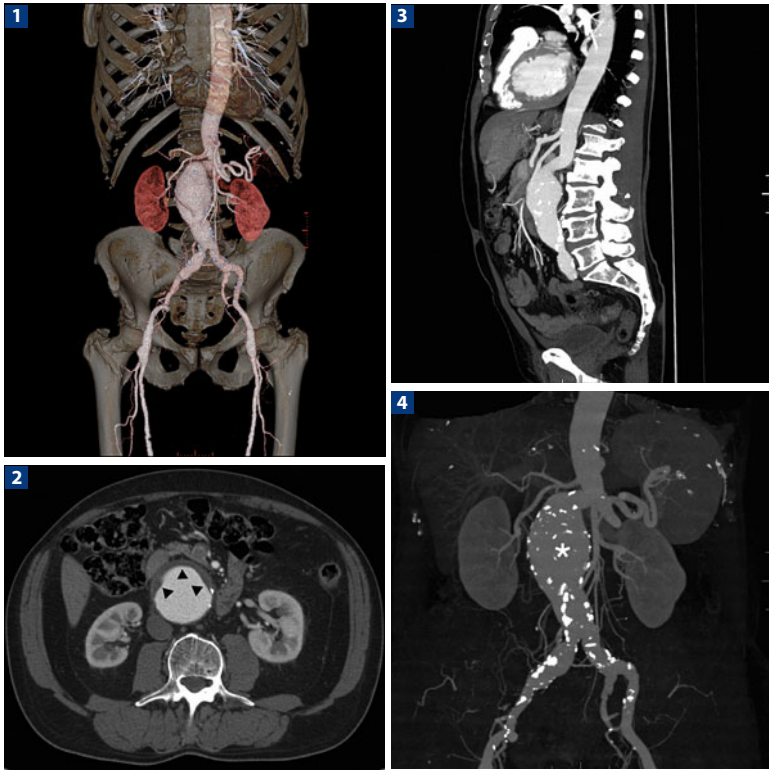








Aneurysm of the subrenal abdominal aorta with parietal thrombotic apposition. **1** VR reconstruction provides a panoramic view of a concentric aneurysm of the subrenal abdominal aorta. **2** Axial image shows the size of the aneurysm and the eccentric location of the thrombotic appositions on the anterior wall (*arrowheads*). **3**, **4** Three-dimensional sagittal and coronal MIP reconstructions demonstrate the relationships with the origin (*asterisk*) of the main splenic vessels

## Study Protocol

**Patient preparation:** A 6-h fast prior to the examination; 18G intravenous catheter in an antecubital vein.

**Iodine flow rate:** 2.0 gI/s.

| CM concentration (mgI/mL) | Flow rate (mL/s) |
| --- | --- |
| 300 | 6.7 |
| 320 | 6.2 |
| 350 | 5.7 |
| 370 | 5.4 |
| 400 | 5.0 |

**CM volume:** (Scan time + trigger delay)*flow rate.

**Saline flush:** 50 ml of saline at the same flow rate.

**Pre-contrast scan:** Unnecessary.

**Post-contrast scan:**
CM injection protocol: Injection time = scan time + 8-s trigger delay.
Trigger delay: 8 s from reaching the value of 100 HU with ROI in abdominal aorta using a bolus tracking technique.
Scan protocol:
Arterial phase. The diagnostic protocol provides lower kV values (80–100 kV) with fixed mA (200 mA); alternatively, automated techniques to reduce mA can be used. Spiral with maximum values of pitch and thin collimation.
Scan region: From the diaphragmatic dome to the pelvis.

## References

Albrecht T, Meyer BC (2007) MDCT angiography of peripheral arteries: technical considerations and impact on patient management. Eur Radiol 17 Suppl 6:F5-F15

Heijenbrok-Kal MH, Kock MC, Hunink MG (2007) Lower extremity arterial disease: multidetector CT angiography meta-analysis. Radiology 245:433-439

Kock MC, Dijkshoorn ML, Pattynama PM et al (2007) Multi-detector row computed tomography angiography of peripheral arterial disease. Eur Radiol 17:3208-3222

**1** This 2D axial image in the arterial phase shows the bifurcated endoprosthesis with type I endoleak (*asterisk*) arising from the distal end of the left iliac arm.
**2** Oblique MIP reconstruction shows the origin of the endoleak (*arrow*) at the distal end of the left iliac arm due to an ineffective seal at the end of the graft.
**3** Sagittal MIP reconstruction shows the type I endoleak. Note the beam-hardening artifacts due to the metallic stent. **4** On VR reconstruction, the calcified wall of the aneurysmal sac with the presence of the endoleak can be seen

## Study Protocol

**Patient preparation:** A 6-h fast prior to the examination; 18G intravenous catheter in an antecubital vein.

**Iodine flow rate:** 2.0 gI/s.

| CM concentration (mgI/mL) | Flow rate (mL/s) |
|---|---|
| 300 | 6.7 |
| 320 | 6.2 |
| 350 | 5.7 |
| 370 | 5.4 |
| 400 | 5.0 |

**CM volume:** (Scan time + trigger delay)*flow rate.

**Saline flush:** 50 ml of saline at the same flow rate.

**Pre-contrast scan:** Necessary to evaluate hyperdense components of the stent.

**Post-contrast scan:**
CM injection protocol: Injection time = scan time + 8-s trigger delay.
Trigger delay: 8 s after the value of 100 HU is reached, with the ROI in the abdominal aorta, using a bolus-tracking technique.
Scan protocol:
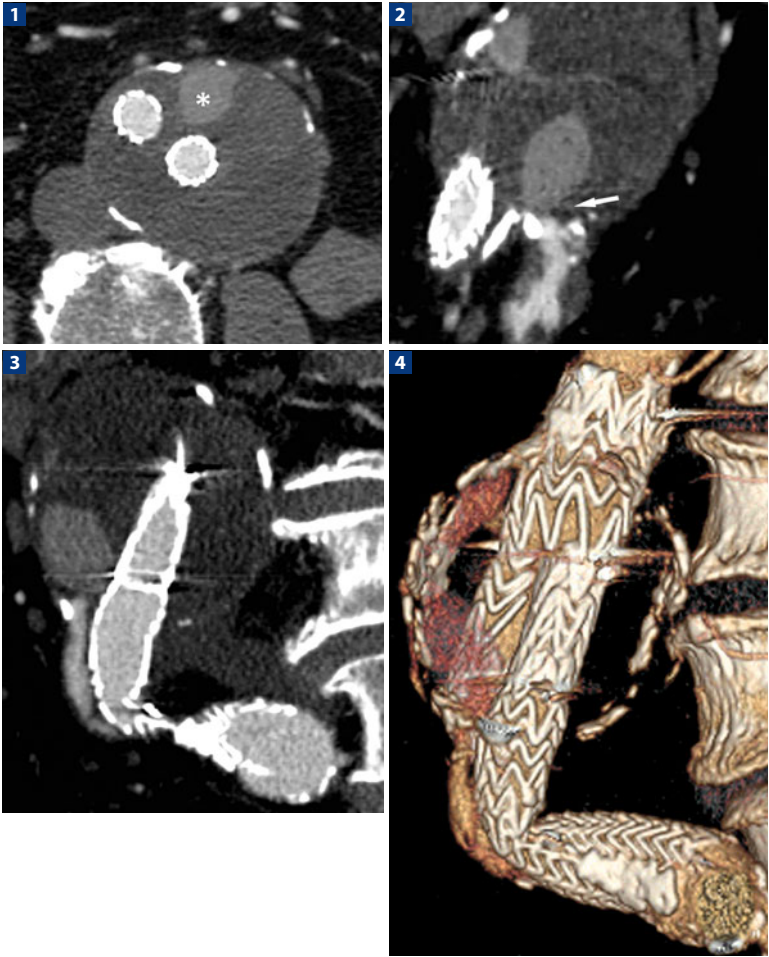Arterial phase and a late phase with a 180-s delay to assess the late endoleak are mandatory. The diagnostic protocol provides lower kV values (80 –100 kV) with fixed mA (200 mA); alternatively, automated techniques to reduce mA can be used.
Spiral with maximum values of pitch and thin collimation.
Scan region: From the diaphragmatic dome to the pelvis.

## References

Barbiero G, Baratto A, Ferro F et al (2008) Strategies of endoleak management following endoluminal treatment of abdominal aortic aneurysms in 95 patients: how, when and why. Radiol Med 113:1029-1042

Iezzi R, Cotroneo AR, Filippone A et al (2008) Multidetector-row computed tomography angiography in abdominal aortic aneurysm treated with endovascular repair: evaluation of optimal timing of delayed phase imaging for the detection of low-flow endoleaks. J Comput Assist Tomogr 32:609-615

Rydberg J, Lalka S, Johnson M et al (2004) Characterization of endoleaks by dynamic computed tomographic angiography. Am J Surg 188:538-543

# VASCULAR – Aortic Endoprosthesis with Type II Endoleak
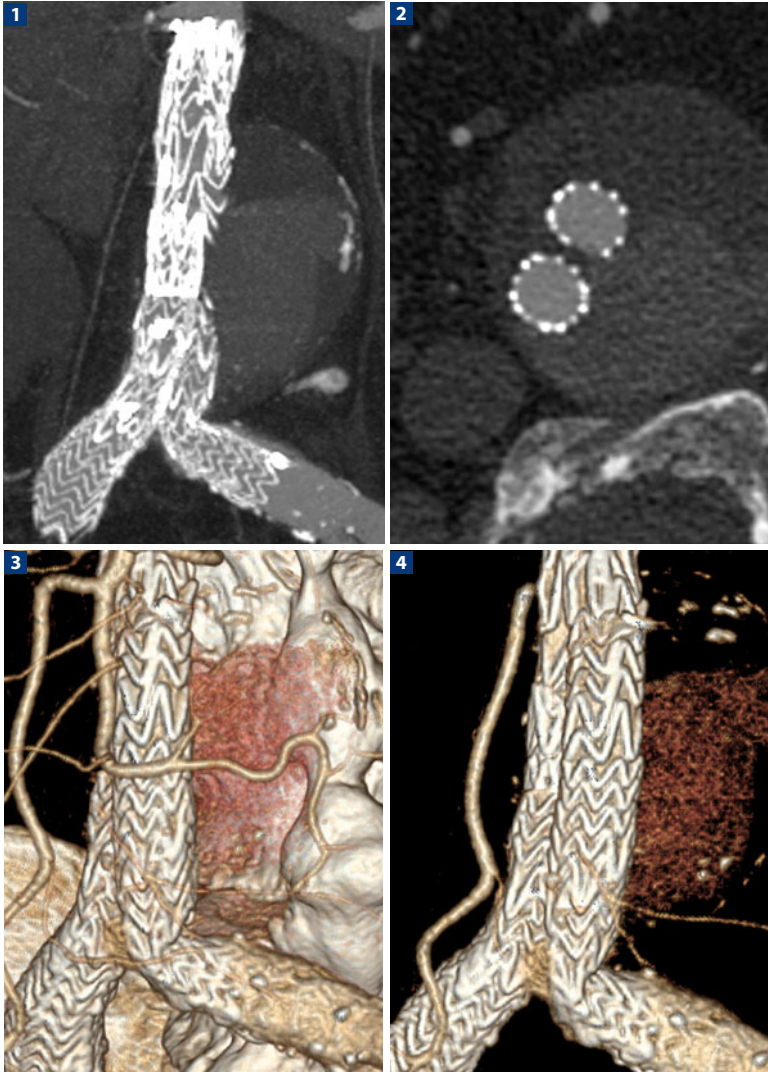








Bifurcated endoprosthesis with associated type II endoleak of the aneurysm due to refilling by the lumbar vessels. **1** Oblique MIP reconstruction. **2** The 2D axial image shows the extensive endoleak posterior to the endoprosthesis. **3**, **4** VR reconstructions: details of the endoprosthesis and the endoleak. Note the calcifications of the aneurysm

## Study Protocol

**Patient preparation:** A 6-h fast prior to the examination; 18G intravenous catheter in an antecubital vein.

**Iodine flow rate:** 2.0 gI/s.

| CM concentration (mgI/mL) | Flow rate (mL/s) |
| --- | --- |
| 300 | 6.7 |
| 320 | 6.2 |
| 350 | 5.7 |
| 370 | 5.4 |
| 400 | 5.0 |

**CM volume:** (Scan time + trigger delay)*flow rate.

**Saline flush:** 50 ml of saline at the same flow rate.

**Pre-contrast scan:** Necessary to evaluate hyperdense components of the stent.

**Post-contrast scan:**
CM injection protocol: Injection time = scan time + 8-s trigger delay.
Trigger delay: 8 s after the value of 100 HU is reached, with the ROI in the abdominal aorta, using a bolus- tracking technique.
Scan protocol:
Arterial phase and a late phase with a 180-s delay to assess the late endoleak are mandatory. The diagnostic protocol provides lower kV values (80 –100 kV) with fixed mA (200 mA); alternatively, automated techniques to reduce mA can be used.
Spiral with maximum values of pitch and thin collimation.
Scan region: From the diaphragmatic dome to the pelvis.

## References

Chernyak V, Rozenblit AM, Patlas M et al (2006) Type II endoleak after endoaortic graft implantation: diagnosis with helical CT arteriography. Radiology 240:885-693
Saba L, Pascalis L, Montisci R et al (2008) Diagnostic sensitivity of multidetector-row spiral computed tomography angiography in the evaluation of type-II endoleaks and their source: comparison between axial scans and reformatting techniques. Acta Radiol 49:630-637
Tolia AJ, Landis R, Lamparello P, Rosen R, Macari M (2005) Type II endoleaks after endovascular repair of abdominal aortic aneurysms: natural history. Radiology 235:683-686

# VASCULAR – Aortic Endoprosthesis with Peri-prosthetic Inflammation
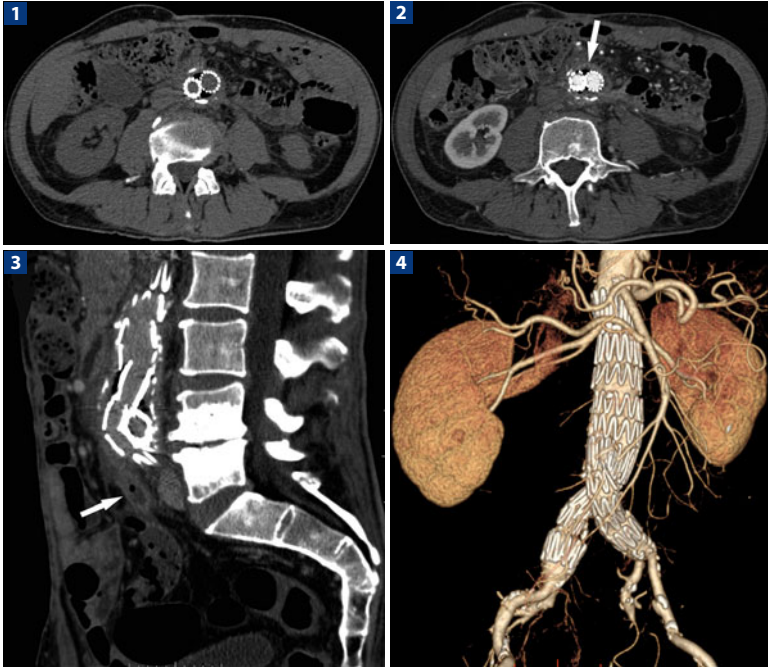


**1** In this axial non-enhanced axial image, a small peri-prosthetic gaseous collection at the level of the iliac arms is already evident.   **2** Contrast-enhanced 2D axial image in the arterial phase confirms the peri-prosthetic collection (*arrow*), with no signs of blood extravasation.   **3** Sagittal MPR image clearly shows the peri-prosthetic collection as well as a more caudal collection (*arrow*) also probably due to abscess formation.   **4** VR reconstruction: detail of the bifurcated endoprosthesis

## Study Protocol

**Patient preparation:** A 6-h fast prior to the examination; 18G intravenous catheter in an antecubital vein.

**Iodine flow rate:** 2.0 gI/s.

| CM concentration (mgI/mL) | Flow rate (mL/s) |
| --- | --- |
| 300 | 6.7 |
| 320 | 6.2 |
| 350 | 5.7 |
| 370 | 5.4 |
| 400 | 5.0 |

**CM volume:** (Scan time + trigger delay)*flow rate.

**Saline flush:** 50 ml of saline at the same flow rate.

**Pre-contrast scan:** Necessary to evaluate hyperdense components of the stent.

**Post-contrast scan:**
CM injection protocol: Injection time = scan time + 8-s trigger delay.
Trigger delay: 8 s after the value of 100 HU is reached, with the ROI in the abdominal aorta, using a bolus-tracking technique.
Arterial phase and a late phase with a 180-s delay to assess the late endoleak are mandatory. The diagnostic protocol provides lower kV values (80–100 kV) with fixed mA (200 mA); alternatively, automated techniques to reduce mA can be used.
Scan protocol:
Spiral with maximum values of pitch and thin collimation.
Scan region: From the diaphragmatic dome to the pelvis.

## References

Chernyak V, Rozenblit AM, Patlas M et al (2006) Type II endoleak after endoaortic graft implantation: diagnosis with helical CT arteriography. Radiology 240:885-693

Saba L, Pascalis L, Montisci R et al (2008) Diagnostic sensitivity of multidetector-row spiral computed tomography angiography in the evaluation of type-II endoleaks and their source: comparison between axial scans and reformatting techniques. Acta Radiol 49:630-637

Tolia AJ, Landis R, Lamparello P, Rosen R, Macari M (2005) Type II endoleaks after endovascular repair of abdominal aortic aneurysms: natural history. Radiology 235:683-686

# VASCULAR – Celiac Trunk Stent









**1** Two-dimensional axial image shows the presence of a stent at the level of the origin of the celiac trunk with evaluation of the trunk patency itself. **2** Two-dimensional sagittal reformatted image. **3** Detail and **4** general MIP reconstructions provide a lateral view of the stent

## Study Protocol

**Patient preparation:** A 6-h fast prior to the examination; 18G intravenous catheter in an antecubital vein.

**Iodine flow rate:** 2.0 gI/s.

| CM concentration (mgI/mL) | Flow rate (mL/s) |
| --- | --- |
| 300 | 6.7 |
| 320 | 6.2 |
| 350 | 5.7 |
| 370 | 5.4 |
| 400 | 5.0 |

**CM volume:** (Scan time + trigger delay)*flow rate.

**Saline flush:** 50 ml of saline at the same flow rate.

**Pre-contrast scan:** Necessary to evaluate hyperdense components of the stent.

**Post-contrast scan:**
CM injection protocol: Injection time = scan time + 8-s trigger delay.
Trigger delay: 8 s after the value of 100 HU is reached, with the ROI in the abdominal aorta, using a bolus-tracking technique.
Scan protocol:
Arterial phase and a late phase with a 180-s delay to assess the late endoleak are mandatory. The diagnostic protocol provides lower kV values (80–100 kV) with fixed mA (200 mA); alternatively, automated techniques to reduce mA can be used.
Spiral with maximum values of pitch and thin collimation.
Scan region: From the diaphragmatic dome to the pelvis.

## References

Ferrari R, De Cecco CN, Iafrate F et al (2007) Anatomical variations of the coeliac trunk and the mesenteric arteries evaluated with 64-row CT angiography. Radiol Med 112:988-998

Grierson C, Uthappa MC, Uberoi R et al (2007) Multidetector CT appearances of splanchnic arterial pathology. Clin Radiol 62:717-723

Smith CL, Horton KM, Fishman EK (2006) Mesenteric CT angiography: a discussion of techniques and selected applications. Tech Vasc Interv Radiol 9:150-155

An aorto-bifemoral bypass in a patient with occlusion of the left common iliac artery and multiple fibrocalcific plaques causing significant stenosis of the right iliac axis. **1** VR reconstruction. **2** Sagittal MIP reconstruction: proximal anastomosis of the graft on the anterior wall of the subrenal aorta. **3** VR reconstruction: distal bifemoral anastomosis; in such cases, the anastomoses may be the site of occlusion such that their patency should also be evaluated. **4** Oblique MIP reconstruction shows the distal anastomosis of the left femoral artery. Note the extensive calcifications of the common femoral artery and the patency of the graft

## Study Protocol

**Patient preparation:** A 6-h fast prior to the examination; 18G intravenous catheter in an antecubital vein.

**Iodine flow rate:** 2.0 gI/s.

| CM concentration (mgI/mL) | Flow rate (mL/s) |
|---|---|
| 300 | 6.7 |
| 320 | 6.2 |
| 350 | 5.7 |
| 370 | 5.4 |
| 400 | 5.0 |

**CM volume:** (Scan time + trigger delay)*flow rate.

**Saline flush:** 50 ml of saline at the same flow rate.

**Pre-contrast scan:** Unnecessary.

**Post-contrast scan:**
CM injection protocol: Injection time = scan time + 8-s trigger delay.
Trigger delay: 8 s after the value of 100 HU is reached, with the ROI in the abdominal aorta, using a bolus-tracking technique.
Scan protocol:
Arterial phase is mandatory. The diagnostic protocol provides lower kV values (80–100 kV) with fixed mA (200 mA); alternatively, automated techniques to reduce mA can be used.
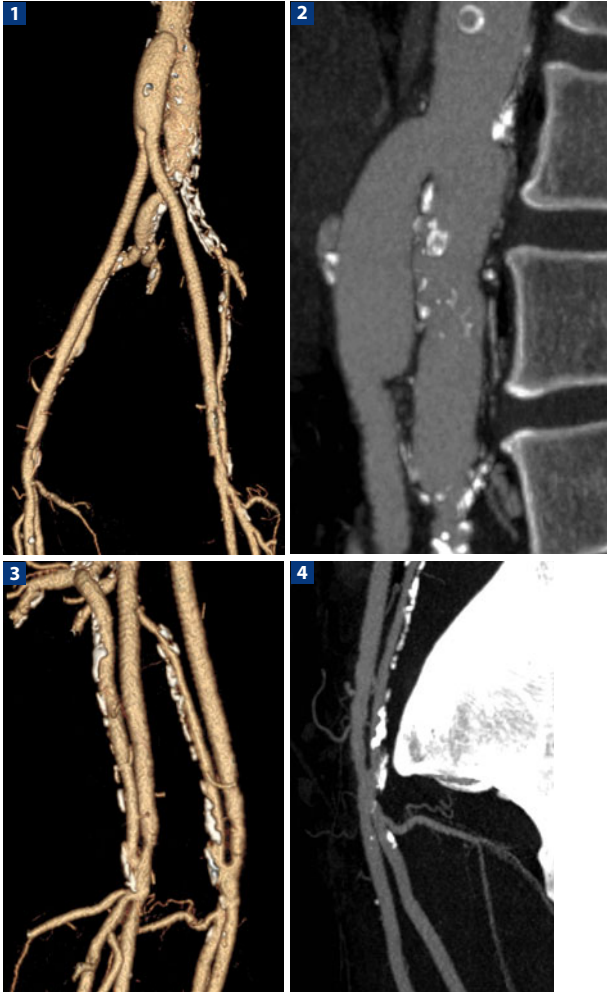Spiral with maximum values of pitch and thin collimation.
Scan region: From the diaphragmatic dome to the knee.

## References

Fleischmann D, Hallett RL et al (2006) CT angiography of peripheral arterial disease. J Vasc Interv Radiol 17:3-26

Lopera JE, Trimmer CK, Josephs SG (2008) Multidetector CT angiography of infra-inguinal arterial bypass. RadioGraphics 28:529-548

Willmann JK, Baumert B, Schertler T et al (2005) Aortoiliac and lower extremity arteries assessed with 16-detector row CT angiography: prospective comparison with digital subtraction angiography. Radiology 236:1083-1093

# VASCULAR – Bifurcation Endoprosthesis and Patent Femoro-femoral Bypass
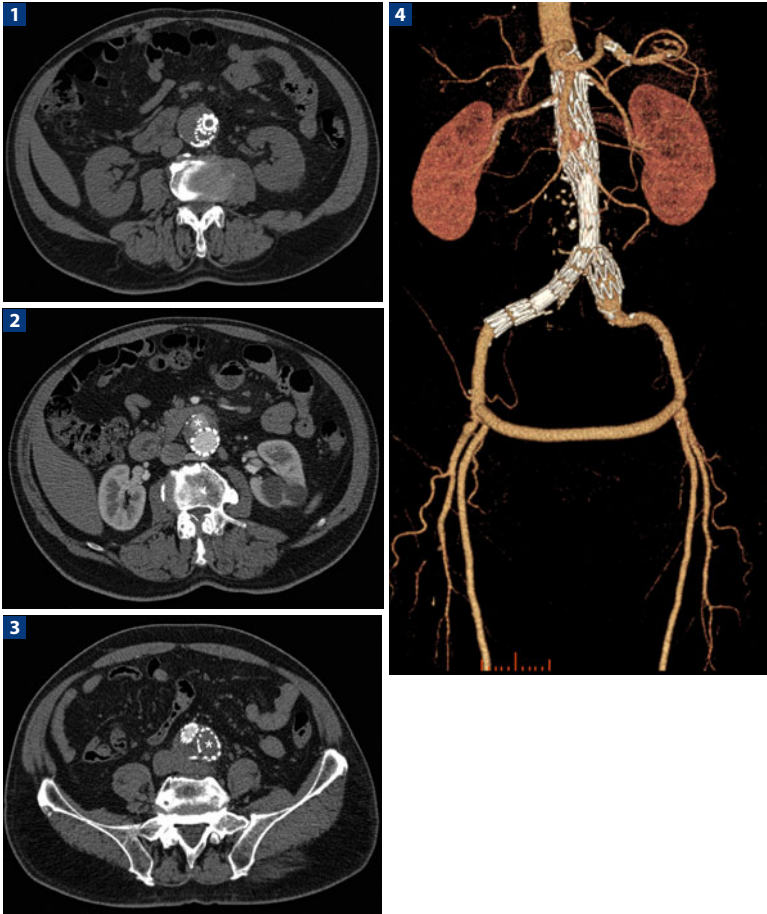








**1** Non-enhanced axial image shows a bifurcated endoprosthesis with the presence of a stent in the left iliac arm of the prosthesis. **2** Axial image in the arterial phase reveals an endoleak in the anterior region of the aneurysm (*asterisk*). **3** Contrast-enhanced axial image shows complete occlusion of the left iliac arm of the prosthesis (*asterisk*). **4** Panoramic VR reconstruction shows the presence of the endoprosthesis and the patent femoro-femoral bypass

## Study Protocol

**Patient preparation:** A 6-h fast prior to the examination; 18G intravenous catheter in an antecubital vein.

**Iodine flow rate:** 2.0 gI/s.

| CM concentration (mgI/mL) | Flow rate (mL/s) |
|---|---|
| 300 | 6.7 |
| 320 | 6.2 |
| 350 | 5.7 |
| 370 | 5.4 |
| 400 | 5.0 |

**CM volume:** (Scan time + trigger delay)*flow rate.

**Saline flush:** 50 ml of saline at the same flow rate.

**Pre-contrast scan:** Necessary to evaluate hyperdense components of the stent.

**Post-contrast scan:**
CM injection protocol: Injection time= scan time + 8-s trigger delay.
Trigger delay: 8 s after the value of 100 HU is reached, with the ROI in the abdominal aorta, using a bolus-tracking technique.
Scan protocol:
Arterial phase and a late phase with a 180-s delay to assess the late endoleak are mandatory. The diagnostic protocol provides lower kV values (80–100 kV) with fixed mA (200 mA); alternatively, automated techniques to reduce mA can be used.
Spiral with maximum values of pitch and thin collimation.
Scan region: From the diaphragmatic dome to the knee.

## References

Chernyak V, Rozenblit AM, Patlas M et al (2006) Type II endoleak after endoaortic graft implantation: diagnosis with helical CT arteriography. Radiology 240:885-693

Saba L, Pascalis L, Montisci R et al (2008) Diagnostic sensitivity of multidetector-row spiral computed tomography angiography in the evaluation of type-II endoleaks and their source: comparison between axial scans and reformatting techniques. Acta Radiol 49:630-637

Tolia AJ, Landis R, Lamparello P, Rosen R, Macari M (2005) Type II endoleaks after endovascular repair of abdominal aortic aneurysms: natural history. Radiology 235:683-686

# VASCULAR – Lower Limbs-Peripheral Arterial Disease
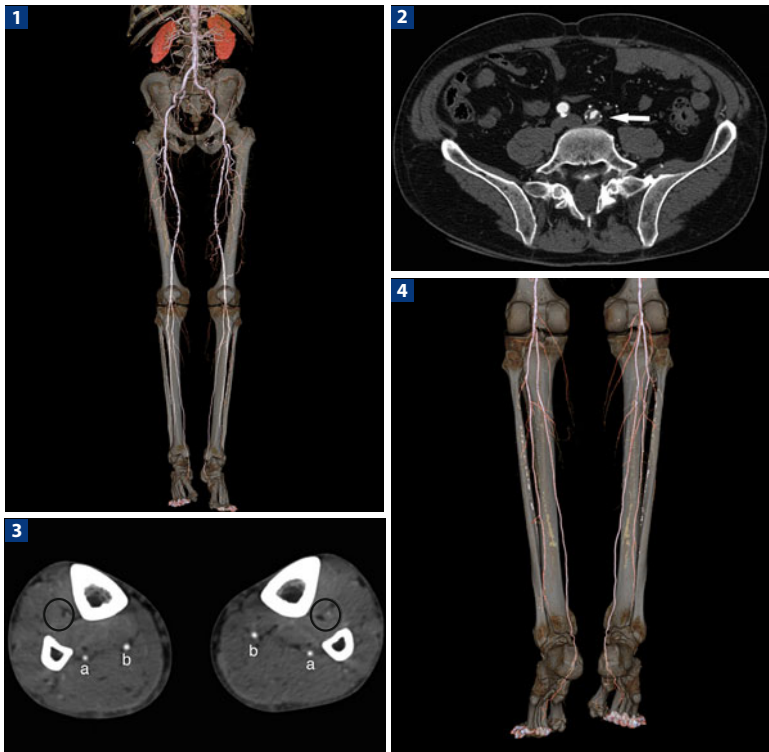








The study provides a perfect representation of the arteries of the lower limb down to the dorsalis pedis arteries. **1** Panoramic VR reconstruction with transparency of the skeletal structures. **2** Axial image at the level of the iliac bifurcation. Note the stenosis of the left common iliac artery with a not hemodynamically significant reduction in the lumen (*arrow*). **3** Axial image at the level of the arterial vessels of the lower limbs. Note the perfect representation of the interosseous (**a**) and posterior tibial (**b**) arteries, with bilateral stenosis of the anterior tibial arteries (*black circles*). **4** VR reconstruction of the vessels of the lower limbs

## Study Protocol

**Patient preparation:** A 6-h fast prior to the examination; 18G intravenous catheter in an antecubital vein.

**Iodine flow rate:** 2.0 gI/s and 1.2 gI/s.

| CM concentration (mgI/mL) | Flow rate (mL/s) |
| --- | --- |
| 300 | 6.7/4 |
| 320 | 6.2/3.7 |
| 350 | 5.7/3.4 |
| 370 | 5.4/3.2 |
| 400 | 5.0/3 |

**Pre-contrast scan:** Unnecessary.

**Post-contrast scan:**
CM injection protocol:
Fixed injection time: 35 s (for patients between 60 and 90 kg).
Biphasic protocol: 1/3 of CM at 2 gI/s followed by 2/3 of CM at 1.2 gI/s every s after the threshold of 100 HU is reached in the ascending aorta using a bolus-tracking technique.
Saline flush: 50 ml of saline at the same flow rate.
Scan protocol: An arterial phase is mandatory. The diagnostic protocol provides lower kV values (80–100 kV) with fixed mA (200 mA); alternatively, automated techniques to reduce mA can be used.
Scan region: From the diaphragmatic dome to the foot.

## References

Fleischmann D, Hallett RL et al (2006) CT angiography of peripheral arterial disease. J Vasc Interv Radiol 17:3-26

Lopera JE, Trimmer CK, Josephs SG (2008) Multidetector CT angiography of infrainguinal arterial bypass. Radiographics 28:529-548

Willmann JK, Baumert B, Schertler T et al (2005) Aortoiliac and lower extremity arteries assessed with 16-detector row CT angiography: prospective comparison with digital subtraction angiography. Radiology 236:1083-1093

# EMERGENCY – Post-traumatic Arterio-porto-biliary Fistula of the Liver
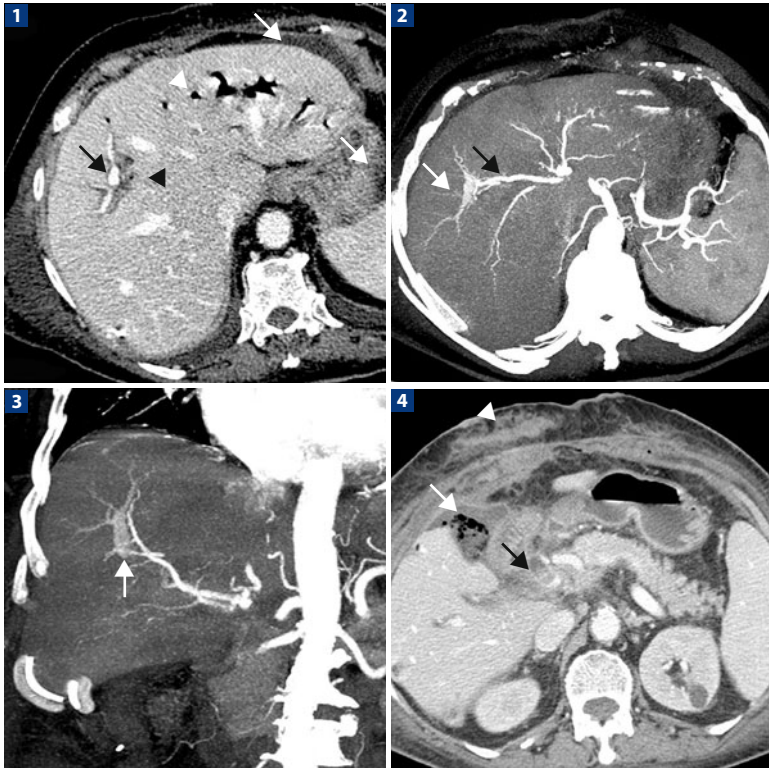


**1** Small lesion with pseudoaneurysmal aspect in segment VIII of the liver (*black arrow*), adjacent to intraparenchymal dilated biliary branches containing hyperdense blood clots (*black arrowhead*). In the portal phase, there are no hepatic parenchymal lacerations and only a minimal layer of hemoperitoneum (*white arrows*). Aerobilia in the intraparenchymal left branches (white arrowhead) is evident.   **2** Axial MIP reconstruction obtained in the arterial phase identifies a simultaneous opacification of a segmental arterial branch (*black arrow*) and an intrahepatic segmental portal branch (*white arrow*).   **3** Coronal MIP reconstruction in the arterial phase documents a mild post-traumatic fistula between the arterial branch of segment VIII and its corresponding portal branch (*arrow*).   **4** Axial scan performed in equilibrium phase shows blood clots in the lumen of the common biliary duct (*black arrow*). There is a small abscess in the subhepatic space (*white arrow*) and a hematoma of the abdominal wall (*arrowhead*)

## Study Protocol

**Patient preparation:** The examination is performed in emergency. No preparation is possible.

**CM volume:** 500–600 mgI (iodine dose) per kg body weight.

| Patient weight (kg) | < 60 | < 80 | > 80 |
|---|---|---|---|
| **CM concentration (mgI/mL)** | | | |
| 300 | 100 | 130 | 150 |
| 320 | 95 | 125 | 140 |
| 350 | 85 | 115 | 130 |
| 370 | 80 | 110 | 120 |
| 400 | 75 | 100 | 110 |
| **CM injection flow rate (mL/s)** | **1.6 gI/s** | **1.8 gI/s** | **2.0 gI/s** |
| **CM concentration (mgI/mL)** | | | |
| 300 | 5.3 | 6.0 | 6.7 |
| 320 | 5.0 | 5.6 | 6.2 |
| 350 | 4.6 | 5.1 | 5.7 |
| 370 | 4.3 | 4.8 | 5.4 |
| 400 | 4.0 | 4.5 | 5.0 |

**Pre-contrast scan:** Required for the identification of intraparenchymal blood and to search for sentinel clots.

**Post-contrast scan:**
The bolus-tracking monitoring technique is used.
Early arterial phase: 10 s after threshold of 100 H. ROI placed at the level of the diaphragmatic dome, to evaluate the arterial vasculature and to identify vascular abnormalities (arteriovenous fistula).
Portal phase: 60-70 s from the start of CM injection, to evaluate the portal tree and to identify parenchymal lesions.
Equilibrium phase: 180 s from the start of CM injection to verify active extravasation of CM due to high-flow hemorrhage.

**Comments:** Traumatic pseudoaneurysms of the hepatic artery branches account for 2–3% of all injuries due to blunt trauma of the liver; those associated with an arteriovenous fistula or biliary fistula are rare. In the case illustrated above, the three abnormalities were present simultaneously. The ability to separately study the arterial and venous vessels, the liver parenchyma, and the bile duct with a triphasic MDCT study of the liver has been the keystone in the diagnosis of this extremely rare pathology. The patient, who had a post-traumatic obstructive jaundice, in fact, was successfully treated with embolization of the arterio-portal fistula.

## References

Becker H, MarKus PM (1994) Bile ducts lesions in liver trauma. Chirurg 65:766-774

Fragulidis G, Marinis A, Polidorou A et al (2008) Managing injuries of hepatic duct confluente variants after major hepatobiliary surgery: an algorithmic approach. World J Gastroenterol 14:3049-3053

Samek P, Bober J, Vrzgula A et al (2001) Traumatic hemobilia caused by false aneurysm of replaced right hepatic artery: case report and review. J Trauma 51:153-158
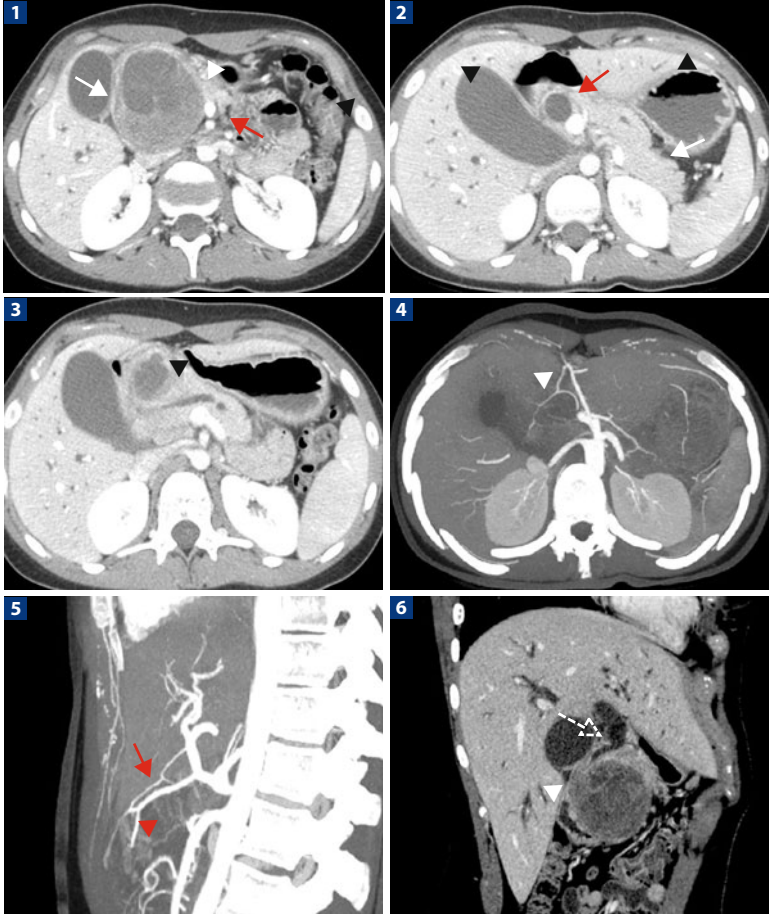
**1** In this adolescent patient, the axial scan in the portal phase shows a neoformation occupying the cephalo-pancreatic region (*white arrow*). The mass is encapsulated, with a micro-and macrocytic appearance; it adheres to the head of the pancreas, which is compressed and deflected toward the midline (*arrowhead*). The superior mesenteric vein is medialized (*red arrow*).   **2** An axial scan also acquired in the portal phase shows the distended common bile duct (*red arrow*) and gallbladder lumen (*arrowheads*). The body and tail of the pancreas are normal (*white arrow*). **3** Wirsung dilation (*arrowhead*) is observed.   **4** MIP reconstruction, in the axial plane and arterial phase, shows the pancreatic-duodenal artery shifted forwards and to the left from the midline (*arrowhead*).   **5** Sagittal MIP reconstruction in the arterial phase confirms displacement of the pancreatic-duodenal artery forwards (*arrow*). The artery has thin walls and is of normal caliber; thin arterial branches from ▶

## Study Protocol

**Patient preparation:** The examination is performed in emergency. No preparation is possible.

**CM volume:** 500–600 mgI (iodine dose) per kg body weight.

| Patient weight (kg) | < 60 | < 80 | > 80 |
|---|---|---|---|
| **CM concentration (mgI/mL)** | | | |
| 300 | 100 | 130 | 150 |
| 320 | 95 | 125 | 140 |
| 350 | 85 | 115 | 130 |
| 370 | 80 | 110 | 120 |
| 400 | 75 | 100 | 110 |
| **CM injection flow rate (mL/s)** | **1.6 gI/s** | **1.8 gI/s** | **2.0 gI/s** |
| **CM concentration (mgI/mL)** | | | |
| 300 | 5.3 | 6.0 | 6.7 |
| 320 | 5.0 | 5.6 | 6.2 |
| 350 | 4.6 | 5.1 | 5.7 |
| 370 | 4.3 | 4.8 | 5.4 |
| 400 | 4.0 | 4.5 | 5.0 |

**Pre-contrast scan:** Low dose, useful to detect dystrophic calcification and intralesional hemorrhage.

**Post-contrast scan:** The bolus-tracking monitoring technique is used.
Late arterial phase: 18-23 s after threshold of 100 H. ROI placed at the level of the diaphragmatic dome, to evaluate the arterial vasculature and to identify vascular abnormalities (arteriovenous fistula).
Portal phase: 60-70 s from the start of CM injection, to evaluate the portal tree and to identify parenchymal lesions.

**Comments:** The localization of a multiloculated expansive cystic mass in the anterior para-renal space, contiguous with the pancreatic head and compressing the extrahepatic bile duct, results in a difficult differential diagnosis that includes cystic pancreatic neoplasms. In the case above, i.e., obstructive jaundice in a pediatric patient, the arterial phase was instrumental to assess the anatomical relationships with the pancreatic-duodenal artery, allowing diagnosis of a retroperitoneal tumor with compression of the pancreatic head. After surgery, histological examination showed a lymphangiomatosis, and the pancreas was not resected.

## References

Candanedo-Gonzales F, Luna-Pèrez P (2000) Cystic lynphangioma of the mesentery. Clinical, radiological, and morphological analysis. Rev Gastroenterol Mex 65:6-10

Colovic RB, Grubor NM, Micey MT et al (2008) Cystic lynphangioma of the pancreas. World J Gastroenterol 14:6873-6875

Ravasse P, Le Treust M, Levesque C et al (1995) Cystic retroperitoneal lynphangioma: a tumor of polymorphic clinical manifestations. A propos of three cases. Arch Pediatr 2:232-236

◄ the superior mesenteric artery and supplying the mass (*arrowhead*) are visible.
**6** Oblique coronal reconstruction obtained in the portal phase confirms distention of the common bile duct at the middle third (*dotted arrow*), compression and deviation of the duct's retro-pancreatic aspect, and a neoformation (*arrowhead*), located below the head of pancreas, which is, consequently, markedly compressed

# EMERGENCY – Bleeding Colonic Diverticulum
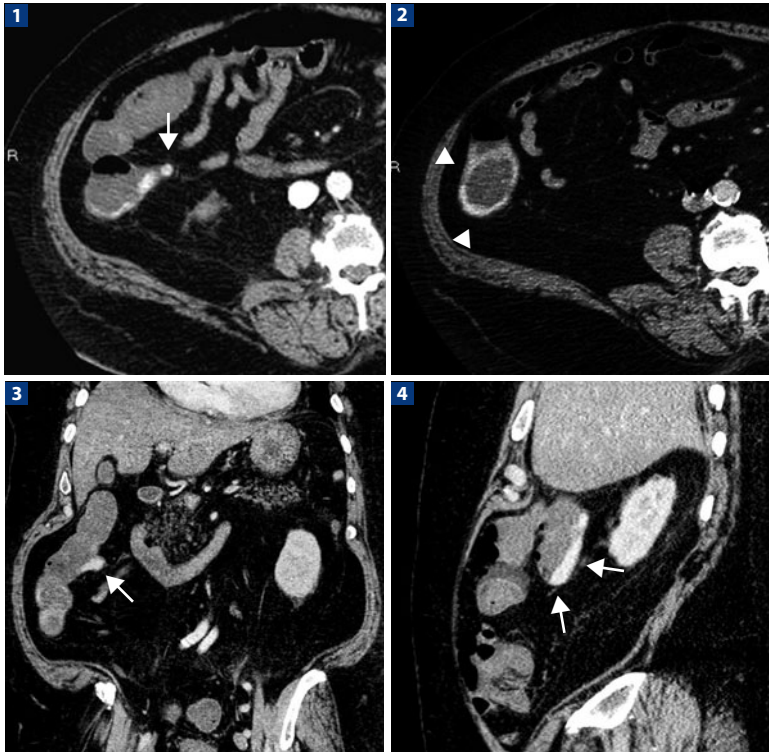


**1** Axial scan obtained in the arterial phase shows active bleeding in a diverticular formation (*arrow*) of the ascending colon. Contrast medium is seen in the inferior vena cava due to the use of the right common femoral vein as the venous access site. **2** Peripheral concentric distribution of the extravasated contrast medium in the colonic lumen (*arrowheads*) during venous phase. **3** MPR coronal reconstruction highlights the profile of the diverticulum in the medial ascending colon (*arrow*). **4** MPR sagittal reconstruction shows contrast medium in the colonic lumen (*arrows*)

## Study Protocol

**Patient preparation:** The examination is performed in emergency. No preparation is possible.

**CM volume:** 500–600 mgI (iodine dose) per kg body weight.

| Patient weight (kg) | < 60 | < 80 | > 80 |
|---|---|---|---|
| CM concentration (mgI/mL) | | | |
| 300 | 100 | 130 | 150 |
| 320 | 95 | 125 | 140 |
| 350 | 85 | 115 | 130 |
| 370 | 80 | 110 | 120 |
| 400 | 75 | 100 | 110 |
| **CM injection flow rate (mL/s)** | **1.6 gI/s** | **1.8 gI/s** | **2.0 gI/s** |
| CM concentration (mgI/mL) | | | |
| 300 | 5.3 | 6.0 | 6.7 |
| 320 | 5.0 | 5.6 | 6.2 |
| 350 | 4.6 | 5.1 | 5.7 |
| 370 | 4.3 | 4.8 | 5.4 |
| 400 | 4.0 | 4.5 | 5.0 |

**Pre-contrast scan:** Useful to detect bleeding collections and clots.

**Post-contrast scan:**
Early arterial phase: 10 s after threshold of 100 H. ROI placed at the level of the diaphragmatic dome, to evaluate arterial enhancement of the colonic wall.
Portal phase: 60-70 s from the start of CM injection to detect bleeding, if not visible in the arterial phase.
Equilibrium phase: 180 s from the start of CM injection to verify extravasation of CM from active bleeding, especially in cases of low-flow.

**Comments:** Intestinal arterial bleeding, especially related to diverticulosis, is often due to chronic inflammation of telangiectasias of diverticula lining mucosa. In the patient above, histological examination after surgery (emergency right hemicolectomy for severe intestinal bleeding) showed an angiodysplasia of the arterial vessels, causing intraluminal bleeding that resulted in a rapid and severe anemia (Hb value at the time of CT examination was 6.8 g/dl). The precise location of the bleeding avoided the need for a colonoscopy and angiography, thus significantly reducing both the time to surgery and the diagnostic and topographical indications for the surgical team.

## References

Kazuoki H, Nobutoshi M, Takayuki M et al (2009) Colonic diverticular bleeding: precise localization and successful management by a combination of CT angiography and interventional radiology. Abdoml Imaging (published on line Oct 24)

Kinouchi M, Kuroda F, Doi T et al (2005) A case of bleeding from ascending colon diverticula diagnosed by abdominal enhanced CT. Journal of Abdominal Emergency Medicine 25:929-932

Kuhle WG, Sheiman RG, Sheiman E (2003) Detection of active colonic hemorrhage with use of helical CT: findings in a swine model. Radiology 228:743-752
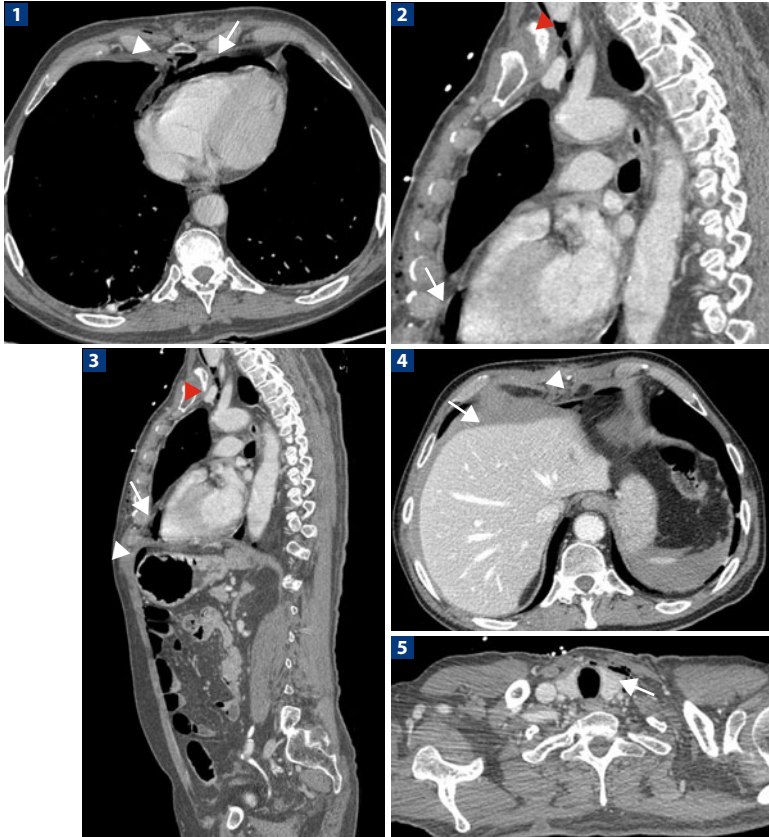
**1** Axial scan of the chest through the ventricular chambers documents a pneumopericardial flap (*arrow*). The break point of the pericardium, where the weapon penetrated (*arrowhead*), is clearly visible.   **2** Sagittal reconstruction of the chest confirms the presence of pneumopericardium (*arrow*) as well as air bubbles filtering up through the cervical region (*arrowhead*).   **3** Sagittal reconstruction of the thoraco-abdominal region shows a pneumopericardial flap (*arrow*) and pneumomediastinal air bubbles that involve the cervical region (*red arrowhead*). In the antero-upper abdomen, a layer of free air (pneumoperitoneum) surrounds the gastric fundus (*white arrowhead*).   **4** Axial scan of the abdomen confirms pneumoperitoneum (*arrowhead*) and documents the presence of a hemopneumoperitoneal flap in the perihepatic and perisplenic regions (*arrow*).   **5** Axial scan passing through the base of the neck confirms the presence of pneumomediastinal air bubbles filtering up through the cervical region (*arrow*)

## Study Protocol

**Patient preparation:** The examination is performed in emergency. No preparation is possible.

**CM volume:** 500–600 mgI (iodine dose) per kg body weight.

| Patient weight (kg) | < 60 | < 80 | > 80 |
|---|---|---|---|
| **CM concentration (mgI/mL)** | | | |
| 300 | 100 | 130 | 150 |
| 320 | 95 | 125 | 140 |
| 350 | 85 | 115 | 130 |
| 370 | 80 | 110 | 120 |
| 400 | 75 | 100 | 110 |
| **CM injection flow rate (mL/s)** | **1.6 gI/s** | **1.8 gI/s** | **2.0 gI/s** |
| **CM concentration (mgI/mL)** | | | |
| 300 | 5.3 | 6.0 | 6.7 |
| 320 | 5.0 | 5.6 | 6.2 |
| 350 | 4.6 | 5.1 | 5.7 |
| 370 | 4.3 | 4.8 | 5.4 |
| 400 | 4.0 | 4.5 | 5.0 |

**Pre-contrast scan:** Low dose, useful to detect and evaluate pneumopericardium and/or pneumoperitoneum.

**Post-contrast scan:**
The bolus-tracking monitoring technique is used.
Arterial phase: 10 s after threshold of 100 H. ROI placed at the level of the ascending aorta, to evaluate arterial damage.
Portal phase: 60-70 s from the start of CM injection, to evaluate the parenchyma and CM extravasation.

**Comments:** This case involved a male wounded with a knife in the anterior chest wall, causing pneumomediastinum and pneumopericardium without evidence of active bleeding or bruising in the chest. CT study of the abdomen showed pneumoperitoneum without signs of solid-organ injuries (liver and spleen). Intraperitoneal free air and blood could have been caused by two events: involvement of the gastric fundus by the weapon or injury from the pericardial sac or diaphragm with secondary drainage of the pericardial hematoma in the abdominal cavity and migration of the pneumopericardium in the peritoneal cavity through the diaphragm opening. Surgery confirmed the second hypothesis, showing a lesion in the pericardial sac and a lesion of the diaphragm, in the absence of perforation of the supramesocolic and submesocolic hollow viscera.

## References

Carrick MM, Pham HQ, Scott BG et al (2007) Traumatic rupture of the pericardium. Ann Thorac Surg 83:1554

Lee SY, Lee SJ, Jeon CW (2008) Pneumopericardium occurring after stab wound to the chest. Am J Surg 196:e10-e11

Romano L, Giovine S, Rossi G et al (1999) Rupture of the pericardium with luxation of the heart after blunt trauma. Emerg Radiol 6:252-254

# EMERGENCY – Volvulus in a Left Paraduodenal Hernia



**1, 2** Axial scans performed, respectively, in the arterial and the portal phase show dilation and tortuosity of the mesenteric vessels, both arterial and venous ("whirlpool sign"), indicative of an intestinal volvulus (*white arrows*). However, the intestinal loops involved retain normal wall thickness and homogeneously enhance. **3, 4** Axial scans, performed in portal phase, show the peritoneal gap in the left paraduodenal region, in which the bowel loops are also herniated (*white arrows*). Aero-hydrodistension of the loop located immediately over of the herniated jejunal loops (*red arrow*) is also clearly demonstrated. The typical "vortex" appearance of the involved mesenteric vessels is extremely important for the diagnosis of volvulus

## Study Protocol

**Patient preparation:** Intravenous catheter (at least 20G).

**CM volume:** 500–600 mgI (iodine dose) per kg body weight.

| Patient weight (kg) | < 60 | < 80 | > 80 |
|---|---|---|---|
| **CM concentration (mgI/mL)** | | | |
| 300 | 100 | 130 | 150 |
| 320 | 95 | 125 | 140 |
| 350 | 85 | 115 | 130 |
| 370 | 80 | 110 | 120 |
| 400 | 75 | 100 | 110 |
| **CM injection flow rate (mL/s)** | **1.6 gI/s** | **1.8 gI/s** | **2.0 gI/s** |
| **CM concentration (mgI/mL)** | | | |
| 300 | 5.3 | 6.0 | 6.7 |
| 320 | 5.0 | 5.6 | 6.2 |
| 350 | 4.6 | 5.1 | 5.7 |
| 370 | 4.3 | 4.8 | 5.4 |
| 400 | 4.0 | 4.5 | 5.0 |

**Pre-contrast scan:** Useful to detect dystrophic calcification and intraluminal or intraparietal hemorrhage of the involved intestinal loops.

**Post-contrast scan:**
The bolus-tracking monitoring technique is used.
Early arterial phase: 10 s after threshold of 100 H. ROI placed at the level of the diaphragmatic dome, to evaluate arterial enhancement of the intestinal wall and, eventually, ischemia.
Portal phase: 60-70 s from the start of CM injection, to evaluate the mesenteric venous branches and to detect expansive lesions.

**Comments:** Paraduodenal internal hernia is a rare condition that corresponds to the passage of intestinal loops through an intra-abdominal peritoneal orifice (congenital or acquired). Paraduodenal hernias can occur to the left or to the right, with a ratio of 3:1; the clinical manifestations may be non-specific, asymptomatic, intestinal ischemia, or bowel occlusion. In the case illustrated above, multi-phase study allowed optimal visualization of the abnormal course of the mesenteric vessels and the bowel loop herniated in the peritoneal breach, excluding ischemia. Surgery confirmed the diagnosis of intestinal volvulus in a paraduodenal hernia. Due to the accuracy and timeliness of the diagnosis, loop resection was unnecessary.

## References

Blachar A, Federle MP, Dodson SF (2001) Internal hernia: clinical and imaging findings in 17 patients with emphasis on CT criteria. Radiology 218:68-74

Iannucci JD, Grand D, Murphy BL (2009) Sensitivity and specificity of eight CT signs in the preoperative diagnosis of internal mesenteric hernia following Roux-en-Y gastric bypass surgery. Clin Radiol 64:373-380. Epub 2008 Dec 16
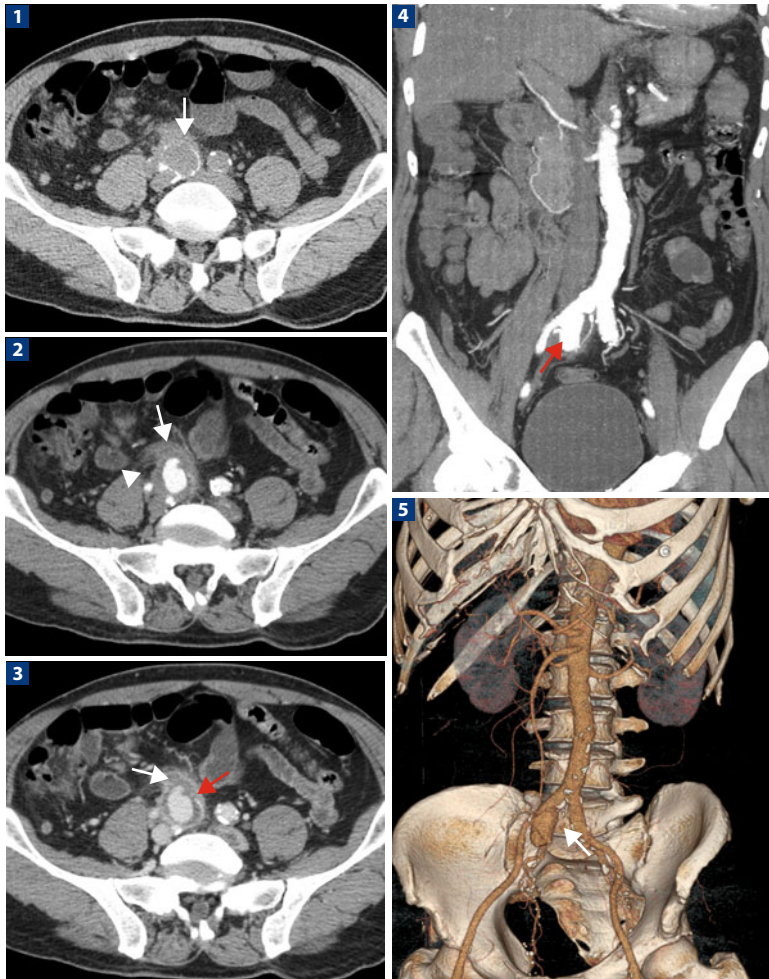
**1** Pre-contrast axial scan shows an aneurysm of the right common iliac artery. Note the calcified walls with interruption of the anterior margin (*arrow*). **2** Arterial phase shows parietal fissuring with passage of contrast medium (*arrowhead*); an ileal loop adherent to the vascular wall (*arrow*) is visible. **3** Late phase clearly illustrates rupture of the aneurysm (*red arrow*) and its irregular wall (*white arrow*). **4** Coronal MIP reconstruction shows the right common iliac artery aneurysm and its fissuring. **5** VR reconstruction shows the three-dimensional aspect of the aneurysmal sac (*arrow*)

## Study Protocol

**Patient preparation:** The examination is performed in emergency. No preparation is possible.

**CM volume:** 500–600 mgI (iodine dose) per kg body weight.

| Patient weight (kg) | < 60 | < 80 | > 80 |
|---|---|---|---|
| **CM concentration (mgI/mL)** | | | |
| 300 | 100 | 130 | 150 |
| 320 | 95 | 125 | 140 |
| 350 | 85 | 115 | 130 |
| 370 | 80 | 110 | 120 |
| 400 | 75 | 100 | 110 |
| **CM injection flow rate (mL/s)** | **1.6 gI/s** | **1.8 gI/s** | **2.0 gI/s** |
| **CM concentration (mgI/mL)** | | | |
| 300 | 5.3 | 6.0 | 6.7 |
| 320 | 5.0 | 5.6 | 6.2 |
| 350 | 4.6 | 5.1 | 5.7 |
| 370 | 4.3 | 4.8 | 5.4 |
| 400 | 4.0 | 4.5 | 5.0 |

**Pre-contrast scan:** Useful to detect densitometric changes in the aorta wall and retroperitoneal effusion.

**Post-contrast scan:**
The bolus-tracking monitoring technique is used.
Arterial phase: 8 s after threshold of 100 H. ROI placed at the level of the diaphragmatic dome.
Equilibrium phase: 180 s from the start of CM injection, necessary to detect active bleeding and to evaluate hypoperfusion of the abdominal organs.

**Comments:** Aorto-iliac fistula usually occurs when early atherosclerotic ulcer penetrates the adventitia and adheres to the wall of adjacent bowel loops. Most patients, initially, have sporadic episodes of melena, which may lead to fulminant digestive hemorrhage. An appropriate MDCT study highlights the early adherence between the aneurysm and intestinal loops, and wall thickening of the adjacent loop; more rarely, it reveals air bubble in the aneurysmal thrombus. These signs and the episodes of melena require immediate surgical evaluation, sometimes preceded by endoscopy. Extravasation of CM from the lumen of the aneurysm to the intestinal loop is always a late sign, with very high mortality.

## References

Hayashi H, Kumazaki T (2005) Multidetector-row CT. Evaluation of aortic disease. Radiat Med 23:1-9

Lawlor DK, De Rose G, Harris KA et al (2004) Primary aorto-iliac enteric fistula: report 6 new cases. Vasc Endovascular Surg 38:281-286

Milona S, Ntai S, Pomoni M et al (2007) Aorto-enteric fistula: CT findings. Abdom Imaging 32:393-397

# EMERGENCY – Mechanical Obstruction of the Small Intestine by Gallstone Ileus
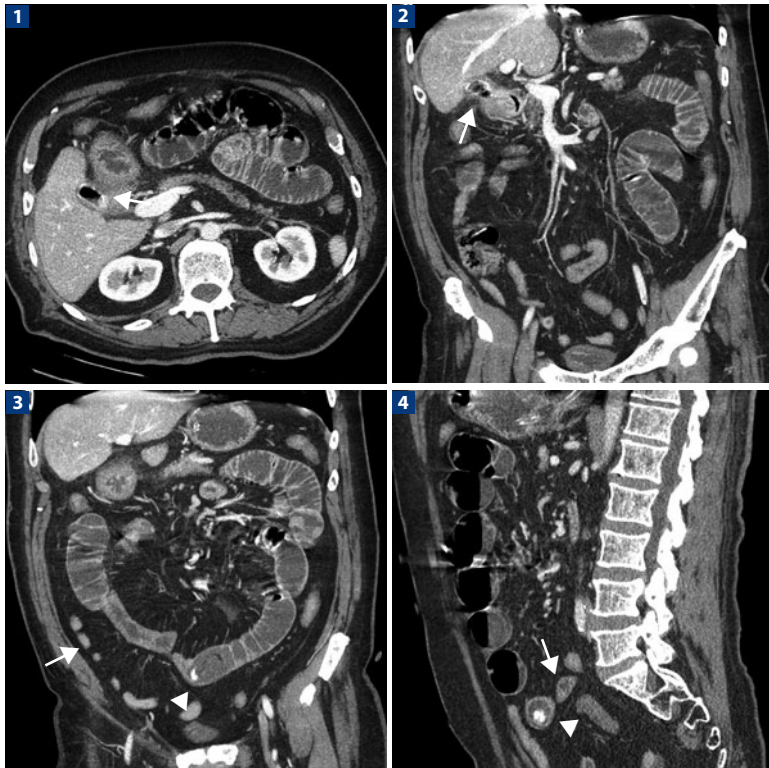


**1**, **2** Axial and coronal scans in the portal phase show the ileal-jejunal loops with regular perfusion of the wall and lumen distended by fluid-filled, hypertonic folds. The gallbladder-duodenal fistula (*arrows*) is clearly visible. **3**, **4** Coronal and sagittal reconstructions show jejunoileal overdistension extending to the pelvic cavity, where a "transition zone" is visible. Upstream of this zone, the dilated ileal loop has a rounded hyperdense formation in the lumen (*arrowheads*). The downstream loops are collapsed (*arrows*)

## Study Protocol

**Patient preparation:** The examination is performed in emergency. No preparation is possible.

**CM volume:** 500–600 mgI (iodine dose) per kg body weight.

| Patient weight (kg) | < 60 | < 80 | > 80 |
|---|---|---|---|
| **CM concentration (mgI/mL)** | | | |
| 300 | 100 | 130 | 150 |
| 320 | 95 | 125 | 140 |
| 350 | 85 | 115 | 130 |
| 370 | 80 | 110 | 120 |
| 400 | 75 | 100 | 110 |
| **CM injection flow rate (mL/s)** | **1.6 gI/s** | **1.8 gI/s** | **2.0 gI/s** |
| **CM concentration (mgI/mL)** | | | |
| 300 | 5.3 | 6.0 | 6.7 |
| 320 | 5.0 | 5.6 | 6.2 |
| 350 | 4.6 | 5.1 | 5.7 |
| 370 | 4.3 | 4.8 | 5.4 |
| 400 | 4.0 | 4.5 | 5.0 |

**Pre-contrast scan:** Useful to detect dystrophic calcification of the intestinal wall and intraluminal or intraparietal hemorrhage.

**Post-contrast scan:**
The bolus-tracking monitoring technique is used
Early arterial phase: 10 s after threshold of 100 H. ROI placed at the level of the diaphragmatic dome, to evaluate arterial enhancement of the colonic wall.
Portal phase: 60-70 s from the start of CM injection, to evaluate the portal branches and perfusion of the intestinal loops, also to characterize any endoluminal expansive lesions.

**Comments:** Gallstone ileus is a mechanical occlusive syndrome resulting from the migration of one or more stones from the biliary tract to the bowel. The pathogenesis is due to a gallbladder lithiasis complicated by biliary-enteric fistula. The fistula develops between the gallbladder and duodenum, colon, stomach, jejunum, or ileum and allows the passage of stones in the intestinal lumen, resulting eventually, in mechanical obstruction. In the case illustrated above, the presence of the gallbladder-duodenal fistula, signs of intestinal obstruction, and the retrieval of gallstones in the small bowel were diagnostic of gallstone ileus. The diagnosis was confirmed at subsequent surgery, with extraction of the gallstones.

## References

Farooq A, Memon B, Memon MA (2007) Resolution of gallstone ileus with spontaneous evacuation of gallstone. Emerg Radiol 14:421-423

Lassandro F, Gagliardi N, Scuderi M et al (2004) Gallstone ileus analysis of radiological findings in 27 patients. Eur J Radiol 50:23-29

Leen GLS, Finlay M (1990) CT diagnosis of gallstone ileus. Acta Radiol 31:497-498

Ripolles T, Miguel-Dasit A, Errando J et al (2001) Gallstone ileus: increased diagnostic sensitivity by combining plain film and ultrasound. Abdom Imaging 26:401-405

# EMERGENCY – Bleeding Jejunal Gastrointestinal Stromal Tumor
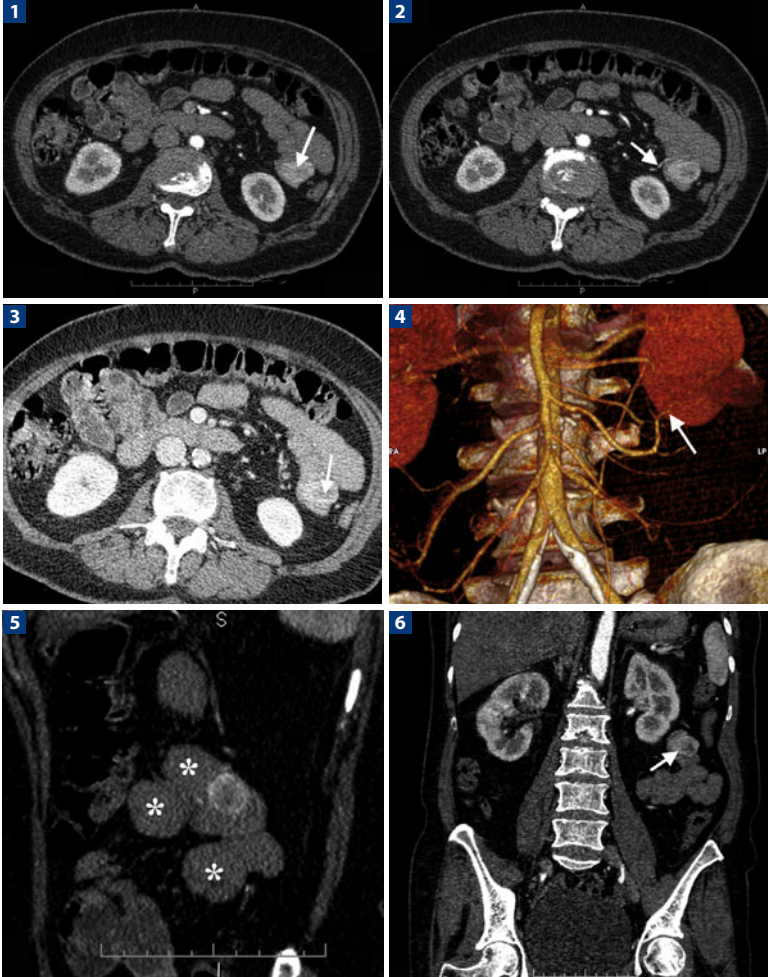












**1** Axial scan in arterial phase shows an expansive mass occupying one of the first jejunal loops (*arrow*). The lesion is characterized by an intense peripheral vascular enhancement with a central hemorrhagic area. **2** Axial scan in arterial phase: a mesenteric arterious vessels supplies the lesion (*arrow*). **3** Axial scan in portal phase: an expansive mass in the first jejunal loops within the hemorrhagic area inside (*arrow*); an endovisceral hyperdensity referable to active bleeding is not visible. **4** VR reconstruction angiography: a mesenteric arterial branch (*arrow*), originating from the superior mesenteric artery, supplies the lesion. **5** Sagittal MPR reconstruction in arterial phase: a hyperdense endovisceral ▶

## Study Protocol

**Patient preparation:** The examination is performed in emergency. No preparation is possible.

**CM volume:** 500–600 mgI (iodine dose) per kg body weight.

| Patient weight (kg) | < 60 | < 80 | > 80 |
|---|---|---|---|
| **CM concentration (mgI/mL)** | | | |
| 300 | 100 | 130 | 150 |
| 320 | 95 | 125 | 140 |
| 350 | 85 | 115 | 130 |
| 370 | 80 | 110 | 120 |
| 400 | 75 | 100 | 110 |
| **CM injection flow rate (mL/s)** | **1.6 gI/s** | **1.8 gI/s** | **2.0 gI/s** |
| **CM concentration (mgI/mL)** | | | |
| 300 | 5.3 | 6.0 | 6.7 |
| 320 | 5.0 | 5.6 | 6.2 |
| 350 | 4.6 | 5.1 | 5.7 |
| 370 | 4.3 | 4.8 | 5.4 |
| 400 | 4.0 | 4.5 | 5.0 |

**Pre-contrast scan:** Useful to detect calcification or clots, signs of active bleeding.

**Post-contrast scan:**
Arterial phase: 8 s after threshold of 100 H. ROI placed at the level of the diaphragmatic dome, to evaluate the visceral wall and arterial enhancement of the lesion; in cases of active massive bleeding, the spreading of CM into the lumen is visible.
Portal phase: 60-70 s from the start of CM injection.
Equilibrium phase: 180 s from the start of CM injection. This phase can play a crucial role in the detection of bleeding sources in case of low-flow.

**Comments:** Gastrointestinal stromal tumors (GISTs) comprise 20% of small intestinal tumors. The diagnosis of GIST can be accidental, with non-specific symptoms such as abdominal pain or gastrointestinal bleeding. The above case was that of a 58-year-old woman with melena. All the phases acquired were important to identify the jejunal lesion, characterized by intense and early enhancement, without evidence of endolesional bleeding. The jejunal lesion was resected and histological examination indicated its mesenchymal origin.

## References

Bartolotta TV, Taibbi A, Galia M et al (2006) Gastrointestinal stromal tumour: 40-row multislice computed tomography findings. Radiol Med 111:651-660

Chi-Ming Lee, Hsin-Chi Chen, Ting-Kai Leung et al (2004) Gastrointestinal stromal tumor: computed tomographic features. World J Gastroenterol 5; 10:2417-2418

Kim JY, Lee JM, Kim KW, Park HS et al (2009) Ectopic pancreas: CT findings with emphasis on differentiation from small gastrointestinal stromal tumor and leiomyoma. Radiology 252:92-100

◄ lesion; the adjacent jejunal loops have a spastic reflex (*asterisks*).   **6** Coronal MPR reconstruction in arterial phase: an expansive formation occupies one of the first jejunal loops, about 30 cm from the ligament of Treitz (*arrow*)

# EMERGENCY – Phytobezoar-induced Mechanical Intestinal Obstruction
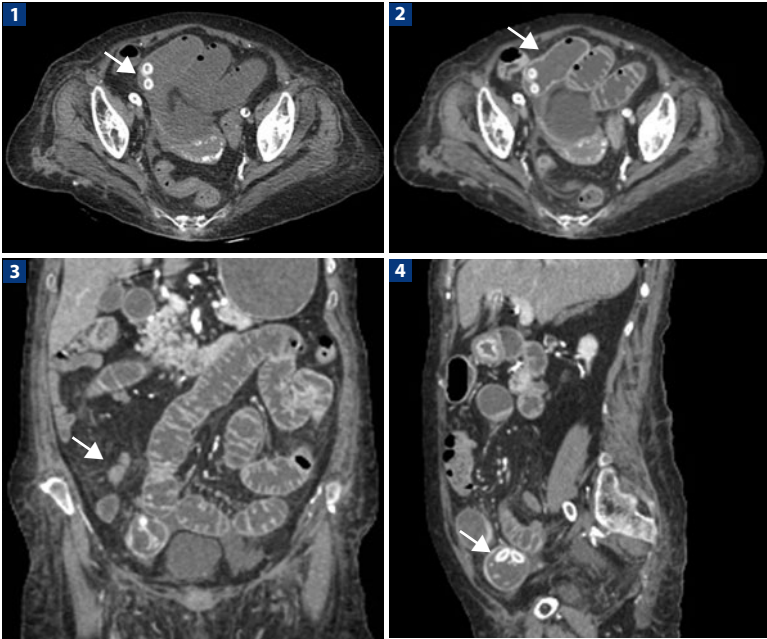


**1** Proximal and middle Ileal and jejunal loops are dilated by liquid content. Prior to the administration of contrast medium, a foreign body within the lumen (*arrow*) is clearly visible. **2** The wall of the involved loop shows physiological enhancement (*arrow*). **3** Coronal MPR reconstruction shows the homogeneous enhancement of the ileal loop walls. The mesentery seems normal but the downstream loops are collapsed (*arrow*). **4** Sagittal MPR reconstruction clearly shows a foreign body (*arrow*) suggestive of hypodense material surrounding central hyperdense nuclei. The phytobezoar resulted in mechanical obstruction of the small intestine

## Study Protocol

**Patient preparation:** The examination is performed in emergency. No preparation is possible.

**CM volume:** 500–600 mgI (iodine dose) per kg body weight.

| Patient weight (kg) | < 60 | < 80 | > 80 |
|---|---|---|---|
| **CM concentration (mgI/mL)** | | | |
| 300 | 100 | 130 | 150 |
| 320 | 95 | 125 | 140 |
| 350 | 85 | 115 | 130 |
| 370 | 80 | 110 | 120 |
| 400 | 75 | 100 | 110 |
| **CM injection flow rate (mL/s)** | **1.6 gI/s** | **1.8 gI/s** | **2.0 gI/s** |
| **CM concentration (mgI/mL)** | | | |
| 300 | 5.3 | 6.0 | 6.7 |
| 320 | 5.0 | 5.6 | 6.2 |
| 350 | 4.6 | 5.1 | 5.7 |
| 370 | 4.3 | 4.8 | 5.4 |
| 400 | 4.0 | 4.5 | 5.0 |

**Pre-contrast scan:** Useful to detect the phytobezoar.

**Post-contrast scan:**
The bolus-tracking monitoring technique is used.
Early arterial phase: 10 s after threshold of 100 H. ROI placed at the level of the diaphragmatic dome, to evaluate arterial enhancement of the intestinal wall.
Portal phase: 60-70 s from the start of CM injection, to evaluate parietal enhancement of the involved loops.

**Comments:** Phytobezoars are compact clusters of vegetal material. Hypochlorhydria, antral decreased mobility, and reduced chewing are the most important predisposing factors. Most bezoars are asymptomatic but they occasionally cause small-bowel obstruction and determine, as illustrated above, a hydromechanical ileus with gaseous distension of the jejunoileal loops upstream. In the above patient, surgery showed dilation of the ileal loops up to about 40 cm from the ileocecal valve, where there was a sharp caliber reduction caused by the phytobezoar.

## References

Andrus Ch, Ponsky JL (1988) Bezoars: classification, pathophysiology and treatment. Am J Gastroenterol 83:476-478

Di Mizio R, Scaglione M (eds) (2007) Ileo meccanico dell'intestino tenue. Aspetti TC e correlazioni eco-radiografiche. Springer-Verlag Italia, Milano

Zissin R, Osadchy A, Gutman V et al (2004) CT findings in patients with small bowel obstruction due to phytobezoar. Emerg Radiol 10:197-200

# EMERGENCY – Iatrogenic Injury of the Right Diaphragmatic Artery by Thermo-ablation of a Liver Nodule
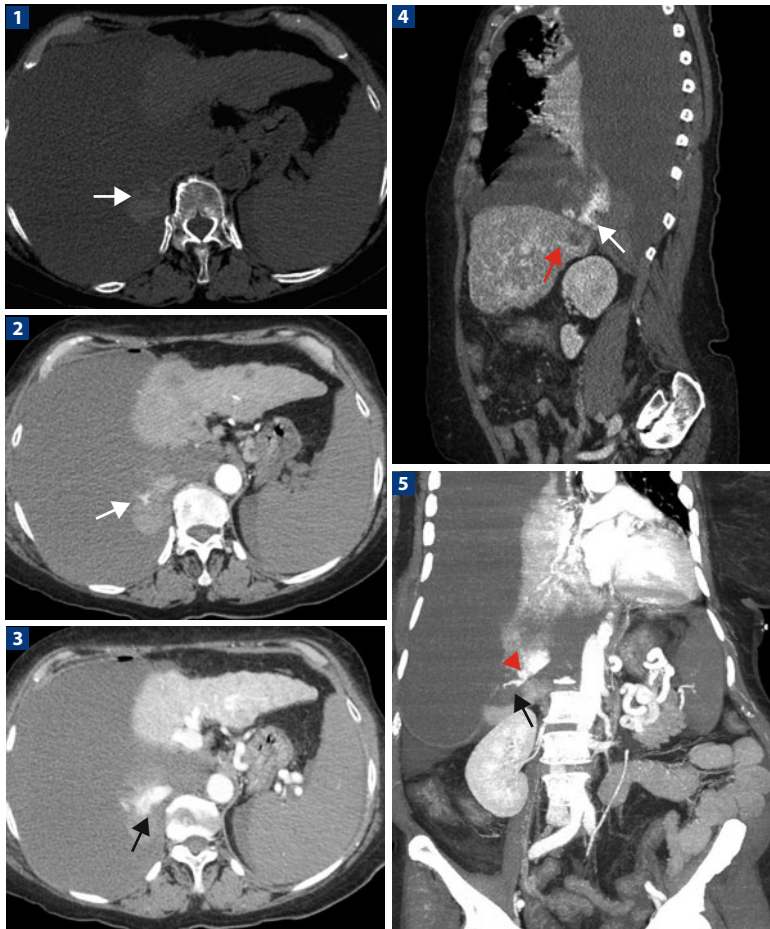


**1** The pre-contrast scan clearly shows a large right pleural effusion with a hyperdense formation indicative of a blood clot (*arrow*). **2** In arterial phase, there is a small site of active bleeding inside the clot (*arrow*). **3** Venous phase, there is an increase in the active bleeding (*arrow*). **4** Sagittal reconstruction shows a hypodense region of the liver (*arrow*), the outcome of thermo-ablation, and a hyperdensity of the surrounding diaphragm caused by active bleeding (*white arrow*). **5** Coronal MIP image, in venous phase, shows an interruption of the diaphragm profile above the thermo-ablation treatment site (*arrow*), where signs of active bleeding (*arrowhead*) can be appreciated

## Study Protocol

**Patient preparation:** The examination is performed in emergency. No preparation is possible.

**CM volume:** 500–600 mgI (iodine dose) per kg body weight.

| Patient weight (kg) | < 60 | < 80 | > 80 |
|---|---|---|---|
| **CM concentration (mgI/mL)** | | | |
| 300 | 100 | 130 | 150 |
| 320 | 95 | 125 | 140 |
| 350 | 85 | 115 | 130 |
| 370 | 80 | 110 | 120 |
| 400 | 75 | 100 | 110 |
| **CM injection flow rate (mL/s)** | **1.6 gI/s** | **1.8 gI/s** | **2.0 gI/s** |
| **CM concentration (mgI/mL)** | | | |
| 300 | 5.3 | 6.0 | 6.7 |
| 320 | 5.0 | 5.6 | 6.2 |
| 350 | 4.6 | 5.1 | 5.7 |
| 370 | 4.3 | 4.8 | 5.4 |
| 400 | 4.0 | 4.5 | 5.0 |

**Pre-contrast scan:** Useful to detect hemorrhages and sentinel clots.

**Post-contrast scan:**
The bolus-tracking monitoring technique is used.
Early arterial phase: 10 s after threshold of 100 H. ROI placed at the level of the diaphragmatic dome, to evaluate the arteries and to identify vascular abnormalities (arteriovenous fistula).
Portal phase: 60-70 s from the start of CM injection to detect parenchymal lesion and evaluate portal branches.
Equilibrium phase: 180 s from the start of CM injection to verify extravasation of CM from high-flow bleeding.

**Comments:** MDCT accurately detects active bleedings and is currently the best imaging modality when an iatrogenic hemorrhage is suspected. In the patient above, the source of bleeding (diaphragmatic artery) was related to a region of necrosis of the diaphragmatic dome, just above the site where the hepatic lesion was thermo-ablated. The patient underwent selective arteriography and embolization of the right diaphragmatic artery.

## References

Keckler S, Welch M, Danks RR (2006) Blunt injury to the right inferior phrenic artery without associate hepatic injury. Injury Extra 37:218-219

Mizobata Y, Yokota J, Yaijma Y et al (2000) Two cases of blunt hepatic injury with active bleeding from the right inferior phrenic artery. J Trauma 48:1153-1155

Sung Wook Shin, Young Soo Do, Sung Wook Choo et al (2006) Diaphragmatic weakness after trascatheter arterial chemoembolization of inferior phrenic artery for treatment of hepatocellular carcinoma. Radiology 241:581-588
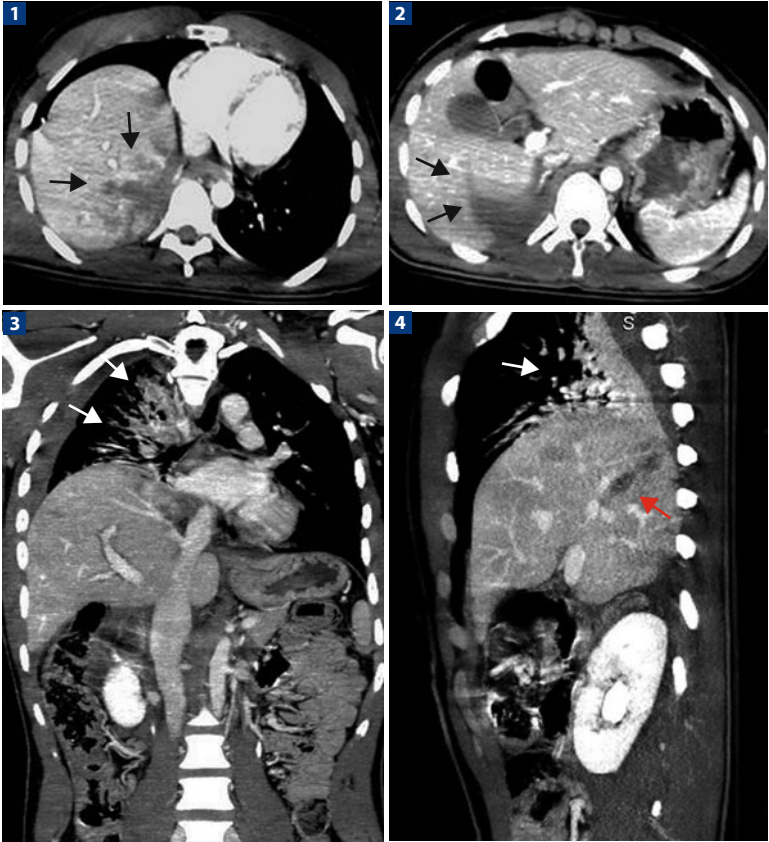
**1** Axial scan of the liver dome shows a large parenchymal contusion of segment VII (*arrows*). **2** Wide notch of segment VI between the thoracic and abdominal cavities, corresponding to the "collar sign" (*arrows*). **3** Coronal MPR reconstruction shows intrathoracic displacement of most of the liver and corresponding vascular structures. An area of atelectasia of the lung parenchyma (*arrows*) can also be seen. **4** Sagittal MPR reconstruction with evidence of parenchymal contusion and laceration of segment VII (*red arrow*) and corresponding atelectasia of the lung (*white arrow*)

## Study Protocol

**Patient preparation:** The examination is performed in emergency. No preparation is possible.

**CM volume:** 500–600 mgI (iodine dose) per kg body weight.

| Patient weight (kg) | < 60 | < 80 | > 80 |
|---|---|---|---|
| **CM concentration (mgI/mL)** | | | |
| 300 | 100 | 130 | 150 |
| 320 | 95 | 125 | 140 |
| 350 | 85 | 115 | 130 |
| 370 | 80 | 110 | 120 |
| 400 | 75 | 100 | 110 |
| **CM injection flow rate (mL/s)** | **1.6 gI/s** | **1.8 gI/s** | **2.0 gI/s** |
| **CM concentration (mgI/mL)** | | | |
| 300 | 5.3 | 6.0 | 6.7 |
| 320 | 5.0 | 5.6 | 6.2 |
| 350 | 4.6 | 5.1 | 5.7 |
| 370 | 4.3 | 4.8 | 5.4 |
| 400 | 4.0 | 4.5 | 5.0 |

**Pre-contrast scan:** Useful to detect bleeding and sentinel clots.

**Post-contrast scan:**
The bolus-tracking monitoring technique is used.
Early arterial phase: 10 s after threshold of 100 H. ROI placed at the level of the diaphragmatic dome, to evaluate the arteries and to detect vascular abnormalities caused by trauma.
Portal phase: 60-70 s from the start of CM injection, to detect parenchymal lesions and to evaluate portal branches.
Equilibrium phase: 180 s from the start of CM injection to verify extravasation of CM from active bleeding.

**Comments:** Hemi-diaphragm injuries are rare in closed abdominal trauma and require early and accurate diagnosis to evaluate possible displacement of intrathoracic abdominal organs and associated thoraco-abdominal damage. The ability of MDCT to perform high-quality MPR reconstructions makes it the technique of choice to evaluate these lesions. In the patient above, much of the liver is herniated into the chest cavity, causing a significant stretch of vascular structures. The multi-phasic approach allowed accurate evaluation of the injured vessels, the hepatic artery, and the portal vein, which is extremely important for patient management. The patient was immediately subjected to a repositioning of the right hemi-diaphragmatic rupture of the liver.

## References

Larici AR (2002) Helical CT with sagittal and coronal reconstructions: accuracy for detection of diaphragmatic injury. AJR Am J Roentgenol 179:451-457

Rees O, Mirvis SE, Shanmuganathan K (2005) Multidetector-row CT of right hemidiaphragmatic rupture caused by blunt trauma: a review of 12 cases. Clin Radiol 60:1280-1289

# EMERGENCY – Abdominal Aortic Aneurysm with Aorto-caval Fistula
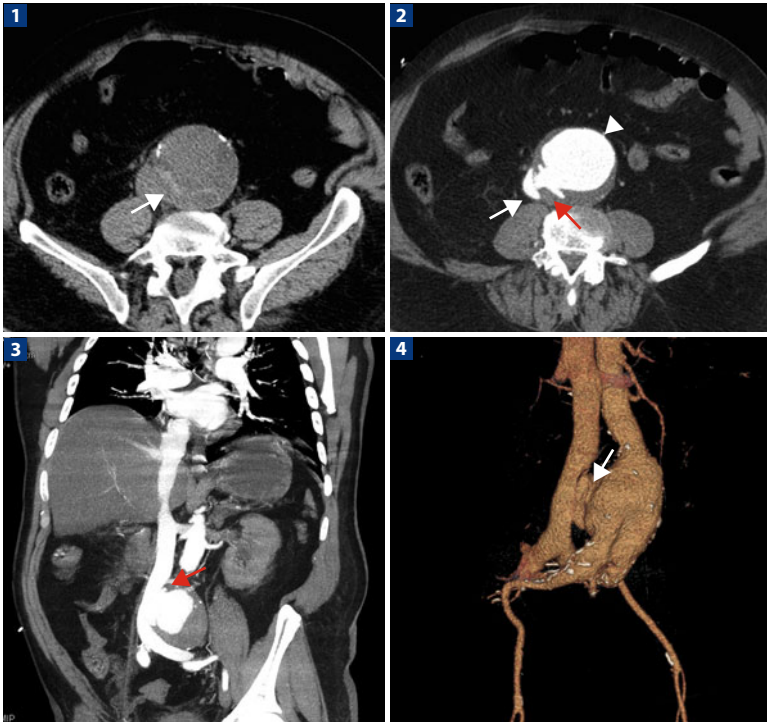


**1** Pre-contrast axial scan shows an aneurysm of the abdominal aorta with parietal thrombotic apposition, calcification, and peripheral hyperdensity of the lumen (*arrow*).    **2** The arterial phase shows a simultaneous enhancement of the inferior vena cava (*white arrow*) and aorta (*arrowhead*); also clearly visible is the link between the aortic lumen and the caval lumen (*red arrow*).    **3** Coronal MIP reconstruction in arterial phase shows hyperflow in the caval lumen and fistula between the aorta and inferior vena cava (*arrow*).    **4** VR reconstruction allows an accurate evaluation of the two vessels involved (*arrow*)

## Study Protocol

**Patient preparation:** The examination is performed in emergency. No preparation is possible.

**CM volume:** 500–600 mgI (iodine dose) per kg body weight.

| Patient weight (kg) | < 60 | < 80 | > 80 |
|---|---|---|---|
| **CM concentration (mgI/mL)** | | | |
| 300 | 100 | 130 | 150 |
| 320 | 95 | 125 | 140 |
| 350 | 85 | 115 | 130 |
| 370 | 80 | 110 | 120 |
| 400 | 75 | 100 | 110 |
| **CM injection flow rate (mL/s)** | **1.6 gI/s** | **1.8 gI/s** | **2.0 gI/s** |
| **CM concentration (mgI/mL)** | | | |
| 300 | 5.3 | 6.0 | 6.7 |
| 320 | 5.0 | 5.6 | 6.2 |
| 350 | 4.6 | 5.1 | 5.7 |
| 370 | 4.3 | 4.8 | 5.4 |
| 400 | 4.0 | 4.5 | 5.0 |

**Pre-contrast scan:** Useful to evaluate densitometric changes in the aorta and retroperitoneum.

**Post-contrast scan:**
The bolus-tracking monitoring technique is used.
Arterial phase: 8 s after threshold of 100 H. ROI placed at the level of the diaphragmatic dome.
Equilibrium phase: 180 s from the start of CM injection to evaluate parenchymal perfusion of the abdominal organs and, possibly, to detect active bleeding.

**Comments:** Spontaneous aorto-caval fistulas complicate about 3–4% of atherosclerotic infrarenal aneurysms. Usually, the abnormal communication originates above the iliac bifurcation, as a result of a chronic inflammatory of aneurysm causing adhesions between the two vessels. Early diagnosis is important for patient survival, as death is often related to acute heart failure. MDCT in the arterial phase highlights the synchronous enhancement of the inferior vena cava and the aorta, with signs of right heart overload. Axial scans using high collimation directly show the fistula between the infrarenal aorta and vena cava. In the case above, the patient was treated surgically with the placement of an aorto-iliac graft.

## References

Coulier B, Tilquin O, Etienne PY (2004) Multidetector row CT diagnosis of aortocaval fistula complicating aortic aneurysm: a case report. Emerg Radiol 11:100-103

Rubin G (2003) MDCT imaging of the aorta and peripheral vessels. Eur J Radiol 45:S42-49

Schwartz SA, Talijanovic AM, Smyth S et al (2007) CT findings of rupture, impeding rupture, and contained rupture of abdominal aortic aneurysms. AJR Am J Roentgenol 188:W58-W62

# EMERGENCY – Ileal Volvulus Complicated by Intestinal Ischemia
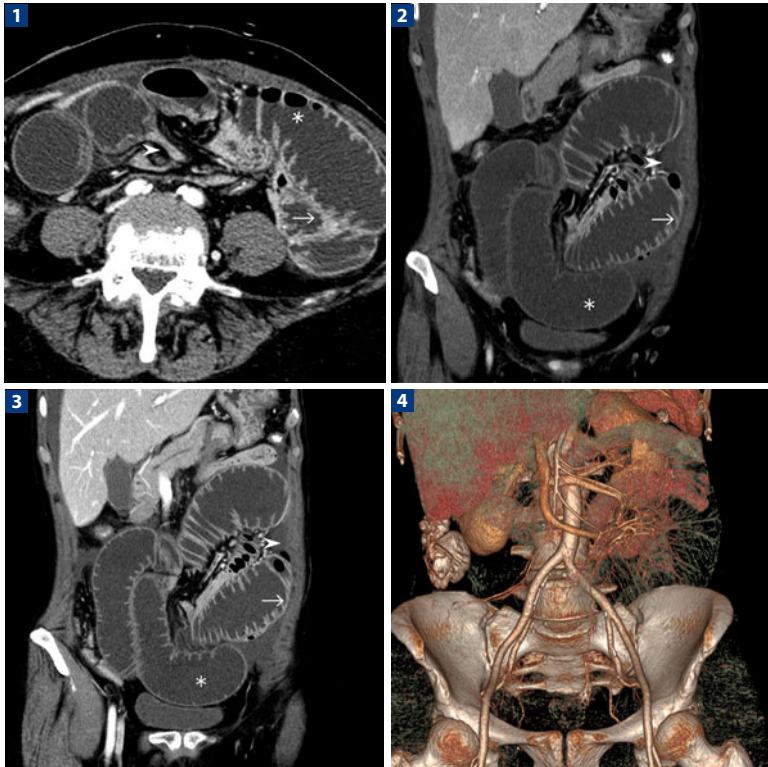


**1** Axial arterial phase scan reconstruction shows marked bowel dilatation, with evidence of a fluid level (*asterisk*), mucosal thickening (*arrow*) and the transition loop (*arrowhead*).   **2, 3**  Arterial and enteric phases with coronal reconstruction show the marked bowel dilatation (*asterisk*), mucosal thickening (*arrow*), and vascular mucosal damage due to the volvulus and the ascites (*arrowhead*).   **4**  VR reconstruction better shows the bowel involvement of the ileocolic artery

## Study Protocol

**Patient preparation:** The examination is performed in emergency. No preparation is possible.

**CM volume:** 500–600 mgI (iodine dose) per kg body weight.

| Patient weight (kg) | < 60 | < 80 | > 80 |
|---|---|---|---|
| **CM concentration (mgI/mL)** | | | |
| 300 | 100 | 130 | 150 |
| 320 | 95 | 125 | 140 |
| 350 | 85 | 115 | 130 |
| 370 | 80 | 110 | 120 |
| 400 | 75 | 100 | 110 |
| **CM injection flow rate (mL/s)** | **1.6 gI/s** | **1.8 gI/s** | **2.0 gI/s** |
| **CM concentration (mgI/mL)** | | | |
| 300 | 5.3 | 6.0 | 6.7 |
| 320 | 5.0 | 5.6 | 6.2 |
| 350 | 4.6 | 5.1 | 5.7 |
| 370 | 4.3 | 4.8 | 5.4 |
| 400 | 4.0 | 4.5 | 5.0 |

**Pre-contrast scan:** Useful for evaluation of ileocolic involvement.

**Post-contrast scan:**
Arterial phase: Useful for the evaluation of the splanchnic vessels.
Enteric phase: Allows better evaluation of wall enhancement.

**Scan delay:** The bolus-tracking monitoring technique is used.
Early arterial phase: 10 s after the threshold of 100 HU is reached.
Enteric phase: 75 s from the start of CM injection.

## References

Yikilmaz A, Karahan OI, Senol S et al (2011) Value of multislice computed tomography in the diagnosis of acute mesenteric ischemia. Eur J Radiol 80:297-302. PubMed PMID: 20719444

Menke J (2010) Diagnostic accuracy of multidetector CT in acute mesenteric ischemia: systematic review and meta-analysis. Radiology 256(1):93-101. Review. PubMed PMID: 20574087

Furukawa A, Kanasaki S, Kono N et al (2009) CT diagnosis of acute mesenteric ischemia from various causes. AJR Am J Roentgenol 192(2):408-416. Review. PubMed PMID: 19155403

# EMERGENCY – Perforated Peptic Ulcer
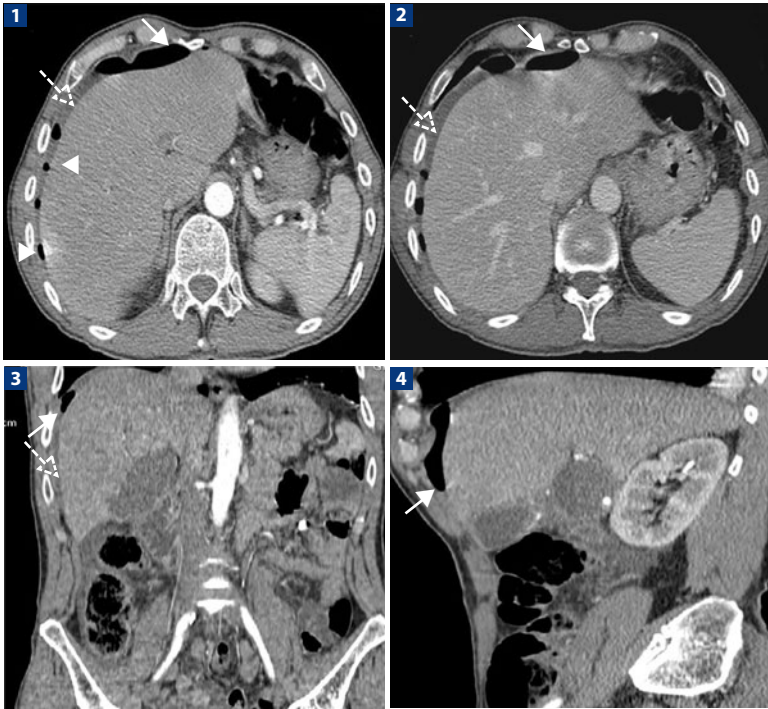


**1**, **2** After hollow viscus perforation, peri-hepatic free air is clearly visible (*white arrow*), associated with small gas bubbles (*white arrowhead*), and fluid effusion (*dashed arrow*). **3** Coronal MPR reconstruction in arterial phase confirms the presence of peri-hepatic free air (*white arrow*) and fluid effusion (*dashed arrow*) while excluding these findings in the submesocolic recess. **4** Sagittal MPR reconstruction shows free air confined to the peri-hepatic region (*arrow*)

## Study Protocol

**Patient preparation:** The examination is performed in emergency. No preparation is possible.

**CM volume:** 500–600 mgI (iodine dose) per kg body weight.

| Patient weight (kg) | < 60 | < 80 | > 80 |
|---|---|---|---|
| **CM concentration (mgI/mL)** | | | |
| 300 | 100 | 130 | 150 |
| 320 | 95 | 125 | 140 |
| 350 | 85 | 115 | 130 |
| 370 | 80 | 110 | 120 |
| 400 | 75 | 100 | 110 |
| **CM injection flow rate (mL/s)** | **1.6 gI/s** | **1.8 gI/s** | **2.0 gI/s** |
| **CM concentration (mgI/mL)** | | | |
| 300 | 5.3 | 6.0 | 6.7 |
| 320 | 5.0 | 5.6 | 6.2 |
| 350 | 4.6 | 5.1 | 5.7 |
| 370 | 4.3 | 4.8 | 5.4 |
| 400 | 4.0 | 4.5 | 5.0 |

**Pre-contrast scan:** Useful to detect bleeding and/ or sentinel clots.

**Post-contrast scan:**
The bolus-tracking monitoring technique is used.
Early arterial phase: 10 s after threshold of 100 H. ROI placed at the level of the diaphragmatic dome, to evaluate arterial vascularization of the parenchyma and hollow viscus.
Portal phase: 60-70 s from the start of CM injection, to evaluate the portal branches and parenchyma.

**Comments:** In the case described above, corresponding to non-traumatic acute abdomen, the CT protocol (arterial phase followed by portal phase) allowed the exclusion of complications (especially ischemia) affecting intestinal loops. Free air and free fluid in the supramesocolic recesses suggested the diagnosis of gastrointestinal perforation. Surgery revealed peritonitis caused by a perforated peptic ulcer.

## References

Grassi R, Romano S, Pinto A et al (2004) Gastro-duodenal perforations: conventional plain film, US and CT findings in 166 consecutive patients. Eur J Radiol 50:30-36

Pinto A, Scaglione M, Giovine S et al (2004) Quaranta pazienti con perforazione gastro-intestinale: confronto tra la sede dei reperti TC spirale multidetettore di perforazione e la sede di perforazione riscontrata all'intervento chirurgico. Radiol Med 108:208-217

Pinto A, Scaglione M, Pinto F et al (2000) Helical computed tomography diagnosis of gastrointestinal perforation in the elderly patient. Emerg Radiol 7:259-262

# EMERGENCY – Active Bleeding in a Hematoma of the Back
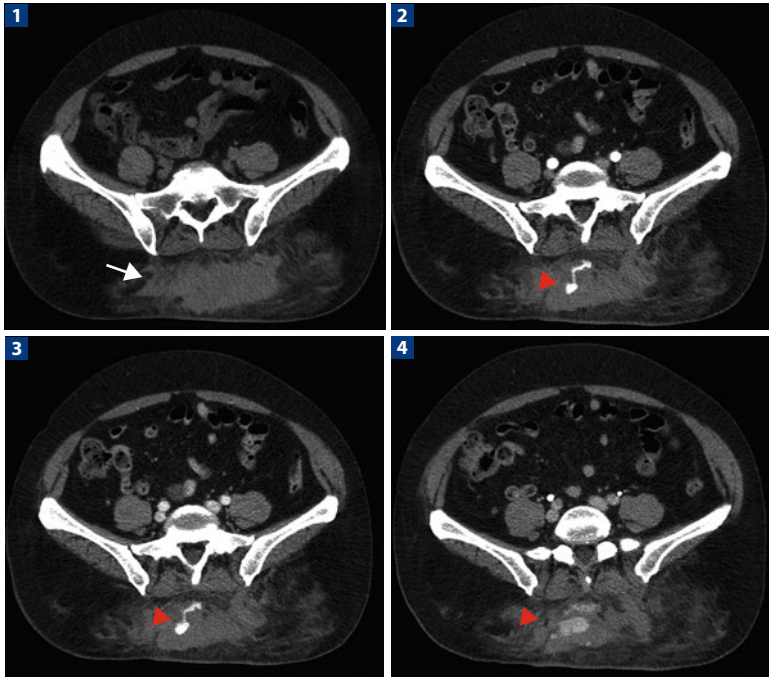


**1** Pre contrast axial CT scan shows an extensive hematoma of the right gluteus muscle (*arrow*).   **2**, **3**, **4** Arterial, portal, and delayed acquisition phases show a rounded lesion of about 3 cm (*arrowheads*) with distinct margins, within the hematoma in the right gluteus muscle, with similar enhancement and wash-out of arteries, suggesting gluteal artery pseudoaneurysm. Note that the shape of lesion does not change in the three post-contrast acquisition phases

## Study Protocol

**Patient preparation:** The examination is performed in emergency. No preparation is possible.

**CM volume:** 500–600 mgI (iodine dose) per kg body weight.

| Patient weight (kg) | < 60 | < 80 | > 80 |
|---|---|---|---|
| **CM concentration (mgI/mL)** | | | |
| 300 | 100 | 130 | 150 |
| 320 | 95 | 125 | 140 |
| 350 | 85 | 115 | 130 |
| 370 | 80 | 110 | 120 |
| 400 | 75 | 100 | 110 |
| **CM injection flow rate (mL/s)** | **1.6 gI/s** | **1.8 gI/s** | **2.0 gI/s** |
| **CM concentration (mgI/mL)** | | | |
| 300 | 5.3 | 6.0 | 6.7 |
| 320 | 5.0 | 5.6 | 6.2 |
| 350 | 4.6 | 5.1 | 5.7 |
| 370 | 4.3 | 4.8 | 5.4 |
| 400 | 4.0 | 4.5 | 5.0 |

**Pre-contrast scan:** Useful to detect bleeding collections and clots.

**Post-contrast scan:**
The bolus-tracking monitoring technique is used.
Early arterial phase: 10 s after threshold of 100 H. ROI placed at the level of the diaphragmatic dome.
Portal phase: 60-70 s from the start of CM injection.
Equilibrium phase: 180 s from the start of CM injection to detect extravasation of CM from active low-flow bleeding.

**Comments:** Traumatic active bleeding must be searched for in every anatomic region. A multiphasic approach is crucial to distinguish these injuries from pseudoaneurysms. Extravasation of CM enlarges during the delayed phase (from "jet" to "pooling") while pseudoaneurysms maintain their rounded morphology in all phases acquired, without dimensional changes and showing enhancement relative to vessels. In the case presented above, there were no bone fractures.

## References

Anderson SW, Soto JA, Lucey BC et al (2008) Blunt trauma: feasibility and clinical utility of pelvic CT angiography performed with 64-detector row CT. Radiology 246:410-519

Ptak T, Rhea JT, Novelline RA (2001) Experience with a continuous, single-pass whole-body multidetector CT protocol for trauma: the three minute multiple trauma CT scan. Emerg Radiol 8:250-256